



Richmond, Craig J. (2009) *Applications for imidazophenanthridine-based heterocycles*. PhD thesis.

<http://theses.gla.ac.uk/1406/>

Copyright and moral rights for this thesis are retained by the author

A copy can be downloaded for personal non-commercial research or study, without prior permission or charge

This thesis cannot be reproduced or quoted extensively from without first obtaining permission in writing from the Author

The content must not be changed in any way or sold commercially in any format or medium without the formal permission of the Author

When referring to this work, full bibliographic details including the author, title, awarding institution and date of the thesis must be given

Applications for Imidazophenanthridine - based Heterocycles



University
of Glasgow

Craig J. Richmond

A thesis submitted to the University of Glasgow
for the degree of Doctor of Philosophy

Department of Chemistry

October 2009

Abstract

The physical properties and reactivity of 2,3-dihydro-1*H*-imidazo[1,2-*f*]phenanthridinium cations (DIPs) and analogous heterocycles have been investigated. The adapted syntheses developed were applied to a range of aryl amines and more elaborate substrates, such as bifunctional aminoquinolinium cations and amino functionalised polyoxometalates (POMs).

1,2,3,12*b*-tetrahydroimidazo[1,2-*f*]phenanthridines (TIPs), an intermediate in the 3-step cascade synthesis of DIPs, have also been isolated. Derivatisation of the TIP structure at the imidazo-*N* position enables control of the reactivity of the intermediate with respect to electronic potential and pK_a , allowing isolation of a selection of TIP structures. Correlations between these parameters and reaction outcome have been made and other influences such as steric and solvent effects have also been investigated.

Investigation of the structure and properties of the TIP framework led to the discovery of a pH dependent cyclisation between the ring-closed TIP form and the ring-open aminoethylphenanthridinium (AEP) form. The complementary TIP and AEP forms can be further manipulated by oxidation or reduction to convert them to their “pH-inert” forms, DIP and aminoethyldihydrophenanthridine (AEDP). These four interchangeable states formed the basis of a redox “lockable” molecular switch that could be useful for molecular level information processing and data storage.

The pH dependent cyclisation between the TIP and AEP forms was also investigated as a targeting mechanism for potential intercalating antitumour agents. The system looks to exploit the pH difference between cancerous tissues and normal tissue to combine high cytotoxicity with high selectivity, a desirable trait that is unfortunately absent in most chemotherapeutic agents. Preliminary *in vitro* assays have shown the TIP/AEP frameworks to have IC_{50} values in the μM range in human ovarian cancer cell lines, comparable to cisplatin and the closely related DIP intercalaters.

Acknowledgements

It would not have been possible to carry out the work presented forthwith without the efforts of a number of individuals; I would therefore like to thank the following people:

Firstly, **Professor Lee Cronin**, not only for giving me the opportunity and freedom to work on such interesting and enjoyable projects, but for convincing me to do a PhD in the first place (still no regrets!).

Second in command so second on the list, **Dr. De-Liang Long**. His expertise in X-Ray Diffraction and crystallography on the other hand is second to none and I appreciate all his help in obtaining the crystal structures and for his organisation of the lab as a whole.

Dr. Alexis Parenty, for taking me under his wing, for giving me ideas and encouraging me to come up with my own, then for being there when they didn't work!, for continuing to whistle the delightful melodies of radio 1 (even hours after Carsten had switched it off!), for inviting me to see "the real France", and for being a great mentor (although I don't think I picked up any tips on cleanliness and organization from him).

Dr. Graham Newton, the "fiercest of the fierce", who told me that I could do a PhD and still have time for football. **Dr. Phil Kitson**, who will remain on my "phone a friend list" indefinitely, how can one man know so much trivia?! **Scott Mitchell**, **Donnie Carmichael** and **Stuart Blain**, for sharing the whole PhD experience from start to finish. **Roslyn Eadie**, heiress to the organic kingdom.

To all the postdoc team, in particular, **Dr. Yufei Song**, **Dr. Pradeep Chullikkattil**, **Dr. Haralampos Miras**, **Dr. Ryo Tsunashima**, **Dr. Carsten Streb**, and **Dr. Geoff Cooper**, who have all contributed in one way or another to this work.

My collaborators; **Dr. Jane Plumb** of the Beatson laboratories, and **Dr. Graeme Cooke**, **Dr. Stuart Caldwell** and **Catherine MacLean**, from the Cooke group; and my students, **Amanda Spence** and **Ruksana Mohammed**.

The support staff in the Chemistry Department; **Jim McIver**, for all his technical support and help (that *@#>! hydrog!); **Dr. David Adam**, for keeping the NMR system running so smoothly; **Jim Tweedie**, for MS analysis; **Kim Wilson**, for elemental analysis; **Jim Gallagher**, for his help during my brief flirtation with the SEM; **Alex Burns** and **Tony Ritchie**, without whom the department couldn't survive; **Ted Easdon**, **Alec James** and **Shawn Maidwell**, down in stores; **Stuart Mackay** and the rest of the IT support staff; and all those in the admin and accounts offices.

All the members of the Cronin Group, past and present, especially the Aragon & Three Judges regulars (you know who you are!), and my friends and colleagues from the department.

And now at the risk of sounding like Gwyneth Paltrow, I want to thank my Mum and Dad, and the rest of the family (including Richard) because I definitely couldn't have gotten this far without them. Y finalmente mi novia, no sólo por su ayuda con esta tesis sino por todo lo demás. Gracias, tq.

Preface

This thesis presents original synthetic work carried out by Craig John Richmond at the University of Glasgow, in the Soddy Laboratory, under the supervision of Prof. Leroy Cronin, during the period of September 2006 to October 2009.

“I wish that I knew what I know now...”

Rod Stewart

Abbreviations

AEDP	Aminoethyldihydrophenanthridine
AEP	Aminoethylphenanthridinium
aq.	Aqueous
Boc	<i>tert</i> -butoxycarbonyl
BEP	5-(2-Bromoethyl)-phenanthridinium bromide
BEDP	5-(2-Bromoethyl)-5,6-dihydrophenanthridine
CI	Chemical ionisation
conc.	Concentrated
COSY	Correlation spectroscopy
CBPQT ⁴⁺	Cyclobis(paraquat- <i>p</i> -phenylene)
CTDIQ ³⁺	Cyclotris(2,3-dihydro-1 <i>H</i> -imidazo[1,2- <i>a</i>]quinoline)
CV	Cyclic voltammetry
d	Day(s)
decomp.	Decomposed
DIP	Dihydroimidazophenanthridinium
DMF	Dimethylformamide
DMSO	Dimethylsulfoxide
DNA	Deoxyribonucleic acid
DNP	1,5-dioxynaphthalene
EI	Electron impact
eq.	Equivalent
ES	Electrospray
FAB	Fast atom bombardment
g	Gram
h	Hour(s)

IC ₅₀	Concentration of drug to inhibit growth in 50% of sample tissues
IR	Infrared
L	Litre
M	Molar
MHz	Megahertz
min	Minute(s)
mp	Melting point
MS	Mass spectroscopy
MTT	3-(4,5-dimethylthiazol-2-yl)-2,5-diphenyl-2 <i>H</i> -tetrazolium bromide
NA	Not applicable
NAD ⁺ /NADH	Nicotinamide adenine dinucleotide
NBS	<i>N</i> -Bromosuccinimide
NMR	Nuclear magnetic resonance
NOE	Nuclear Overhauser Effect
ORTEP	Oak Ridge Thermal Ellipsoid Plot
rt	Room temperature
SAR	Structure Activity Relationship
TBA	Tertiary butylammonium
TEA	Triethylamine
THF	Tetrahydrofuran
TIP	Tetrahydroimidazophenanthridine
Ts	Tosyl
UV	Ultra violet

Table of Contents

ABSTRACT	I
ACKNOWLEDGEMENTS.....	II
PREFACE	IV
ABBREVIATIONS	V
TABLE OF CONTENTS	VII
INTRODUCTION	1
1 FUNCTIONAL ORGANIC MATERIALS.....	1
1.1 Intuition or Inquisition?	1
1.2 Macrocycles	3
1.2.1 Aza-Crowns and Crown Ethers.....	3
1.2.2 Rigid Macrocycles	6
1.3 Molecular Machines and Devices	10
1.3.1 Principles and Definitions	10
1.3.2 Molecular Devices	11
1.3.3 Molecular Machines.....	14
2 APPLICATIONS OF HETEROCYCLIC CHEMISTRY	17
2.1 Heterocycles in Nature	17
2.2 Heterocycles in Drug Synthesis	19
2.3 Heterocycles and Cancer.....	20
2.3.1 Cancer as a disease.....	20
2.3.2 Causes of cancer.....	20
2.3.3 Treatments for cancer.....	21
2.4 2,3-dihydro-1 <i>H</i> -imidazo[1,2- <i>f</i>]phenanthridinium (DIP) heterocycle	26
2.4.1 DIP Applications in Anti-cancer Therapies	26
2.4.2 DIP Synthesis	27
2.4.3 DIP Applications in Inorganic-Organic Hybrid Materials.....	30
AIMS.....	34
RESULTS AND DISCUSSION	35
3 MACROCYCLIC POLYCATIONS	35
3.1 4-Aminoquinoline Macrocycles.....	35
3.2 3-Aminoquinoline Macrocycles.....	40
4 TIP SYNTHESIS – UNDERSTANDING THE REACTION	45

4.1	Prevention of oxidation by BEP.....	45
4.2	Method development.....	47
4.3	Electronic effects of amine substituents.....	51
4.4	Steric effects of amine substituents.....	58
4.5	TIP structure analysis.....	62
5	LOCKABLE MOLECULAR SWITCH	70
5.1	pH Controlled Reversible Cyclisation	70
5.2	Redox Susceptibilities.....	73
5.3	Realization of Dual-mode Switching.....	75
5.4	Operation of the Molecular Switch.....	76
5.5	Amine Derivatisation for Surface Tethered Devices	85
6	TIP/AEP/DIP BIOACTIVITY COMPARISON	89
6.1	pH Controlled Selectivity of AEP/TIPs	89
6.2	AEP/TIP/DIP Comparison Library.....	91
6.3	MTT Dye-based Microtitration Assay Results	99
7	POLYOXOMETALATE ORGANIC HYBRIDS	110
7.1	TRIS-base Phenanthridine Ligands	110
7.2	Phenanthridine Aldehyde Ligands	116
7.3	Neutral Phenanthridine Ligands.....	119
8	CONCLUSIONS AND FUTURE WORK	123
8.1	Macrocyclic Polycations	123
8.2	TIP Synthesis and Applications	125
8.3	Lockable Molecular Switch	126
8.4	Bioassay Results	129
8.5	IP-POM Hybrids	129
	EXPERIMENTAL.....	132
9	EXPERIMENTAL	132
9.1	Materials.....	132
9.2	Instrumentation	133
9.3	Methods.....	134
9.4	Electrochemical Data	135
9.4.1	Cyclic voltammetry studies of DIPs (12a, b, i, j, t).....	135
9.4.2	Cyclic voltammetry studies of DIP 12b and AEP 13b.....	137

9.4.3	Square wave voltammetry studies of DIP 12b and AEP 13b	138
9.5	UV Spectra Conditions (Ref. Figure 33)	139
9.6	Fluorescence Spectra Conditions (Ref. Figure 33)	139
9.7	In Situ Monitored ¹ H NMR Experiments.....	140
9.7.1	TIP-AEP hydride transfer initiation via acidification (Ref. Figure 19)	140
9.7.2	Bromoaniline isomer comparison (Ref. Figure 20)	140
9.7.3	Adamantyl and isobutyl comparison (Ref. Figure 21 & Figure 22)	141
9.7.4	4-fluorophenyl-TIP/AEP cyclisation reversibility (Ref. Figure 30)	141
9.7.5	Monophasic isobutyl-AEP/TIP conversion via pH jump (Ref. Figure 34).....	141
9.7.6	Incremental isobutyl-AEP/TIP conversion in biphasic system (Ref. Figure 35) 141	
9.7.7	Br ₂ oxidation of isobutyl-TIP (Ref. Figure 40).....	142
9.7.8	BEP methoxy adduct formation (Ref. Figure 50)	142
9.7.9	TRIS-cage-TIP (Ref. Figure 52)	142
9.8	In Situ Monitored UV Switching Experiments.....	142
9.8.1	pH switching of isobutyl-AEP/TIP (Ref. Figure 36)	142
9.8.2	NaBH ₄ reduction of isobutyl-AEP (Ref. Figure 37).....	143
9.8.3	Br ₂ oxidation of isobutyl-TIP (Ref. Figure 39).....	143
9.9	MTT Assays	143
9.10	Crystallography	144
9.10.1	1-(4-Fluorophenyl)-1,2,3,12b-tetrahydroimidazo[1,2- <i>f</i>]phenanthridine (11n)..	145
9.10.2	2-(1-Methyl-2,6,7-trioxa-bicyclo[2.2.2]oct-4-yl)-3,4-dihydro-2 <i>H</i> ,12 <i>bH</i> -1-oxa- 2,4 <i>a</i> -diazatriphenylene (28).....	146
9.11	Syntheses and Analytical Data.....	148
9.11.1	4-Amino-1-methylquinolinium toluene-4-sulfonate (3).	148
9.11.2	1-Methyl-1 <i>H</i> -quinolin-4-ylideneamine (4).	148
9.11.3	3-Amino-1-methylquinolinium- <i>p</i> -toluenesulfonate (7).	149
9.11.4	3-Acetylaminoquinoline (8).	150
9.11.5	3-Acetylamino-1-methylquinolinium <i>p</i> -toluenesulfonate (9).	151
9.11.6	5-(2-Bromoethyl)-phenanthridinium bromide (10).....	152
9.11.7	1-Cyclohexyl-1,2,3,12b-tetrahydroimidazo[1,2- <i>f</i>]phenanthridine (11a).	153
9.11.8	1-Isobutyl-1,2,3,12b-tetrahydroimidazo[1,2- <i>f</i>]phenanthridine (11b).....	153
9.11.9	1-Cyclopentyl-1,2,3,12b-tetrahydroimidazo[1,2- <i>f</i>]phenanthridine (11c).	154

9.11.10	1-Dodecyl-1,2,3,12b-tetrahydroimidazo[1,2-f]phenanthridine (11d).	155
9.11.11	1-Tert-butyl-1,2,3,12b-tetrahydroimidazo[1,2-f]phenanthridine (11e).	155
9.11.12	1-Adamantyl-1,2,3,12b-tetrahydroimidazo[1,2-f]phenanthridine (11f).....	156
9.11.13	1-(4-Dimethylaminophenyl)-1,2,3,12b-tetrahydroimidazo[1,2-f]phenanthridine (11g).	157
9.11.14	1-(4-Methoxyphenyl)-1,2,3,12b-tetrahydroimidazo[1,2-f]phenanthridine (11h).	157
9.11.15	1-(3,4-imethoxyphenyl)-1,2,3,12b-tetrahydroimidazo[1,2-f]phenanthridine (11i).	158
9.11.16	1-(Phenyl)-1,2,3,12b-tetrahydroimidazo[1,2-f]phenanthridine (11j).	159
9.11.17	1-(3,5-Dimethylphenyl)-1,2,3,12b-tetrahydroimidazo[1,2-f]phenanthridine (11k)...	160
9.11.18	1-(2-Fluorophenyl)-1,2,3,12b-tetrahydroimidazo[1,2-f]phenanthridine (11m).	160
9.11.19	1-(4-Fluorophenyl)-1,2,3,12b-tetrahydroimidazo[1,2-f]phenanthridine(11n).	161
9.11.20	1-(3-Trifluoromethylphenyl)-1,2,3,12b-tetrahydroimidazo[1,2-f]phenanthridine (11p).	162
9.11.21	1-(4-Bromophenyl)-1,2,3,12b-tetrahydroimidazo[1,2-f]phenanthridine (11r).	163
9.11.22	1-(4-Methylacetatephenyl)-1,2,3,12b-tetrahydroimidazo[1,2-f]phenanthridine (11s).	163
9.11.23	1-(3,4-Difluorophenyl)-1,2,3,12b-tetrahydroimidazo[1,2-f]phenanthridine (11t).	164
9.11.24	1-(3,4,5-Trifluorophenyl)-1,2,3,12b-tetrahydroimidazo[1,2-f]phenanthridine (11u).	165
9.11.25	1-(3-Methoxyphenyl)-1,2,3,12b-tetrahydroimidazo[1,2-f]phenanthridine (11y).	166
9.11.26	1-(3-Chloro-4-fluorophenyl)-1,2,3,12b-tetrahydroimidazo[1,2-f]phenanthridine (11z).	166
9.11.27	1-(3-Cyano-phenyl)-1,2,3,12b-tetrahydro-imidazo[1,2-f]phenanthridine (11a')	167
9.11.28	1-Cyclohexyl-2,3-dihydro-1H-imidazo[1,2-f]phenanthridinium bromide (12a).	168

9.11.29	1-(3,4-Dimethoxyphenyl)-2,3-dihydro-1 <i>H</i> -imidazo[1,2- <i>f</i>]phenanthridinium bromide (12i).	169
9.11.30	1-Phenyl-2,3-dihydro-1 <i>H</i> -imidazo[1,2- <i>f</i>]phenanthridinium bromide (12j).	170
9.11.31	1-(4-Fluorophenyl)-2,3-dihydro-1 <i>H</i> -imidazo[1,2- <i>f</i>]phenanthridinium bromide (12n).	171
9.11.32	1-(3-Trifluoromethylphenyl)-2,3-dihydro-1 <i>H</i> -imidazo[1,2- <i>f</i>]phenanthridinium bromide (12p).	172
9.11.33	1-(3,4-Difluorophenyl)-2,3-dihydro-1 <i>H</i> -imidazo[1,2- <i>f</i>]phenanthridinium bromide (12t).	173
9.11.34	1-Methyl-2,3-dihydro-1 <i>H</i> -imidazo[1,2- <i>f</i>]phenanthridinium bromide (12b').	174
9.11.35	1-(2-Hydroxyethyl)-2,3-dihydro-1 <i>H</i> -imidazo[1,2- <i>f</i>]phenanthridinium bromide (12f').	175
9.11.36	1-Methoxycarbonylmethyl-2,3-dihydro-1 <i>H</i> -imidazo[1,2- <i>f</i>]phenanthridinium bromide (12g').	176
9.11.37	1-Carboxymethyl-2,3-dihydro-1 <i>H</i> -imidazo[1,2- <i>f</i>]phenanthridinium bromide (12h').	177
9.11.38	1-(4-Hydroxy-phenyl)-2,3-dihydro-1 <i>H</i> -imidazo[1,2- <i>f</i>]phenanthridin-4ium bromide (12i').	177
9.11.39	5-(2-Cyclohexylaminoethyl)-phenanthridinium chloride; hydrochloride (13a).	178
9.11.40	5-(2-Isobutylaminoethyl)-phenanthridinium chloride; hydrochloride (13b).	179
9.11.41	5-(2-Cyclopentylaminoethyl)-phenanthridinium chloride; hydrochloride (13c).	180
9.11.42	5-(2-(4-Methoxyphenyl)-aminoethyl)-phenanthridinium chloride; hydrochloride (13h).	181
9.11.43	5-(2-(3,4-Dimethoxyphenyl)-aminoethyl)-phenanthridinium chloride; hydrochloride (13i).	182
9.11.44	5-(2-Phenylaminoethyl)-phenanthridinium chloride; hydrochloride (13j).	183
9.11.45	5-(2-(3,5-Dimethylphenyl)-aminoethyl)-phenanthridinium chloride; hydrochloride (13k).	184

9.11.46	5-(2-(4-Fluorophenyl)-aminoethyl)-phenanthridinium chloride; hydrochloride (13n).	185
9.11.47	5-(2-(3-Trifluoromethylphenyl)-aminoethyl)-phenanthridinium chloride; hydrochloride (13p).....	186
9.11.48	5-(2-(3,4-Difluorophenyl)-aminoethyl)-phenanthridinium chloride; hydrochloride (13t).....	187
9.11.49	5-(2-Methylaminoethyl)-phenanthridinium chloride; hydrochloride (13b')..	188
9.11.50	5-(2-Cycloheptylaminoethyl)-phenanthridinium chloride; hydrochloride (13c')..	189
9.11.51	5-(2-Butylaminoethyl)-phenanthridinium chloride; hydrochloride (13d')	190
9.11.52	5-(2-Nonylaminoethyl)-phenanthridinium chloride; hydrochloride (13e')	191
9.11.53	5-(2-Dodecylaminoethyl)-phenanthridinium chloride; hydrochloride (13j') ..	192
9.11.54	5-(2-Isobutylaminoethyl)-6 <i>H</i> -phenanthridine(14b)	193
9.11.55	AEDP disulfide (15).....	194
9.11.56	AEP disulfide (16).....	195
9.11.57	TIP disulfide (17)	196
9.11.58	DIP disulfide (18).....	197
9.11.59	[4-(5-[1,2]Dithiolan-3-yl-pentanoylamino)-phenyl]-carbamic acid tert-butyl ester (19).....	197
9.11.60	5-[1,2]Dithiolan-3-yl-pentanoic acid (4-amino-phenyl)-amide (20)	198
9.11.61	5-[1,2]Dithiolan-3-yl-pentanoic acid [4-(2,3-dihydro-12 <i>bH</i> -imidazo[1,2- <i>f</i>]phenanthridin-1-yl)-phenyl]-amide (21).....	199
9.11.62	1-[4-(5-[1,2]Dithiolan-3-yl-pentanoylamino)-phenyl]-2,3-dihydro-1 <i>H</i> -imidazo [1,2- <i>f</i>]phenanthridin-4-ylum bromide (22)	200
9.11.63	1-Methyl-4-nitro-2,6,7-trioxabicyclo[2.2.2]octane (23)	201
9.11.64	1-Methyl-2,6,7-trioxabicyclo[2.2.2]oct-4-ylamine (24)	201
9.11.65	<i>N</i> -(1-methyl-2,6,7-trioxa-bicyclo[2.2.2]oct-4-yl)-hydroxylamine (27).....	202
9.11.66	2-(1-Methyl-2,6,7-trioxa-bicyclo[2.2.2]oct-4-yl)-3,4-dihydro-2 <i>H</i> ,12 <i>bH</i> -1-oxa-2,4a-diaza-triphenylene (28)	203
9.11.67	5-(2-(1-methyl-2,6,7-trioxa-bicyclo[2.2.2]oct-4-yl)-hydroxylaminoethyl)-phenanthridinium chloride; hydrochloride (29).....	204
9.11.68	1-[4-(5,5-Dimethyl-[1,3]dioxan-2-yl)-phenyl]-2,3-dihydro-1 <i>H</i> -imidazo[1,2- <i>f</i>]phenanthridin-4-ylum bromide (31)	205

9.11.69	1-(4-Formylphenyl)-2,3-dihydro-1 <i>H</i> -imidazo[1,2- <i>f</i>]phenanthridin-4-ylum bromide (32).....	206
9.11.70	TRIS-Dawson 1-(4-formylphenyl)-2,3-dihydro-1 <i>H</i> -imidazo[1,2- <i>f</i>]phenanthridin -4-ylum salt (33).....	207
9.11.71	4-[2-(6-Oxo-6 <i>H</i> -phenanthridin-5-yl)-ethylamino]-benzaldehyde (34).....	208
9.11.72	LiAlH ₄ DIP reduction.	209
9.11.73	AEDP acidic oxidation.....	210
PUBLICATIONS.....		211
REFERENCES		212

Introduction

1 FUNCTIONAL ORGANIC MATERIALS

1.1 Intuition or Inquisition?

Research in all areas of science can be viewed as a blend of great human minds mixed with varying degrees of good fortune. It would be wonderful to think that the huge leaps forward scientific research has given us, particularly in the 20th century, have been the product of design and forethought however this would be slightly naive and in most cases wrong. The truth is that many of the greatest discoveries have been largely serendipitous in nature and the final applications were rarely considered from the outset. It is not my aim to detract from the successes attributed to the people involved in these discoveries, since it was their knowledge and creative thinking that highlighted the gravity of their discoveries in the context of the “real world”; it is merely to point out the inherent uncertainty of research. This marriage of labour and luck has proved to be a fitting partnership and has led to some truly incredible discoveries; namely Penicillin and Cisplatin being amongst some of the most famous examples.¹

As time has passed, the observations and subsequent knowledge gained from research has always allowed others to build upon it, and so the rate of development in all scientific areas has steadily increased with time. This was famously noted in a correspondence between Isaac Newton and Robert Hooke in reference to the works of René Descartes;

“What Descartes did was a good step. You have added much several ways, and especially in taking the colours of thin plates into philosophical consideration. If I have seen a little further it is by standing on the shoulders of Giants”

The contributions of such eminent scientists has led us to the fortunate position we are in today, where so much has been learned that it is now possible to use this knowledge and apply it to the physical, sociological and ecological problems of today’s world. As a result the research community are now able to approach research with a greater focus on application rather than speculation. Where speculative research creates new techniques

and materials without fully knowing what the final applications may be, whilst application driven research has a defined problem that researchers aim to solve using the knowledge and techniques available. Neither approach, however, can work on its own, and in reality any successful research project will always involve aspects of both.

The successful growth and development of the global pharmaceutical industry is a testament to the benefits of this combined approach. The use of plant and herbal extracts to treat illness has been known and practiced around the globe for centuries however it was only realized that the activities of such extracts could be attributed to a single organic molecule after isolation and characterisation of the active components. The early 19th century saw the isolation of morphine and quinine and demonstrated their activity as analgesics and antipyretics, concurrent with the effects observed from the extracts of poppy plants and cinchona bark.¹ Many other active compounds were discovered and used for clinical application over the years but many diseases and illnesses were still prevalent at the start of the 20th century. With the high demand for new treatments coupled with the prospect of high financial rewards and social distinction there was great opportunity and incentive for chemists and biologists to apply this newfound knowledge in the search for drugs. As fractional distillation and synthetic techniques improved it became more and more viable for total synthesis to replace the previous methods of natural product isolation, fermentation, and semi-synthesis; leading to the birth of the pharmaceutical industry as we know it.¹ Synthetic and analytical techniques have since developed in a somewhat symbiotic fashion with the growth of this economical giant, as the industry exploit the discoveries of the researchers who are in turn rewarded by the financial success the commercial products bring to the industry. Many of the pharmaceutical products on today's market are therefore a result of the greater understanding of fundamental chemical and biological processes, and the application of this knowledge to the synthetic strategies of 'drug design'.² The true significance of a single discovery therefore may not be realised until it is placed in the context of others, from the past, present, or even the future.

So although the pharmaceutical industry may have provided an initial incentive for the expansion of research in organic chemistry, many new organic compounds have fulfilled their potential by finding applications elsewhere. Examples of such discoveries include

polymers, dyes and macrocycles. From these discoveries, entire new areas of organic chemistry have emerged and they are considered to be distinct areas of research in their own right, the products from which have found applications in materials design, catalysis and many other areas in addition to medicine.³⁻⁵

1.2 Macrocycles

1.2.1 Aza-Crowns and Crown Ethers

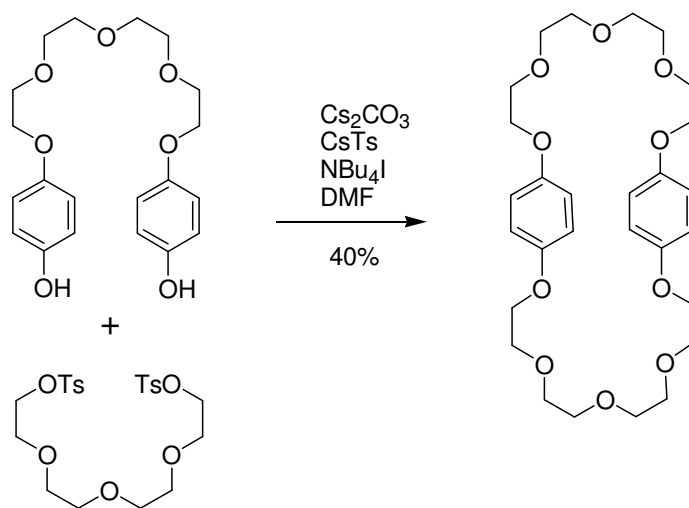
Macrocycles are defined as “*cyclic systems with rings greater than nine members*”,⁶ and is an umbrella term that covers a vast number of cyclic architectures. These include; cyclophanes, calixarenes, cyclodextrins, aza-crowns, thia-crowns, crown ethers, cucurbiturils, cryptands, torands, and spherands as some of the most prevalent in the literature.⁵⁻¹¹ The structures range in composition and complexity but one thing that remains common to all is their application in host-guest molecular recognition systems.¹²⁻¹⁷

Crown ethers are probably the simplest of the examples given above in terms of structure however this does not necessarily make their syntheses trivial. Their synthesis relies on the Williamson ether method either in linear or convergent syntheses to produce medium to large ring crown ethers with a diversity of functionalities.^{10,18} Scheme 1 shows the synthesis of a chiral 18-crown-6 macrocycle from diethyl tartrate and diethylene glycol.¹⁹ Although the individual reaction steps are fairly straight forward; acetal protection/deprotection, transesterification, tosylation and ether formation; the overall yields are rarely very high as the final cyclisation step is subject to competitive formation of linear and cyclic oligomers of different sizes. For example in the synthesis shown in Scheme 1, combination of the individual reactants in a 1:1 ratio rather than 2:2 forms the 9-crown-3 derivative in addition to the desired 18-crown-6 product.



Scheme 1. Synthesis of 1,1',4,4'-tetra-*O*-benzyl-2,2':3,3'-bis-*O*-oxydiethylene-di-*L*-threitol.

One method of improving the selectivity of the ring forming reaction for particular sizes is to use a template. An example that utilizes this method of template directed macrocycle formation is the synthesis of bis-*p*-phenylene-34-crown-10 described by Ouchi *et al.*²⁰ The final ring closing step in this synthesis employs caesium toluenesulfonate as a template which gives yields as high as 40% for the desired product (Scheme 2).



Scheme 2. Conditions for the ring closing step in the synthesis of bis-*p*-phenylene-34-crown-10.

Chiral crown ethers have found applications as chiral resolving agents and chiral reagents for enantioselective reactions,^{21,22} while the benzo crown ethers have been used to form rotaxanes and catenanes through complexations with guests containing π -electron deficient recognition sites such as viologens.^{23,24} More traditional uses of crown ethers exploit their ability to solubilize metal cations in organic solvents for use as phase transfer catalysts.²⁵

The properties exhibited by the crown ether hosts is largely determined by the ring size and composition and the additional functionalities incorporated in their design; the simplest example that demonstrates this tunable behaviour is the preferential binding affinities of K^+ and Na^+ cations by 18-crown-6 and 15-crown-5 respectively, where a slight change in ring size results in a reversal in selectivity.^{18,26} The effects of ring composition are highlighted by the increasing affinity of aza-oxa crowns for heavy metals with increasing nitrogen content: $\text{Log } K$ values for 18 membered macrocycles and Pb^{2+} follow the series $[18]O_6 < [18]N_2O_4 < [18]N_4O_2 < [18]N_6$.^{6,27} Aza-oxa crowns are particularly valuable as the introduction of the nitrogen donor atoms not only alters the binding selectivity but also allows for further binding functionality to be introduced to create lariat crowns and cryptands.^{28,29}

The importance of nitrogen donors in macrocycle chemistry is highlighted by the fact that over half of all synthetic macrocycles contain nitrogen donors.⁶ Macrocyclic polyamines (aza-crowns) are highly versatile ligands as they can be functionalised to a greater extent than crown ethers allowing greater control over binding selectivity. The aza-crowns also follow a similar but more specific binding trend to crown ethers with respect to ring size vs guest size. The reason for the increase in binding specificity is due to the differences in the ligand-guest orbital interactions. Oxygen donor atoms are harder electron donors and therefore interact better with the hard cations of the alkali metal series whereas the softer nitrogen centres have a higher affinity for the softer transition metals. The valence orbitals of the S-block metals are spherical and therefore offer no directional influence on the interactions with the electron-donating p-orbitals of the oxygens. The valence orbitals of d-block transition metals however have very defined geometries and so interactions with the nitrogen donor atoms are much more specific. The series of binding constants for mononuclear complexes of Ni^{2+} cations and aza-crowns, $[9]N_3 < [12]N_6 > [21]N_7 > [24]N_8$, can be explained by the favourable binding contributions from 6 nitrogen centers over 3 to form stable hexacoordinate complexes but when 7 and 8 nitrogens are introduced no additional binding effects are seen as the metal center is coordinatively saturated.⁶ Aza-crowns form stable dinuclear transition metal complexes when the ring contains >6 nitrogen donors. The high binding affinities of aza-crowns to heavy metals like Pb, Hg and Ni prompted investigations into their use as biological immobilizing agents for these toxic metals.³⁰ Other potential biological applications that have been investigated include;

ligands for MRI contrast agents, antimicrobial, psychotropic, antiarrhythmic, vasodilating and antihypertensive agents^{6,31}. The basicity of the nitrogen centers in aza-crowns also means that they are almost fully protonated at physiological pH, they have shown high affinity for biologically relevant anions such as AMP, ADP and ATP and therefore have applications as receptors for these substrates as well.^{32,33}

1.2.2 Rigid Macrocycles

In any host-guest relationship the selectivity and strength of binding is governed by the nature of both components. The crown macrocycles discussed previously have demonstrated how variations in charge, donor atom type, number of donor atoms, overall ring size, and additional ring functionality, can be manipulated to alter the selectivity towards different guest molecules. One point that was not discussed was the effect of rigidity on such binding events. Torands are fused-ring analogues of sexipyridine that were synthesised in the early 1990s.^{34,35} These macrocyclic frameworks are very rigid, which has a dramatic effect on cation binding. The calculated stability constants for the Na⁺ and the K⁺ complexes with the torand shown in Figure 1 are 14.7 and 14.3 respectively, which are remarkably even stronger than complexes with cryptands and cryptaspherands of similar size.³⁶⁻³⁹

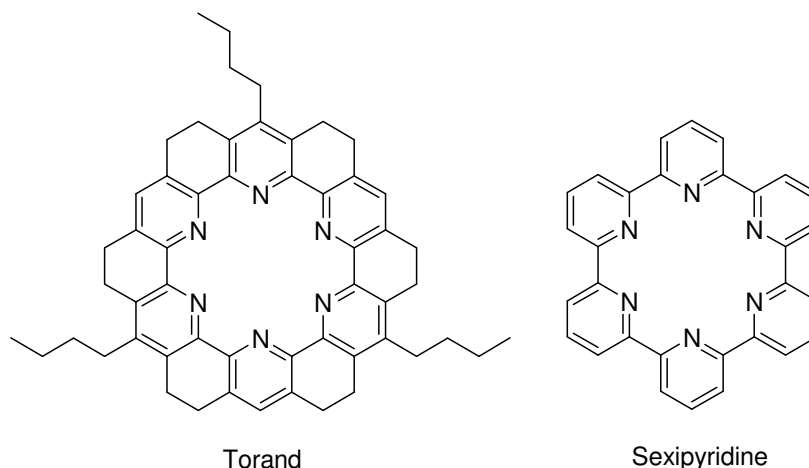
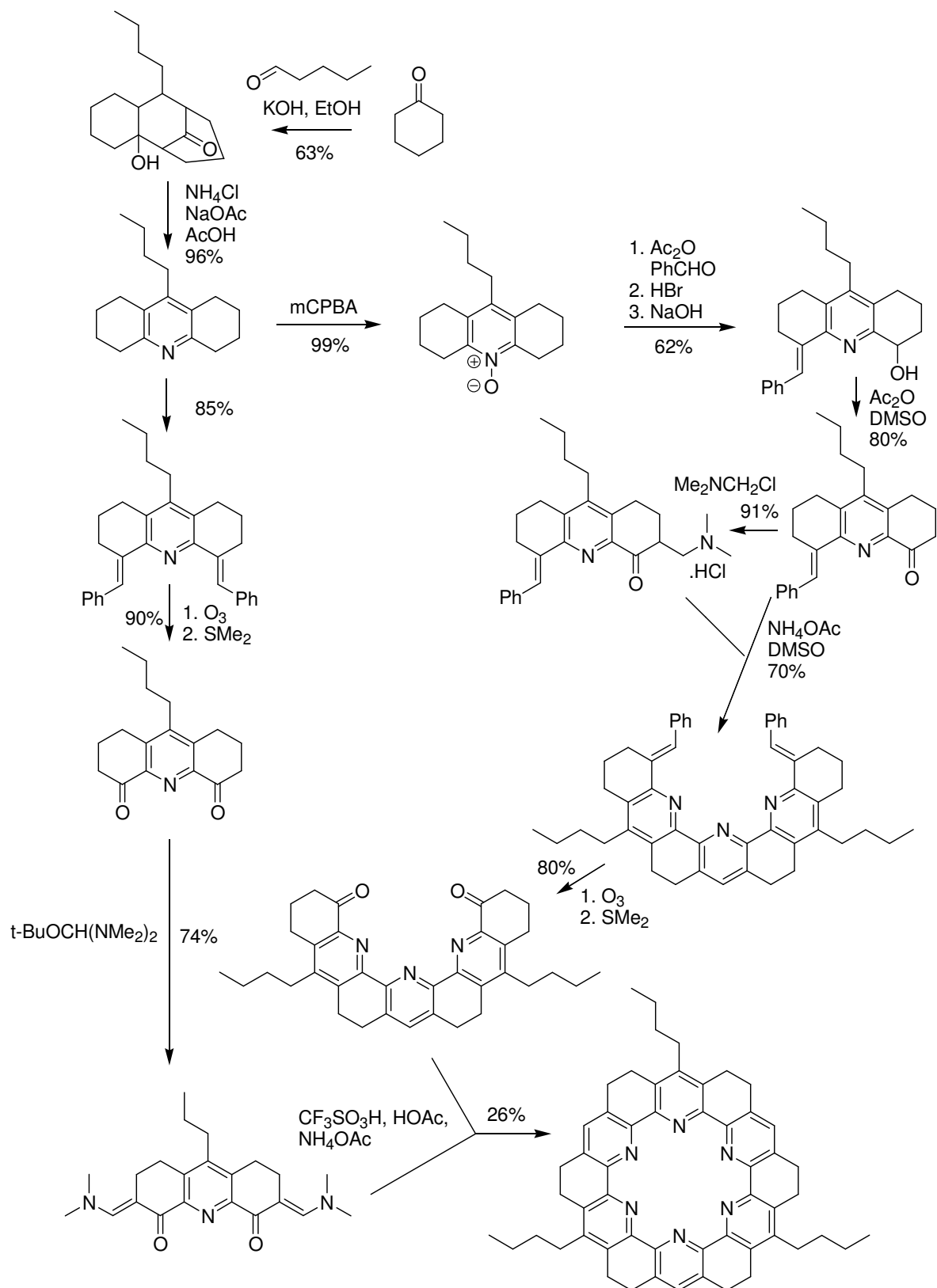


Figure 1. Structures of sexipyridine and the fused-ring torand analogue

Synthesis of the torand framework is fairly long but straightforward, with all steps except the final step proceeding with moderate to high yields (Scheme 3).



Scheme 3. Synthetic route to tributyldecacyclohexaazakekulene

In fact the group of T.W Bell who first synthesised the compound claim that the individual steps are sufficiently simple that a single person could prepare over 1g in less than 1 month.³⁸ The synthetic methodologies developed also offer access to larger torand rings and rings functionalised with other substituents. The reason these reactions proceed without any template is that the rigid non-cyclic precursors are pre-organised with geometries that favour cyclisation over linear oligomerisation. The cucurbiturils are another class of macrocycles that have very rigid frameworks and are able to be synthesized without a template.^{40,41} These “pumpkin shaped” guest systems have shown high affinity for organic dye molecules making them of great interest for applications in waste treatments.^{42,43}

The synthetic macrocycle frameworks available offer access to almost every type of intermolecular interaction, electrostatic, hydrogen bonding, hydrophobic etc. It is even now possible to combine different types of macrocyclic motifs to form hybrid ring systems such as calixarene azacrowns and calixarene crowns.^{44,45} This ability to combine these systems enables host systems to be tailored to optimally interact with a specific guest of interest. The work carried out by the groups of Sauvage, Lehn, and Stoddart has used this strategy to full effect, which has resulted in some remarkably complex and beautifully interconnected architectures.⁴⁶⁻⁵⁴ Figure 2 shows Sauvage’s Cu(I) templated assembly of interlocked phenanthroline crown macrocycles⁵⁵ and Stoddart’s CBPQT⁴⁺/DNP polyrotaxane.⁵⁶

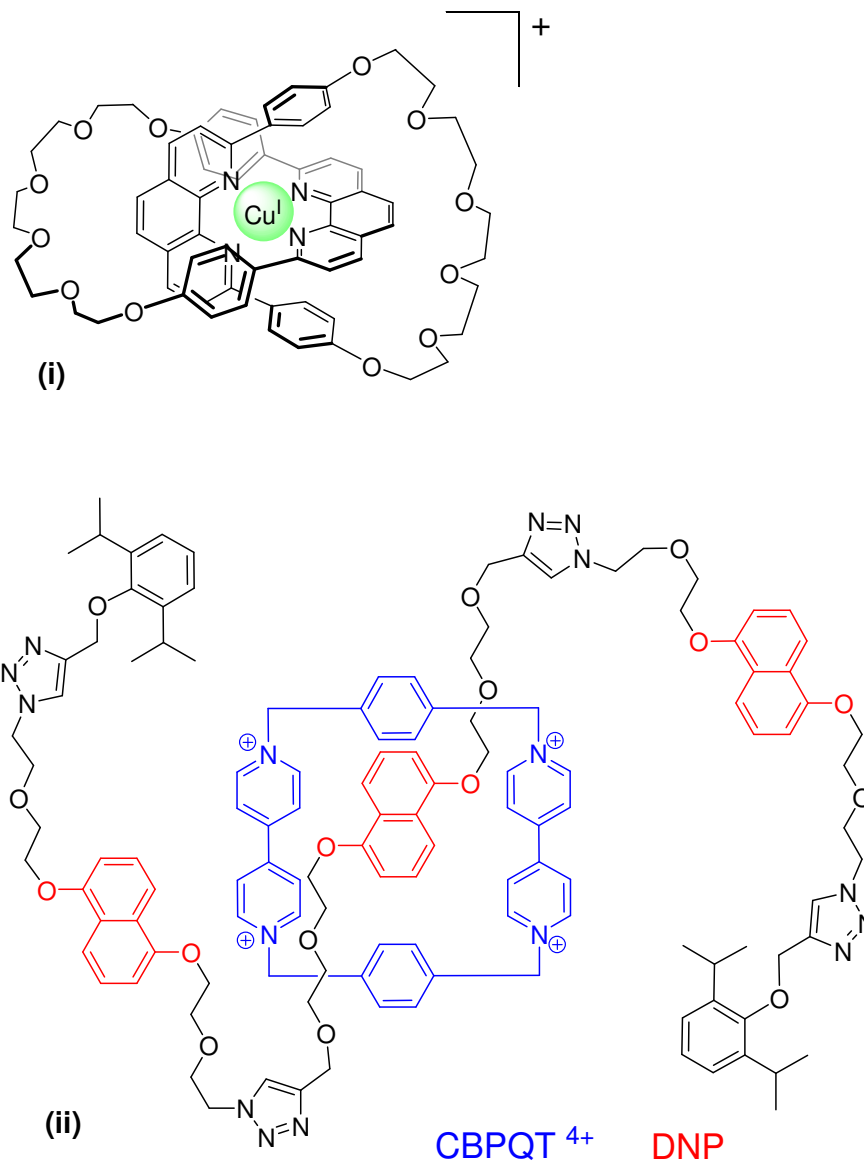


Figure 2. (i) Sauvage's [2]catenate complex; (ii) Stoddart's CBPQT⁴⁺/DNP polyrotaxane.

1.3 Molecular Machines and Devices

1.3.1 Principles and Definitions

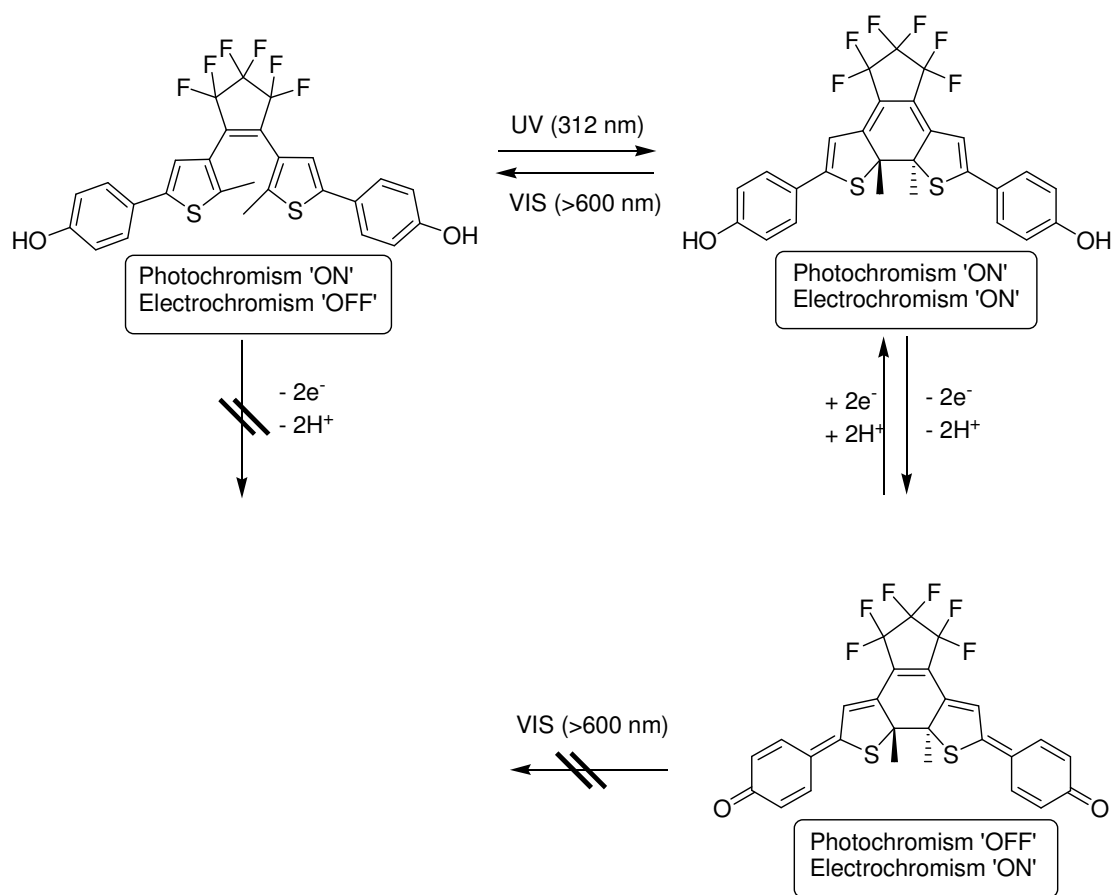
The Oxford dictionary definition for a device is: *A thing made or adapted for a particular purpose, especially a piece of mechanical or electronic equipment.* And a machine is: *An apparatus using mechanical power and having several parts, each with a definite function and together performing a particular task.*⁵⁷ It can therefore be taken from this that a machine is simply a combination of mechanical devices with moving parts. In the macroscopic world it is easy to find examples for both, for example; light bulbs, lenses, electrical heaters, even explosives, are all examples of devices; cars, planes, blenders, drills, are all examples of machines. In the molecular world the boundaries between these two functioning entities becomes less clear though since the definition of motion is not as straightforward. Brownian motion for example exists in all materials and results in the random movement of particles with respect to each other even if the object itself remains stationary. The *cis-trans* isomerisation of azo-dyes involves movement of the two nitrogen substituents relative to one another from a point of reference within the molecule whilst the molecule itself may remain in the same position in space. Rotaxanes are interlocked ring and axle supramolecular assemblies that can exhibit translational movement of the ring along the length of the axle, the ring can therefore move with respect to the axle position, again whilst the complete assembly remains in the same place. The term “motion” or “movement” can therefore be seen to rely heavily on the point of reference you choose to take, this can be more easily explained when considering similar examples in the “real world”. If you consider two passengers on a train at a station there are numerous cases that can arise by moving the objects in relation to one another, for example; if the train moves then the train and the passengers move in relation to the station but not each other; or if the passengers swap seats then they have moved in relation to each other but not in relation to the train or the station. The two molecular scale examples given previously can therefore be considered as similar processes i.e. conformational changes in the azo molecule or rotaxane assembly, or different processes i.e. isomerization of the aza molecule or ring shuttling of the macrocyclic ring along the axle, depending what point of reference you choose. In the world of supramolecular chemistry the point of reference is generally considered to be taken from any molecular framework that is connected through strong

covalent bonds. Interconnected frameworks that move with respect to each other through the manipulation of weaker intermolecular interactions can be classed as “machines”, isolated molecular arrangements that alter their configuration or conformation are not considered as moving and are therefore classed as “devices”.⁵⁸ Molecular shuttles,⁵⁹ valves⁶⁰ and motors⁶¹ perform a function via movement of their components and are examples of “molecular machines”; molecular switches,^{62,63} sensors,⁶⁴ and wires⁶⁵ perform a function without movement and are examples of “molecular devices”.

1.3.2 Molecular Devices

The types of molecular devices that have been synthesised to date include wires, sensors, and switches. The function of these molecular devices perform the same basic functions as their macroscopic equivalents: a wire allows the transport of electrons along its length and is usually part of a more complex device that involves other input and an output devices; a sensor generates a recordable or quantifiable signal in the presence of a particular physical stimulus; a switch is very similar to a sensor except the external input signal is deliberately applied to control the output. With the high levels of interest and subsequent growth of the field there are now many examples of nano scale devices⁵⁸ but it is inappropriate to discuss more than one or two in detail here. The examples chosen demonstrate the versatility of the molecular frameworks and stimuli that can be used to create such devices.

The first example was created in 1994 by Jean-Marie Lehn’s group where they used photochromic and electrochemical properties to control the switching states of a bisphenol perfluorocyclopentene (Scheme 4).^{66,67}



Scheme 4. Operation of the dual-mode optical-electrical molecular switching device. (redrawn without permission)⁶⁶

The system utilises the photoconversion of the dithienylethene moiety to switch between the “open”, non-conjugated and the “closed”, conjugated states via irradiation with UV and visible light.⁶⁸ The additional hydroquinone functionality also allows the system to be electrochemically manipulated to switch to the “locked” quinoid state. The three states are all distinguishable by their absorbance spectra and the subsequent colour changes observed; open (colourless), closed (blue), locked (violet). This type of switch can therefore operate in a write-lock-read-unlock-erase manner and could ultimately be used as an optical switching device capable of high density information storage.

The second example also exhibits an optical output but uses three inputs in a cooperative fashion to create a sensor with AND Boolean logic (Figure 3).⁶⁹

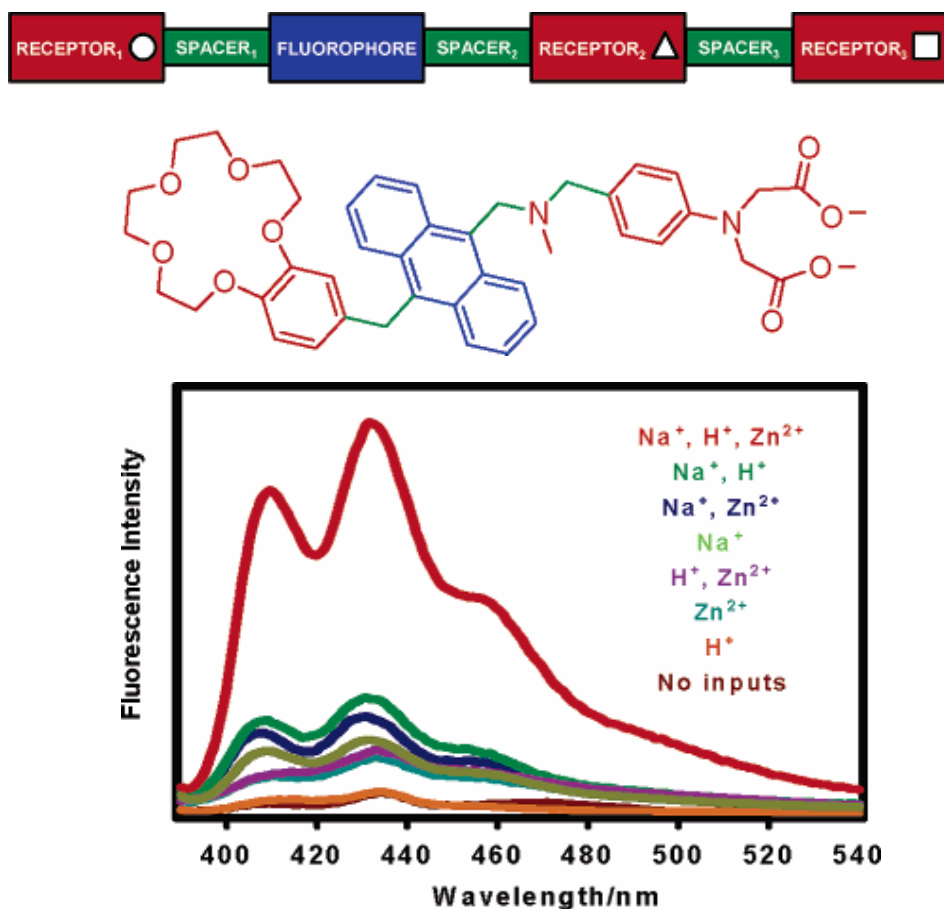


Figure 3. Structure and fluorescence intensity for the triple input sensor. (images adapted and reproduced without permission)⁶⁹

The structure of the sensor molecule has three recognition sites; (i) a crown ether receptor for Na^+ cations; (ii) a tertiary amine moiety for H^+ ions; and (iii) a phenyliminodiacetate receptor for Zn^{2+} cations. From the emission spectra it can be seen that the fluorescence output for the system is only high when all three inputs, Na^+ , H^+ and Zn^{2+} , are all high, any other combination of inputs results in a low output, thus exhibiting AND logic. The system exploits the photoinduced electron transfer (PET) quenching of the fluorescent anthracene unit by the electrons from the crown ether oxygens, tertiary amine nitrogen and carboxylate anions when in the unbound state, only when all three receptors are bound are the PET processes inhibited and fluorescence observed. This type of system could find use in the fast screening of specific medical conditions, for instance, renal failure is indicated

by elevated levels of creatinine, urea, and potassium.⁷⁰ An appropriately designed sensor could therefore be used in the preliminary diagnosis of this condition.

1.3.3 Molecular Machines

Molecular machines use mechanical motion to do work in order to perform their function; the motion can be harmonic,⁷¹ rotational⁶¹ or linear⁵⁹ and the function will be dependent upon the inherent properties of the translational states. One of the most impressive examples demonstrated to date for the application of molecular machines was the work of David Leigh *et al*, who created a photoisomerizable bistable [2]rotaxane capable of reversibly altering the polarity of a gold surface when they were physisorbed as monolayers (Figure 4).⁷²

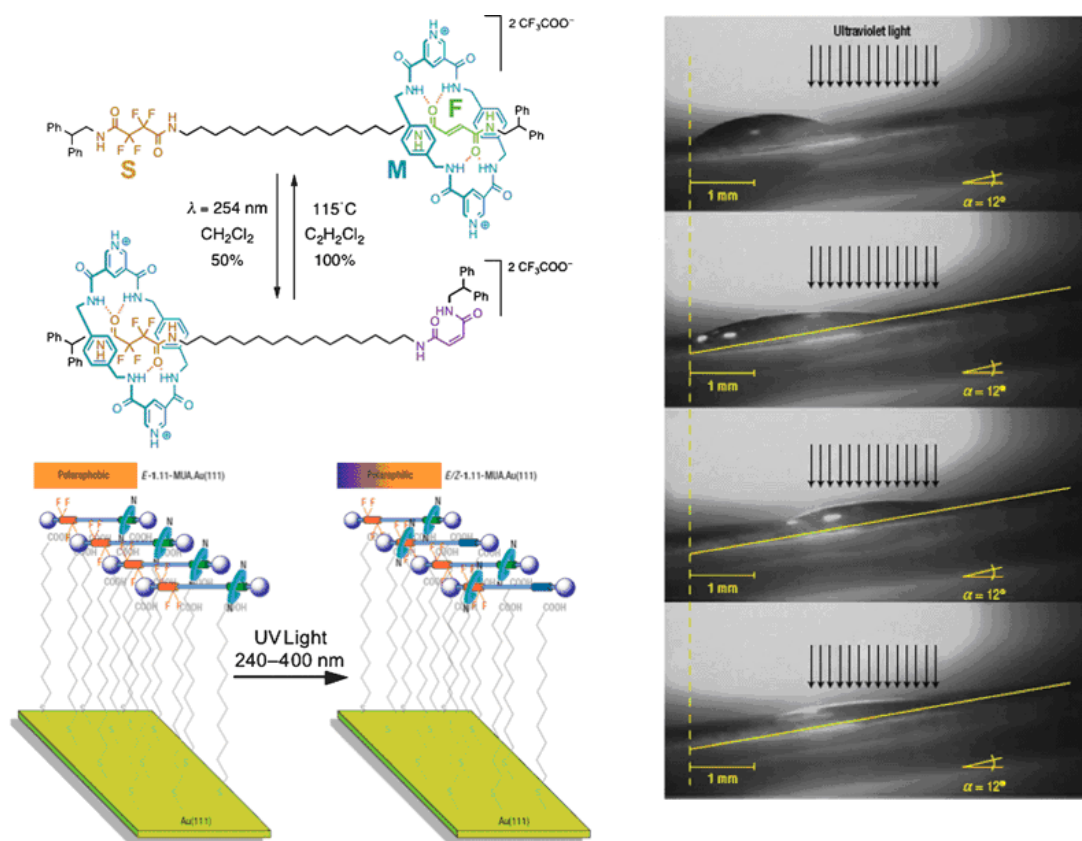


Figure 4. Structure of the photoisomerizable bistable [2]rotaxane and images of the irradiation experiment used to transport a droplet of diiodomethane. (image adapted and reproduced without permission)⁷³

The [2]rotaxane consists of a hydrophilic fumaramide unit and a hydrophobic tetrafluorosuccinamide unit on its dumbbell component, and a dipyridinium tetramide-based macrocycle ring component. The macrocycle binds preferentially to the hydrophilic fumaride station in the “zero” or “ground” state, leaving the hydrophobic tetrafluorosuccinamide unit exposed. Photoisomerization of the fumaride by irradiation with UV light (254 nm) results in translation of the macrocycle to the tetrafluorosuccinamide station, thus shielding the hydrophobic region. When the [2]rotaxane assembly was physisorbed as a monolayer on a Au(III) surface with 11-mercaptopundecanoic acid the surface polarity could be changed when irradiated with UV light. When specific sections of the surface were irradiated, a droplet of diiodomethane could be transported across the surface against gravity at slopes of up to 12°. This technology could be useful in the development of lab-on-a-chip and microfluidic devices.

Another elaborate example of a molecular machine that highlights the complexity that it is now possible to incorporate in their design is the “molecular elevator” (Figure 5).⁷⁴ Its design and function are a result of the combination of the linear motion developed in the synthesis of a [2]rotaxane molecular shuttle⁷⁵ and the tripodal geometry used to create “triply-threaded two-component superbundles”.⁷⁶ The acid-base controlled recognition between the crown ether and the amino and viologen stations results in translational movement of the entire triphenylene platform. The distance between the triphenylene and 1,3,5-triphenylbenzene platforms can therefore be altered at will and could be useful for selective release of guests intercalated within this binding pocket.

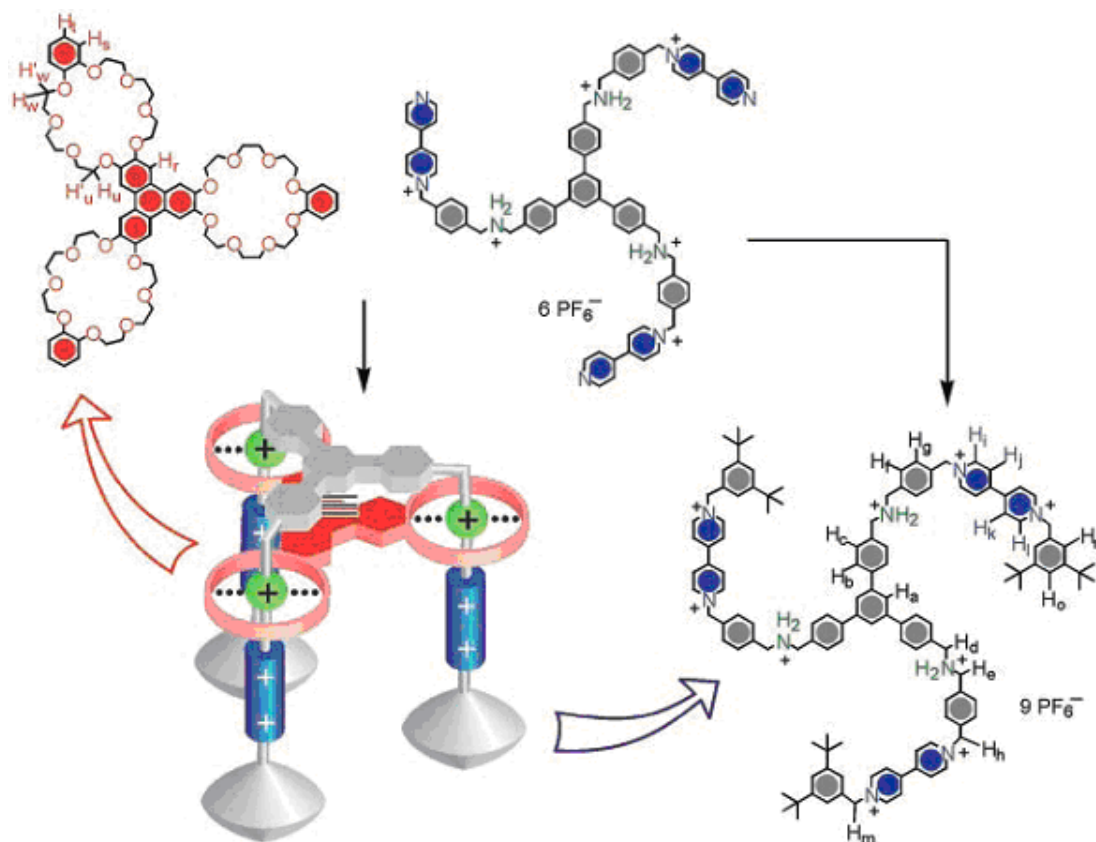


Figure 5. Structures and assembly of the “molecular elevator”. (image adapted and reproduced without permission)⁷⁴

The examples shown above are only a very brief highlight of some of the chemistry being carried out in this rapidly growing area of research. The synthetic craftsmanship and innovative design of such structures is sure to continue and will inevitably lead to greater fundamental understanding of the processes involved as well as applications in materials science and drug delivery.

2 APPLICATIONS OF HETEROCYCLIC CHEMISTRY

Heterocycles are a class of organic compounds that have applications in a wide range of modern research, from drugs^{77,78} and organic synthesis⁷⁹; to materials for energy transfer^{80,81} and even hydrogen storage.⁸² This diversity in their applications comes from the array of properties exhibited by the numerous possible heterocyclic structures and the subsequent interactions they have with other chemical and biological systems.⁸³ Some heterocycles can act as nucleophiles, others as electrophiles, acids, bases, reductants, oxidants, and so on. These properties are controlled by the size and shape of the ring and the number, type, and position of the heteroatoms. Controlling these parameters is crucial when designing new frameworks for functional organic molecules and materials.

2.1 Heterocycles in Nature

There is no better architect than nature and evolution, which has utilized organic building blocks for millions of years to create some truly astonishing structures. You simply have to look at the crystal structures of a plant light-harvesting complex,⁸⁴ or a strand of DNA,⁸⁵ or a virus protein coat⁸⁶ to appreciate the structural complexity that can be achieved. However nature is not only a master of design but also of function, which it has demonstrated through the exploitation of simple organic molecules or metal cations to control complex biological pathways.⁸⁷ Nature has therefore found a use for many heterocyclic frameworks to carry out tasks such as cell signaling, structural integration, and catalysis.⁸⁷

The neurotransmitter, serotonin, is a perfect example of how nature uses heterocycles to control signal transduction.⁸⁸ The majority of the human body's total serotonin is located in the gut, where it is used to regulate intestinal movements. The remainder is synthesized in serotonergic neurons in the central nervous system, where it has a vital role in virtually all brain functions, including memory, mood, appetite, motor function, and body temperature.⁸⁸ The size and complexity of structure is therefore obviously not a direct indication of its importance.

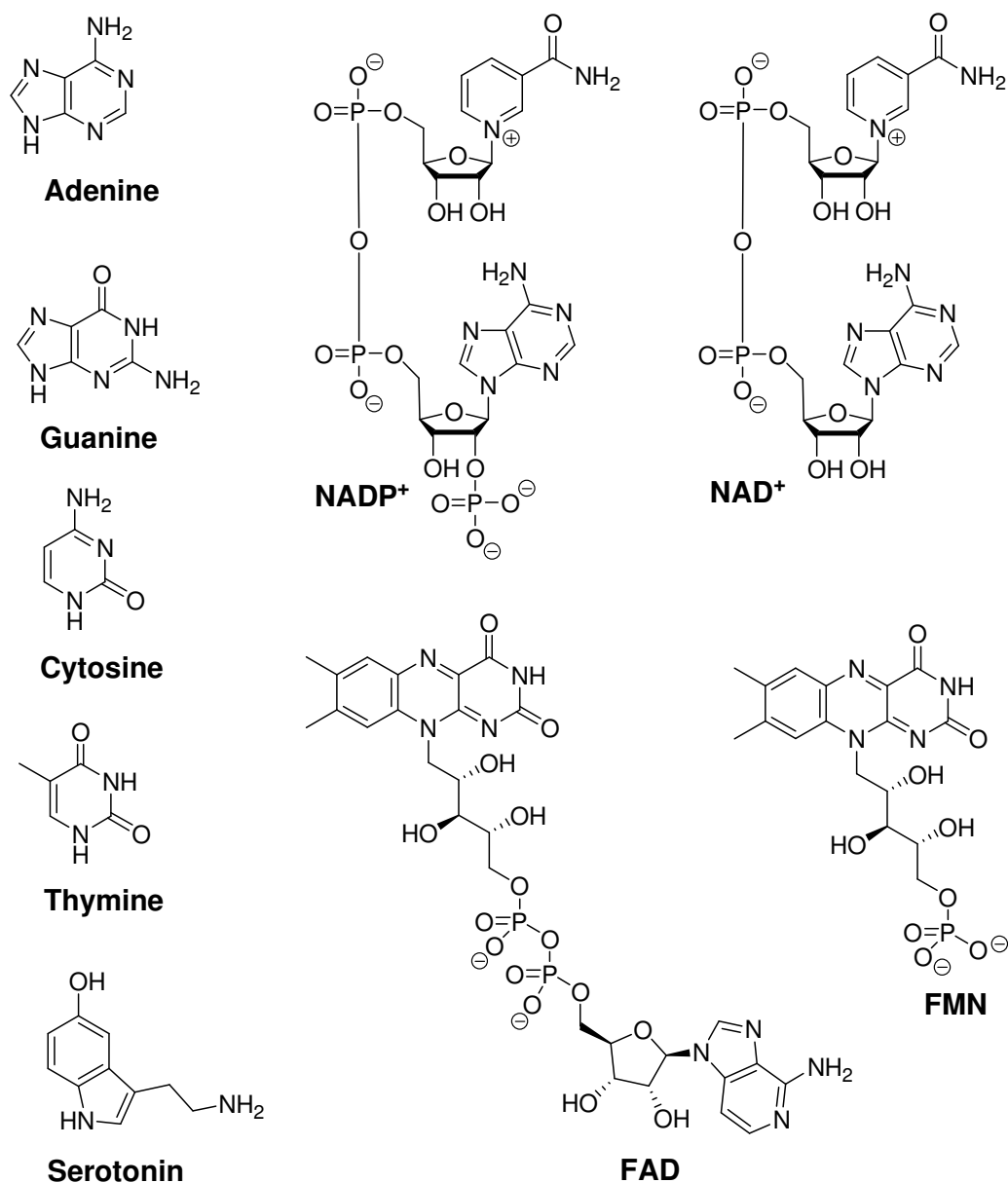


Figure 6. Structures of natural heterocycles.

DNA is one of, if not the most important molecule in any living organism as it contains the genetic information that is essential for reproduction.⁸⁹ The structure was unknown until 1953, when Watson and Crick proposed the double-stranded helical structure that is so commonly known today.⁸⁵ The integrity of the entire structure is highly dependent upon 4 molecules, which are of course the aromatic heterocycles guanine, cytosine, thymine and adenine. The two linear strands of DNA are held together by hydrogen bonding

interactions between these heteroaromatic bases. The complimentary nature of the hydrogen bonding arrangement is also what allows for selective insertion of the corresponding nucleotides during replication and transfer of genetic information. The π -stacking of these base-pairs also aids in stabilising the helical structure.

A large proportion of essential processes in living organisms, including those of signal transduction and DNA replication mentioned above, are dependent upon the action of enzymes to perform under physiological conditions.⁹⁰ The catalytic activity of enzymes is often dependent not only upon the primary peptide sequence and absolute 3D protein structure but also on the involvement of additional species called cofactors. Cofactors can be metal cations such as Mg^{2+} , Zn^{2+} and Fe^{3+} or they can be small organic molecules such as pyridines and flavins.⁹⁰ The pyridine derivatives NAD (nicotinamide adenine dinucleotide) and NADP (nicotinamide adenine dinucleotide phosphate); and flavins, FAD (flavin adenine dinucleotide) and FMN (flavin mononucleotide), are essential cofactors for the action of dehydrogenases and oxidoreductases.⁹¹ These enzymes and their cofactors are used as hydrogen transfer catalysts for the oxidation and reduction of the enzyme substrates.

2.2 Heterocycles in Drug Synthesis

The reliance on heterocycles and other small molecules for biological pathways is a very important factor in drug design for medicinal chemists. The interaction of small molecules with larger, more complex structures provides an opportunity for the manipulation of pathways and their resulting physical traits through the actions of low molecular weight drugs.² As mentioned previously enzymes are involved in almost all biological transformations and commonly interact with small molecules,⁹⁰ they are therefore perfect drug targets. The most common actions of drugs acting on protein targets are through binding at the active site (competitive/non-competitive inhibitors) or by inducing structural changes through binding elsewhere (allosteric inhibition).⁹² Inactivation (or activation) of the targeted enzyme has a knock-on effect further down the line in the pathway, bringing about changes in the substrate/product levels that cause the physical condition. An example of such a condition is antifreeze poisoning, where the ethylene glycol enters the

biological pathway via ADH (Alcohol Dehydrogenase) and subsequently produces the toxic substance, oxalic acid. This condition is treated by administering a large dose of ethanol, the natural substrate of ADH, to prevent the ethylene glycol entering the pathway by competing for the enzyme sites.⁹²

2.3 Heterocycles and Cancer

2.3.1 Cancer as a disease

Cancer is unfortunately not as simple to treat as it is a result of *multiple* errors in cell signaling pathways. It is not a single disease but a term used to cover over 200 different diseases resulting from different cellular defects, which affect various organs throughout the body.⁹² They are all classed under the same term “cancers” because they all result in the uncontrolled growth of cancerous cells in the form of tumours. Tumours can be either benign or malignant: A tumour is benign when the new growth of cells is localized and can usually be removed by surgery; a tumour is malignant when the cancer cells are mobile and can be distributed around the body, setting up new growths in different areas making them very difficult to treat.

2.3.2 Causes of cancer

The uncontrolled growth is a result of genetic defects in the genes responsible for controlling the cell cycle. The cell cycle is the general process involving the life and death of a cell and is strictly controlled by a number of checkpoints to ensure that only the correct DNA sequences are replicated in order for the new daughter cells to function properly. Genetic defects are actually very common but during normal cell replication they are either repaired, or if repair is not possible, then the cell is terminated so the defect is not passed on. However if the genetic defects occur within the genes coding for proteins involved in the control pathways then the chances of cells becoming cancerous begin to increase. Almost all cancers have a defect in at least one of these “control genes”, for example cyclins and CDKs (cyclin dependent kinases) are proteins that regulate cell growth and division and defects in their genes have been detected in 90% of human

cancers. The loss of a fully functioning regulation and repair mechanism consequently makes further mutations easier to be passed on unchecked. The subsequent build up of genetic defects then leads to cancerous cells which have the following characteristics: abnormal cell function, insensitive to growth inhibitor signals, abnormalities in cell cycle regulation, evasion of apoptosis (no cell death), increased telomerase activity (limitless division), angiogenesis (generation of blood vessels) and eventually metastasis (cancer spreading).⁹²

Although spontaneous DNA damage can occur through natural errors in the replication process, the majority are caused by a number of external factors; chemicals such as alkylating agents,⁹³ intercalating agents^{94,95} and heavy metals;^{96,97} radiation such as UV, X-ray and gamma;⁹⁸ viruses like the human papillomavirus;⁹⁹ and even lifestyle and diet.¹⁰⁰ The natural safeguards in the regulatory pathways of the cell cycle are very efficient at removing minor defects that result from acute exposures to these carcinogens but longer, more frequent exposures increase the risk of more serious damage.¹⁰¹ If the damaged DNA is not repaired and undergoes replication then this altered DNA sequence is carried through cell division and becomes a permanent mutation in that cell lineage. For a cell to become cancerous it has to obtain mutations in at least 5 genes.¹⁰¹ These mutations are not acquired by a single cell but through a sequential process of acquisition and expansion, where the number of initial mutant cells expands and they then acquire a second mutation, then a third, and so on; with each successive mutation becoming more likely, as more and more of the normal regulatory processes are lost. Hence why prolonged exposure to mutagens through activities like smoking and working with asbestos increase the incidence of cancer in these demographics.¹⁰¹

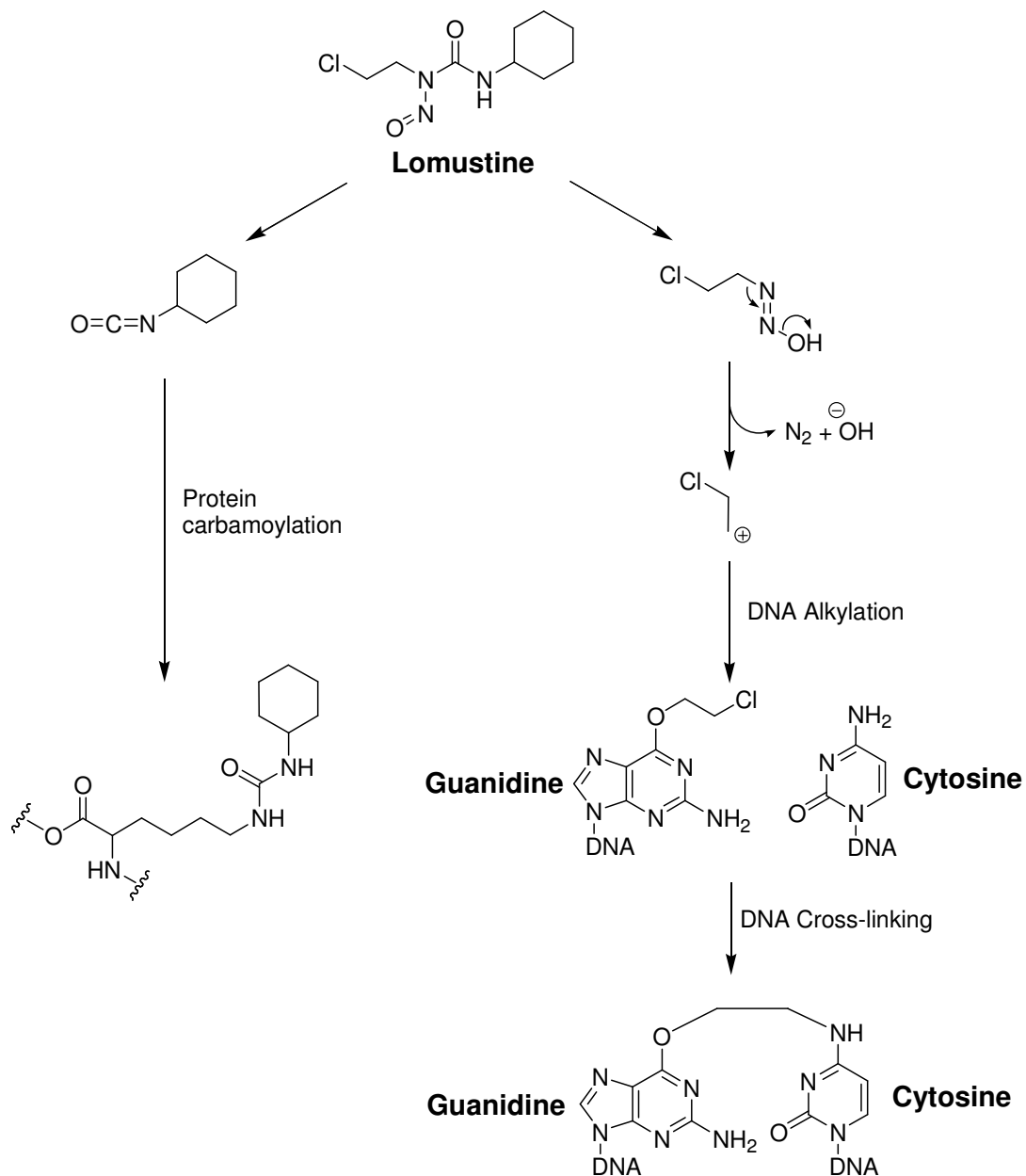
2.3.3 Treatments for cancer

Although there are many newly developing cancer treatments under investigation such as gene therapy, antibody-directed enzyme prodrug therapy (ADEPT), virus-directed enzyme prodrug therapy (VDEPT) and gene-directed enzyme prodrug therapy (GDEPT), the three traditional and most common methods for treatment of cancers are surgery, radiotherapy, and chemotherapy.¹⁰² All three methods offer particular benefits and drawbacks: Surgery cannot guarantee complete removal of all cancerous cells due to their ability to invade

neighbouring and far away tissues through metastasis, whilst selectivity and toxicity pose a large problem for both radiation and chemical treatments. Often a combination of surgery, radiotherapy, and chemotherapy, which have complimentary modes of action, leads to the most effective treatments.¹⁰¹

Chemotherapy is the term used for the treatment of cancer and other diseases through chemical means.¹⁰³ The drugs available for chemotherapy treatments of cancer can fall into a number of categories depending on their mode of action; alkylating agents, mitotic inhibitors, antimetabolites, and topoisomerase inhibitors are the most common.¹⁰⁴

Alkylating agents target DNA directly through alkylation of the nucleophilic nitrogens of the DNA base-pairs such as *N*-1 and *N*-3 of adenine, *N*-3 of cytosine, and *N*-7 of guanine. Alkylation of guanine units is particularly effective in causing mutations since the alkyl-guanine favours the unnatural enol tautomer, which base-pairs with thymine rather than cytosine, resulting in miscoded regions in the DNA. However the most potent action of alkylating agents is the cross-linking of DNA, where the DNA strands become covalently linked and can no longer be replicated or translated.¹⁰⁵ Important alkylating agents include nitrogen mustards, aziridines, nitrosoureas and sulfonic acid esters.¹⁰⁶



Scheme 5. Mechanism of action for Lomustine, a nitrosourea alkylating agent.

Nitrosoureas have a dual mode of action as they decompose in the body to form two active compounds, an alkylating carbocation and a carbamylating isocyanate. The alkylating agent cross-links DNA through reaction with the *O*-6 positions of guanine bases or *N*-3 positions of cytosine bases. The active isocyanate forms carbamates through reaction with the lysine residues in proteins, which could cause inactivation of DNA repair enzymes, thus increasing its potency. Although cisplatin and other platinum-based chemotherapeutic drugs are not alkylating agents as such, they behave in a similar fashion.¹⁰⁷ These drugs

antagonist. The high uptake of nutrients in rapidly dividing cancer cells is a feature which makes these drugs so effective.

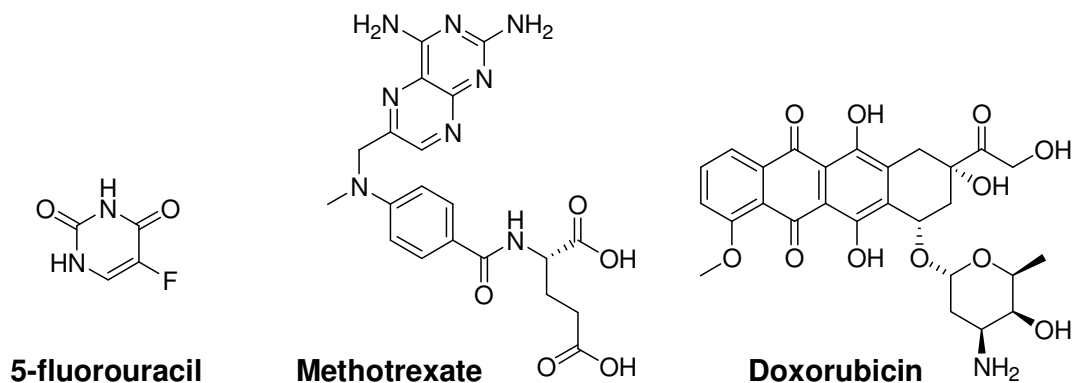


Figure 8. Structures of the antimetabolite drugs 5-fluorouracil and methotrexate; and doxorubicin, a topoisomerase inhibitor.

Doxorubicin is among the class of cytotoxic agents called topoisomerase inhibitors. Topoisomerases are enzymes that unwind and wind DNA during replication and transcription.¹¹⁵ Doxorubicin intercalates DNA and stabilises the complex topoisomerase II forms with DNA after unwinding, the DNA is then no longer available for complexation with other proteins and cannot undergo replication, ultimately leading to cell death.¹¹⁶

The major drawbacks of all chemotherapeutic drugs regardless of their mode of action are those of bioavailability, selectivity, systemic toxicity, and resistance.¹¹⁷ The reasons for the difficulties encountered in targeting cancer cells over healthy cells is due to the fact that the cancer cells are derived from indigenous tissues and therefore share many similarities. New treatments like ADEPT, VDEPT and GDEPT use the combination of genes and viruses to direct or initiate expression of nonhuman enzymes in cancer cells, followed by administration of a prodrug substrate for the enzyme, which is then converted to the active drug only in the cancerous tissues.¹⁰² Exploitation of “the Warburg effect” is also providing promising results for more selective chemotherapeutic agents. The Warburg effect is an observation that most cancer cells predominantly produce energy by glycolysis and lactic acid fermentation in the cytosol, rather than by oxidation of pyruvate in mitochondria like most normal cells.¹¹⁸ This change in the primary metabolic pathways

creates distinctions in cancerous tissues, namely increased expression of glycolytic enzymes and increased acidity,¹¹⁹ that could offer new targets and more selective treatments.¹²⁰

2.4 2,3-Dihydro-1*H*-imidazo[1,2-*f*]phenanthridinium (DIP) heterocycle

2.4.1 DIP Applications in Anti-cancer Therapies

Previous work within the Cronin research group led to the discovery of a new class of *N*-heterocycles, 2,3-dihydro-1*H*-imidazo[1,2-*f*]phenanthridinium cations.¹²¹ These positively charged aromatic frameworks were shown to have moderate binding affinities for DNA¹²² and were subsequently investigated for their potential application as anticancer agents. The DIP framework was shown to intercalate between the base-pairs of DNA with comparable binding affinities to the well known intercalaters, ethidium bromide and chelerythrine.¹²³ The DIP frameworks were assessed by *in vitro* assays in human ovarian tumour cell lines and showed very high cytotoxicities, some compounds were even more active than carboplatin in these cell lines.¹²⁴ The DIP framework was also shown to have superior metabolic stability, with respect to hydroxide addition and reduction, in comparison to other well known intercalating frameworks.

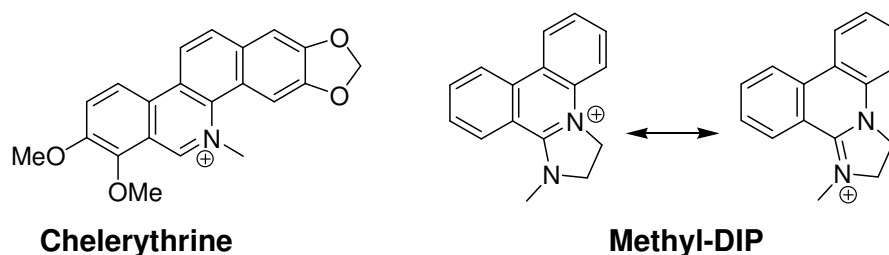


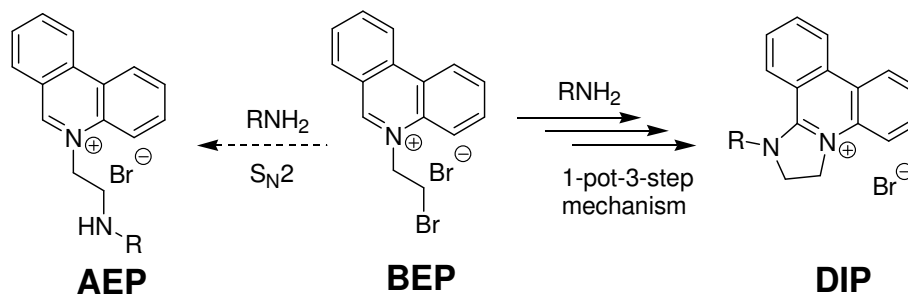
Figure 9. Resonance stabilisation of the positive charge in the DIP moiety compared to the iminium moiety in the phenanthridinium analogue, chelerythrine.

The reasons for this increased stability come from the resonance stabilization of the positive charge in the dihydroimidazolium moiety in comparison to the iminium moiety

of analogous phenanthridinium intercalaters (Figure 9). The initial tests carried out on the DIP frameworks were very positive and developing them into drug candidates looked to be a strong possibility. Further investigations of the library of DIP frameworks that had been synthesised gave much valued SAR information, which indicated a high dependency upon the lipophilicity of the amino side-chain for cytotoxicity.¹²⁵ It was postulated that the DIP frameworks therefore had two types of binding to DNA, intercalation of the dihydrophenanthridinium ring system, and additional minor groove binding of the amino side-chain. The mode of action was therefore likely to arise from interactions with the DNA-protein complexes formed during transcription and replication, similar to topoisomerase inhibitors.¹¹⁶ However the true nature of binding and the mode of action were never confirmed. Results obtained from *in vivo* assays in mice transplanted with human tumour xenografts were unfortunately not as encouraging as the initial *in vitro* studies. Very low therapeutic indices were obtained for a large proportion of the DIP compounds tested. The therapeutic index (TI) is defined as the lethal dose of a drug in 50% of the sample population (LD₅₀) divided by the effective dose (ED₅₀), so a high TI is preferential to a low one as in these cases the effective dose required is much less than the lethal dose. The non-selective effects observed for the DIPs were thought to be caused by non-specific DNA binding or by other mechanisms such as membrane insertion.^{125,126} The low TI for the DIPs meant that the compounds were too toxic for further *in vivo* investigations and the pursuit to develop them into potential chemotherapy agents was halted.

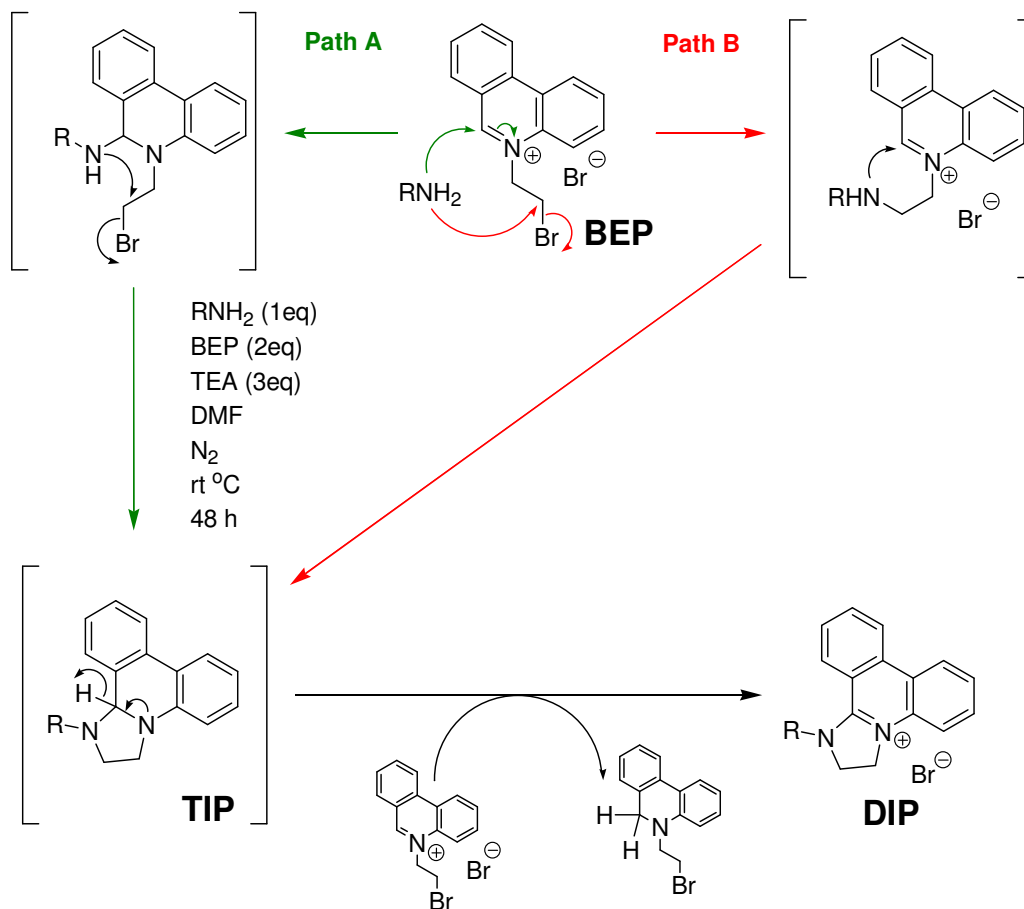
2.4.2 DIP Synthesis

Although the application of the DIP heterocycles as anticancer agents was not as successful as first hoped, their discovery and synthesis in itself is an interesting story. The DIP heterocycles were serendipitously discovered when attempting to substitute the bromoethyl side-chain of 5-(2-bromoethyl)-phenanthridinium bromide (BEP) with primary amines.¹²⁷ Rather than the expected substitution of the bromine via the S_N2 mechanism to produce the 5-(2-aminoethyl)-phenanthridinium bromide (AEP), a series of reactions led to the production of a tetracyclic cation, subsequently characterized as the DIP framework (Scheme 6).



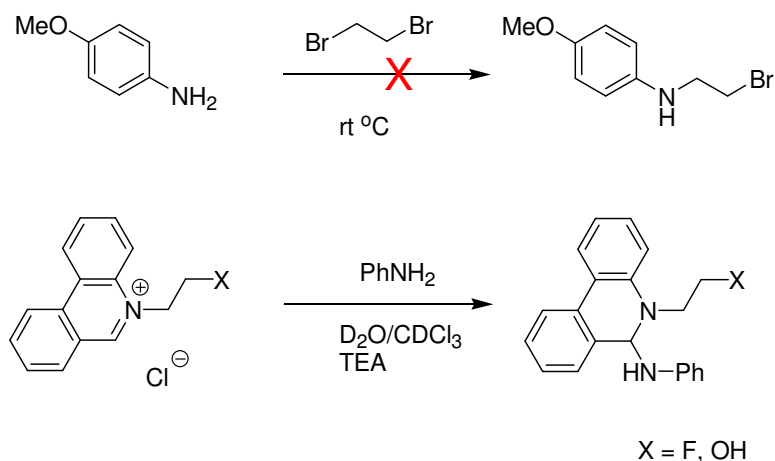
Scheme 6. Possible reactions of the BEP cation with primary amines

Two possible pathways were proposed for the formation of DIP from BEP, both of which involved an addition of the amine to the BEP, followed by cyclisation and finally oxidation to DIP.¹²¹ The oxidant in the final step was identified as a second equivalent of BEP due to the presence of the BEP reduction product, 5-(2-bromoethyl)-5,6-dihydrophenanthridine (BEDP), in the final reaction mixture, and the observation of very low yields for DIP with respect to BEP (< 50%). The cyclic 1,2,3,12*b*-tetrahydroimidazo[1,2-*f*]phenanthridine (TIP) intermediate was characterised *in situ* via MS and NMR spectroscopy. The identification of the order of the first two steps was however not as trivial and required further investigations to identify the correct intermediate species. The BEP framework contains two electrophilic centres which react with the nucleophilic primary amines to give the cyclic TIP intermediate. However it was not apparent whether addition occurred at the iminium moiety or the bromoalkyl moiety first (Scheme 7).



Scheme 7. Possible mechanisms of DIP formation.

Path B involves nucleophilic substitution at the bromoethyl side-chain followed by a 5-*endo-trig* cyclisation, whereas path A involves α -addition at the iminium moiety followed by a 5-*exo-tet* cyclisation. The rules of ring closure proposed by Baldwin *et al*¹²⁸ supported the case for the preference of path A over path B due to the energetically unfavorable 5-*endo-trig* cyclisation required for path B, which was corroborated by observations made during the reactions of suitably functionalized analogues (Scheme 8).



Scheme 8. Reactions confirming the preference of path A over path B.

No reaction was observed when *p*-methoxyaniline was mixed with 1,2-dibromoethane, indicating that intermolecular S_N2 of the alkyl bromide was not possible at room temperature. Addition of primary amines to 5-(2-fluoroethyl)-phenanthridinium and 5-(2-hydroxyethyl)-phenanthridinium chlorides was still possible at room temperature.¹²¹ From this evidence path A was established as the mechanistic route to DIP from BEP. Further investigations were then made to expand and improve the efficiency of the DIP synthesis which led to the development of a biphasic methodology.¹²¹ This methodology used phase separation to convert the BEP starting material to the TIP intermediate almost quantitatively, oxidation by NBS then yielded the DIP product in very high yield (typically > 90%) with respect to the amine and the BEP reactants. Investigations into the use of other solvents and co-oxidants were also made which resulted in a portfolio of complimentary methodologies for generating DIPs from a wide range of amine substrates.^{127,129}

2.4.3 DIP Applications in Inorganic-Organic Hybrid Materials

Many examples for the applications of organic heterocycles in areas out with the traditional biological and medicinal remit have been given so far (see section 1.3 Molecular Machines and Devices). Another such example is that of the combination of DIP heterocycles with inorganic metal oxide species to produce novel inorganic-organic hybrid materials.

Polyoxometalates (POMs) are molecular anionic transition metal oxide clusters, they have active roles in catalysis,^{130,131} medicine,^{132,133} electrochemistry,¹³⁴ and molecular magnetism.^{135,136} The structures that can be formed vary in shape, size, and function; with the synthetic conditions having a direct influence on these properties.¹³⁷ Experimental parameters such as pH, temperature, metal salt composition, cation identity, concentration, and stoichiometry can all affect the self assembly of these metal oxide clusters. Some generic examples of the more common POM clusters are shown in Figure 10.

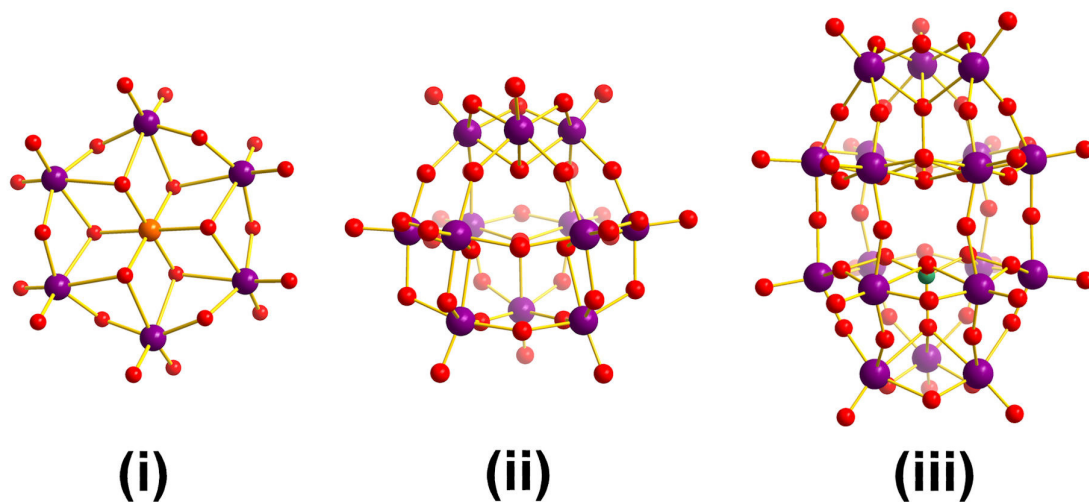


Figure 10. Ball and stick graphical representation of the common POM architectures: (i) $[M_7O_{24}]^{n-}$ Anderson; (ii) $[M_{12}O_{36}(XO_4)]^{n-}$ Keggin; (iii) $[W_{18}O_{54}(XO_4)_2]^{n-}$ Dawson.

A large number of derivatives of the Anderson, Keggin, and Dawson cluster types are known, with variations in the transition metals, counter cations, and heteropolyanions. Alteration of these variables can result in changes in the cluster topology and crystal packing of these architectures, which ultimately affects the physical properties and applications of the bulk material.^{138,139} The introduction of organic components into POM materials can also have a huge effect on the material properties. The organic part can be incorporated within the structure as a ligand metal complex, as a counterion, or as a covalently linked conjugate.¹⁴⁰⁻¹⁴⁴ Although there are recent examples using Huisgen

coupling to create POM-organic hybrids¹⁴⁵ the most common methods for the covalent attachment of organic ligands to POM clusters are through coordination to a lacunary POM structure.^{146,147} This can be achieved by using a flexible triol such as pentaerythritol or TRIS-Base (tris(hydroxymethyl)aminomethane), where the pendant alcohols can displace the terminal hydroxyl ligands of the POM to give the POM-ligand conjugate.^{144,148} This methodology has been used very successfully within the Cronin group to derivatise POM clusters. Cation exchange and cocrystallisation are a much more popular method for the incorporation of organic components within POM materials and there are numerous examples of these types of compounds.¹⁴⁹⁻¹⁵¹

POM clusters with TBA counter cations are readily soluble in polar organic solvents like acetonitrile, acetone, methanol, DMF and DMSO. Cation exchange of the TBA cations with aromatic DIP cations leads to precipitation of highly insoluble aggregates, which have very poor solubility in all solvents except DMSO and DMF.¹⁵² This rapid alteration of the material properties due to this cation exchange reaction can be exploited to create new macro scale inorganic-organic hybrid materials with defined macro scale topologies.¹⁵³ When single crystals of a polyoxometalate (POM) species $[(C_4H_{10}NO)_{40}[W_{72}Mn_{12}O_{268}X_7]$, where $X = Si$ or Ge , were suspended in an aqueous solution of a DIP cation it was observed that a spontaneous microtube growth emerged from the crystal (Figure 11).¹⁵³ This phenomenon was discovered by researchers within the Cronin research group where efforts have been made to gain understanding of the fundamental interactions of the self assembly process and to devise applications for the microtubes formed.



Figure 11. Time-lapse images of a single tube emerging from the POM crystal

The tube growth was shown to be the result of osmotic pressure pumping material out from within a semi permeable membrane that forms around the crystal. When the POM crystal contacts the DIP solution, a membrane forms around the crystal, osmotic pressure builds

up from the diffusion of water across the membrane, the membrane then ruptures and the material is expelled causing microtube growth. The rate of growth and the tube diameter were shown to be a function of the concentration of the DIP solution, and directional control was established through potential differences applied across the bulk sample.¹⁵⁴ The integrity of the microtube structures was explored by injecting a fluorescent dye, upon which complete containment of the dye within the tubes was achieved. The scope of the system was also investigated and similar growth patterns were obtained for a variety of mixtures of POM materials and DIP cations.¹⁵³ This could therefore lead to the design and synthesis of topologically well defined architectures that retain the functionality of the original POM material.

Aims

DIP heterocycles are a relatively new organic framework with interesting physical and biological properties and much work has been carried out in investigating DIPs as intercalating antitumour agents. However little has been done to explore the potential usefulness of these heterocycles and their syntheses in other areas of chemistry. The aim of this project was therefore to expand the chemistry surrounding the synthesis of DIPs to create functionalised derivatives that could find uses in areas out with their initial sphere of biological activity.

In addition to their potential applications as chemotherapeutic agents, the mechanism of formation of DIPs is an intriguing aspect as well. Previous work established that the mechanism involves a 3-step cascade reaction sequence, and although the intermediates had been characterised *in situ*, none of them were isolated. A priority target was to isolate these intermediate structures so their properties could be assessed and new applications could be inspired. Alteration of the reaction conditions and the amino substrates were to be investigated in order to achieve this goal.

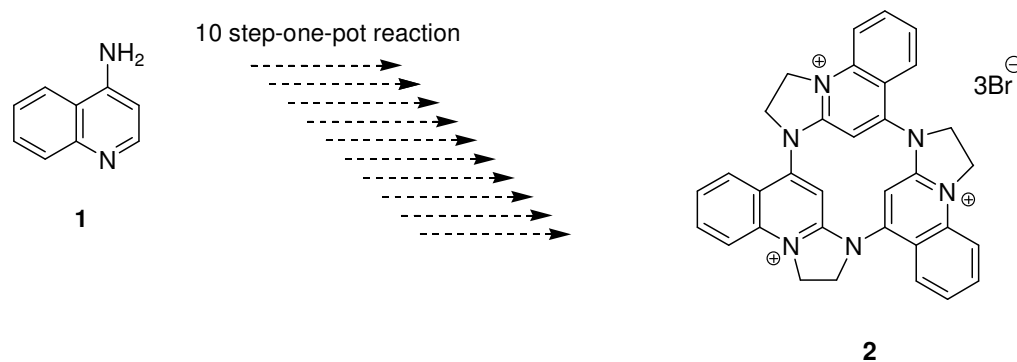
It was also thought that the use of more complex amine substrates would lead to the discovery of new DIP materials with potential applications in areas such as catalysis and supramolecular host-guest chemistry. For example; bifunctionalised quinolinium substrates, containing both amine and imminium moieties, could lead to even more complex sequential multi-step reactions. The proposed products of such reactions were cyclic or acyclic polycations, depending on the orientations of the functional groups and the number of monomeric units, and could be useful for anion binding. Polyoxometalate clusters with covalently bound organic groups show dramatic changes in their physical properties compared to their untethered counterparts. The covalent attachment of DIP-type heterocycles to POMs could therefore achieve similar outcomes. This would require appropriately functionalised linkers to be synthesised and methodologies compatible with the substrates to be developed. Investigations into the compatibility of the DIP chemistry and these complex amine substrates were therefore intended to be another important aspect of this project.

Results and Discussion

3 MACROCYCLIC POLYCATIONS

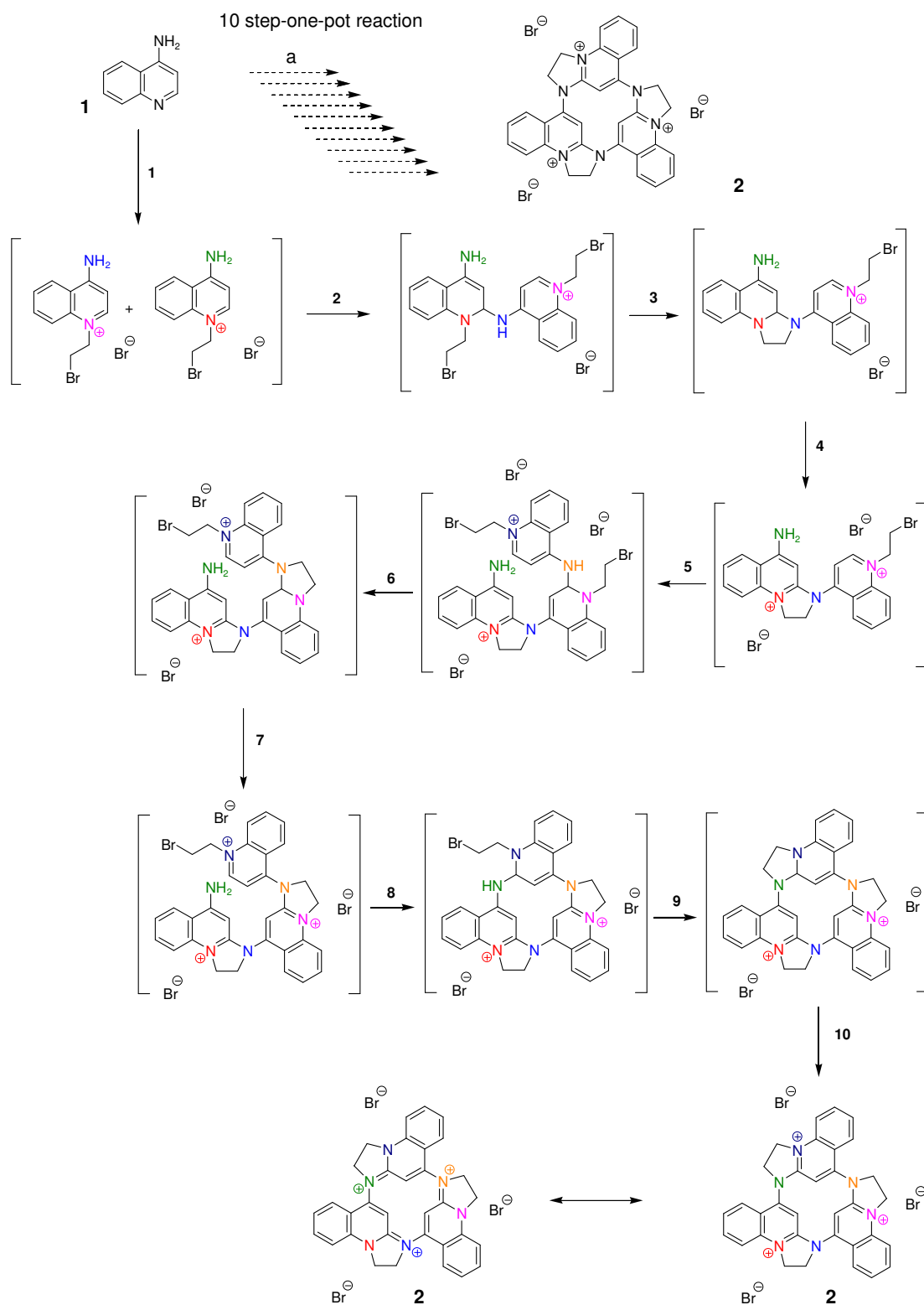
3.1 4-Aminoquinoline Macrocycles

The chemistry of macrocycles has been shown to be a well established research field. Synthetic routes vary from templated single step ring-closing reactions to complex multi-step procedures¹⁵⁵⁻¹⁵⁸ and the product applications are inherently dependent upon the building blocks used to create the final architectures, which may be large/small, aromatic/aliphatic, hydrophobic/hydrophilic, charged/uncharged etc. The synthesis of new macrocyclic cations is therefore an attractive objective for synthetic chemists due to the vast number of potential applications for such targets. The ambitious target devised for this project was that of cyclotris(2,3-dihydro-1*H*-imidazo[1,2-*a*]quinoline) (CTDIQ³⁺, **2**, Scheme 9).



Scheme 9. Proposed CTDIQ³⁺ target.

The high charge and rigid structure of the target **2** would have potential as an anion binder due to its rigid framework and the strong electrostatic interactions it should offer. The proposed route to the target aimed to exploit the facile synthesis of 2,3-dihydro-1*H*-imidazo[1,2-*a*]quinolines (DIQs) developed by Parenty *et al.*,^{121,127} in a multi-step-one-pot reaction with 4-aminoquinoline substrate **1** (Scheme 10). The mechanism involves four main steps; alkylation at the quinoline-*N*, α -addition of amino-*N*, 5-*exo-tet* cyclisation, and oxidation. Repetition of these steps leads to formation of the desired target macrocycle **2**, providing the steps occur in the correct order and with the desired geometry.



Scheme 10. Proposed mechanism for formation of the CTDIQ³⁺ macrocycle. (a) 1,2-dibromoethane, TEA, DMF, N₂, 90°C, 48h

The initial conditions employed were adapted from the 2 step synthesis of DIQs where primarily alkylation of quinoline yields a 1-(2-bromoethyl)-quinolinium bromide substrate for the subsequent multi-step reaction.^{121,127} Combination of these steps had the potential for multiple side-reactions, such as dimerisation, elimination and non-regioselective alkylations, to compete with the desired reaction sequence. Unfortunately this is exactly what was observed. Upon cooling of the reaction mixture after heating for 48 h the reaction was filtered (TEA.HBr crystals collected) and the mother liquor was analysed by MS. The data collected showed no indication of the target molecule, only the initial alkylation product plus undesired byproducts were observed (Figure 12).

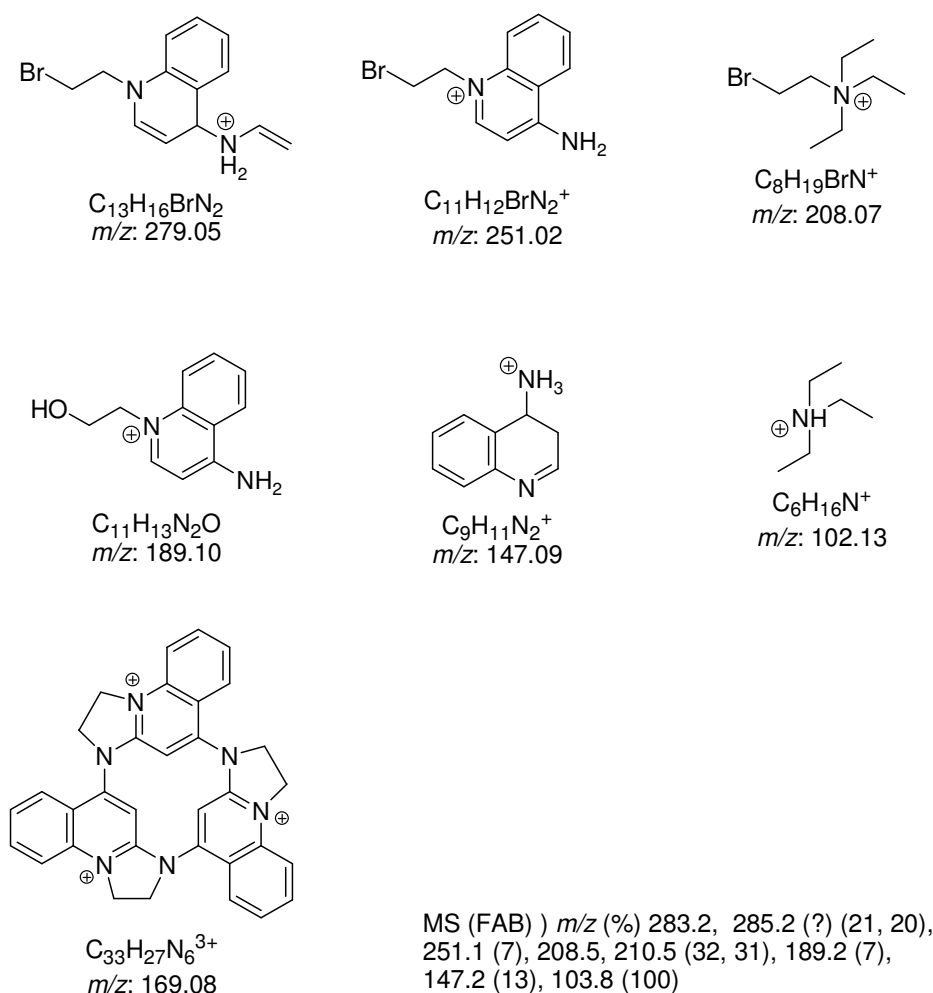
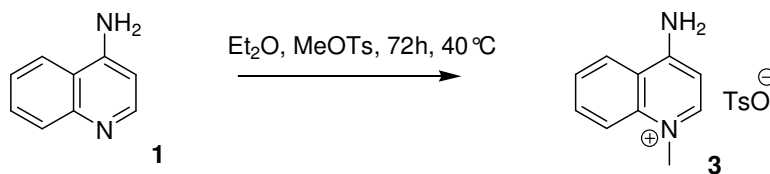


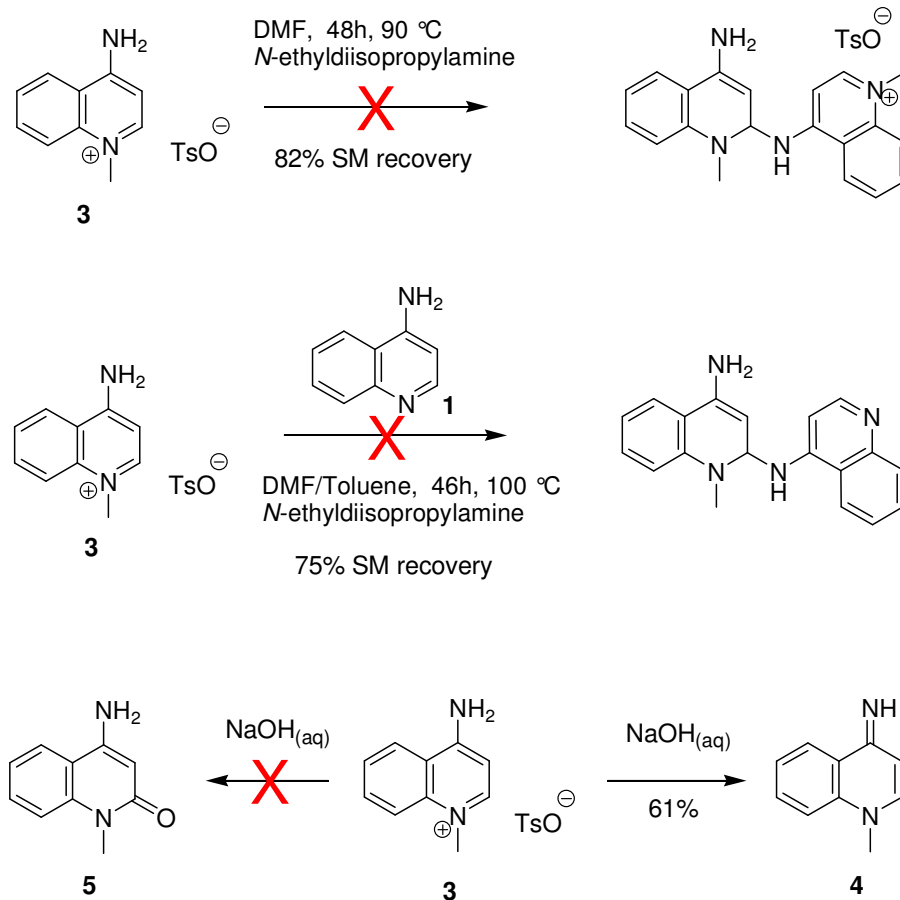
Figure 12. Observed mass ion signals and possible corresponding fragments for the initial one-pot synthesis of CTDIQ³⁺.

The presence of the TEA-bromoethyl conjugate and the lack of any high mass fragments indicated that TEA was reacting as a nucleophile as well as a base and that no α -addition was occurring between aminoquinolinium species in the reaction mixture. Attempts to isolate the 4-amino-1-(2-bromoethyl)-quinolinium bromide via direct alkylation of the 4-aminoquinoline substrate with 1,2-dibromoethane were unsuccessful. The decision was therefore made to move towards a step-wise synthesis of a simplified target in order to gain more insight as to exactly where the reaction was failing and then to adapt the synthesis and build up complexity from there. The new target structure proposed was that of 4-amino-1-methylquinolinium toluene-4-sulfonate **3** (Scheme 11).



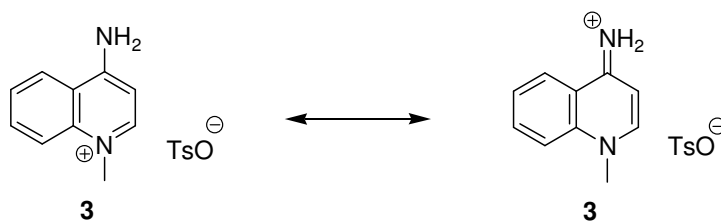
Scheme 11. 4-Amino-1-methylquinolinium toluene-4-sulfonate target.

A series of investigative reactions were performed using the new methylquinolinium substrate (Scheme 12). Refluxing the methylated substrate in DMF and *N*-ethyl-diisopropylamine for 48 h resulted in recovery of the starting material (~80%) after precipitation with Et₂O, the same reaction with the addition of 1 eq of non-alkylated 4-aminoquinoline yielded a similar result. Refluxing in aqueous NaOH yielded the deprotonated compound **4** and not quinolinone **5**.



Scheme 12. Investigative reactions with methylquinolinium substrate.

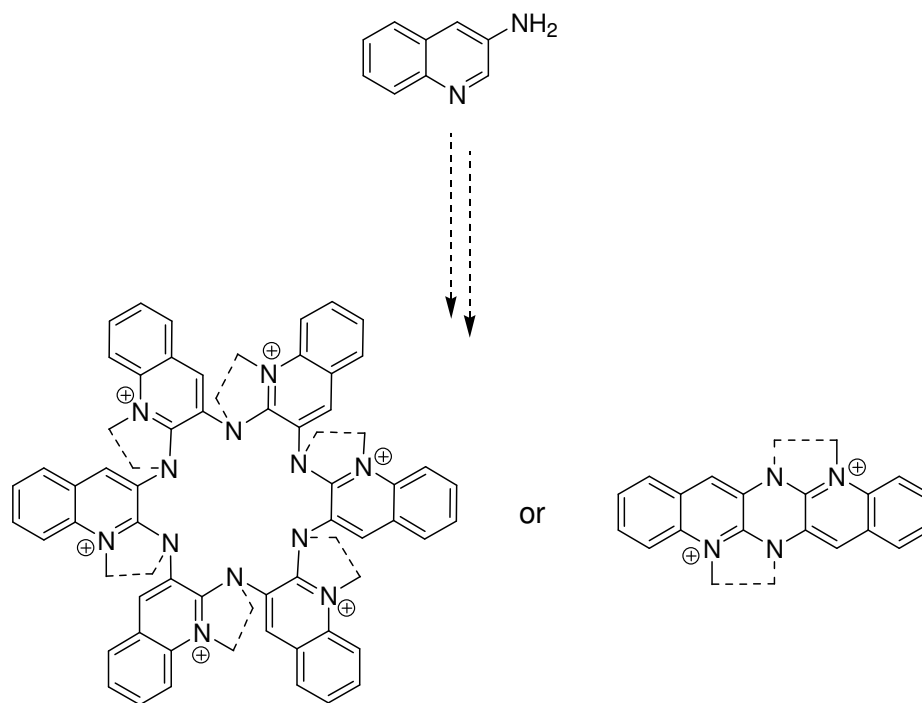
From these results it was concluded that the α -addition step was not occurring due to the conjugation between the two nitrogen centres. The nucleophilicity of the amino-*N* and the electrophilicity of the quinolinium are diminished by delocalisation of the positive charge (Scheme 13). It is also worth noting here that similar α -addition reactions of aryl amines are significantly hindered by bulky substituents ortho to the nucleophilic primary amine (see section 4.4).



Scheme 13. Conjugation of nitrogen centres in 4-aminoquinolinium species.

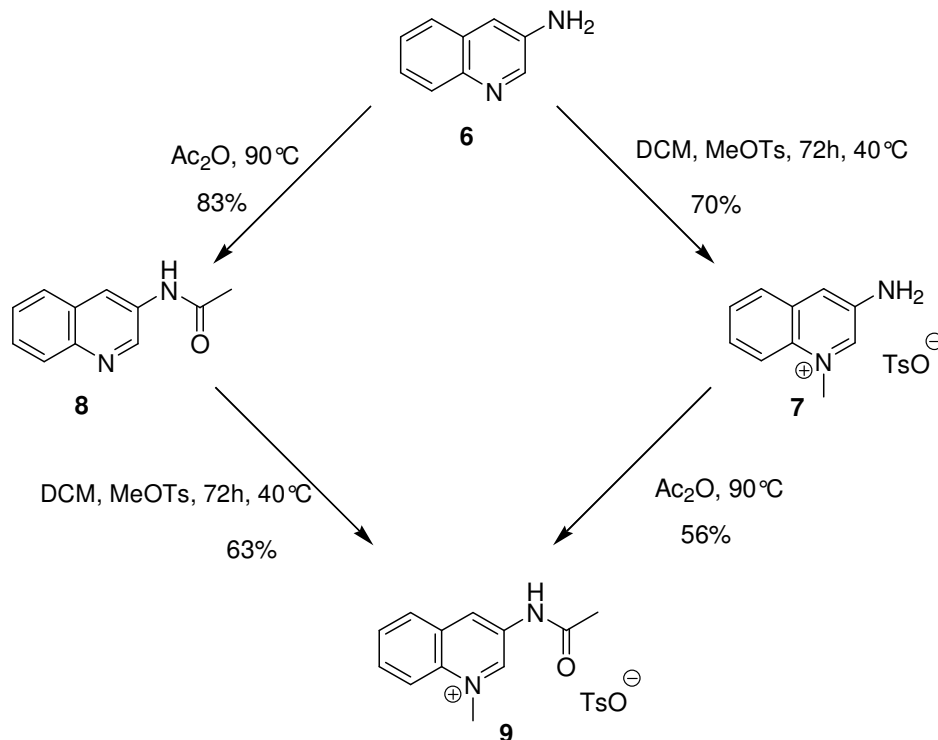
3.2 3-Aminoquinoline Macrocycles

It was proposed that aminoquinolines with different substitution arrangements of the amine functionality relative to the quinoline nitrogen could overcome this problem. The choices of aminoquinoline replacements were limited by consideration of the electronic and geometric properties for each isomer. 3-aminoquinoline contained an unhindered, non-conjugating amino group and retained a geometry that could still potentially lead to a 1 + 1 dimer or a 6-membered macrocyclic product (Scheme 14).



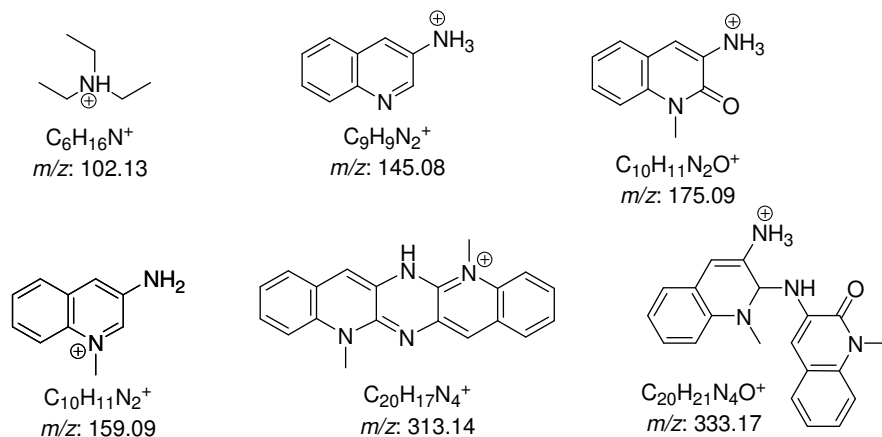
Scheme 14. Possible dimeric and macrocyclic products from reactions of the 3-aminoquinoline substrate.

Direct alkylation of the quinoline-*N* with 1,2-dibromoethane was again unsuccessful so the tactic of methylation was employed and substrate **7** was synthesised (Scheme 15).



Scheme 15. Synthesis and reactions of 3-amino-1-methylquinolinium toluene-4-sulfonate (7).

The nucleophilicity of the amino-*N* both before and after alkylation was tested by reacting substrates **6** and **7** with acetic anhydride. Compound **9** was able to be synthesised via both synthetic routes, confirming that the amine retained its' nucleophilic character even after alkylation of the quinoline-*N*. Unfortunately the successful retention of nucleophilicity did not transfer to the successful production of macrocyclic products. When TEA was added to a solution of methylquinolinium substrate **7** in DMF and the reaction mixture was analysed by MS after 48 h no peaks could be assigned to macrocycles or oligomers of **7**. (Figure 13).

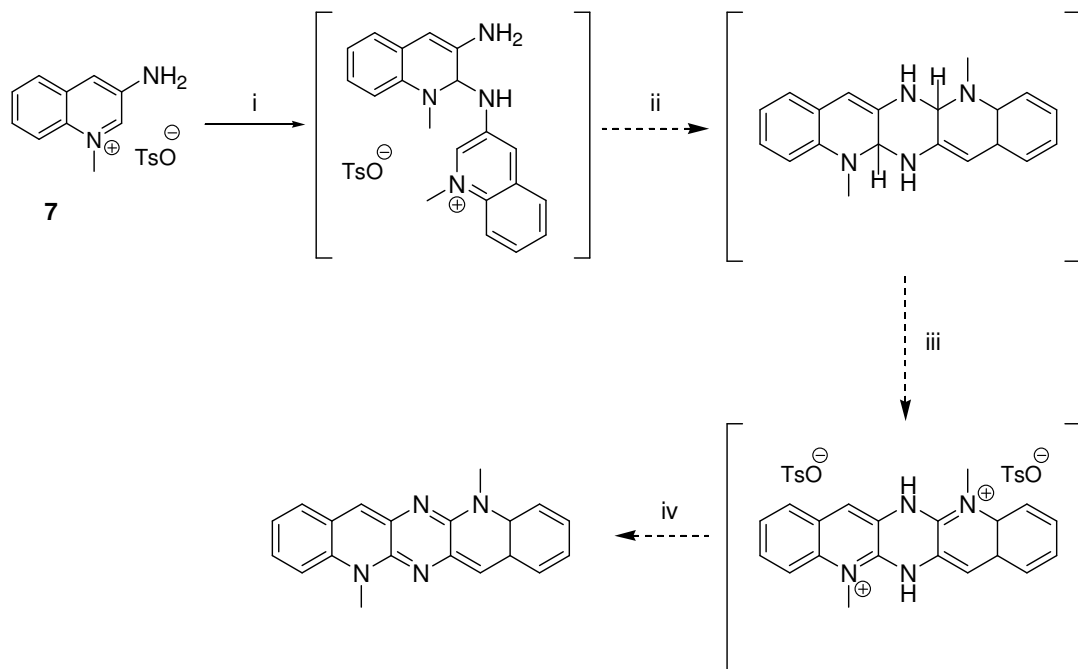


MS (Cl⁺) *m/z* (%) 338.4 (?) (22), 257.3 (?) (24), 175.2 (31), 145.2 (33), 102.2 (100)

Figure 13. Observed mass ion pattern and possible fragments for reaction mixture of compound 7 plus TEA in DMF.

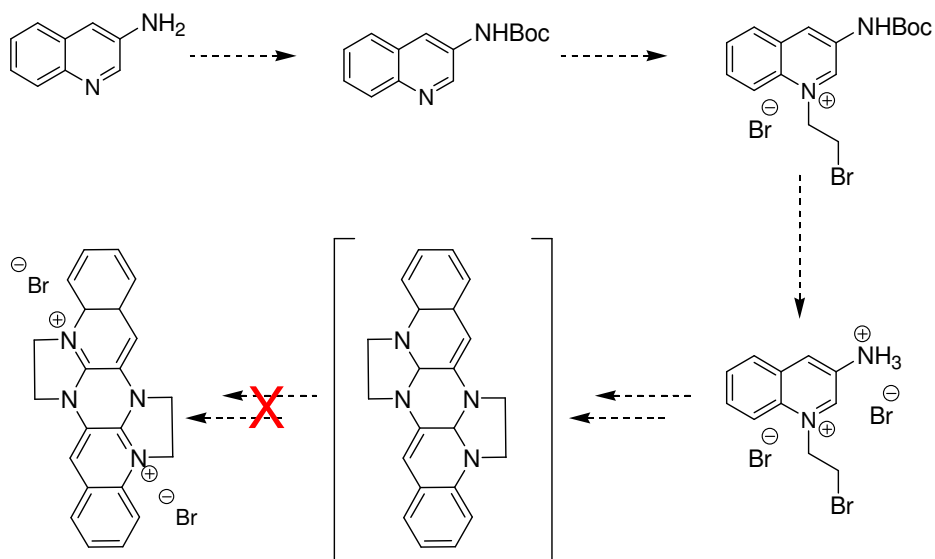
The observation of mass fragments ($m/z = 175.09, 257.3, 338.4$) of higher mass than the methylquinolinium substrate ($m/z = 159.09$) was promising as this indicated that the substrate was reacting under the standard conditions but could just not produce the target structures. The choice of 3-amino-1-methylquinolinium as the framework for the macrocycle building block overcame the problems that had been encountered with the previous 4-aminoquinoline derivatives: The amino-*N* was no longer conjugated with the quinolinium-*N* and there were no ortho substituents to inhibit the α -addition. However the methylated substrate could not yield the desired products as the 5-membered imidazo ring could not be formed.

In order to form a stable macrocyclic framework the 3-aminoquinoline needs to be alkylated with the bromoethyl side-chain necessary for formation of the 5-membered imidazo ring. If cyclisation does not occur prior to the oxidation step then the amino group will leave before oxidation can occur, or a neutral oxidation product will form through deprotonation of the secondary amine centre (Step iv, Scheme 16).



Scheme 16. 3-aminoquinoline dimer (i) 1st α -addition; (ii) 2nd α -addition; (iii) oxidation; (iv) deprotonation

Alkylation of the quinoline-*N* with 1,2-dibromoethane would overcome this problem but protection/deprotection of the amino-*N* would need to be introduced to synthesise the reactive alkylated substrate as the 3-aminoquinoline cannot be directly alkylated with 1,2-dibromoethane (Scheme 17). However it was also proposed that the oxidation step for this substrate would be problematic as it was previously reported that reactions of aryl amines with 1-(2-bromoethyl)-quinolinium bromide do not oxidise easily and the reaction stops after the addition and cyclisation steps.¹²⁷



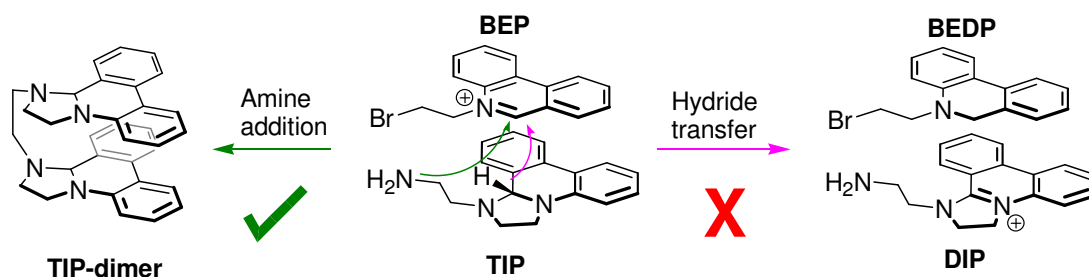
Scheme 17. Synthetic strategy for 1-(2-bromoethyl)-3-aminoquinolinium bromide and subsequent multi-step reactions to dimer product.

The initial aim of utilizing DIP-type reactions to produce macrocyclic architectures was not achieved however the results obtained to date have provided vital information on the reactivity of the electrophilic and nucleophilic centres involved. This has enabled us to completely revise our original hypotheses and design a new blueprint for a suitably reactive substrate. The new framework will specifically require: (i) an unhindered amine; (ii) an aliphatic (or non-conjugated) amine; (iii) a 2-bromoethylquinolinium moiety; (iv) sufficient distance/rigidity between the reactive centres to prevent intramolecular additions; (v) appropriate geometry to allow cyclic products rather than linear oligomers. Adhering to these guidelines should give any future attempts a much greater chance of success.

4 TIP SYNTHESIS – UNDERSTANDING THE REACTION

4.1 Prevention of oxidation by BEP

As discussed earlier, a number of methods for the synthesis of the biologically active DNA intercalating agents, DIPs, have been developed.^{121,124,127} These methods utilise a variety of solvents and oxidizing agents and are applicable to a range of primary amine substrates. Regardless of the changes in the conditions, all the reactions essentially follow the same 3-step mechanism: amine addition, cyclisation and oxidation, proceeding through the ring open α -adduct and ring closed TIP intermediate species. Until now, no examples of the α -adduct had been isolated and only two examples of the TIP had been isolated. The intermediates that could not be isolated were partially characterized *in situ* by MS and NMR spectroscopy.^{127,129} The two TIP structures that were successfully isolated were synthesised from the diamino compounds, ethylenediamine and 4,4'-diaminodiphenyl ether, using monophasic reaction conditions and were fully characterized. Applying the same methodology to monoamines always resulted in DIP formation as these TIP intermediates are rapidly oxidised by the BEP starting material. The oxidation step to form DIPs using BEP as the oxidant requires a formal hydride transfer and so it is likely that the transition state for this will involve π -stacking of the TIP and the BEP to attain the correct geometry for the transfer to occur. In the case of ethylenediamine the first addition and cyclisation reactions could occur as normal but as the second BEP molecule aligns to undergo the “hydride transfer” the pendant amine side chain could undergo a second α -addition and cyclisation, thus consuming the oxidant and preventing oxidation (Scheme 18).

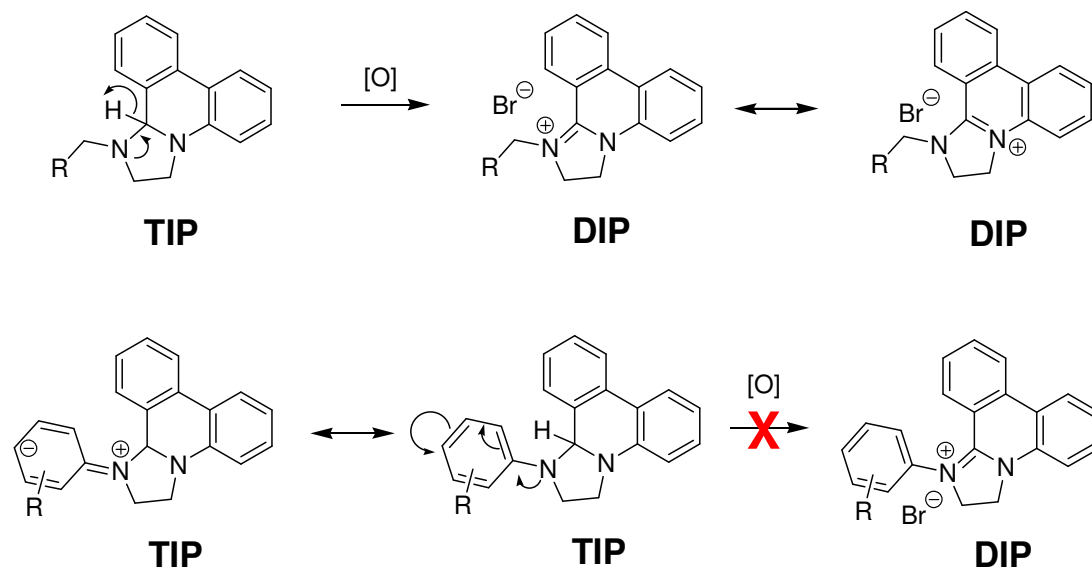


Scheme 18. Prevention of oxidation via second amine addition.

The reaction of the 4,4'-diaminodiphenyl ether is not likely to follow this same hypothesis because of the reduced flexibility of the diphenyl ether link. The inhibition of the oxidation must be due to other factors. The factors affecting the oxidation of aryl-TIPs are discussed later in this section. It should be noted here that both of the TIP dimers can be further oxidised to their DIP analogues by the addition of a further two molar equivalents of BEP or other oxidising agents, the reaction outcome is therefore heavily reliant on the reactant stoichiometry.

For monoamines it is possible to generate the TIP intermediate quantitatively using a biphasic methodology, where the TIP intermediate is separated from the BEP reactant via phase transfer.¹²¹ This method is however limited to hydrophilic primary amines only because the alpha addition step must occur in the aqueous phase. The TIP structures generated from these aliphatic amines are unstable and had only been characterized *in situ* by MS and NMR spectroscopy.^{127,129} It was hypothesised that a synthetic protocol for the isolation of monomeric TIP structures could be developed, providing that the main hurdle of inhibiting the hydride transfer reaction could be overcome.

The reactivity of the TIP structure with respect to oxidation was thought to be highly dependent upon the availability of the *N* lone pair introduced from the amine nitrogen since the inherent high stability of the DIP framework lies within the delocalisation of the positive charge over two conjugated nitrogen centres. Conjugation of the amino-*N* with the side-chain will decrease the ability of this lone pair to stabilize the positive charge in the DIP product, thus reducing the driving force for the oxidation step. Scheme 19 shows the resonance representations of TIP and DIP structures with a non-conjugating alkyl side-chain and a conjugating aryl side-chain.



Scheme 19. Electronic inhibition of TIP oxidation.

4.2 Method development

Aryl amines were an obvious candidate to investigate this electronic effect however they posed a problem as they were incompatible with the synthetic procedures already available. Aryl amines are insoluble in water so the biphasic methodology would separate the amine and BEP reactants and no addition reaction could occur. Monophasic reaction conditions had to be used but the solvent needed to be non-protic to prevent pseudo-base formation of the BEP under the basic reaction conditions yet remain polar enough to solvate the cationic species. DMF and DMSO are both polar aprotic solvents and initial assays carried out in deuterated solvents and analyzed *in situ* by ¹H NMR spectroscopy showed promising results (Figure 14).

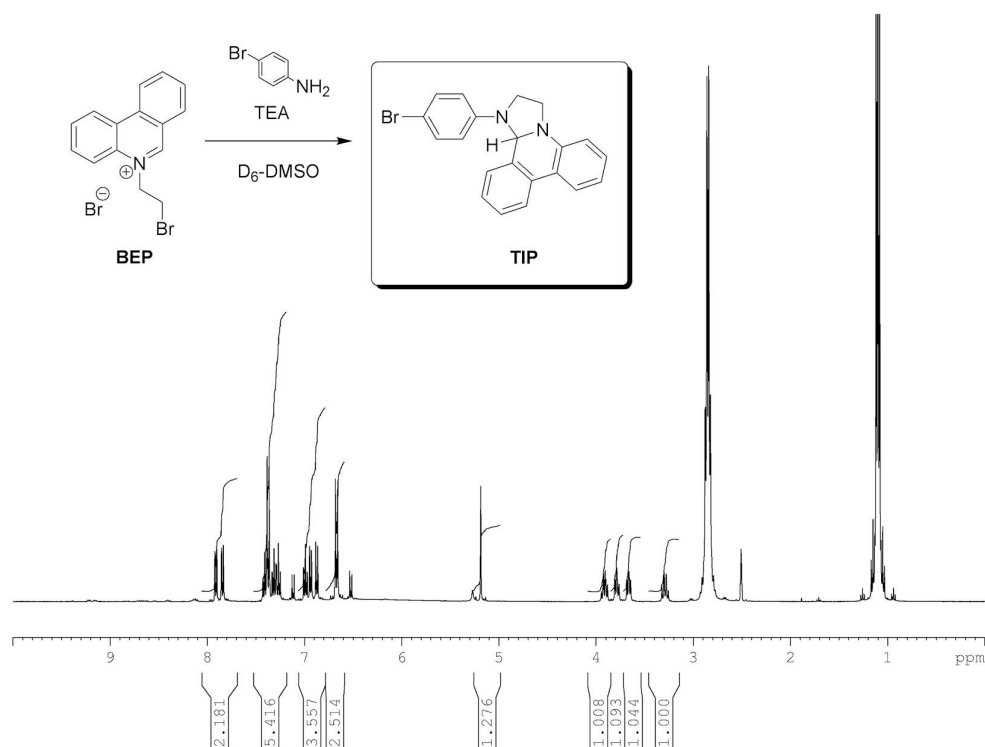


Figure 14. ¹H NMR spectrum of the crude reaction mixture after 15 min. BEP (1eq), 4-bromoaniline (1eq), TEA (3eq). Characteristic high field singlet for TIP α-proton is evident at ~5.2ppm.

The example reaction shows complete conversion of the reactants to the TIP framework with the only byproduct being TEA.HBr, however with the high boiling points of these solvents and their miscibility with water it was thought that isolation and purification of the sensitive products would be problematic. Chloroform was screened as a potential solvent using the same NMR experimental procedure and a similar outcome was observed, almost complete conversion of the BEP and amine to the TIP product (¹H NMR Spectrum shown in Figure 15).

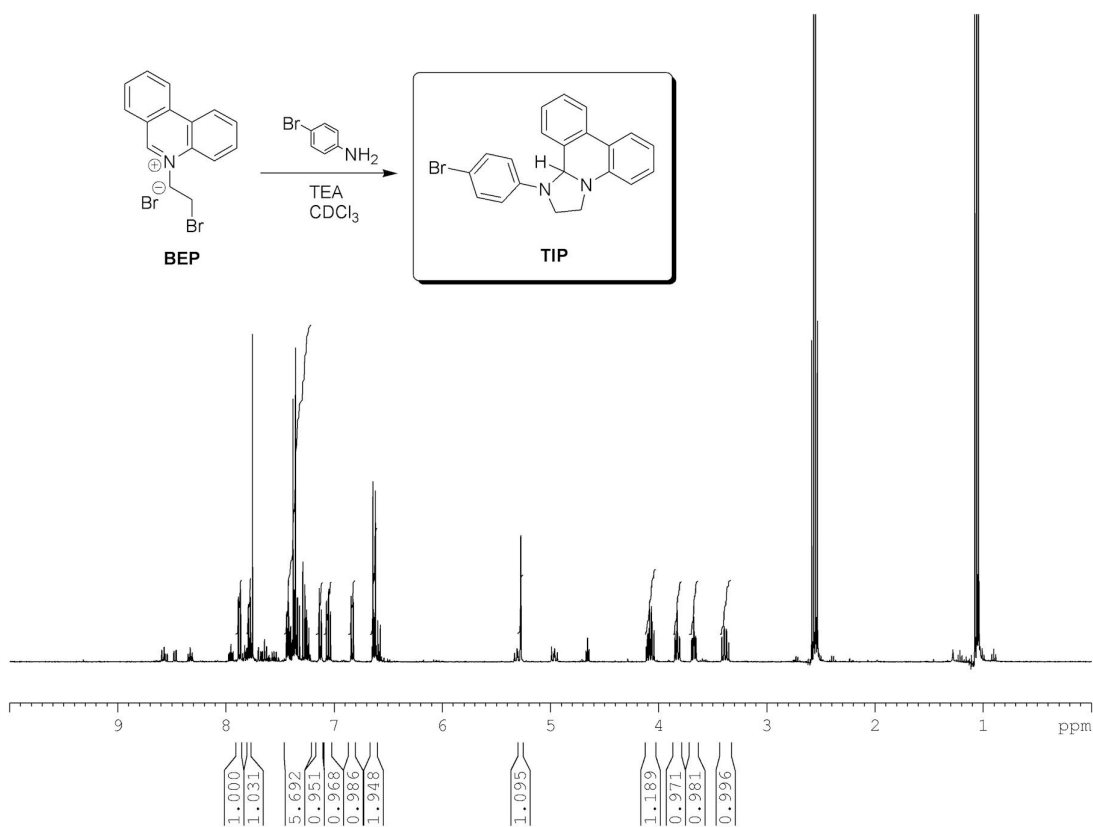
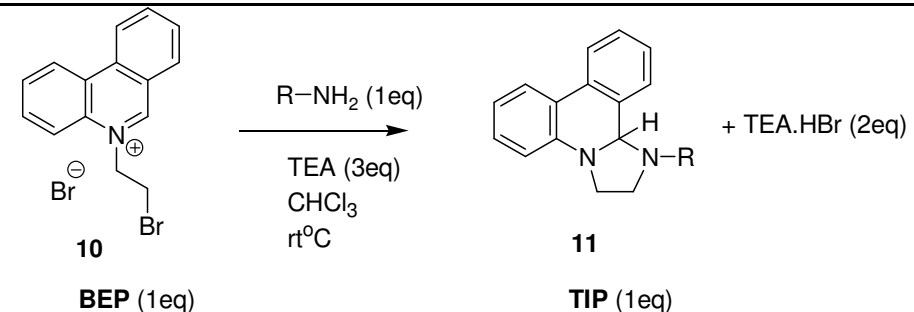
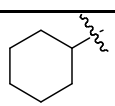
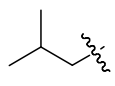
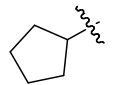
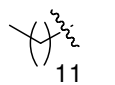
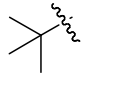
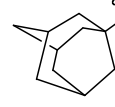
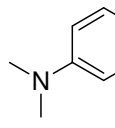
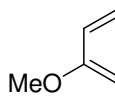
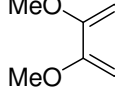
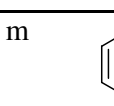
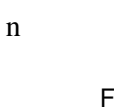
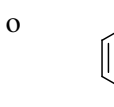
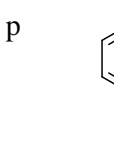
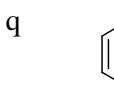
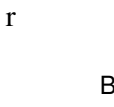
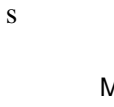
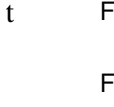
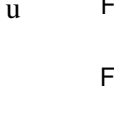
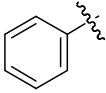
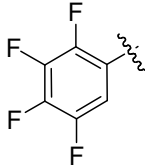
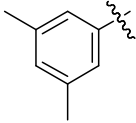
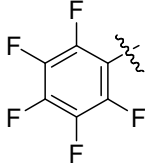
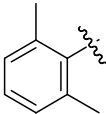
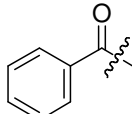


Figure 15. ¹H NMR spectrum of the crude reaction mixture after 3 h. BEP (1eq), 4-bromoaniline (1eq), TEA (3eq). Characteristic high field singlet for TIP α-proton is evident at ~5.2ppm.

Chloroform was subsequently established as the solvent of choice as it overcame the previous issues of product isolation and was still able to solvate the reactants, although somewhat sparingly with respect to BEP. This however proved to be an advantageous trait as it created a visual aid for monitoring the reaction process. The BEP starting material is largely insoluble in chloroform but the products are completely soluble, so as the reactants are consumed the reaction mixture gradually evolves from an off-white suspension to a bright orange solution, thus indicating when the reaction has reached completion. The mother liquor can then be washed with water to remove the salt byproducts, followed by low temperature evaporation of solvent and excess TEA under vacuum to isolate the TIP product. A range of amines were investigated and a number of products containing the desired TIP framework were isolated using this general methodology (Table 1).

Table 1. TIP products obtained via reaction of primary amines with BEP

			
Entry	TIP 11(a-x) R =	pK_a^a Amines a-x	Yield (%) ^b
a		10.57 ± 0 ^c 0.10	
b		10.72 ± 0 ^c 0.10	
c		10.80 ± 0 ^c 0.10	
d		10.80 ± 0 ^c 0.10	
e		10.68 ± 0 ^c 0.10	
f		10.75 ± 70 0.20	
g		6.65 ± 88 ^f 0.12	
h		5.21 ± 89 0.10	
i		4.77 ± 89 0.10	
m		3.20 ± 68 0.10	
n		4.66 ± 85 0.10	
o		1.10 ± 0 ^d 0.10	
p		3.37 ± 76 0.10	
q		2.54 ± 0 ^d 0.10	
r		3.90 ± 78 0.10	
s		2.47 ± 68 0.10	
t		3.64 ± 98 0.10	
u		2.62 ± 60 0.10	

j		4.61 ± 73 0.10	v		1.23 ± 0 ^e 0.10
k		4.84 ± 95 0.10	w		-0.16 ± 0 ^e 0.10
l		4.31 ± 0 ^d 0.10	x		-1.54 ± 0 ^e 0.25

(a) pK_a values calculated using Advanced Chemistry Development (ACD/Labs) Software V8.14 for Solaris (©1994-2009 ACD/Labs); (b) Isolated product yield after normal work-up; (c) Reactive TIPs can not be isolated from monophasic reaction mixture due to consumption via a hydride transfer reaction. Biphasic reaction conditions can overcome the hydride transfer to provide short-lived solutions able to be characterized by MS and NMR spectroscopy; (d) No TIP formed due to steric hinderance; (e) No TIP formed due to reduced amine nucleophilicity (f) 5.0 eq TEA

4.3 Electronic effects of amine substituents

From the list of amine substrates investigated it can be seen that there is indeed a correlation between the availability of the amino-*N* lone pair and reaction success. Increasing the electron withdrawing capacity of the R group reduces the availability of the *N* lone pair for further conjugation and therefore stabilizes the TIP structure. Entries a – e in Table 1 showed no observation of the corresponding TIP products after work-up, which demonstrates that a lack of conjugation from the aliphatic side-chain increases the reactivity of the TIP with respect to oxidation. This was verified by the presence of the oxidation product, DIP, in the product mixture for these reactions. In contrast, aryl amines of varying electron deficiency can be reacted with the BEP starting material to generate the corresponding TIP structures in moderate to excellent yields (Table 1, entries g-u). Partial conjugation of the *N* lone pair to the π -system of the aromatic ring increases the energy barrier for the “hydride transfer” from the TIP to the BEP, therefore allowing complete conversion of the BEP to the TIP product. Direct conjugation of the *N* lone pair to the side-chain in the form of an amide or conjugation to a highly electron deficient aromatic system did not lead to production of any of the corresponding TIP structures (Table 1, entries v-x). This can be explained by the loss of sufficient nucleophilicity through

overcompensating with respect to conjugation of the lone pair. In these cases the majority of the BEP starting material is recovered by filtration; however the presence of phenanthridine in the filtrate indicated conversion of some of the material via an elimination reaction.

In terms of electronic effects, isolation of TIP structures can be seen as a balancing act between having enough nucleophilicity for the primary amine to undergo the first two steps whilst retaining enough electron withdrawing capacity to prevent further oxidation. It was proposed that the pK_a value of the primary amine substrate would be a quick and simple measurement that could be useful in predicting the reaction outcome. From the plot in Figure 16 it can be seen that a window for successful TIP isolation can be estimated for amines with pK_a values of between approximately 2 and 7. It is notable that an absolute correlation between pK_a and reaction outcome cannot be formed as the steric effects of the amine side chains must be also be considered, which are discussed later in this section.

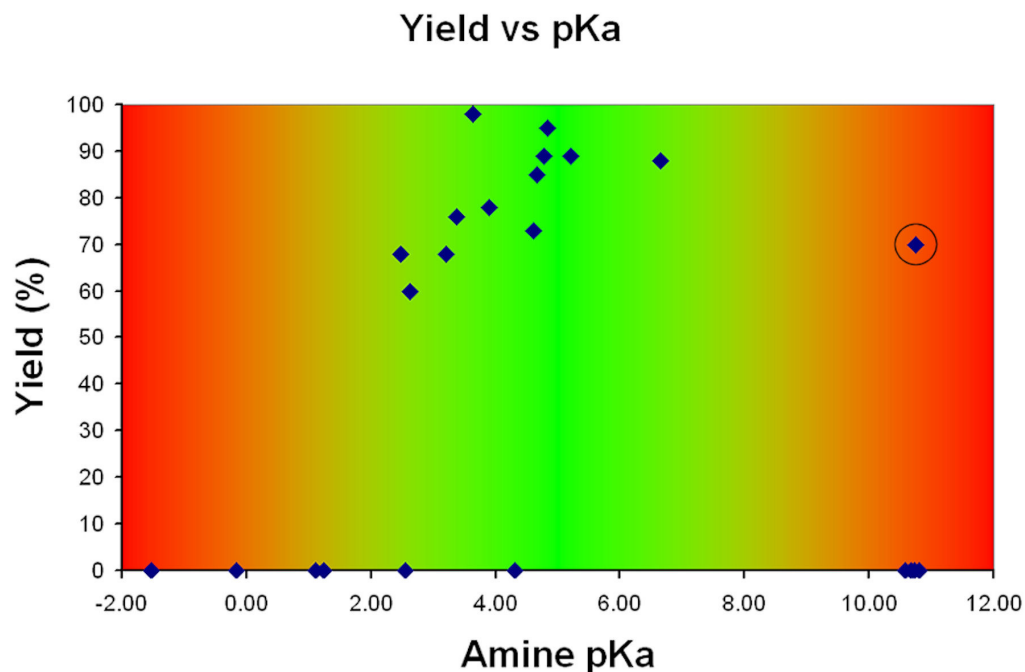


Figure 16. Plot showing TIP Product Yield vs Amine pK_a . Circled data point is for adamantyl-TIP 11f.

The reduction potentials of a selection of DIP analogues **12(a, b, i, j, t)** containing a mixture of aryl and aliphatic side-chains were measured to corroborate the influence of the side-chain on the electronic potential of the DIP framework (Figure 17).

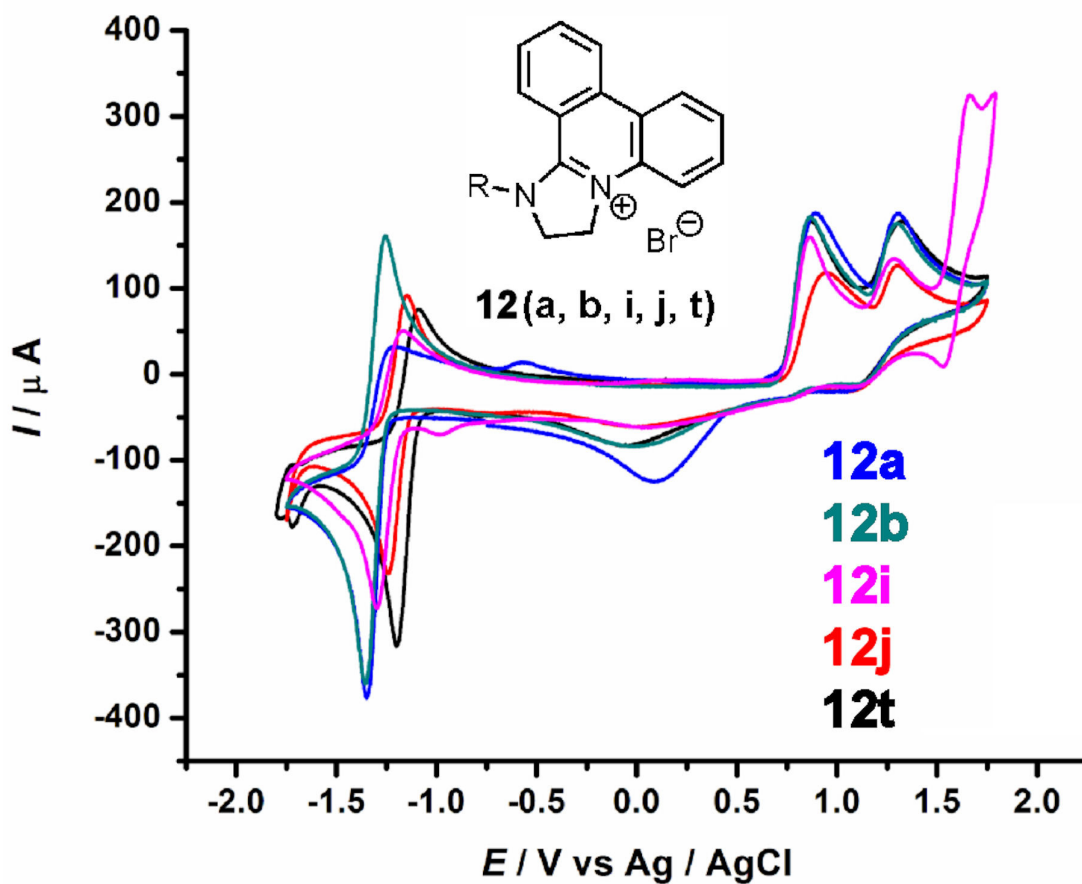


Figure 17. Cyclic Voltammograms of compounds; **12a**, R = cyclohexyl; **12b**, R = isobutyl; **12i**, R = 3,4-dimethoxyphenyl; **12j**, R = phenyl; **12t**, R = 3,4-difluorophenyl; at 100 mV/sec. The reversible reduction waves for all of the DIP compounds occur between *ca.* -1.0 V and -1.5 V. Two irreversible oxidation waves are also observed at *ca.* +0.9 V and +1.3 V

The reversible reduction waves observed for each DIP compound occur between *ca.* -1.0 V and -1.5 V and are assigned to the 2 electron transfer reduction of DIP to TIP. The two irreversible oxidation waves observed at *ca.* +0.9 V and +1.3 V are due to the single electron transfer oxidations of DIP to the radical cation, then to the fully oxidised

imidazophenanthridinium (IP) cation. A plot of the reduction potential values against the amine substituent is shown in Figure 18.

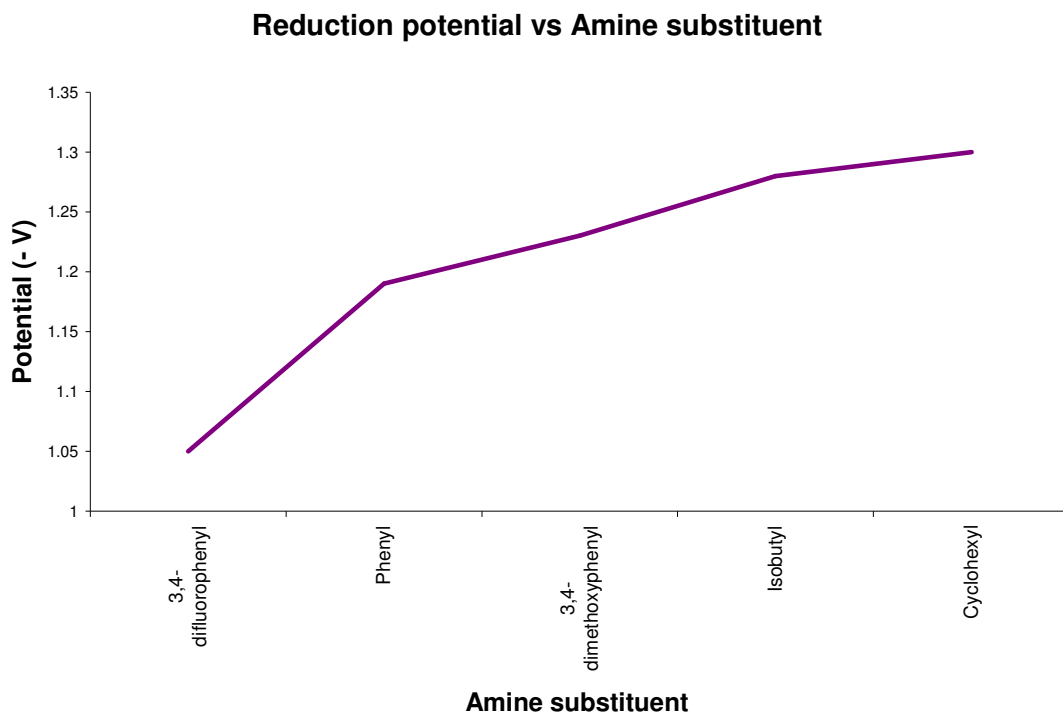
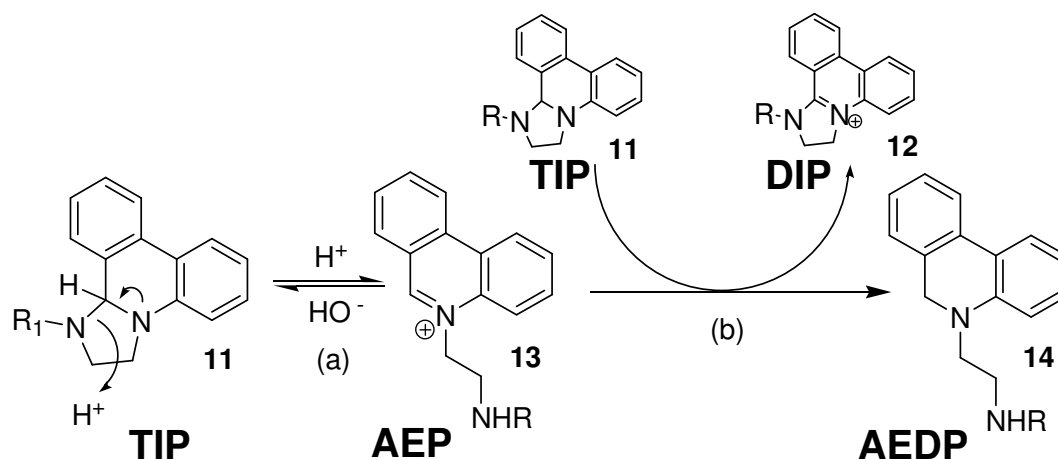


Figure 18. Plot of reduction potential values against the amine substituents. Trend shows an increase in the reduction potentials with decreasing electron withdrawing character of the amine side-chain.

From this data it can be seen that the values for the reduction potentials increase with the decreasing electron withdrawing character of the R groups, this supports the hypothesis that the amine *N* lone pair is involved in stabilizing the positively charged DIP core and that alteration of the R group has a direct influence on this.

Conjugation of the amine side-chain not only affects the electronic potential but also decreases the pK_a of the attached nitrogen centre making it less susceptible to protonation. Preventing protonation of the TIP intermediate is equally as important as preventing oxidation reactions with BEP as protonation of TIP leads to the generation of 5-(2-aminoethyl)-phenanthridinium (AEP) structures **13** via ring opening. This process is

reversible (see section 5.1) however once the AEP core forms it can act as a ‘hydride acceptor’, in a similar fashion to BEP, leading to further oxidation and complete consumption of the TIP in solution (Scheme 20).



Scheme 20. (a) Reversible pH controlled ring opening and closing of TIP-AEP structures; (b) Intermolecular hydride transfer between TIP and AEP to form the oxidation product, DIP, and the reduction product, 5-(2-aminoethyl)-5,6-dihydrophenanthridine (AEDP).

This process is the most likely reason why attempts to isolate TIPs by solvent evaporation of the organic layers from biphasic DIP synthesis procedures have been unsuccessful. Reaction of aliphatic amines such as isopropylamine or isobutylamine with BEP under biphasic conditions will generate a solution of the TIP intermediate in the organic phase.¹²¹ As the incompatible TIP and AEP forms **11** and **13** exist in equilibrium it is easy to see why the relative stability of these aliphatic-TIP analogues are so low, especially in such monophasic solutions: The position of the equilibrium will tend to favor one form over the other depending on the availability of protons in solution and the probability of a successful collision and subsequent hydride transfer between the two forms will be dependent upon concentration. There is no proton source in the organic solution so the TIP is favoured and is stable in mildly basic solutions for a number of hours. However upon removal of the solvent under vacuum the sample is highly concentrated to an oily residue, the probability of the hydride transfer between the TIP and AEP as it forms is now much greater and they will irreversibly react, ultimately leading to the consumption of TIP. This

complicated series of reactions was demonstrated by monitoring the acidification of a solution of isobutyl-TIP in D₆-DMSO with DCI by ¹H NMR spectroscopy. From the spectra in Figure 19 it can be seen that the solution of isobutyl-TIP and isobutylamine (acting as excess base) is converted to an equimolar mixture of isobutyl-DIP and isobutyl-AEDP by addition of DCI.

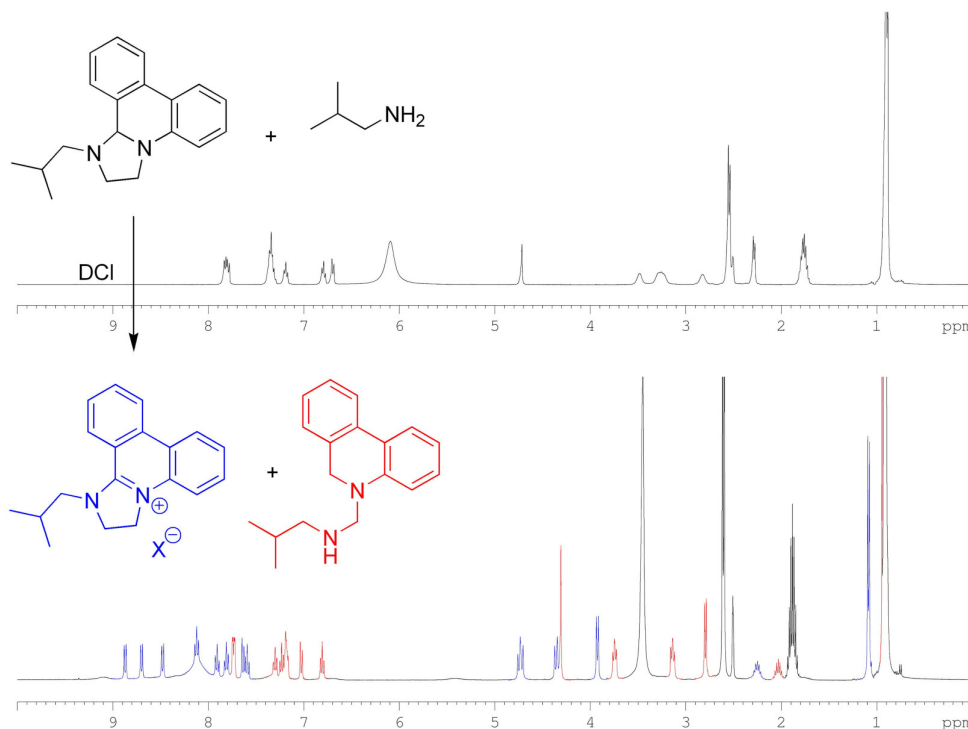


Figure 19. Isobutyl-TIP consumption via protonation and subsequent hydride transfer; structure and assigned peaks for isobutyl-DIP in blue; structure and assigned peaks for isobutyl-AEDP in red.

In the initial solution the excess of the isobutylamine acts as a base so the position of the equilibrium greatly favours the TIP form over the AEP form and the lifetime of any AEP that does form will be too short for any hydride transfer reaction to occur. As the base is neutralised by the addition of the acid, the equilibrium is shifted more towards the AEP form, this allows for both the TIP and AEP forms to coexist in the same solution and undergo the hydride transfer reaction. This produces the equimolar mixture of 5-(2-aminoethyl)-5,6-dihydrophenanthridine (AEDP) and DIP observed.

The thermodynamic driving forces for the hydride transfer reaction are likely to arise from the reduction of steric strain and increased delocalization of the positive charge in the DIP/AEDP products compared to the TIP/AEP reactants. This is corroborated by consideration of the standard electronic potential of the cell, E°_{CELL} . Equations 1, 2 and 3 show the electron half-equations and reduction potentials for the reacting species and the overall redox equation for the hydride transfer.



The resulting electronic potential for the cell is calculated as approximately +0.7 V, which results in a highly negative value for ΔG° from the relationship:

$$\Delta G^\circ = -n F E^\circ_{\text{CELL}}$$

The thermodynamic forces therefore support the agreement for a spontaneous redox reaction under standard conditions.

Although the electrochemical measurements agree with the hypotheses; (i) that a spontaneous hydride transfer occurs between TIP and AEP structures under standard conditions; and (ii) that the electron withdrawing capacity of the amino side-chain can influence the electronic potential for this hydride transfer, they do not support complete inhibition of hydride transfer. Referring back to Figure 17 it can be seen that the reduction potentials for the DIPs with aryl amino side-chains are still very high, $> -1.0 \text{ V}$, which still result in positive values for the electronic potentials, ΔE° , and negative values for ΔG° of hydride transfer. The hydride transfer reaction between aryl TIPs and phenanthridinium based reactants is therefore theoretically possible and there is precedence for the synthesis of aryl-DIPs from aryl-TIPs using BEP as the oxidant.¹²¹ The effects of the aryl side-

chains on the reaction outcome must therefore be a kinetic effect rather than thermodynamic. The rate of the hydride transfer reaction simply becomes relatively slower than the amine addition and cyclisation. Hence the following observations: (i) when the alkyl amine and BEP reactants are present in a 1:1 ratio, *ca.* half of the BEP is converted to DIP and half is converted to BEDP due to the competing hydride transfer; (ii) when an aryl amine and BEP reactants are present in a 1:1 ratio, all of the BEP starting material is converted to TIP since there is no longer competition from the relatively slower hydride transfer; (iii) when either alkyl or aryl amines and BEP reactants are present in a 1:2 ratio, half of the BEP is converted to DIP and half is converted to BEDP since the BEP is in excess with respect to the amine. Electronic effects from the amine substituents contribute to stabilizing the TIP with respect to oxidation and protonation but they are unlikely to be solely responsible, other effects such as sterics must also be considered.

4.4 Steric effects of amine substituents

It was found that steric effects are indeed highly influential on the reaction outcome and have an effect at each stage of the multi-step mechanism. From the series of successfully isolated TIP structures (Table 1, entries f - u) a set of structural isomers were selected to compare these effects. From the comparison of electronically similar isomeric pairs (Table 1, entries k - r) it can be seen that aryl substrates functionalized with bulky substituents at the ortho-positions are unable to form the TIP products unlike those that are either meta or para substituted. The only ortho-functionalized substrate able to undergo conversion to the TIP product was 2-fluoroaniline (Table 1, entry m), where the fluorine atoms relatively small steric bulk is not sufficient to hinder the addition and cyclisation steps. The reactions of 2- and 4-bromoaniline were repeated in D₆-DMSO to allow the difference in reactivity for the two isomers to be directly compared (Figure 20).

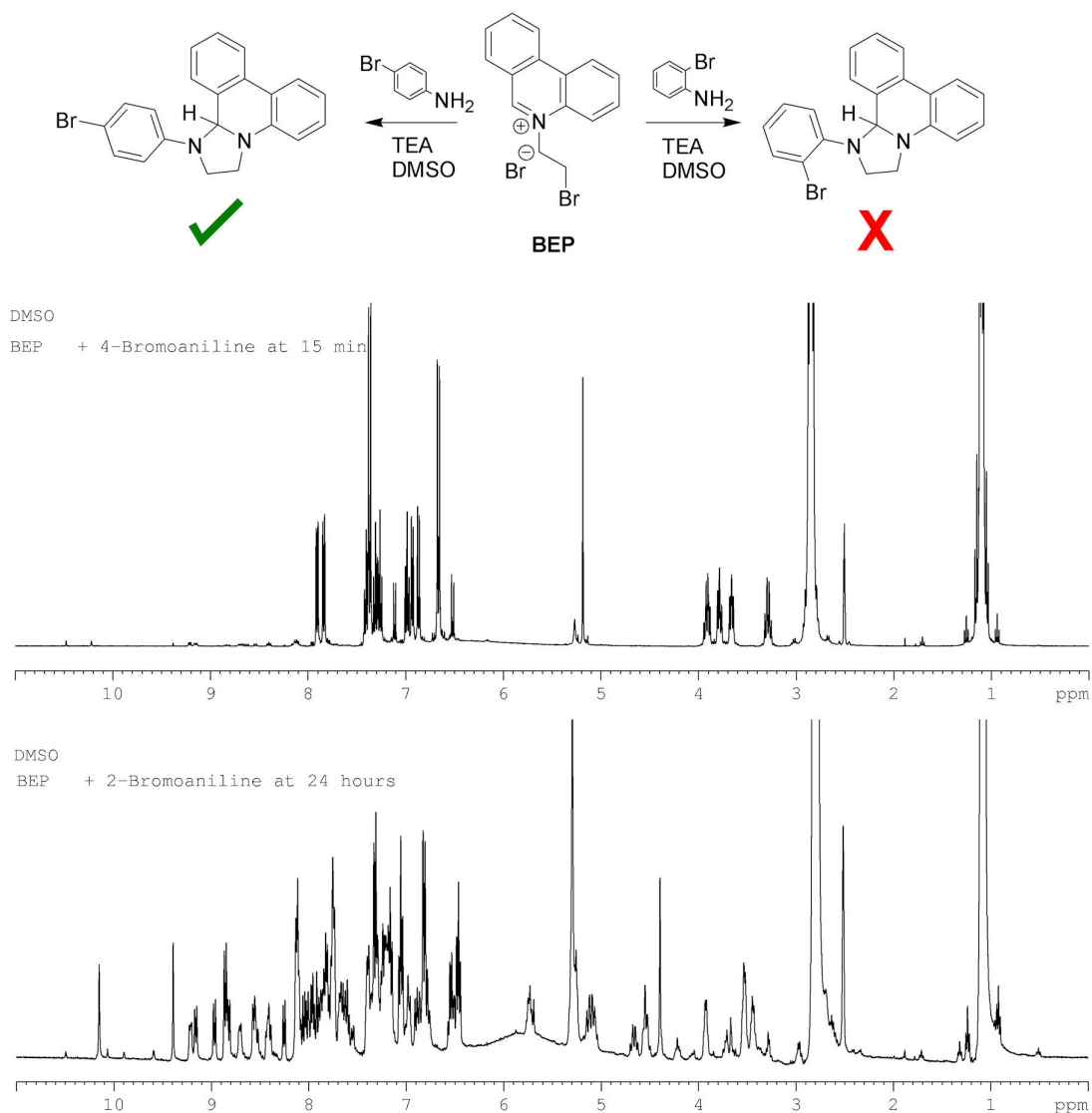
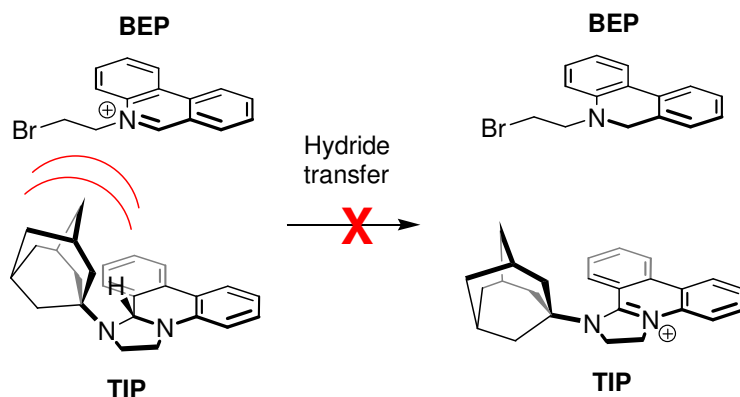


Figure 20. ^1H NMR spectra of the crude reaction mixtures for; (top) BEP (1eq), 4-bromoaniline (1eq), TEA (3eq); and (bottom) BEP (1eq), 2-bromoaniline (1eq), TEA (3eq).

The NMR reactions showed that the BEP starting material was consumed but no signals correlating to the TIP intermediate were observed even after 24 hrs for the reaction of 2-bromoaniline, compared to the reaction of 4-bromoaniline which had reached complete conversion to the TIP in less than 15 min. The ^1H NMR spectrum of the 2-bromoaniline reaction shows a complex mixture of components but some of the signals were able to be assigned to the amine starting material and also phenanthridine. A possible explanation for

this observation could be that in these cases the highly reactive BEP starting material was unable to react with the amine so instead it underwent an elimination reaction in the presence of the TEA base.

The isolation of the TIP analogue of adamantamine (Table 1. entry f) was a very important discovery as this highlighted the stabilization of the TIP structure primarily through steric effects rather than electronic inhibition. The amine substrate is a non-conjugated aliphatic amine with a relatively high pK_a value of 10.75. With no conjugation of the amino-*N* lone pair and the adamantyl group it can be assumed that this compound will have a similar electronic potential to other aliphatic TIP analogues. The inhibition of the hydride transfer and subsequent TIP stabilization must therefore be influenced purely by the steric bulk of the amine side-chain alone. A schematic representation of the steric inhibition of the hydride transfer is shown in Scheme 21.



Scheme 21. Steric repulsion from bulky adamantyl side-chain inhibits the hydride transfer reaction between the TIP and BEP.

To confirm the inhibitory effects of bulkier substituents on hydride transfer, a comparative NMR study of the reactions of isobutyl and adamantyl TIPs **11b** and **11f** with BEP in D_6 -DMSO was carried out. In the former case the reaction resulted in almost instant conversion of TIP **11b** to DIP **12b** as the BEP reactant is reduced, whereas in the latter case both TIP **3f** and BEP reactants were clearly visible in the reaction mixture even after 9 hours.

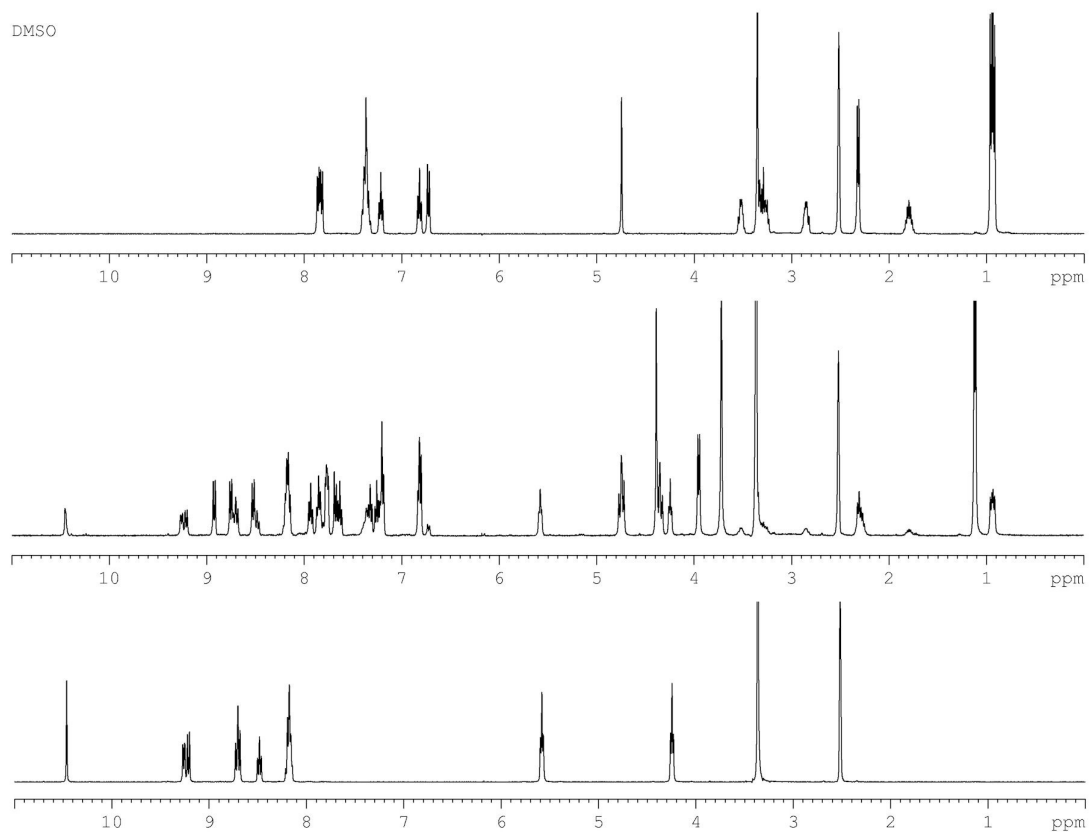


Figure 21. ^1H NMR spectra of; (top) solution of isobutyl-TIP 12b in DMSO; (bottom) solution of BEP oxidant in DMSO; (middle) mixed TIP and BEP solutions after 5 min. Note the residual BEP peaks in the mixture are from the slight excess with respect to TIP.

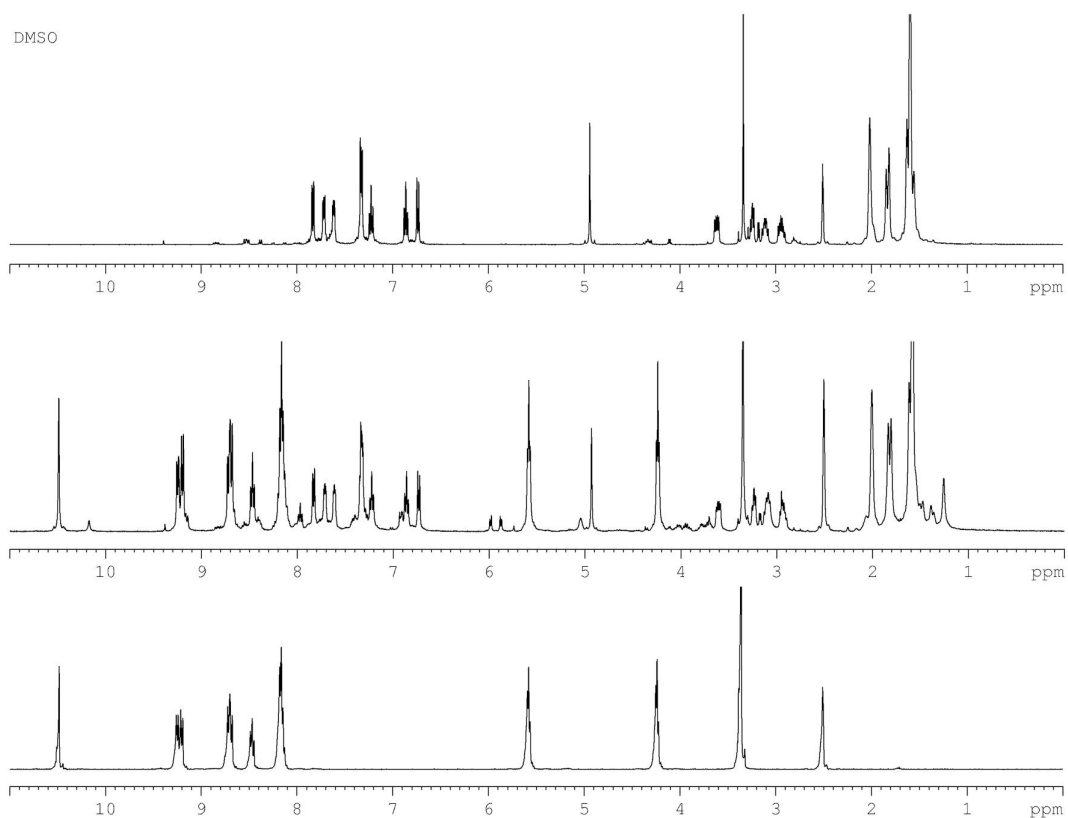


Figure 22. ^1H NMR spectra of; (top) solution of adamantyl-TIP **12f** in DMSO; (bottom) solution of BEP oxidant in DMSO; (middle) mixed solutions after 9 hours.

As both amines involved have almost exactly the same $\text{p}K_{\text{a}}$ (10.72 vs 10.75, Table 1 entries b and f) the difference in reactivity these TIPs exhibit towards the BEP oxidant must come from the difference in steric bulk of the side-chain alone. To explain this steric inhibition, more detailed structural information for the TIP framework was required.

4.5 TIP structure analysis

The isolated TIP frameworks were fully characterized by traditional techniques: melting point, ^1H and ^{13}C NMR, IR, MS, HRMS and elemental analysis, all of which were in agreement with the proposed TIP structure. A very distinctive aspect of the TIP structures was the presence of a sharp singlet at ~ 5 ppm in the ^1H NMR spectra due to the α -proton. The ^1H NMR spectrum of dimethylphenyl-TIP **11k** is shown in Figure 23.

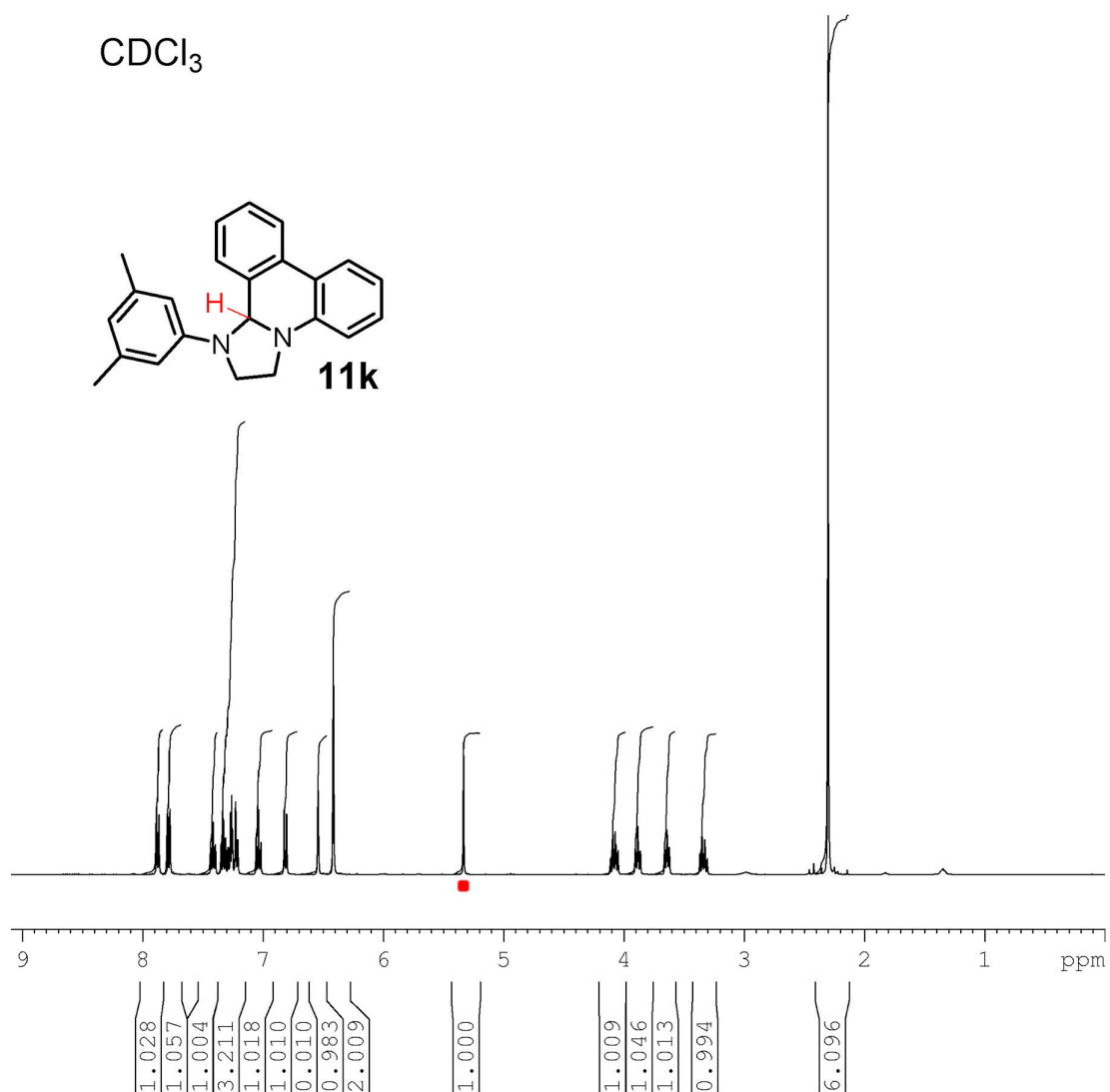


Figure 23. ¹H NMR spectrum for dimethylphenyl-TIP 11k with the distinctive α -proton singlet highlighted red.

The assignment of the remaining proton signals was not as trivial due to the high number of overlapping signals and identical coupling constants so a COSY spectrum was also obtained (Figure 24).

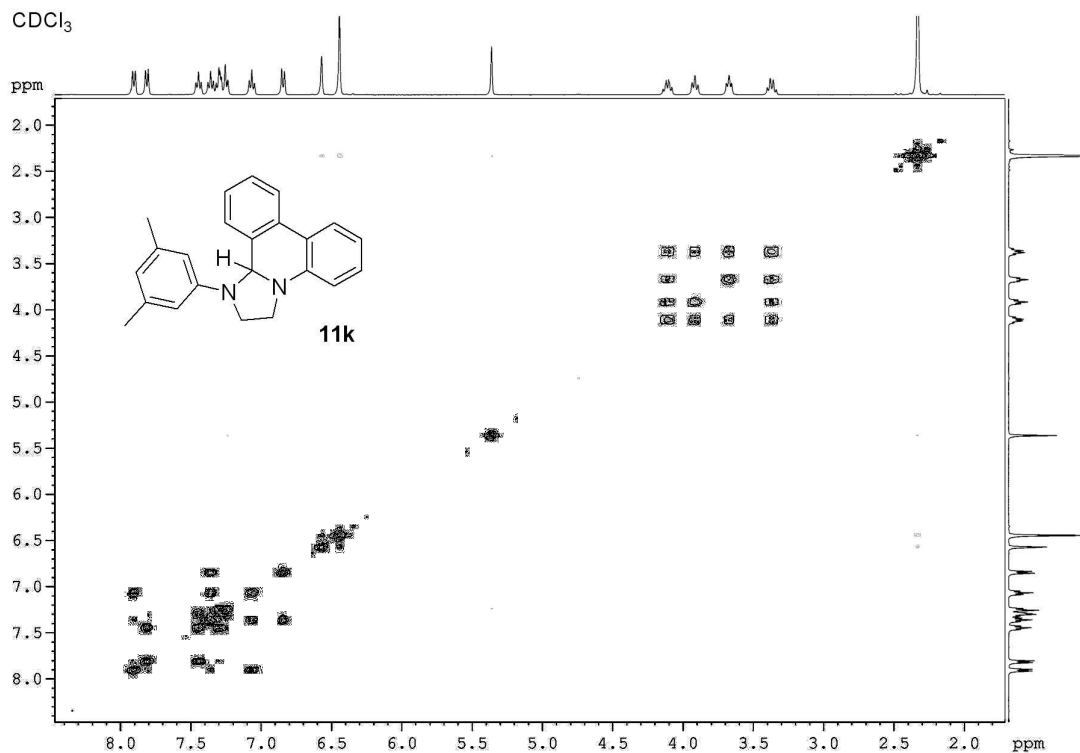


Figure 24. COSY plot for dimethylphenyl-TIP 11k. Note the lack of coupling for the α -proton singlet and the highly symmetrical splitting patterns for the aliphatic ring protons.

From this plot, almost all of the individual proton assignments could be made. These assignments are shown in Figure 25. An interesting feature of this spectrum is the unexpectedly simple splitting pattern for the aliphatic ring protons. The chiral centre makes all protons in the ring inequivalent and individual coupling should therefore be observed between all of them to give rise to four signals with ddd splitting. Indeed four signals are observed however none appear to be split in this manner, two appear to be quartets, and two appear to be triplets in the 1D proton spectrum. The COSY spectrum shows two that H_i & H_l (Figure 25) couple to each other as well as the other two remaining ring protons, H_j & H_k , and are therefore ddd's, but because the J values are all equivalent they appear as quartets. The remaining two protons, H_j & H_k , show the same identical coupling to the other two protons, but do not couple to each other, and therefore appear as triplets. The lack of coupling between protons H_j & H_k is due to the dihedral angle between these two C-H bonds giving J values of 0 from the Karplus equation:

$$J_{jk} = A + B\cos^2\Phi \quad (0^\circ \leq \Phi \leq 180^\circ)$$

A and B are experimentally determined constants; the maximum coupling is observed when $\Phi = 180^\circ$ or 0° ; and the minimum coupling is observed when $\Phi = 90^\circ$, as is the case here.

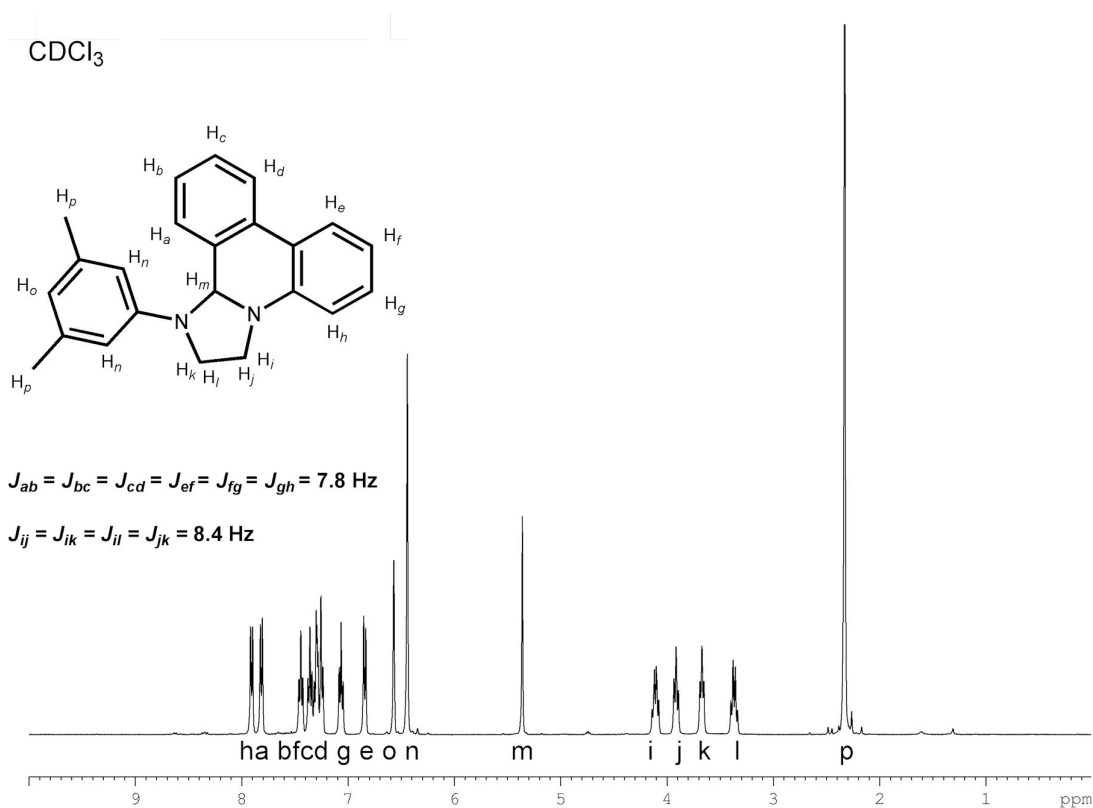
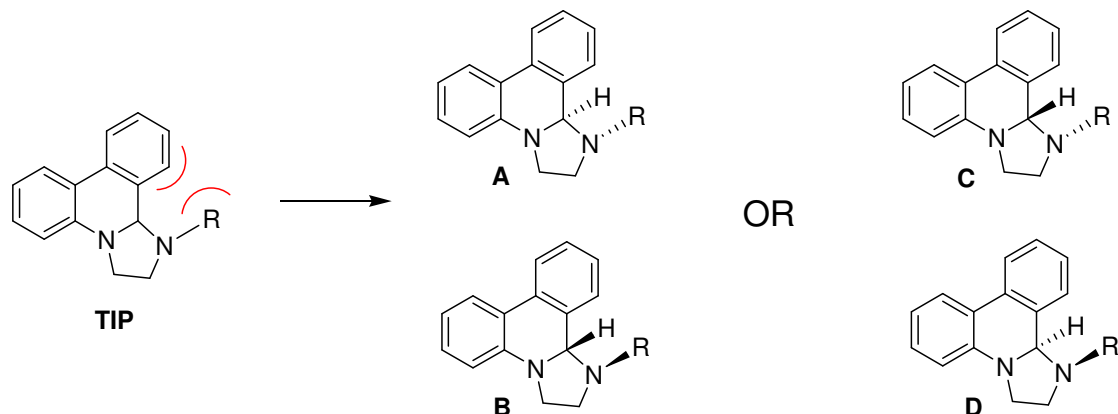


Figure 25. ¹H NMR spectrum of dimethylphenyl-TIP 11k with assigned signals.

The higher level of saturation in the TIP ring system induces non-planarity and creates uncertainty over the spatial positioning of the relevant substituents, the α -carbon and the amine side-chain. As the proximity of the R group to the phenanthridine ring system is very close when they are in the same plane, energetically unfavourable steric clashes force the R group out of the plane of the phenanthridine (Scheme 22). The position of the R

group with respect to the α -proton can therefore either be *syn*, A and B; or *anti*, C and D (note there is no energy difference between enantiomers).



Scheme 22. Possible conformations of TIP structure.

The hypothesis of steric inhibition could only be plausible if the orientation of the amine side-chain and the α -proton of the TIP are in a *syn* configuration with respect to each other, if they were *anti* then the size of the amine side-chain would be of little consequence to the outcome of the hydride transfer reaction. Fortunately crystals suitable for single crystal X-Ray diffraction were able to be grown for a TIP structure, 1-(4-fluorophenyl)-TIP, **11n**. Evaporation of a saturated diethyl ether solution of **11n** yielded large rod-shaped crystals from which the absolute structure was determined (Figure 26.) The structure crystallised as a racemate for which the R enantiomer is shown, the image shows the phenyl side chain deflecting out of the plane of the phenanthridine ring system as expected but most importantly in the same direction as the α -proton.

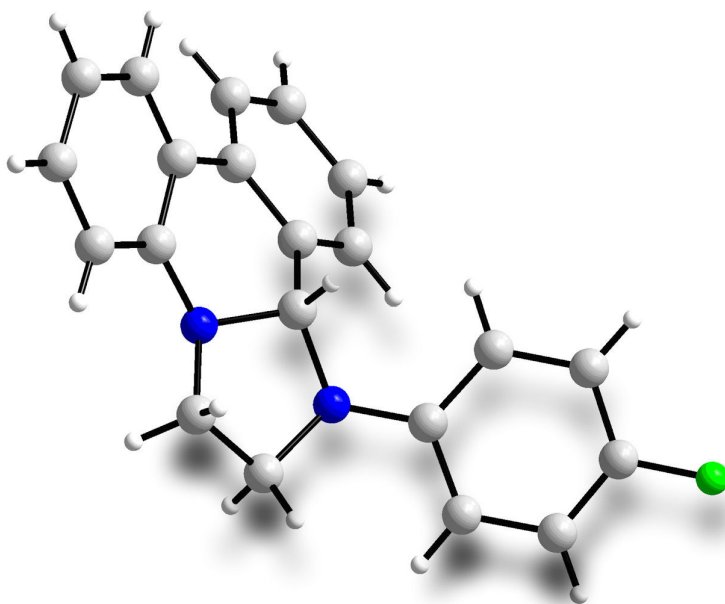


Figure 26. Ball and stick representation for structure 11n shows phenyl side-chain and α -proton in *syn* arrangement.

The crystal structure gave absolute confirmation of the structural conformation in the solid state but information on the conformation in solution was still required. Taking into consideration the favourable and unfavourable energy contributions for all of the possible conformations, the following arguments can be made to identify the *syn* arrangement as the predominant conformation in solution as well. For the envelope conformation of the 5-membered ring there are four possible conformations that can interconvert by ring flipping and pyramidal inversion processes (Figure 27). Since the 5-membered ring is part of a fused-ring system, the ring flipping process is severely inhibited and the system is effectively “locked” in the conformations where the α -proton is axial (H_{ax}). The two possible conformations remaining can then either accommodate the amine R-group on the same face as the α -proton (*Syn*; R_{eq} , H_{ax}) or on the opposite face to the α -proton (*Anti*; R_{ax} , H_{ax}). In ring systems where pyramidal inversion is possible, equatorial substituents are preferred.¹⁵⁹ The (*Syn*; R_{eq} , H_{ax}) conformation is therefore theoretically the most stable arrangement, and will be the most predominant conformer in solution as well as that observed for the crystal structure.

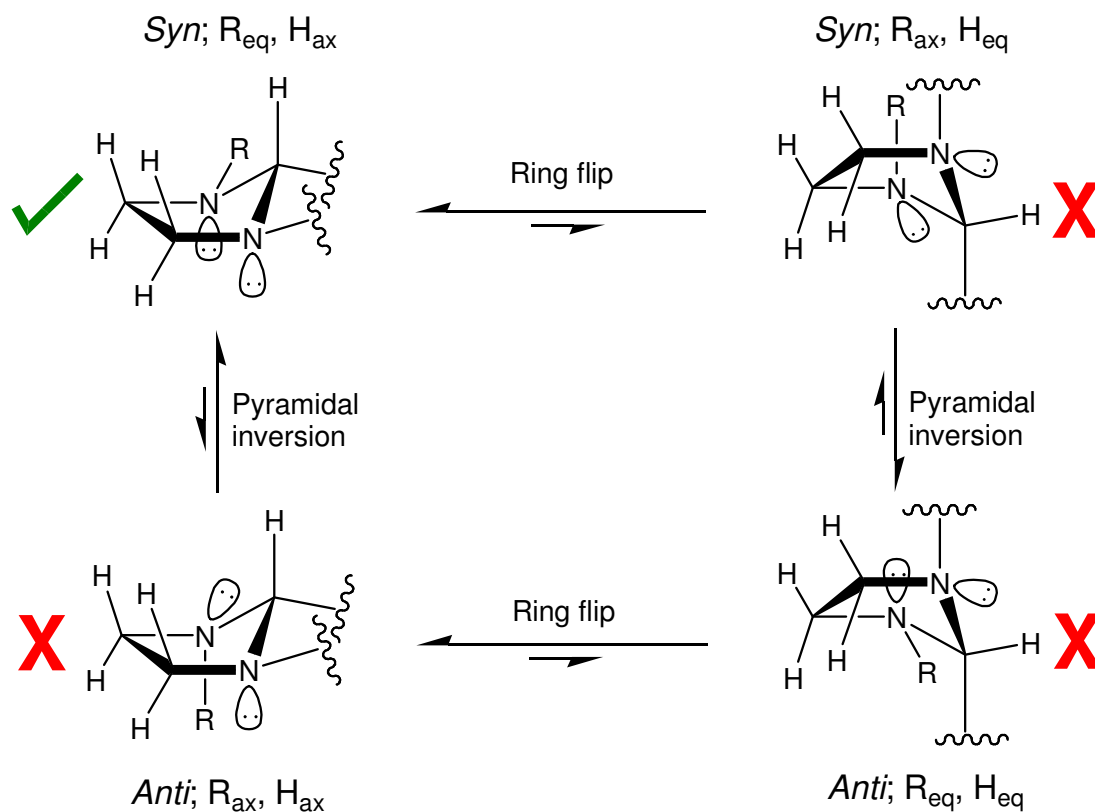


Figure 27. Energetically favourable and unfavourable conformations of TIP heterocycles.

Irradiation of the α -proton signal (5.29 ppm in CDCl_3) for a sample of 4-fluorophenyl-TIP **11n** also gave a strongly positive NOE with the phenyl ring protons meta to the fluorine (6.71 ppm in CDCl_3). The spectra are shown in Figure 28. It is important to note here that pyramidal inversion is faster than the NMR experiment timescale therefore it is impossible to state that the (*Syn; R_{eq}, H_{ax}*) conformation is the sole, or even the major conformation existing in the solution state, it simply proves that this conformation is accessible at room temperature in solution.

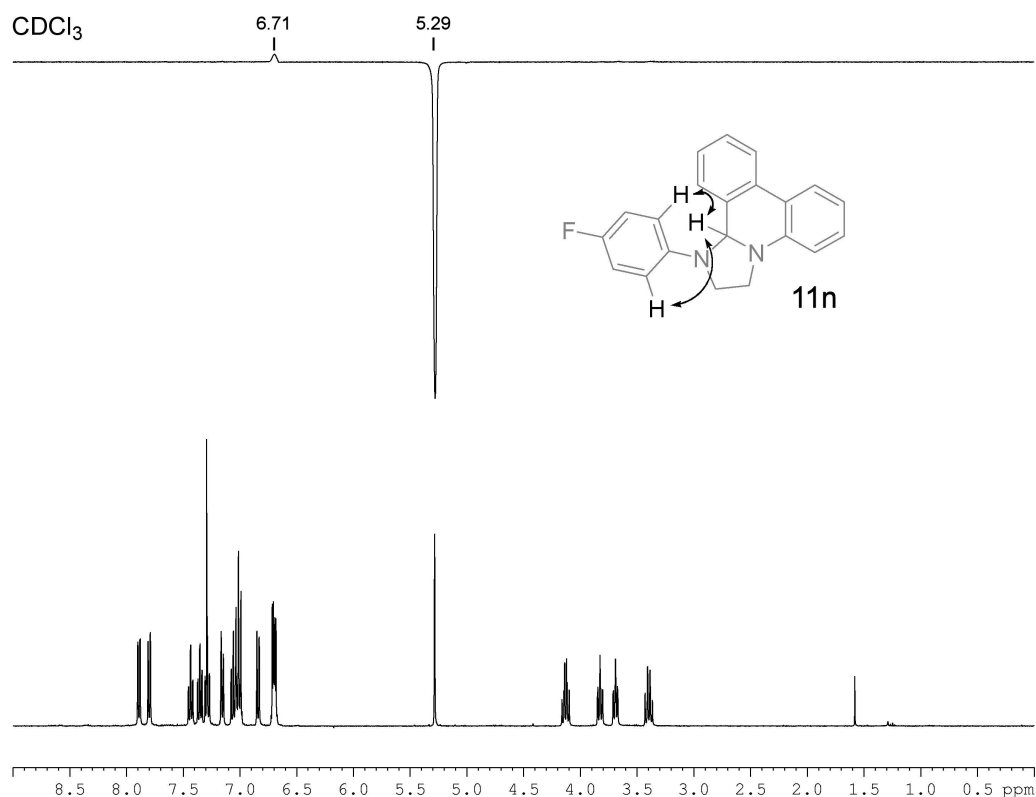
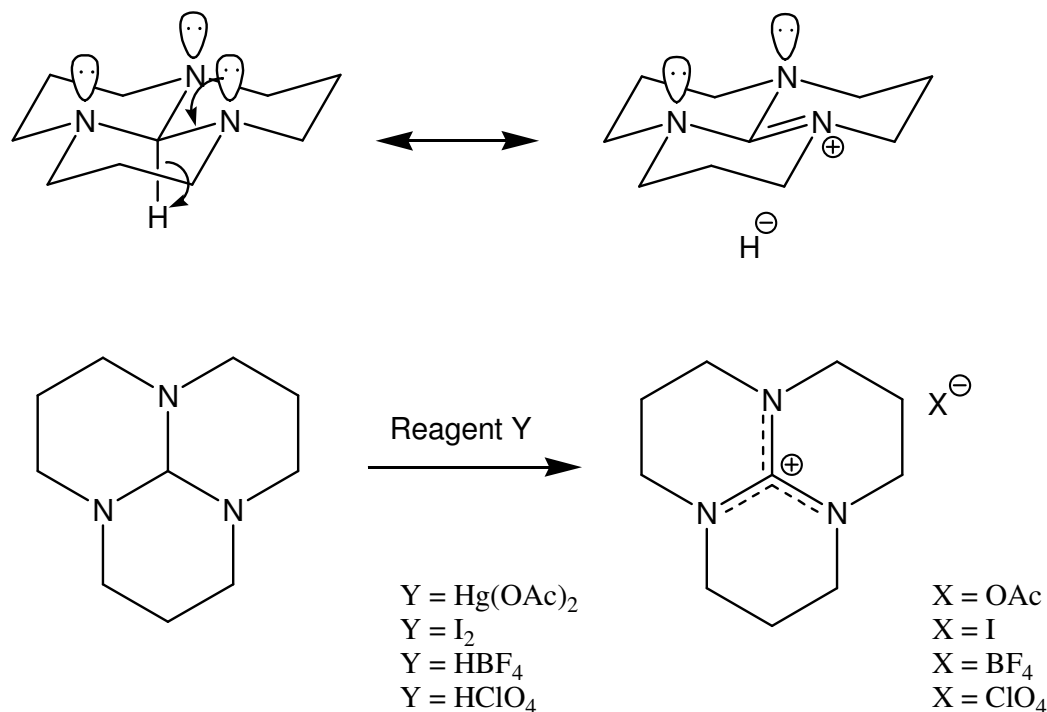


Figure 28. ^1H NMR spectrum and overlaid NOE spectrum for 4-fluorophenyl-TIP 11n.

Incidentally this structural data could also offer another explanation for the high reducing power of the TIP framework. The proposed conformation requires both *N* lone pair orbitals to align antiperiplanar to the C-H bond (See Figure 27, *Syn*; R_{eq} , H_{ax}). Tricyclic orthoamide structures can adopt a similar arrangement which greatly affect the properties of the C-H bond.¹⁵⁹ The anti periplanar arrangement permits mixing of the lone-pair orbitals with the σ_{CH}^* , weakens the C-H bond, and increases the electron density at the methine hydrogen.^{160,161} Scheme 23 shows a perhydrotriazaphenalane structure and some reactions that demonstrate its reductive nature.



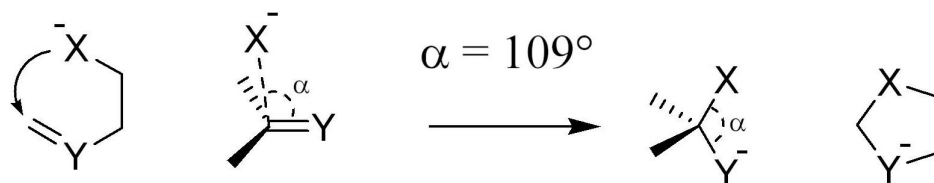
Scheme 23. (top) graphical representation of the anomeric effect from the *N* lone pair orbitals; (bottom) reactions of a perhydrotriazaphenalane with common oxidants.

5 LOCKABLE MOLECULAR SWITCH

5.1 pH Controlled Reversible Cyclisation

The isolation of the TIP framework allowed investigations of their physical and chemical properties to be carried out. One result of these investigations was the behaviour of the TIPs in acidic media, where protonation of the ring nitrogen leads to ring opening to form a dicationic AEP species (see section 4.3). The reversibility of this ring opening/closing was initially thought to be irreversible due to the selection rules proposed by Baldwin *et al.*^{128,162-164} These rules state that a *5-endo-trig* cyclisation is energetically disfavoured due to the preferred angle of nucleophilic attack, $\alpha = 109^\circ$, only being achievable through severe distortion of bond angles and distances.

5-endo-trig



5-exo-tet

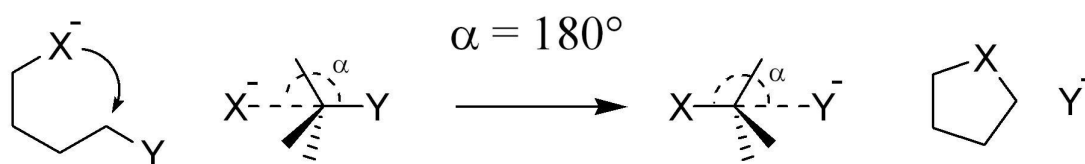
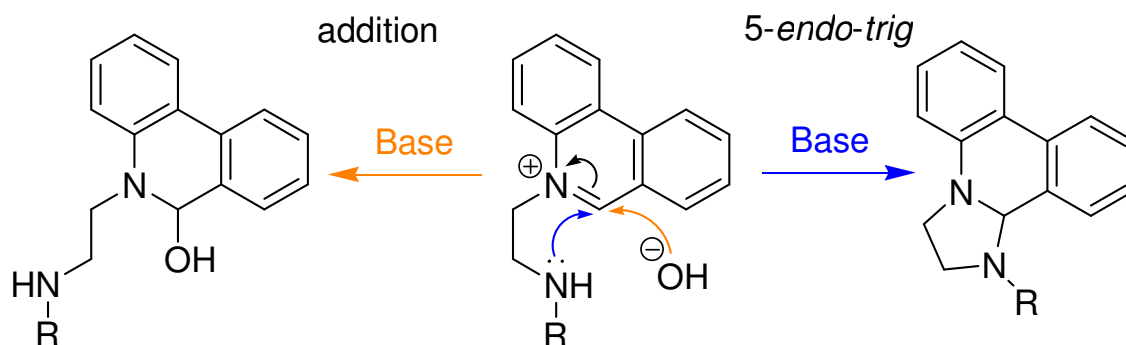


Figure 29. Diagram showing preferred trajectories for terminal atoms in selected 5-membered ring cyclisations.

The distance in the chain length between terminal atoms is not sufficient to achieve the desired 109° trajectory required for the *5-endo-trig* cyclisation but it is long enough to allow the 180° angle required for a *5-exo-tet* cyclisation. In the mechanism for DIP formation these selection rules are obeyed as the cyclic TIP intermediate was proved to form via an α -addition step followed by a *5-exo-tet* cyclisation rather than an S_N2 substitution followed by a *5-endo-trig* cyclisation.¹²¹ In cases where there is an option for 2 cyclic products these rules are generally obeyed, although there are a few exceptions.¹⁶³

In the case of the TIP/AEP cyclisation it was initially thought that rather than undergo the disfavoured *5-endo-trig* cyclisation of the amine, an intermolecular addition of hydroxide would be preferred.



Scheme 24. Scheme showing the possible α -addition or cyclisation products for the reaction of AEPs in aqueous base.

At the time, distinction between the two possible products was ambiguous because MS and NMR spectroscopy were the only techniques available since the compounds could not be isolated. Isolation of the stable TIP structures was an important discovery in answering this question. The first reaction to corroborate the preference for cyclisation over hydroxide addition was the reversible acid-base initiated ring opening and closing of 4-fluorophenyl-TIP. Both the TIP and AEP structures had been isolated and unambiguously characterised, so this was an ideal model for this investigation. A solution of 4-fluorophenyl-TIP in D_6 -DMSO was acidified by addition of DCl followed by basification with TEA and the solution was analysed by ^1H NMR spectroscopy throughout (Figure 30).

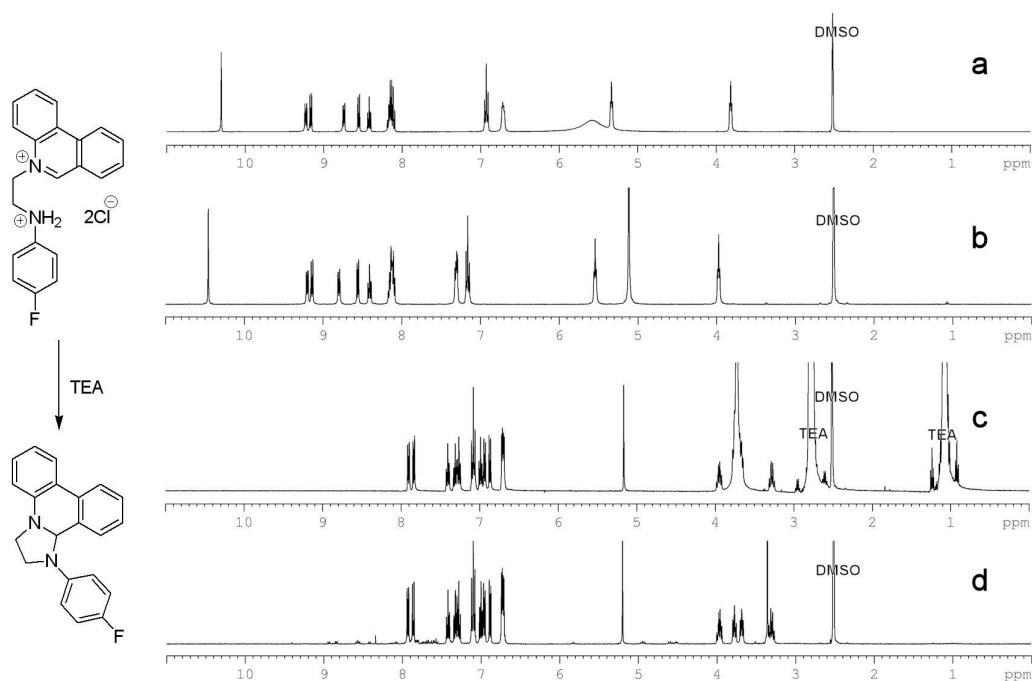


Figure 30. ^1H NMR spectra showing AEP – TIP cyclisation: (a) reference spectrum of characterised 4-fluorophenyl-AEP dichloride salt; (b) experiment spectrum after DCl addition; (c) experiment spectrum after TEA addition; (d) reference spectrum of characterised 4-fluorophenyl-TIP.

This reaction confirmed the quantitative conversion of the AEP to the TIP upon addition of TEA, however the solvent is aprotic and the base is non-nucleophilic, so it is not an exact comparison for hydroxide addition. A second experiment was therefore carried out, where a biphasic solution of isobutyl-AEP in water and EtOAc was basified by addition of Na_2CO_3 , and after separation of the phases, NBS was added to the organic phase which resulted in precipitation of isobutyl-DIP. The yield of DIP collected by filtration was quantitative with respect to the AEP starting material, confirming that deprotonation and cyclisation is preferred even in the presence of nucleophilic bases like hydroxide.

5.2 Redox Susceptibilities

The equilibrium between the AEP and TIP forms was discussed earlier to highlight the issue of “hydride transfer” from TIP species to AEP and the problems this creates for isolation of these compounds (see section 4.3). The presence of this potential for hydride

transfer is a result of the contrasting redox properties of the AEP and TIP structures, TIPs contain a tetrahydroimidazo moiety which is easily oxidised and is therefore a “hydride donor”, AEPs contain a phenanthridinium moiety which can be easily reduced and is therefore a “hydride acceptor”. To investigate the solution electrochemistry of these compounds, cyclic (CV) and square wave (SWV) voltammetries were obtained for the isobutyl-DIP and isobutyl-AEP structures (CV diagrams shown in Figure 31, for SWV data see experimental section 9.4.3).

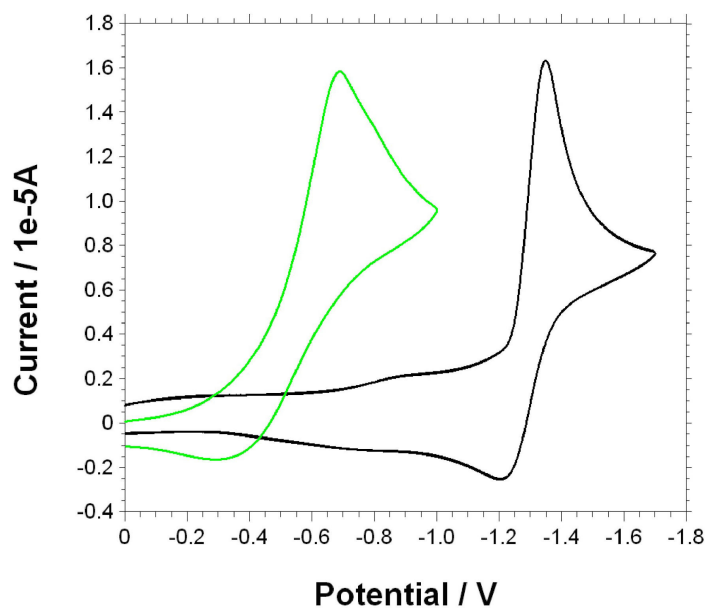


Figure 31. Cyclic voltammograms of isobutyl-DIP (black) and isobutyl-AEP (green)

The CV data shows a pseudoreversible redox wave for the isobutyl-DIP, whereas the redox wave for the isobutyl-AEP is irreversible. SWV estimates the reduction potential of the isobutyl-DIP and isobutyl-AEP to be -1.3 V and -0.6 V respectively, which was in correspondence with our expectation that the DIP-based system is significantly harder to reduce than the AEP species. Such a large difference in reduction potentials is in agreement with our spectroscopic data, confirming the possibility of hydride transfer (see section 4.3).

5.3 Realization of Dual-mode Switching

Combination of the pH controlled cyclisation and the contrasting redox properties provided an opportunity to combine these two aspects to produce a 4-pole switchable organic system. The phenanthridine-based TIP and AEP heterocycles form the reversible switching mode as the two forms are interchangeable and can be converted from one to the other under pH control. These two forms can then also be further manipulated through exploitation of their redox potentials to convert them to their respective “pH-inert” forms, DIP and AEDP, which forms the irreversible switching mode or “locking” mechanism. Figure 32 shows how the 4 forms are connected within the switch.

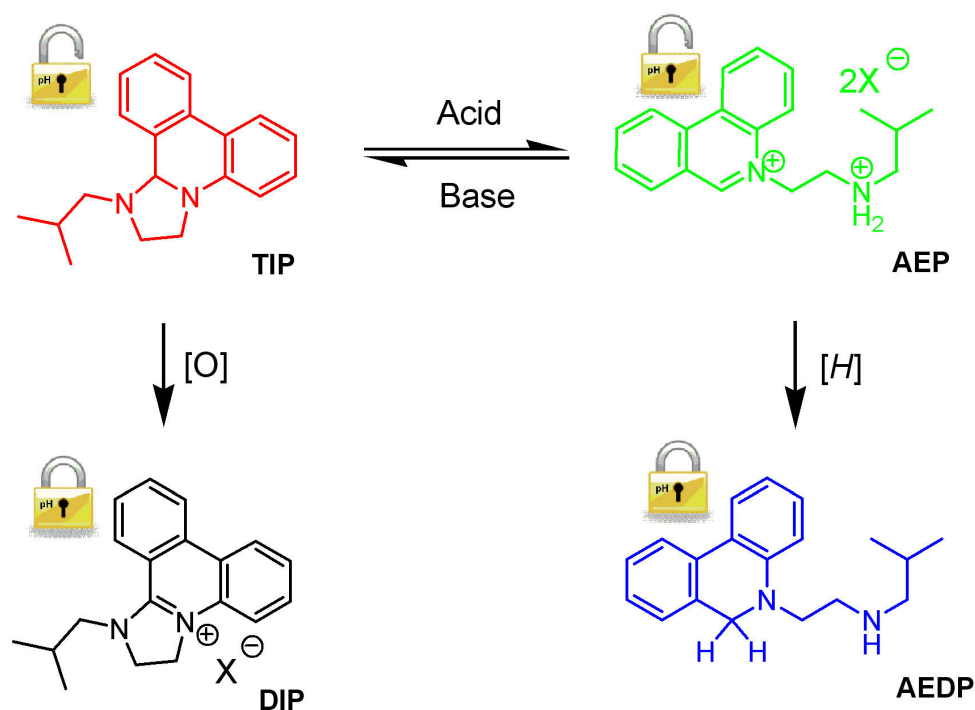


Figure 32. Scheme showing the reversible pH switching and irreversible redox switching modes.

Since the DIP and AEDP forms are inert to pH with respect to the cyclisation, the reduction and oxidation steps can be seen to irreversibly lock the pH switching mechanism.

5.4 Operation of the Molecular Switch

Although synthetic routes to each of the four switchable states were available a suitable method to identify each of the states and observe the switching mechanism *in situ* had to be devised. All structural forms had very good chromophores and were therefore active to both UV absorption and fluorescence emission spectroscopy, the spectra for each of the four structural forms are shown in Figure 33.

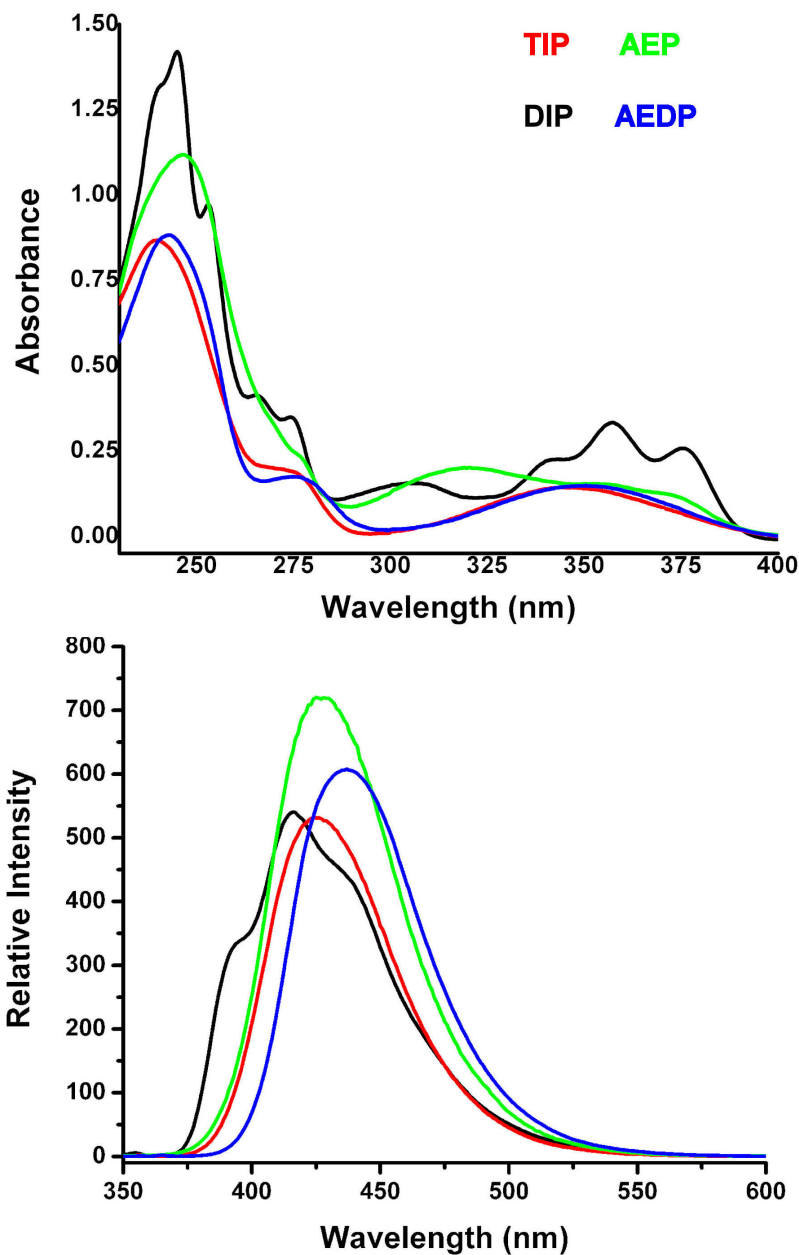


Figure 33. UV absorption (top) and fluorescence emission (bottom) spectra for the isobutyl TIP (red), AEP (green), DIP (black) and AEDP (blue).

Both UV and fluorescence spectra appeared to give similar levels of structural distinction however a combination of UV and ^1H NMR spectroscopy were chosen as the most appropriate analytical techniques for structural evaluation and performance evaluation. A series of experiments were designed to demonstrate the behavior of the system in solution using these techniques. Due to the contrasting properties of the key switchable states, the TIP (neutral, hydride donor) and the AEP (positive charge, hydride acceptor) the system behaved very differently when in monophasic and biphasic conditions.

When pH controlled switching was attempted in monophasic conditions the system was susceptible to the intermolecular hydride transfer, forming the “pH inert” DIP and AEDP forms and terminating the reversible switching (See section 4.3). However the cyclisation process could be carried out under monophasic conditions by using a pH swing,^{165,166} since the proton transfer and cyclisation processes are faster than the hydride transfer when the proton availability is at either extreme. The TIP and AEP can therefore interconvert rather than disproportionate to DIP and AEDP. This was demonstrated using a ^1H -NMR spectroscopy experiment where an excess of triethylamine (~12 eq) was added to a solution of AEP in D_6 -DMSO (Figure 34).

The fast addition of a large excess of triethylamine causes a pH jump to highly basic levels thus rapidly reducing the availability of protons in solution and increasing the rate of conversion of AEP to TIP. The increased rate of deprotonation and cyclisation with respect to the hydride transfer means the AEP can be rapidly and quantitatively converted to the TIP as the length of time both forms remain in solution is no longer sufficient to allow hydride transfer to occur. Although this demonstrates that the reversible cyclisation step can occur in a single phase it was deemed to be inappropriate for repeated switching as it would be highly inefficient with respect to acid and base consumption and decreased analytical sensitivity through dilution. It was thought that a biphasic system would be a more robust technique for achieving repeatable “clean” switching.

DMSO

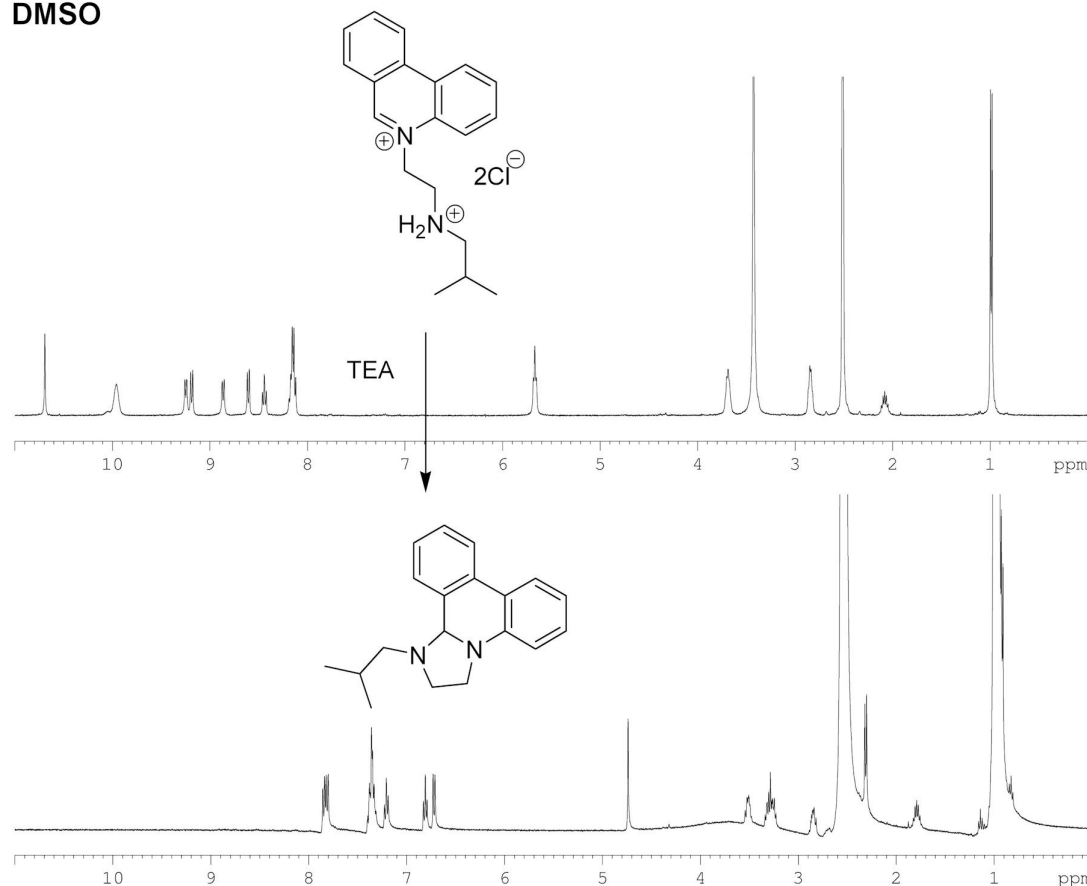


Figure 34. ¹H NMR Spectra showing AEP-TIP cyclisation in monophasic DMSO via rapid pH swing.

When a biphasic solution of isobutyl-AEP in D₂O and CDCl₃ was incrementally made more basic with sodium carbonate additions, the cyclisation to isobutyl-TIP and phase transfer could be observed by monitoring both phases with ¹H NMR spectroscopy. The series of spectra showed a gradual growth of the isobutyl-TIP peaks in the chloroform phase, using cyclohexane as an internal reference (Figure 35). After basification (pH >12) of the aqueous phase no AEP could be detected in the D₂O phase. Conversely gradual reduction of isobutyl-TIP peaks with respect to cyclohexane in the chloroform phase was observed upon acidification with DCl. Clean spectra of the isobutyl-AEP were obtained for the D₂O phase both before and after the reaction. The deprotonation, cyclisation and

phase transfer process was faster than could be observed on the NMR timescale therefore conversion essentially occurred instantly upon addition of acid or base.

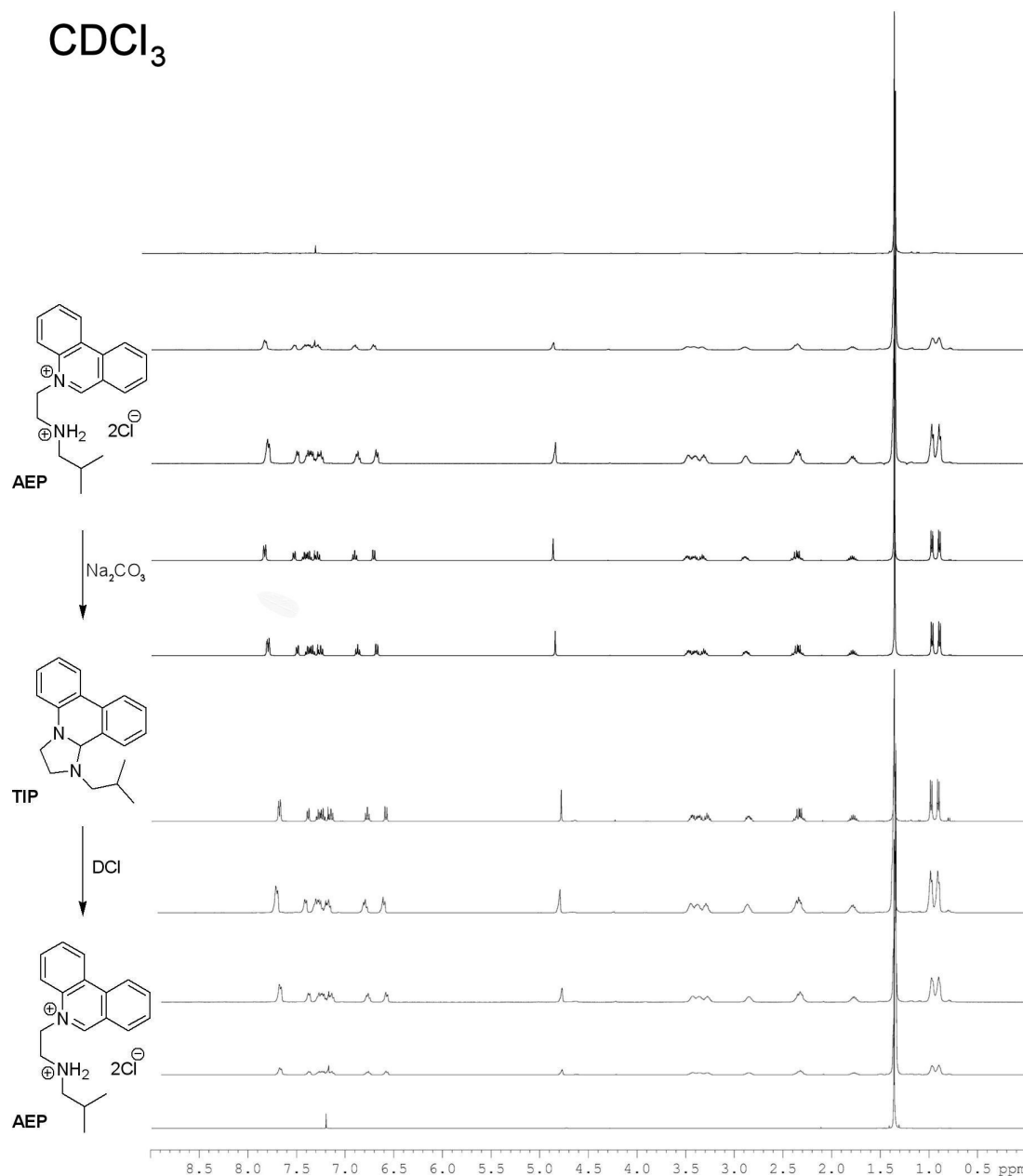


Figure 35. Series of ¹H NMR spectra showing increasing and decreasing TIP peaks with respect to cyclohexane during basification and acidification steps respectively.

Repetition of the cyclisation and phase transfer under biphasic conditions was also followed over a number of cycles using UV spectroscopy (Figure 36). The isobutyl-AEP showed absorbance maxima at 366 nm and 324 nm and the isobutyl-TIP showed an absorbance maximum at 348 nm. As each form was only soluble in one of the two phases i.e. TIP in the organic phase and AEP in the aqueous phase this allowed both structural and quantitative information to be obtained for each phase. The pH of a biphasic solution of isobutyl-AEP was repeatedly switched from ~3 to ~9 over a total number of three cycles and UV spectra were recorded for each phase throughout. The absorbance at the selected absorbance maxima for each phase can be seen to switch from high to low inversely as pH is altered: When the pH is low the absorbance of the aqueous phase at 324 nm is at its highest, whereas the absorbance of the organic phase is effectively zero as the molecule exists completely in the open AEP form. When the pH is high the absorbance of the organic phase at 348 nm is at its highest and the absorbance of the aqueous phase is effectively zero as the molecule exists completely in the closed TIP form. It can be seen quite clearly from these experiments that the cyclisation and phase transfer process is rapid and essentially quantitative and repeatable without any significant loss of activity.

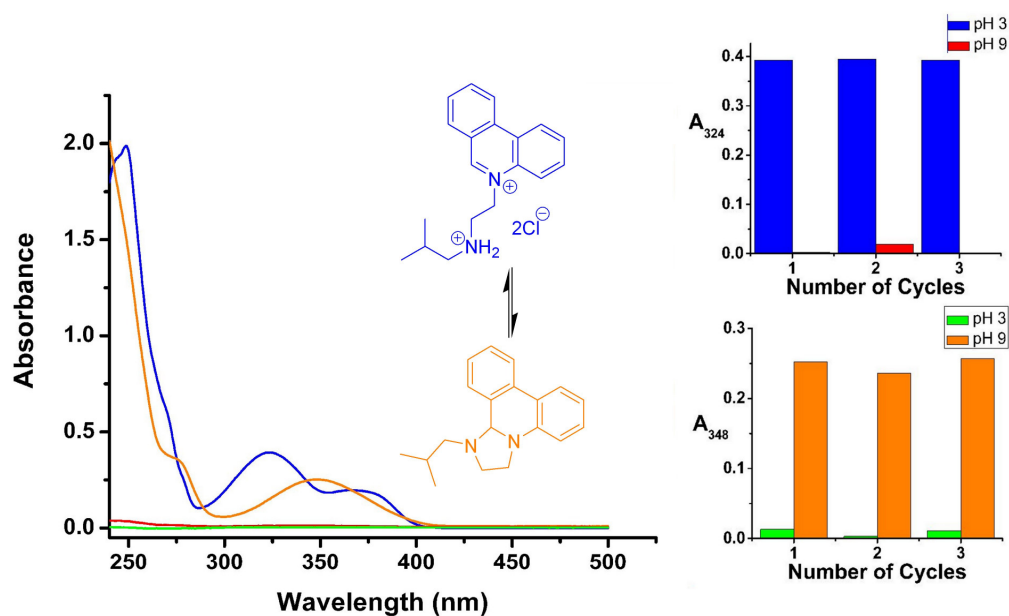


Figure 36. Absorption spectra of DCM and aqueous phases at varying pH: (i) AEP in aqueous phase, pH ~3, blue curve; (ii) Blank DCM phase, pH ~3, red curve; (iii) Blank aqueous phase, pH ~9, green curve; (iv) TIP in DCM phase, pH ~9, orange curve. Inset top: Absorbance changes of aqueous phase at 324 nm. Inset bottom: Absorbance changes of DCM phase at 348 nm.

The complimentary redox activity of the interchangeable forms is what allows for the selective 'locking' of the system in its open or closed state by reduction or oxidation. A set of similar biphasic experiments monitored by UV and $^1\text{H-NMR}$ spectroscopy were therefore used to demonstrate the operation of these processes. When an excess of NaBH_4 was added to a biphasic solution of isobutyl-AEP the complete conversion and phase transfer to a new product with an absorbance maxima at 357 nm was observed using UV spectroscopy (Figure 37).

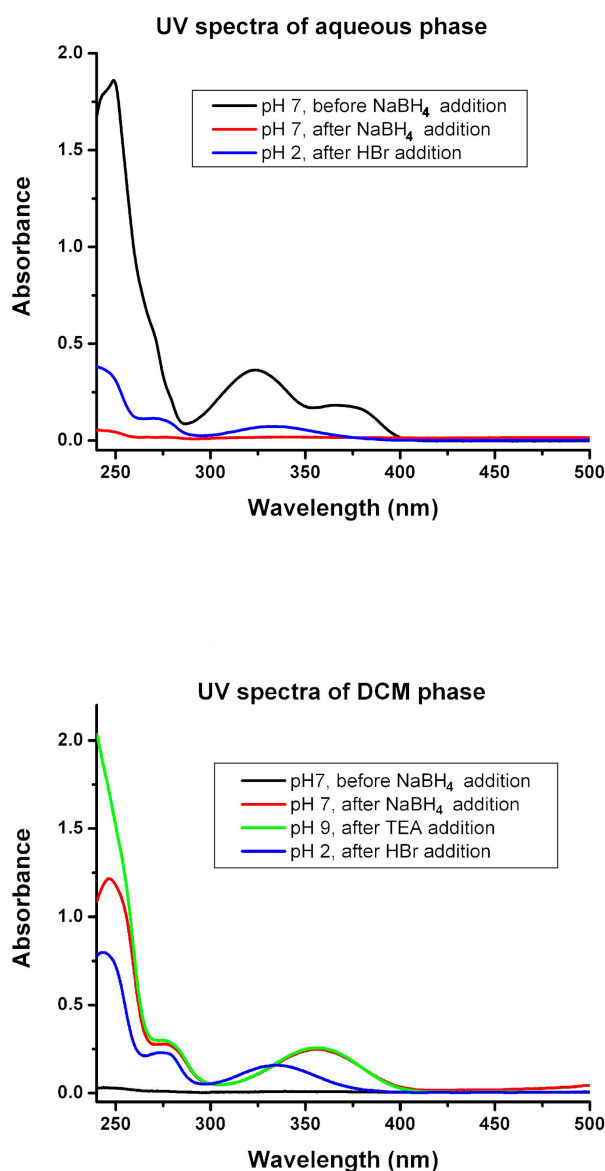


Figure 37. UV spectra of aqueous (top) and DCM (bottom) phases during reduction of AEP to AEDP under biphasic conditions.

By comparison of the black and red curves, the reduction and phase transfer was shown to be equally as efficient as the reversible pH step. The final acidification step (blue curves) shows inhibition of the cyclisation as the AEP is not reformed, a new absorbance is seen due to protonation of the reduced ring-open AEDP form. With the chromophores of the TIP and AEDP being so similar, the absorbance maxima of each are very close, (348 nm and 357 nm, respectively), distinction by UV spectroscopy alone was a little ambiguous. The DCM layer was therefore concentrated under vacuum to isolate the crude reduction product for analysis by ^1H NMR spectroscopy (Figure 38). The spectra of AEDP and TIP are very different, the AEDP spectrum contains a characteristic methylene singlet at 4.3 ppm and the TIP contains an α -proton singlet at 4.8 ppm. The reduction product could therefore be unambiguously identified as the isobutyl-AEDP.

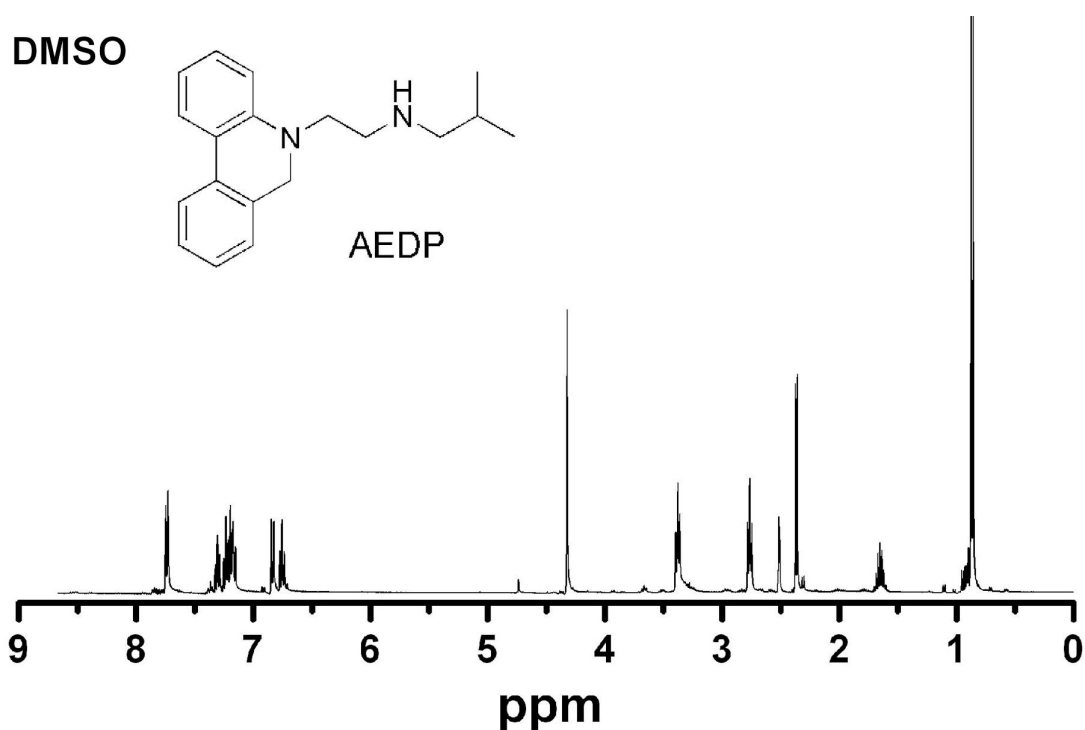


Figure 38. ^1H NMR spectra of the crude reduction product, AEDP.

When bromine was added to a biphasic solution of isobutyl-TIP the oxidation to isobutyl-DIP could be seen by the appearance of the new absorbance maxima at 380 nm, 361 nm & 347 nm in the UV spectrum (Figure 39).

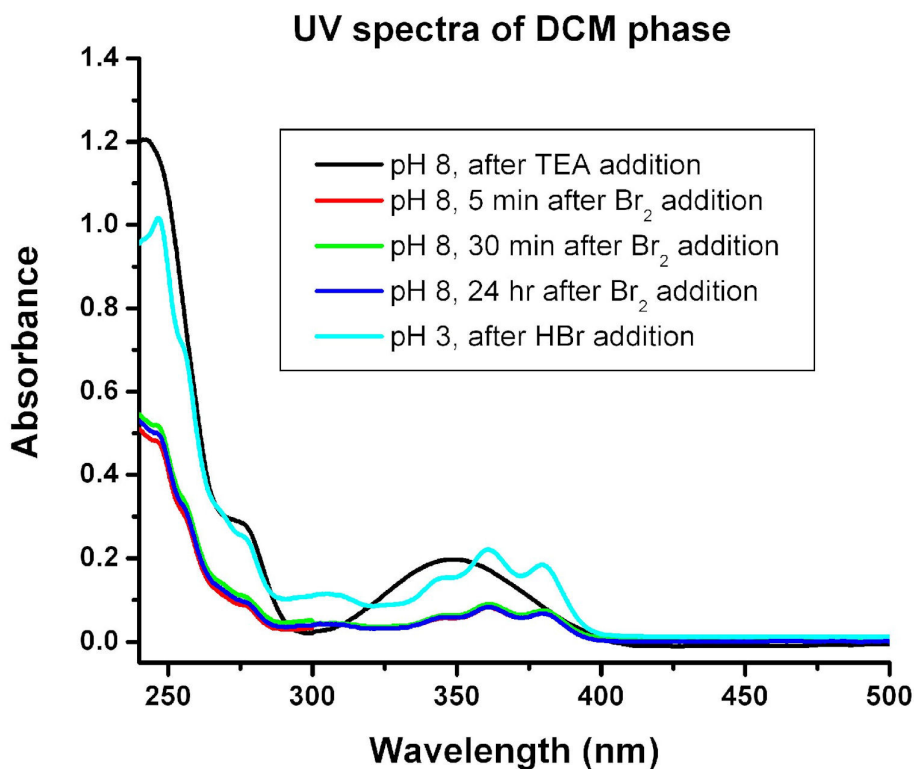


Figure 39. UV spectra of DCM phase during bromine oxidation of TIP to DIP under biphasic conditions.

The initial TIP solution formed in the presence of TEA base and addition of bromine water resulted in oxidation to the DIP. Note that the DIP product is not transferred from the organic phase and the initial absorbance is suppressed by the basic conditions. Decreasing the pH after oxidation did not yield the UV absorption bands correlating to AEP, again demonstrating that the reversible cyclisation process had been inhibited. The changes in the UV spectrum upon re-acidification after oxidation can be explained by protonation reducing any suppression of the DIP absorbance through pseudo-base formation. The UV spectrum of the DIP form is very distinctive and completely different to the spectra of any of the other states, however the same reaction was analysed by ¹H NMR spectroscopy for clarity and completeness (Figure 40). The characteristic ring triplets at 5.01 ppm and 4.64 ppm in the ¹H NMR spectrum unambiguously identified isobutyl-DIP as the sole oxidation product.

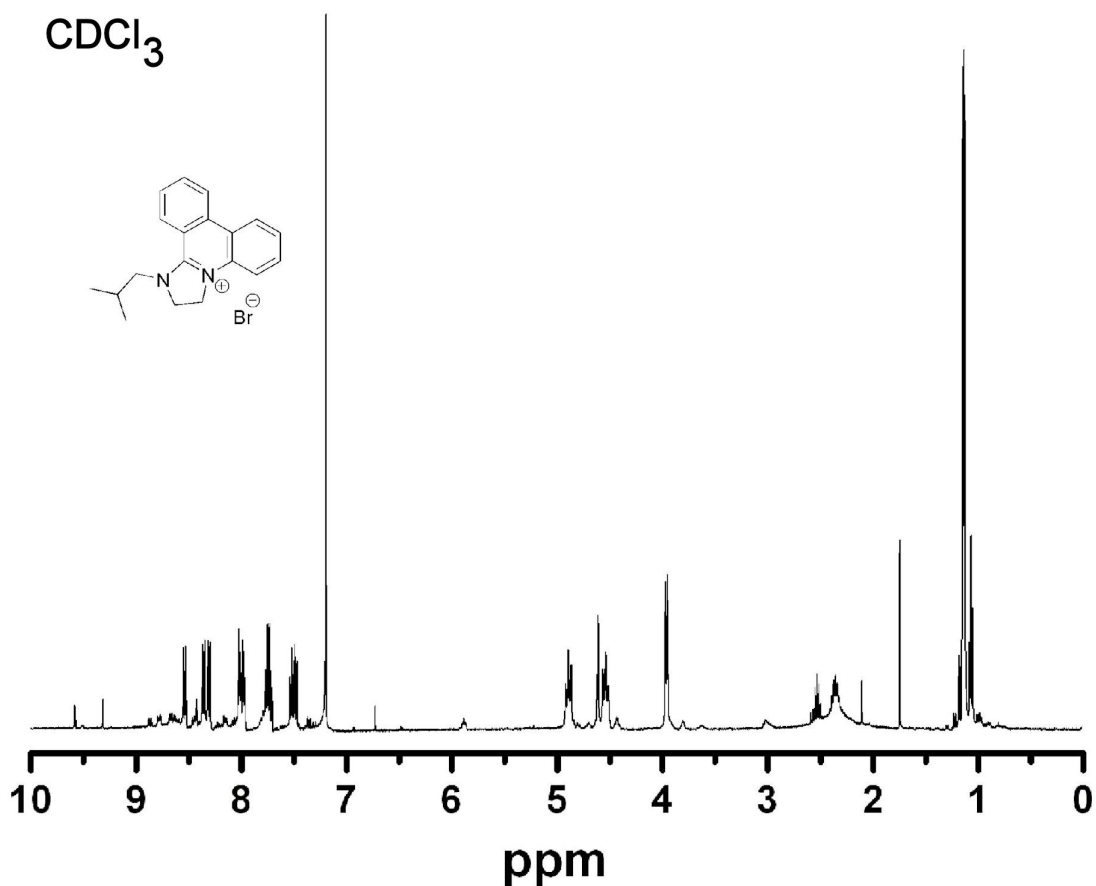


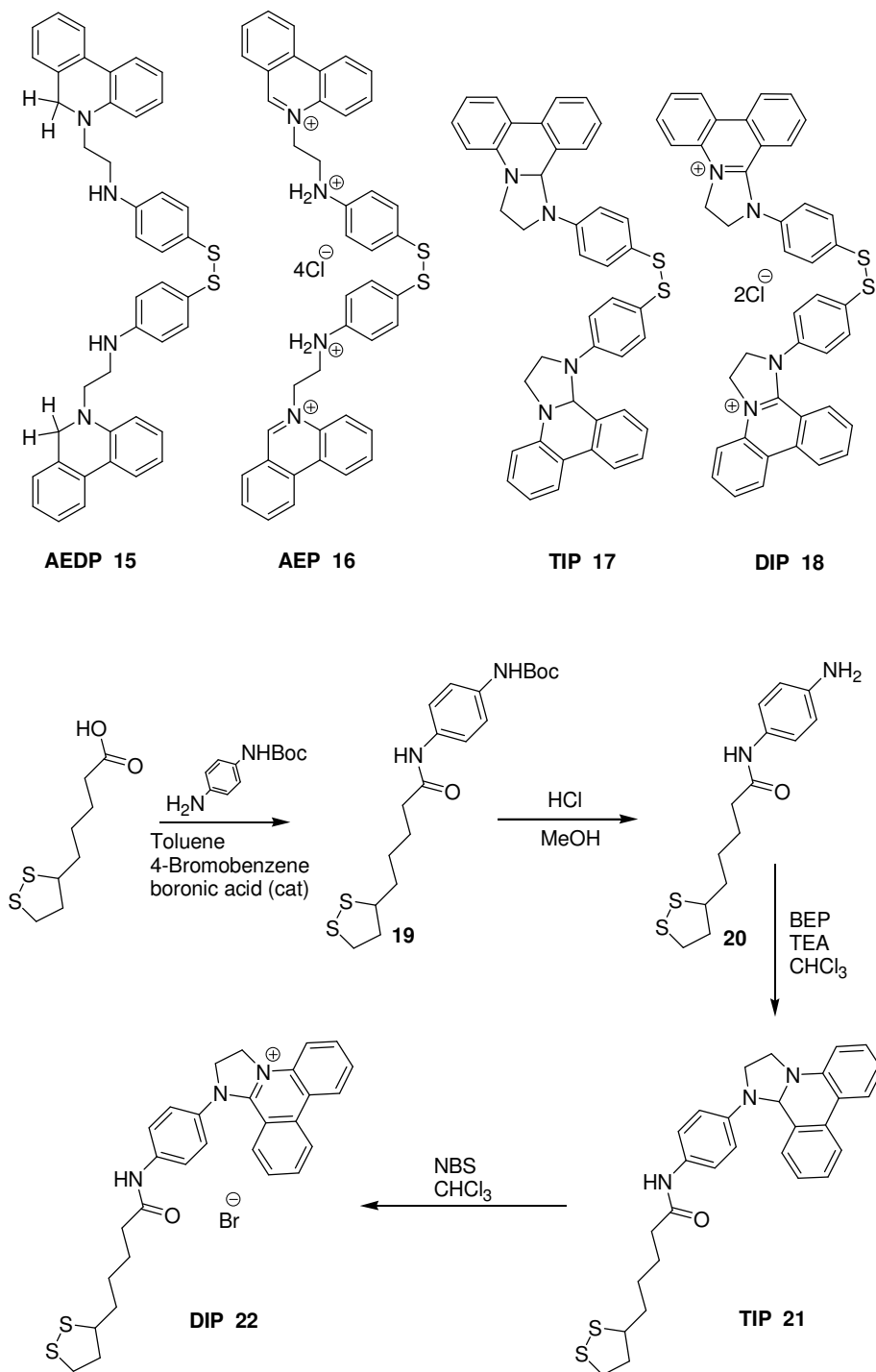
Figure 40. ^1H NMR spectrum of the oxidation product, DIP, in the CDCl_3 phase after addition of Br_2 to a biphasic solution of TIP in $\text{CDCl}_3/\text{D}_2\text{O}$.

The cyclisation process in this heterocyclic molecular system has been shown to operate reversibly in both monophasic and biphasic conditions using pH control and reduction and oxidation can be used to irreversibly inhibit this process. The preferred use of biphasic conditions allows clean reversible operation of the pH modulated cyclisation and repetition over a number of cycles. The selective “locking” oxidation and reduction steps of the TIP and AEP forms are also equally efficient and conversion to the “pH-inert” DIP and AEDP forms is quantitative. This combination of two separate control parameters creates a switchable system with a gated response, where one parameter controls the other, thus allowing for read-write and read only behavior, which is particularly interesting for application in molecular data storage devices. Although the biphasic solution based methodologies used here demonstrates the dual functionality of this system very well, it is unlikely that any “real” molecular devices will incorporate such a feature. It was therefore

proposed to isolate the switchable substrates on solid surfaces with the aim of enhancing performance and creating a more applicable device.

5.5 Amine Derivatisation for Surface Tethered Devices

The synthetic methodologies for DIPs, TIPs and AEPs are not without limitation but on a whole are complimentary and generally applicable for the derivatisation of almost any primary amine. The possibility of creating a framework with an added functionality required for surface adsorption was therefore a fairly trivial task. As one of the most interesting characteristics of the switchable frameworks are their interesting electrochemical properties, gold was chosen as an appropriate substrate because it would allow both structural characterisation and electrochemical information to be obtained via AFM (atomic force microscopy), whilst also offering simple methods for substrate derivatisation. The target compound was therefore required to incorporate an amine functionality compatible with the synthetic methodologies for the introduction of the switchable heterocycles, and a thiol/disulfide functionality for surface adsorption. Due to the nucleophilicity of the thiol functionality, simple amino thiol compounds would not be able to be directly reacted with the BEP framework as competition between the nucleophilic nitrogen and sulfur centres would lead to a mixture of products. Protection of the amino thiol in the form of a disulfide proved to be a successful strategy in the past to generate sulfur-DIP analogues and so was adapted for the synthesis of the other heterocyclic forms. Aryl disulfides are easily adsorbed on gold substrates with similar adsorption behaviour to aryl thiols so disulfide-DIP analogues should still form SAMs.¹⁶⁷ The commercially available 4-aminophenyl disulfide was reacted with BEP to synthesise AEDP, AEP, TIP and DIP analogues **15-18**. Lipoic acid is widely applied as a gold substrate linker and so was also used to synthesise derivatives **21** and **22** (Scheme 25).



Scheme 25. Synthesis of phenanthridine based disulfide conjugates.

Attempts to adsorb **DIP 18** onto the gold substrates were unsuccessful. The gold substrates were pre-washed (sonicated in isopropanol, then acetone, then CHCl_3) then immersed in 1.0 mM solutions of the sample **DIP 18** in CHCl_3 (~6 mg in 10 mL) for 12-24h. The

substrates were removed and rinsed thoroughly with CHCl_3 then EtOH before drying under a flow of nitrogen. There was no evidence of adsorption even for samples that were immersed for up to 5 days. The immersed substrates were characterized by CV and IR and the results obtained were identical to the blank reference substrate. Attempts to adsorb structures **15**, **16** and **17** using the same method also failed to yield any derivatised substrates. The reasons for the lack of adsorption of samples of **15-18** could be due to the relatively short distance between the bulky heterocycles and the gold substrate. When you consider the adsorption mechanism of disulfides there first has to be an association of the disulfide with the gold substrate before the thiolate link can form, this association may be severely hindered by the large heterocyclic systems of structures **15-18**. For samples **16** and **18** there would also be electrostatic repulsion between the positive charges of the heterocycles and the positively charged gold substrate.

Interestingly the solution electrochemistry of the **DIP** disulfide derivative **18** was quite different to that of the isobutyl-DIP. Compound **18** shows non-reversible redox properties as shown in the CV diagram in Figure 41. The first reduction occurred at -0.835 V and the second at -1.44 V. The first reduction peak can be assigned to the disulfide reduction and the second reduction peak is likely to be the DIP – TIP reduction. The irreversible nature of the reduction waves is due to dissociation of S-S bond resulting in deposition on the Pt electrode.

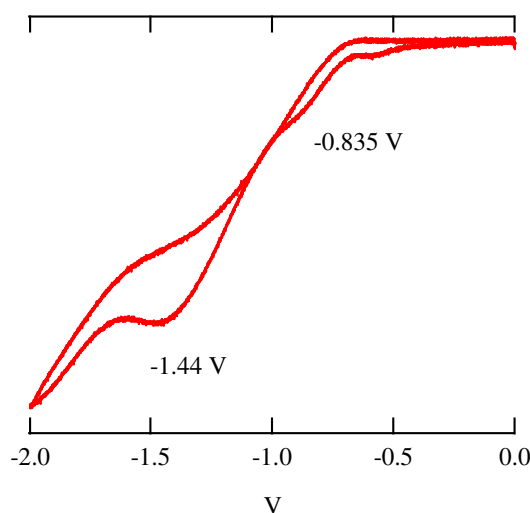
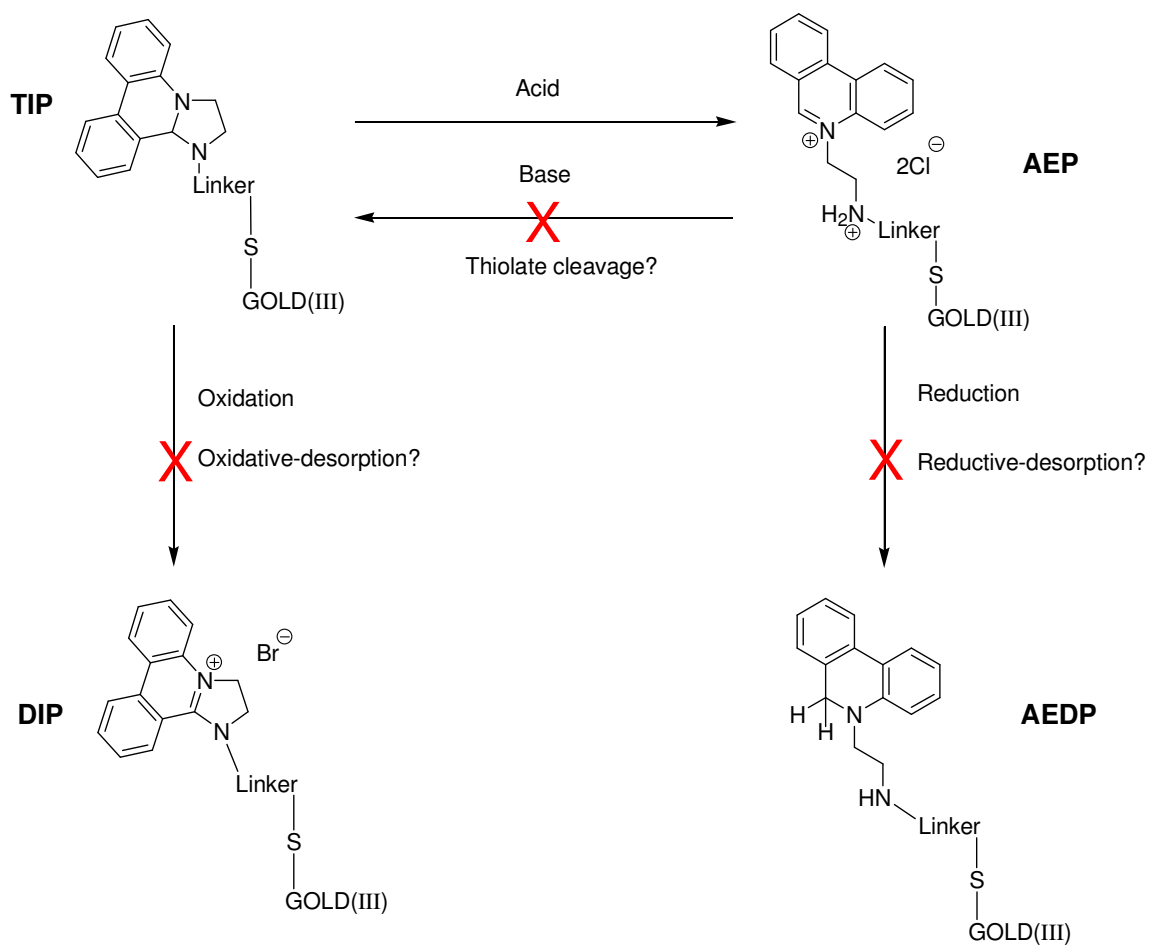


Figure 41. CV of DIP disulfide **18**; Pt working electrode in MeCN with TBABr and Ag/AgCl reference electrode.

Electrochemical deposition of compound **18** was also attempted but no derivatised substrate was obtained via this method either.

The synthesis of lipoic acid derivatives **21** and **22** should have been able to overcome the issues of surface adsorption by providing enough distance and flexibility between the substrate and the heterocycles via the alkyl spacer. Unfortunately this line of investigation was abandoned before the adsorption of these derivatives could be tested. It was realized that the gold-thiolate link and the conditions used for monolayer switching were unlikely to be compatible (Scheme 26).



Scheme 26. Scheme showing incompatibilities between the thiolate link and the switching conditions.

For operation of the switch the derivatised substrates would have to be exposed to a range of oxidative, reductive, acidic, and basic conditions to enable switching between the four heterocyclic forms. Since thiolate-gold SAMs can be cleaved by reductive, oxidative, and basic conditions¹⁶⁸⁻¹⁷¹ it was thought that the monolayers would be destroyed during the switching processes. This would ultimately render the system useless even if adsorption was possible since the derivatised substrate would not be stable during repeated switching. A more robust substrate and linker would therefore need to be used in order to investigate the behaviour of the switch immobilized on a surface. Alkyl silicates are possibly the most appropriate alternative however electrochemical data for these systems could be difficult to obtain.

6 TIP/AEP/DIP BIOACTIVITY COMPARISON

6.1 pH Controlled Selectivity of AEP/TIPs

As mentioned previously a major drawback with the DIP framework was their low therapeutic indices caused by non-selective toxic effects they exhibit in non-cancerous cells (see section 2.4.1). A number of mechanisms for targeting cancer cells have been investigated to create chemotherapeutic agents with increased selectivity, such as biomimics, viral conjugates, and antibody conjugates.¹⁰² Cancer tissues have been shown to have a lower pH compared to regular healthy tissue due to higher quantities of lactic acid produced by the increased levels of glycolytic respiration.¹⁷² It was proposed that the reversibility of the TIP/AEP cyclisation could take advantage of this characteristic to create a pH sensitive system with increased cancer selectivity. The TIP/AEP equilibrium is pH dependent and will therefore express each form as a function of pH, AEP will be favoured at lower pH and TIP will be favoured at higher pH. The planar cationic AEP form should be more active than the non-planar neutral TIP which should then lead to increased cytotoxicity in cancer cells and reduced cytotoxicity in normal cells (Figure 42).

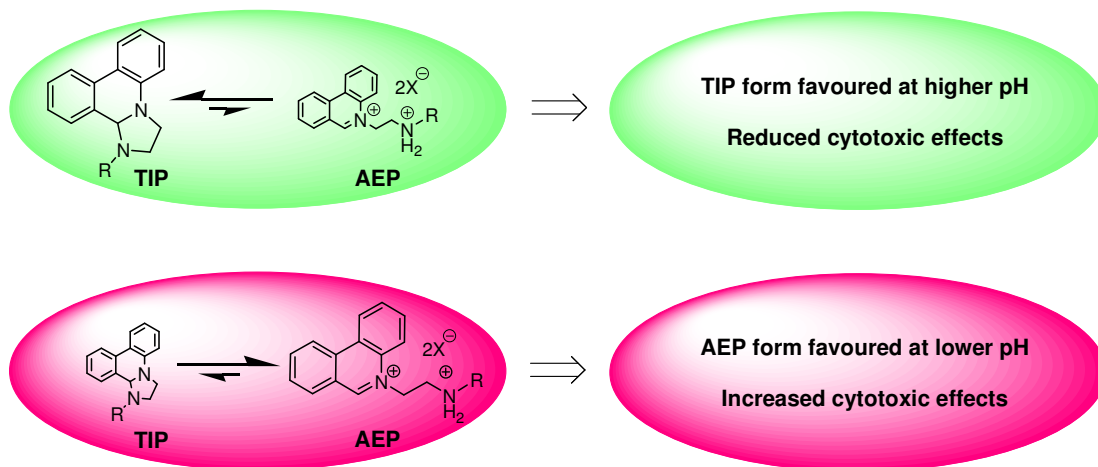


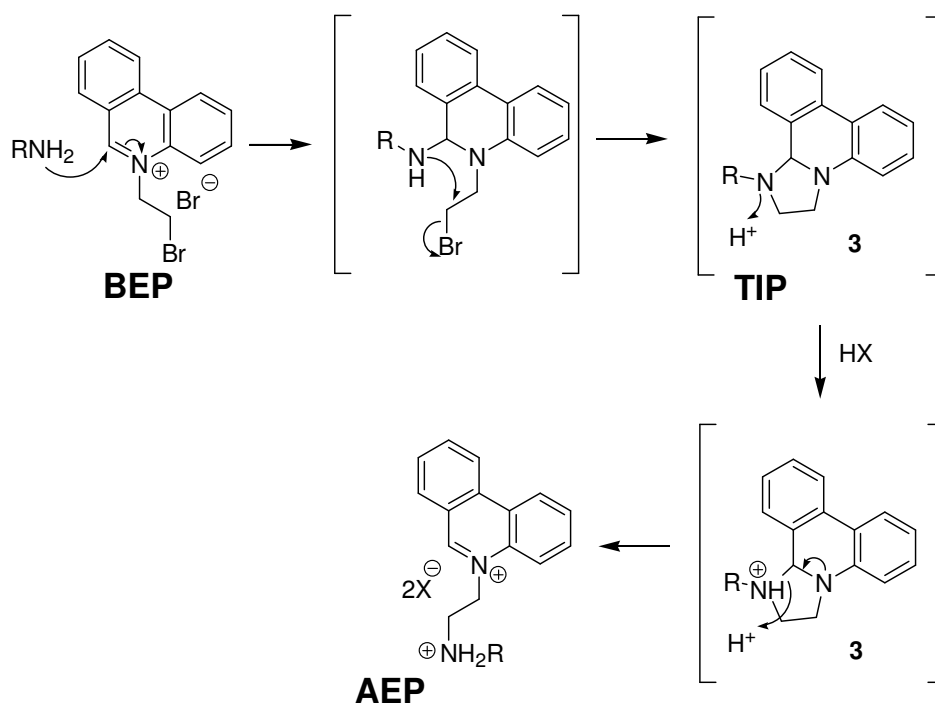
Figure 42. Proposed cytotoxic effects of TIP/AEPs in normal cells (green) and cancer cells (pink).

The TIP form is a neutral, non-planar heterocycle making it a very poor candidate for a DNA binder since the majority of attributes required for DNA affinity have been removed. The lack of positive charge means there will be no electrostatic interactions with the negatively charged DNA phosphate backbone and the loss of aromaticity from the ring system reduces planarity and π -character and therefore reduces DNA intercalation. The only mode of activity that could possibly remain would be via minor groove DNA binding. Non-specific membrane insertion would also be lessened as the TIP framework is not amphiphilic. In contrast the AEP form is a cationic, planar aromatic heterocycle making it a very good candidate for a DNA binder. The high positive charge means there will be strong electrostatic interactions with the negatively charged DNA phosphate backbone, the flat aromatic ring system should intercalate between the DNA base pairs, and minor groove binding by the amine side-chain will also be possible. The amphiphilicity of AEPs containing long alkyl chains could also increase apoptosis in cancer cells via membrane insertion and osmotic bursting.¹²⁶ The application of this system should ultimately lead to an increase in cancer cell termination and reduced cytotoxic effects in normal cells.

6.2 AEP/TIP/DIP Comparison Library

In order to test the pH selectivity hypothesis, firstly a library of compounds had to be synthesised and secondly a method of detecting their efficacy had to be developed. A large library of DIP substrates already exists for which their *in vitro* cytotoxicity was measured using an MTT-dye-based microtitration assay.^{124,125} A similar strategy was therefore selected for this work, where a comparative library of compounds would be synthesised and sent for activity screening using a high throughput MTT assay. Once the initial efficacy levels for the compounds were confirmed the pH dependency of the DNA binding and cytotoxicity could then be investigated.

The general TIP synthesis methodology (see section 4.2) was used to expand the selection of TIP frameworks using a range of structurally diverse aromatic amines. The AEP analogues had never before been synthesised from primary amines so a new methodology had to be developed for the synthesis of this section of the library. The DIP analogues had mostly been synthesised and tested prior to this study so comparative data could be easily sourced, and for those that had not there were numerous methodologies reported that could be followed in order to produce the desired DIPs.^{127,129}



Scheme 27. Mechanism of AEP formation from BEP plus a primary amine.

The AEP frameworks were generated from the same BEP and primary amine starting materials as the TIPs and DIPs so there is therefore significant mechanistic overlap. The initial α -addition and cyclisation steps are identical, however rather than isolation (TIPs) or oxidation (DIPs), a final protonation and ring opening step results in formation of the AEP structure (Scheme 27).

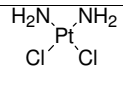
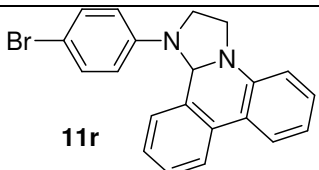
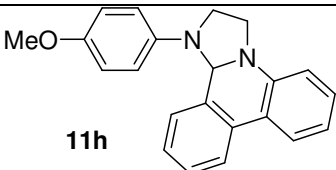
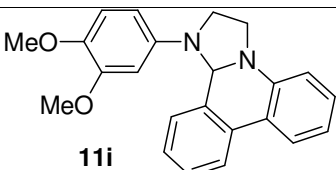
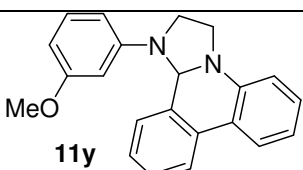
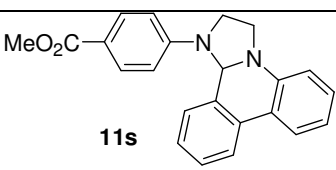
Due to these similarities the synthetic methodologies were equally dependent upon the nature of the amine side-chain. For aliphatic amines a biphasic solvent system was employed for the amine addition and cyclisation steps and the protonation and ring-opening steps. For aromatic amines the TIP first had to be isolated and a monophasic acidification procedure could then be used for the protonation and ring opening steps.

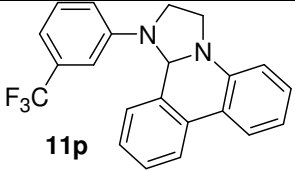
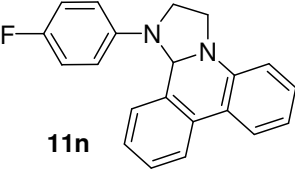
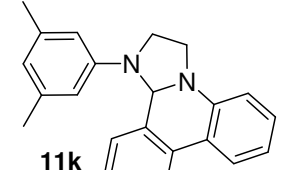
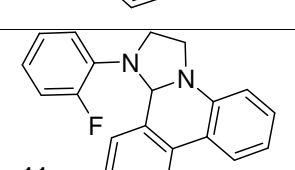
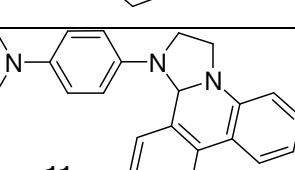
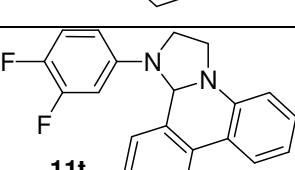
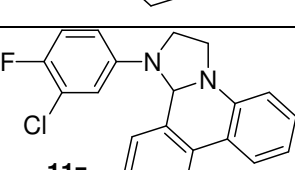
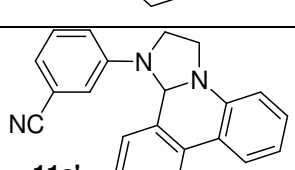
Biphasic methodology for aliphatic AEPs: A solution of the aliphatic amine in a 5% Na_2CO_3 (aq) solution was added to a suspension of the BEP starting material in DCM and the reaction stirred under nitrogen. This allowed for the α -addition step to occur in the aqueous phase and subsequently transfer the α -adduct to the organic phase where cyclisation would provide the TIP intermediate. Separation of the phases then allowed for a solution of the TIP intermediate to be obtained. Extraction of the organic phase with aqueous acid resulted in protonation, ring-opening and phase transfer of the AEP target to the aqueous phase. The acidic aqueous solution of the AEP could then be concentrated under vacuum and precipitated with acetone/EtOAc to yield the AEP dihalide salts.

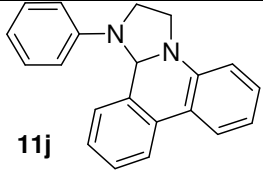
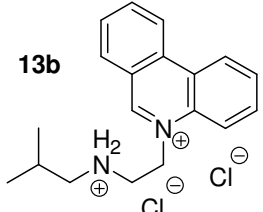
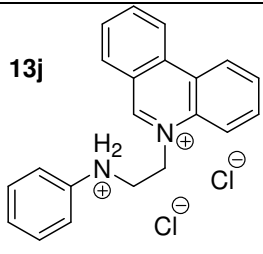
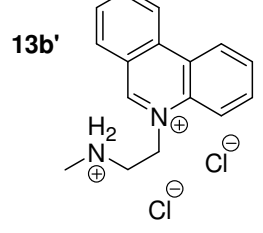
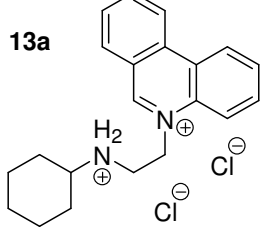
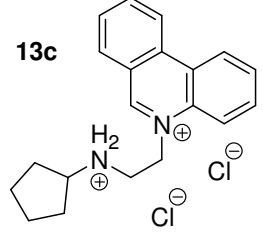
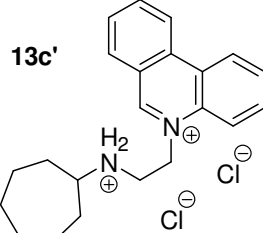
2-step monophasic methodology for aromatic AEPs: The TIP intermediates were generated using the general methodology developed previously (see section 4.2). An additional methanol trituration was carried out to ensure complete removal of the TEA and its hydrobromide salts as they would be difficult to remove from the AEP product salt. A suspension of the TIP intermediate in methanol could then be acidified with concentrated acid to provide a solution of the AEP target. The AEP solution could then be concentrated and the product precipitated by addition of acetone. Both methodologies resulted in the isolation of very pure AEP salt products, however the biphasic methodology tended to result in slightly higher yields. This was due to the TIP intermediate not requiring isolation and purification in this method.

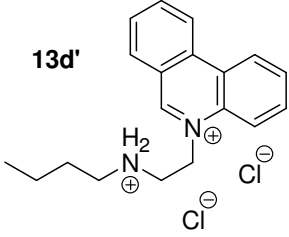
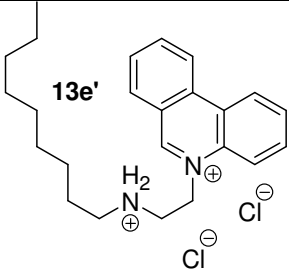
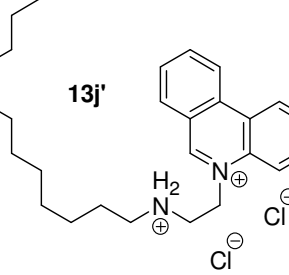
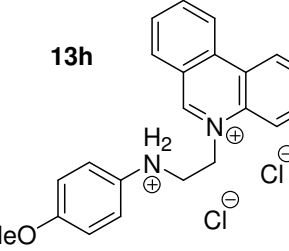
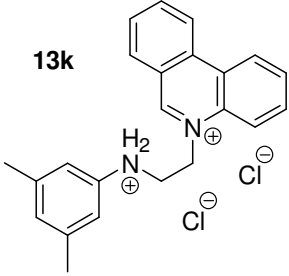
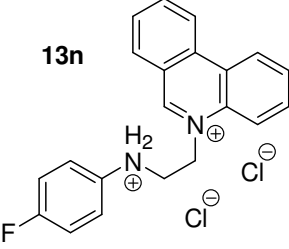
With methods in hand to generate each of the three frameworks to be compared, a small library of compounds was synthesised and screened for cytotoxicity in a selection of cancer cell lines (Table 2). The cytotoxicity measurements were carried out by Dr. Jane Plumb at the Cancer Research UK, Beatson Laboratories in Glasgow.

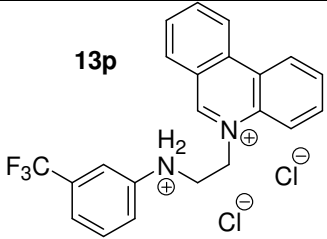
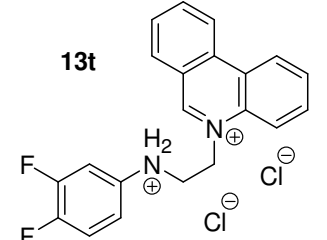
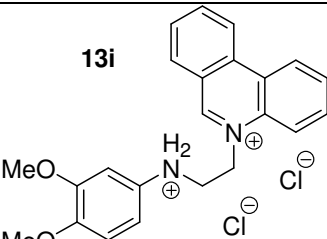
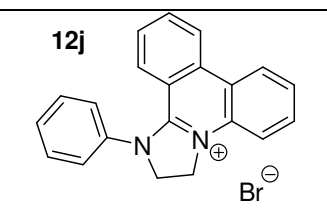
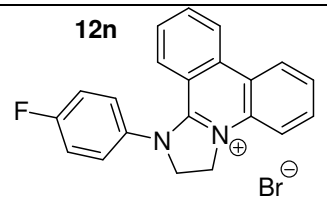
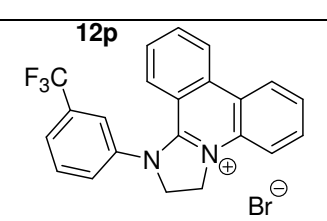
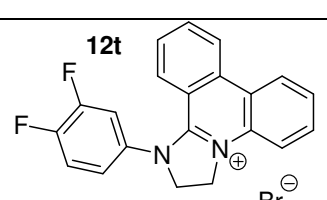
Table 2. TIP/AEP/DIP structures and corresponding IC₅₀ and RF values calculated from MTT assay of A2780, A2780/cp70 and MCP1 cell lines.

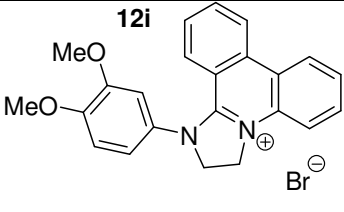
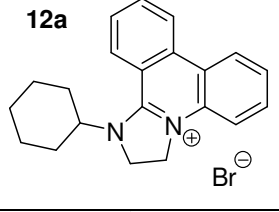
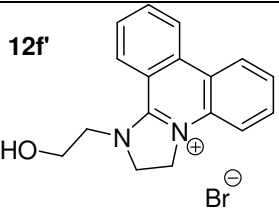
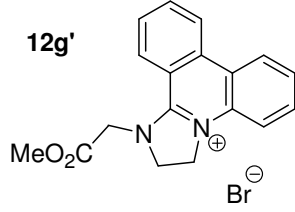
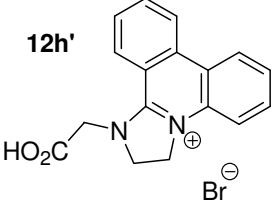
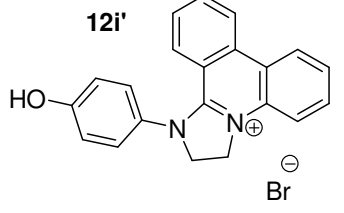
Structure	IC ₅₀ (μM)			RF	
	A2780	A2780/cp70	MCP1	CP70/ A2780	MCP1/ A2780
 Cisplatin	0.12 ± 0.04	2.04 ± 0.23	0.47 ± 0.05	16.7	3.9
 11r	4.91 ± 0.52	10.3 ± 0.6	3.97 ± 0.18	2.1	0.8
 11h	1.74 ± 0.54	2.57 ± 0.40	1.05 ± 0.04	1.5	0.6
 11i	84.3 ± 5.1	28.1 ± 1.9	57.9 ± 1.4	0.3	0.7
 11y	1.78 ± 0.12	5.93 ± 0.66	5.19 ± 3.30	3.3	2.9
 11s	19.6 ± 0.1	35.6 ± 4.3	12.0 ± 0.8	1.8	0.6

 <p>11p</p>	19.4 ± 0.5	33.3 ± 5.3	12.5 ± 0.7	1.7	0.6
 <p>11n</p>	12.35 ± 1.03	22.45 ± 1.13	14.73 ± 1.37	1.8	1.2
 <p>11k</p>	5.63 ± 0.99	2.48 ± 0.17	3.06 ± 0.50	0.4	0.5
 <p>11m</p>	16.90 ± 1.83	24.30 ± 4.07	13.59 ± 1.23	1.4	0.8
 <p>11g</p>	8.45 ± 0.78	4.85 ± 0.53	6.26 ± 0.99	0.6	0.7
 <p>11t</p>	15.57 ± 1.31	25.83 ± 3.80	16.39 ± 1.42	1.7	1.1
 <p>11z</p>	10.50 ± 0.69	18.65 ± 1.42	7.66 ± 0.82	1.8	0.8
 <p>11a'</p>	21.31 ± 2.24	18.62 ± 2.31	17.78 ± 0.61	0.9	0.8

 <p>11j</p>	11.56 ± 1.29	13.26 ± 2.27	14.14 ± 2.22	1.2	1.2
 <p>13b</p>	10.26 ± 1.38	7.24 ± 0.97	9.86 ± 0.75	0.7	1.0
 <p>13j</p>	19.15 ± 0.63	22.90 ± 2.62	19.12 ± 0.98	1.2	1.0
 <p>13b'</p>	17.93 ± 0.61	8.73 ± 1.18	9.54 ± 1.51	0.5	0.5
 <p>13a</p>	7.01 ± 0.50	7.12 ± 1.05	2.98 ± 0.06	1.0	0.4
 <p>13c</p>	7.87 ± 1.06	9.22 ± 1.55	5.12 ± 0.02	1.2	0.7
 <p>13c'</p>	12.09 ± 1.63	11.44 ± 2.20	6.17 ± 0.56	1.0	0.5

<p>13d'</p> 	12.02 ± 2.66	2.61 ± 0.37	4.84 ± 0.22	0.2	0.4
<p>13e'</p> 	9.71 ± 1.00	1.97 ± 0.24	2.66 ± 0.23	0.2	0.3
<p>13j'</p> 	2.27 ± 0.17	0.57 ± 0.11	0.41 ± 0.11	0.3	0.2
<p>13h</p> 	9.18 ± 1.51	6.19 ± 0.47	5.16 ± 0.54	0.7	0.6
<p>13k</p> 	19.74 ± 0.25	12.12 ± 0.37	11.20 ± 2.42	0.6	0.6
<p>13n</p> 	21.13 ± 0.57	33.51 ± 3.03	19.60 ± 1.10	1.6	0.9

<p>13p</p> 	18.67 ± 0.21	25.79 ± 3.07	10.14 ± 0.47	1.4	0.5
<p>13t</p> 	19.56 ± 0.50	23.64 ± 2.73	14.33 ± 1.03	1.2	0.7
<p>13i</p> 	99.17 ± 2.05	103.77 ± 1.83	66.11 ± 3.38	1.1	0.7
<p>12j</p> 	0.73 ± 0.17	1.81 ± 0.11	1.22 ± 0.20	2.5	1.7
<p>12n</p> 	2.56 ± 0.56	3.12 ± 0.13	3.89 ± 0.77	1.2	1.5
<p>12p</p> 	22.31 ± 1.38	7.31 ± 0.91	15.26 ± 2.00	0.3	0.7
<p>12t</p> 	2.01 ± 1.29	3.45 ± 0.37	4.46 ± 0.82	1.7	2.2

<p>12i</p> 	1.56 ± 0.06	3.63 ± 0.63	2.98 ± 0.39	2.3	1.9
<p>12a</p> 	0.84 ± 0.11	2.44 ± 0.03	2.38 ± 0.24	2.9	2.8
<p>12b'</p> 	1.26 ± 0.18	1.46 ± 0.14	5.07 ± 0.90	1.2	4.0
<p>12f'</p> 	3.85 ± 0.15	2.75 ± 0.13	9.65 ± 0.76	0.7	2.5
<p>12g'</p> 	12.91 ± 5.13	13.99 ± 1.07	30.90 ± 2.32	1.1	2.4
<p>12h'</p> 	1.55 ± 0.51	8.94 ± 1.98	26.16 ± 7.68	5.8	16.9
<p>12i'</p> 	0.610 ± 0.099	0.498 ± 0.104	0.801 ± 0.090	0.8	1.3

6.3 MTT Dye-based Microtitration Assay Results

The cell lines that were screened were the human ovarian cancer cell line, *A2780*, and two cisplatin resistant derivatives, *A2780/cp70* and *MCPI*.¹⁷³ Cell line *A2780* contains a functioning *hMLH1* gene whilst the resistant cell lines do not. This loss of gene function in the resistant cell lines is due to hypermethylation of the *hMLH1* promoter, which results in the loss of expression of the *MLH1* component of the DNA mismatch repair pathway. Lack of *MLH1* expression has been shown to be related to cisplatin resistance in these cell lines,^{174,175} which is a major problem since cisplatin is a major chemotherapeutic for the treatment of ovarian cancers.¹⁷⁶

3-(4,5-Dimethylthiazol-2-yl)-2,5-diphenyl-tetrazolium bromide (MTT) is a water soluble, yellow coloured dye which can be converted to a dark-blue coloured formazan by metabolically active cells. This metabolism can be exploited to rapidly determine the quantity of viable living cells after treatment with the target compounds. The colour of the individual wells in the plates corresponds to the conversion of the MTT, which is directly related to the number of living cells within the well. Therefore an indirect relationship between the measured colour change and drug efficacy can be formed. The assay technique was first developed in 1983¹⁷⁷ and is the same assay used to determine the cytotoxicity of the library DIP compounds previously developed within the Cronin group.^{124,125,178} The cytotoxicity measurements were carried out by Dr. Jane Plumb at the Cancer Research UK Beatson Laboratories in Glasgow. The test results shown in Table 2 give the IC_{50} values, defined as the concentration of drug required to kill 50% of the cells; and the RF values, calculated by dividing the IC_{50} value for a given drug for the cisplatin resistant cell lines by that obtained for the cisplatin sensitive *A2780* cell line.

The library of compounds was designed not only to give information on the general cytotoxicity trends of the AEP and TIP forms but also to allow direct comparisons to be drawn between these structures and the DIPs. The library was designed with this in mind so there is a large amount of structural overlap between the three compound families with respect to the amine side-chains. Table 3 and the related plots (Figure 43, 44 and 45) show the reformatted assay results as a function of the amine side-chain and highlight the correlations between the three forms for each cell line.

Table 3. Reformatted MTT assay results for DIP/AEP/TIP comparison

Amine Side-Chain	DIP IC₅₀ (μM)	AEP IC₅₀ (μM)	TIP IC₅₀ (μM)
	A2780	A2780	A2780
	A2780/cp70	A2780/cp70	A2780/cp70
	MCP1	MCP1	MCP1
Methyl	1.26 1.46 5.07	17.93 8.73 9.54	NA (not available)
Cyclohexyl	0.84 2.44 2.38	7.01 7.12 2.98	NA
Cyclopentyl	4.63 6.27 5.66	7.87 9.22 5.12	NA
Cycloheptyl	3.01 4.59 3.03	12.09 11.44 6.17	NA
<i>n</i> -butyl	NA	12.02 2.61 4.84	NA
Nonyl	0.27 0.30 0.47	9.71 1.97 2.66	NA
Dodecyl	0.087 0.052 0.050	2.27 0.57 0.41	NA
Isobutyl	5.12 5.98 4.26	10.26 7.24 9.86	NA
4-Methoxyphenyl	1.45 1.10 0.50	9.18 6.19 5.16	1.74 2.57 1.05
3,5-Dimethylphenyl	NA	19.74	5.63

		12.12	2.48
		11.20	3.06
4-Fluorophenyl	2.56	21.13	12.35
	3.12	33.51	22.45
	3.89	19.60	14.73
3-(trifluoromethyl)-phenyl	22.31	18.67	19.4
	7.31	25.79	33.3
	15.26	10.14	12.5
3,4-Difluorophenyl	2.01	19.56	15.57
	3.45	23.64	25.83
	4.46	14.33	16.39
3,4-Dimethoxyphenyl	1.56	99.17	84.3
	3.63	103.77	28.1
	2.98	66.11	57.9
Phenyl	0.73	19.15	11.56
	1.81	22.90	13.26
	1.22	19.12	14.14

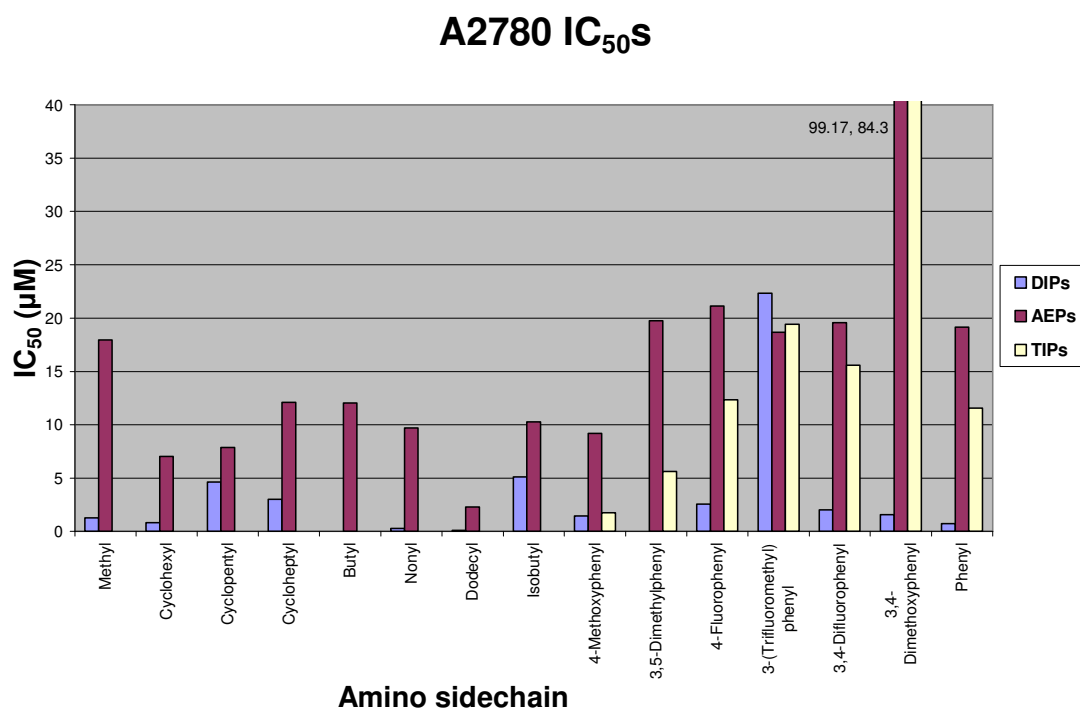


Figure 43. Plot of IC₅₀ values for the DIP, AEP and TIP forms in cell line A2780

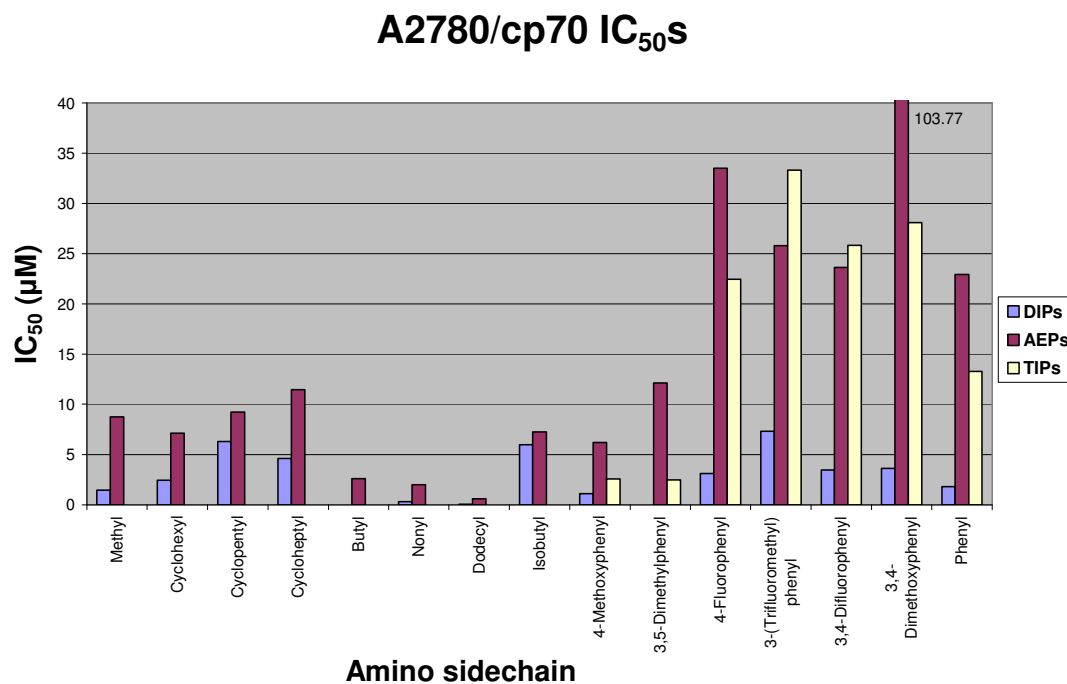


Figure 44. Plot of IC₅₀ values for the DIP, AEP and TIP forms in cell line A2780/CP70

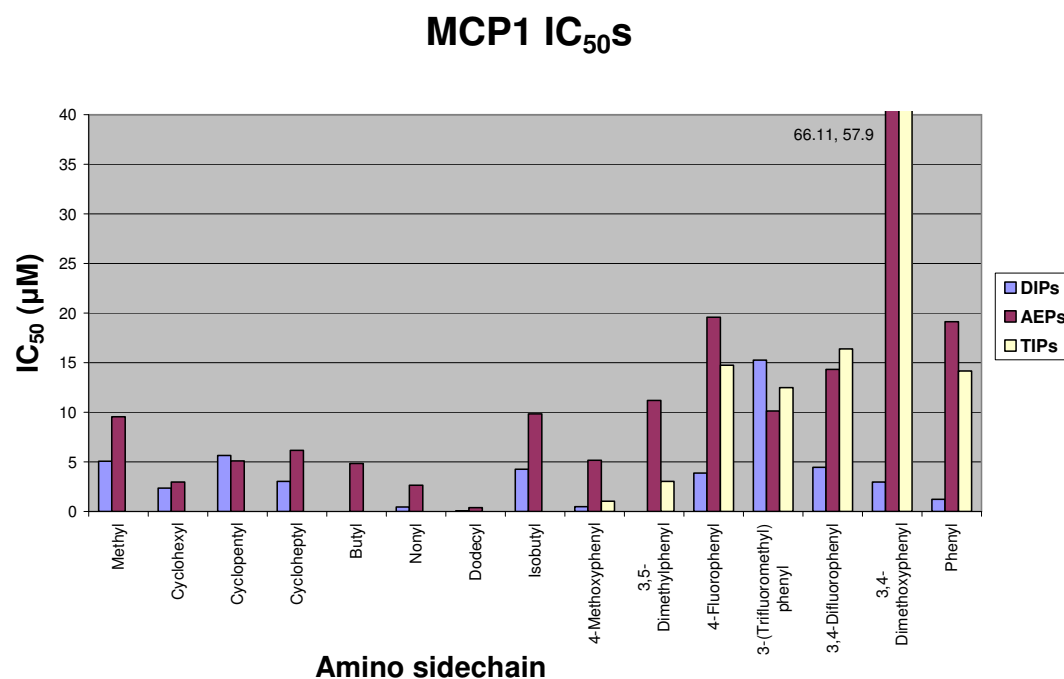


Figure 45. Plot of IC₅₀ values for the DIP, AEP and TIP forms in cell line MCP1

At this point it should be noted that data for TIP structures with aliphatic side-chains are unavailable due to the lack of stability of these heterocycles (see section 4.1) however a number of correlations can be seen to exist from analysis of the data obtained. Firstly it is evident that there is a general trend exhibited in all three cell lines when the three heterocycle forms are directly compared for each respective amine, activity is highest in the DIPs and the TIPs and AEPs have comparatively lower activity. This result was very surprising since the AEP form was expected to have greater activity than the TIPs. The TIP structures themselves are unlikely to possess high DNA affinity for reasons discussed previously therefore their activity is likely to come from a transformation to a more active form either in the cell medium or within the cell itself. As the cell medium is buffered to pH 7.4, conversion of the TIP to AEP is possible and could result in the observed activity. For drug samples with low aqueous solubility, such as the TIPs, DMSO is often used to solvate the drug before addition to the sample wells. There is precedent for the oxidation of TIPs to DIPs in the presence of DMSO as the oxidant therefore these oxidative conditions could result in oxidation of the TIP to DIP which could also be responsible for the higher activity than expected. As the IC₅₀ values for the TIPs correlated more closely

with the AEPs than the DIPs it was proposed that the active species for the TIP compounds was more likely to be the AEP form rather than the DIP form. Linear regression plots of the results agreed with this hypothesis (Figure 46, 47 and 48).

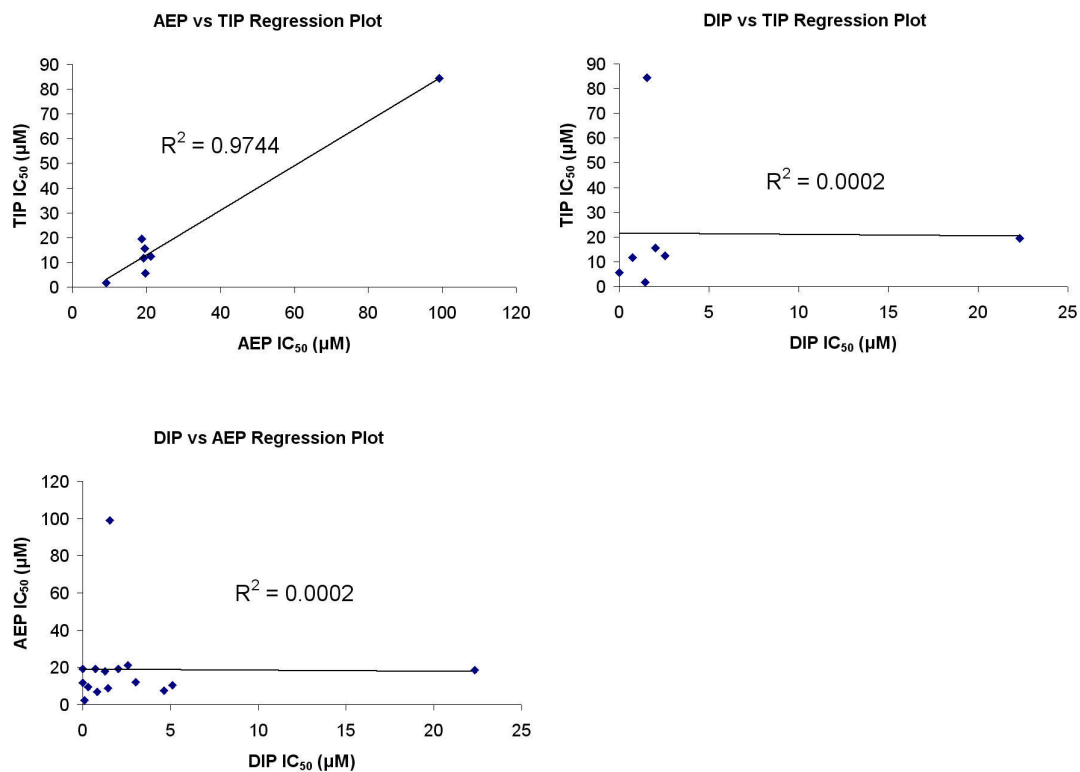


Figure 46. Regression plots of IC_{50} Values for A2780 Cell Line.

The R^2 value for linear regression is very good for the AEP vs TIP plot but not for the DIP vs TIP or DIP vs AEP plots. This indicates that the activities for the AEPs and TIPs are related to each other but not to the DIP activities.

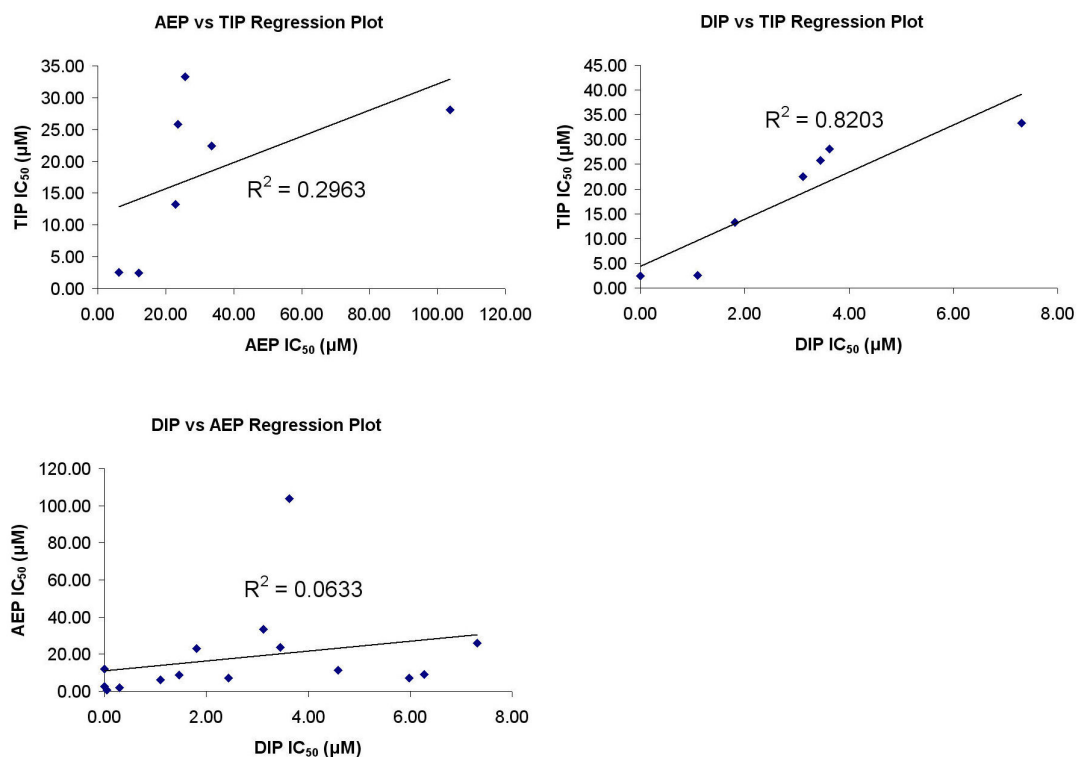


Figure 47. Regression plots of IC₅₀ Values for A2780/CP70 Cell Line.

For the A2780/CP70 cell lines the regression plots again showed possible related activity between AEPs and TIPs but also showed a possible activity relationship between the DIPs and the TIPs.

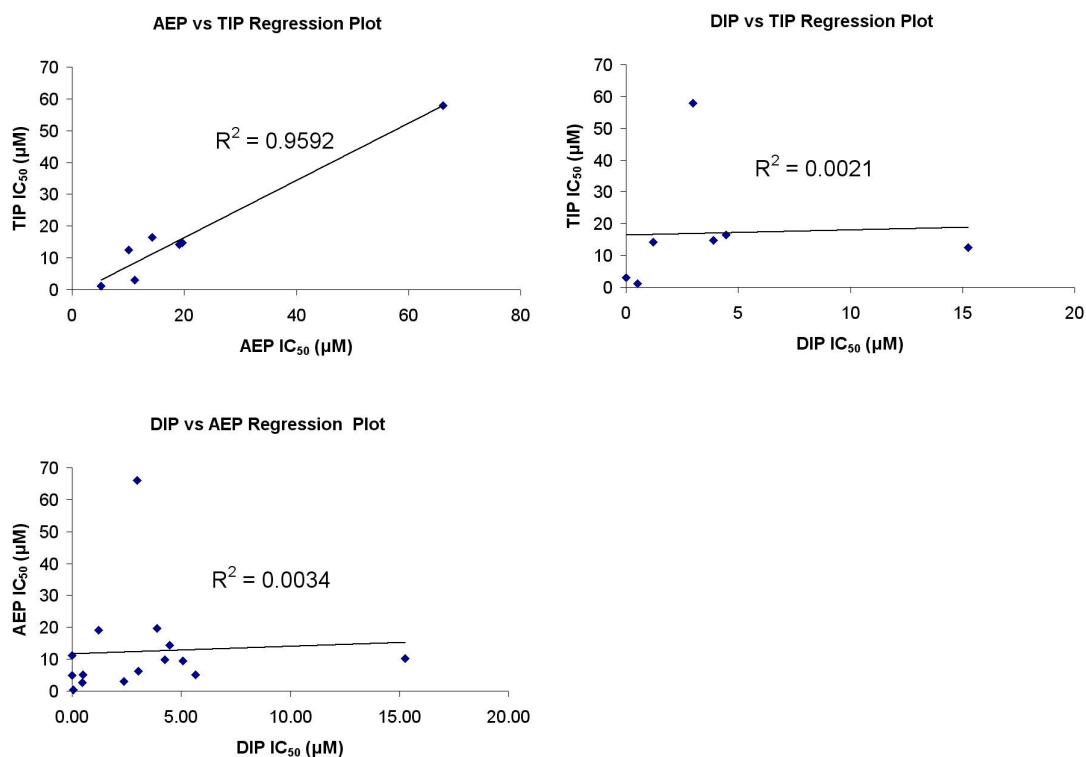


Figure 48. Regression plots of IC₅₀ Values for MCP1 Cell Line.

For the MCP1 cell lines the linear regression plots are again consistent with activity relationships between the TIPs and AEPs only. Taking into consideration the patterns observed in all the data plots, coupled with the small size of the data sets, no conclusions can be drawn with absolute confidence. However there does appear to be a relationship between the TIP and AEP activities that warrants further investigation. Although the general activity of the TIP/AEP compounds appears to be lower than the DIPs the observation of a relationship between the activity of the AEP and TIP forms is far more important in proving the original pH dependence hypothesis. If the results are related, then administering compounds to the cancer cell lines in either the AEP or TIP form leads to *in vitro* conversion to the same form, if the compounds interconvert in a similar fashion *in vivo* then the TIP form should predominate in normal tissues, whilst the AEP form should predominate in the cancerous tissues. As a result of this interconversion, a significant increase in the TI's could be achieved.

Another trend familiar to the data sets is that in all three cell lines, all compounds appear to react uniformly to changes in the amino side-chain (Figure 43, 44 and 45). Linear aliphatic side-chains offer the highest activities and cyclic aliphatic and substituted aromatic side-chains have the lowest activities. This data agrees with the hypothesis of the dual mode binding previously presented for SAR studies of DIP compounds.^{122,125,129} The polyaromatic framework intercalates between the DNA base-pairs to give the initial binding mode and the amino side-chain then offers further attractions via groove binding. Evidence from this previous work by the Cronin group suggests that increasing the minor groove binding ability of the side-chain results in an increase in cytotoxicity, however, it should be noted that increases in DNA binding does not always translate to increased cytotoxicity.¹⁷⁹ The nature of the side-chain is therefore responsible for tuning the binding strength and subsequent cytotoxicity of such compounds. The linear aliphatic side-chains can easily insert into the minor groove of the DNA structure, displacing the ordered water and entropically increasing the net binding energies for such compounds. Cyclic aliphatic and aromatic side-chains are more rigid and are therefore less able to conform to the minor groove of the DNA and therefore have a reduced binding energy which results in the lower activities observed.

The final trend observed was related to the RF values. The RF values compare the sensitivities of the Cisplatin resistant lines, A2780/CP70 and MCP1, with that of the parental A2780 cell line. RF values for Cisplatin are 16.7 and 3.9 for the CP70 and MCP1 cell lines respectively, evidently showing a decrease in activity due to resistance. An RF value of > 1 means that a compound shows cross resistance with cisplatin i.e. whatever makes the cells resistant to platinum also makes them resistant that compound. These compounds would therefore not be very interesting as potential treatments for cancer. DIPs were reported to have general RF values of < 1 which made them highly attractive targets for new anti-cancer therapies.^{124,125} Compounds that give an RF value of < 1 are of interest since they avoid the resistance mechanism for platinum drugs. Also if the RF is very low (< 0.5) it means that the compound is significantly more active in the Cisplatin resistant cells than in the parental lines and there is a possibility that it has even targeted something present in the resistant cell line that is not present in the parental line. Compounds with low RF's could potentially lead to new chemotherapeutic agents that could be used in conjunction with current treatments and allow chemotherapy to continue

when cisplatin resistance develops. The plots of the RF ratios for the AEP, TIP and DIP frameworks with respect to the amino side-chain functionality are shown in Figure 49.

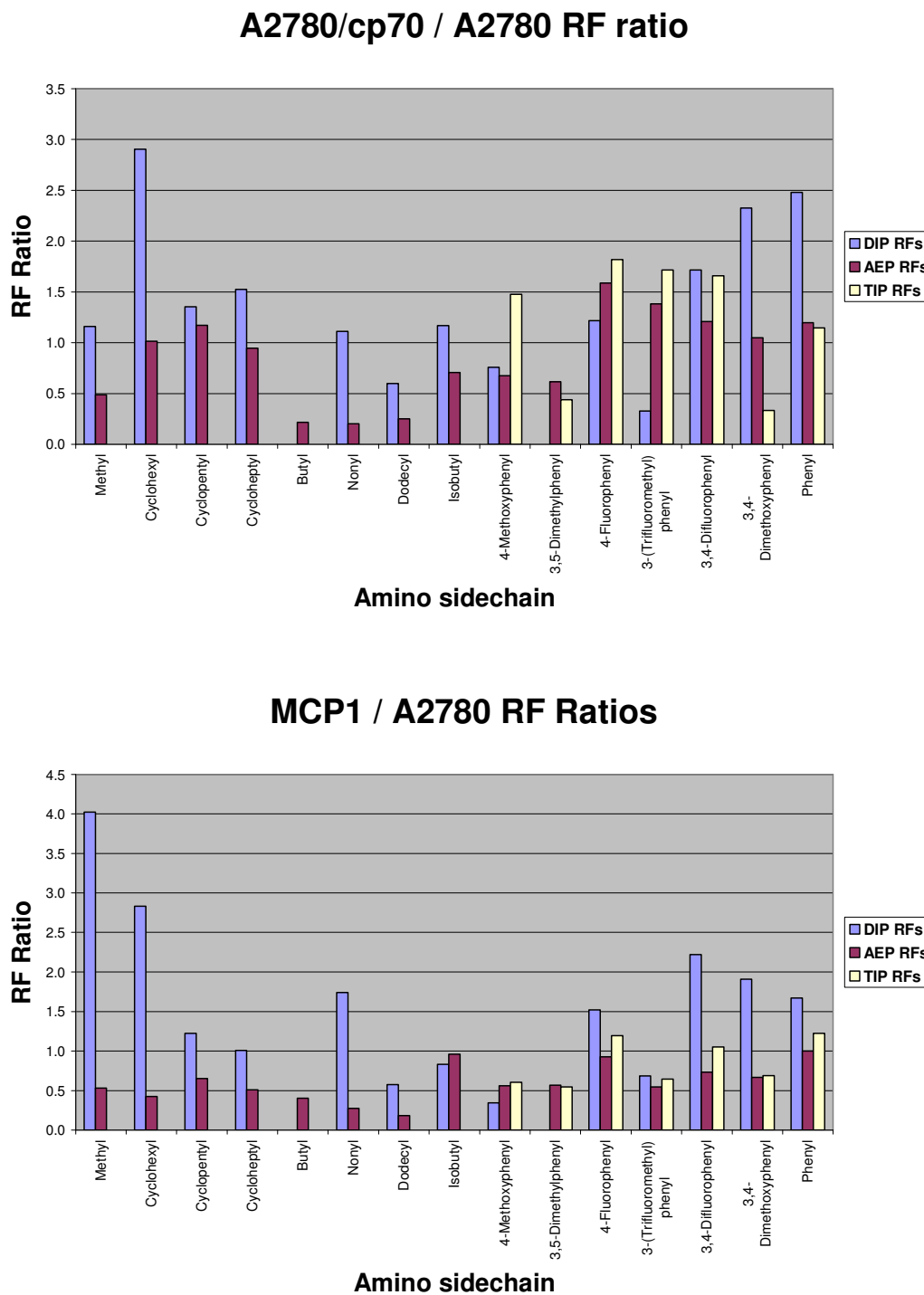


Figure 49. Plot of cp70/A2780 RF ratios (top) and MCP1/A2780 RF ratios (bottom) for AEP, TIP and DIP frameworks as a function of the amino side-chain.

From the RF plots it can be seen that the AEPs and TIPs match, if not slightly better, the DIP compounds with respect to their RF values. For the CP70 data range, the average RF values are 1.2, 0.8 and 1.2 for the DIPs, AEPs and TIPs respectively; for the MCP1 data range, the average RF values are 1.4, 0.6 and 0.8 for the DIPs, AEPs and TIPs respectively. As mentioned previously this is a highly desirable property for new anti-cancer drug candidates as they are either unaffected by the same resistance mechanisms as cisplatin or are possibly even targeting the resistant strains. The lack of susceptibility of these compounds can be explained by their different mode of action to cisplatin. Cisplatin is a transition metal complex that works by covalently cross-linking DNA base pairs and distorting the DNA double helix, preventing replication. The correlation between cisplatin resistance and the loss of MLH1 protein expression suggests the DNA mismatch repair system has a role in generating signals that contribute to the generation of apoptotic activity.¹⁸⁰ The binding mode for AEP/TIPs is suggested to be through intercalation and minor groove binding. However their mechanism for initiating apoptosis must not be associated with the mismatch repair proteins coded for by hMLH1 since they retain, or even increase, their activity in its absence. The uniformly low RF values across the range for the TIPs and AEPs could prove to be very useful as major changes could be made to drug targets to increase their potency without affecting this desirable characteristic.

The comparative cytotoxicity assay of AEP/TIPs/DIPs has yielded the following results: (i) IC₅₀ values for the AEP/TIPs are in the μM concentration range, comparable to DIPs; (ii) The activities of AEPs and TIPs appear to be related, suggesting a common active species; (iii) Interconversion of AEPs and TIPs *in vitro* is thought to be the reason for this association in activity; (iv) RF values for AEP/TIPs are typically ≤ 1 and so are not susceptible to the same resistance mechanisms as cisplatin; (v) consequently the induction of cell death by AEP/TIPs is not dependent upon the mismatch repair function. These initial observations for the AEP/TIP framework warrant further investigation of the system as a possible source of selective chemotherapeutics. However since it is not possible to carry out pH variable assays, the only way to investigate the selectivity aspect would be *in vivo* assays. The next stage for evaluation of compounds would therefore be human tumour xenografts in mice for further clinical development. These tests provide much more data than the *in vitro* assays, such as compound stability and metabolism, bioavailability, tumour suppression, and therapeutic index. A small selection of

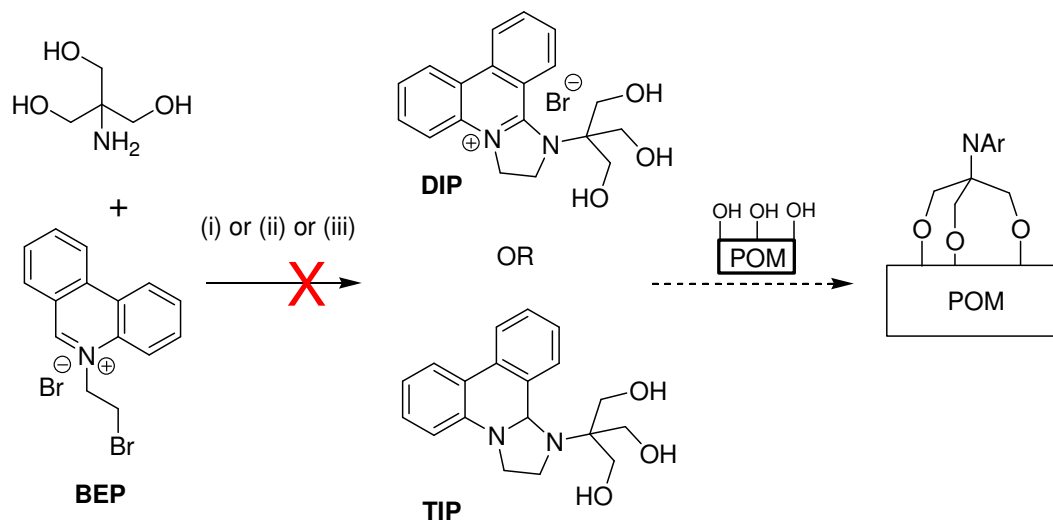
compounds have been selected and will be screened for *in vivo* activity and selectivity using this assay.

7 POLYOXOMETALATE ORGANIC HYBRIDS

7.1 TRIS-base Phenanthridine Ligands

Due to the electrochemical properties reported for many polyoxometalate structures¹⁸¹⁻¹⁸⁴ and the electrochemical properties observed for the phenanthridine based heterocycles discussed earlier it was thought that combination of the two could lead to materials with interesting new electrochemical properties. Derivatization of TRIS-base with various organic functionalities and subsequent “grafting” onto POM structures has been used to successfully derivatize POM clusters.^{144,185} The synthetic strategy proposed for creating phenanthridine-POM conjugates therefore relied upon generation of a suitably functionalised TRIS-ligand.

Since the TRIS-base contains a primary amine functionality, it was thought that reaction with BEP would yield a suitable phenanthridine-TRIS ligand that could then be “grafted” onto the POM cluster. However no phenanthridine-based conjugates were obtained as there were incompatibility issues for all the synthetic strategies available for the reaction of TRIS-base with BEP (Scheme 28).



Scheme 28. Proposed reactions of TRIS-base with BEP.

(i) The monophasic DMF methodology for DIP synthesis involves the reaction of 1 eq of the amine with 1 eq of BEP to produce the TIP intermediate, a second equivalent of BEP is then consumed as the stoichiometric oxidant to yield the DIP product. For large sterically hindered amines this oxidation process is inhibited and so the TIP intermediate cannot be converted to the DIP product; (ii) The biphasic $\text{Na}_2\text{CO}_3/\text{EtOAc}$ methodology for DIP synthesis requires phase transfer of the intermediates to the organic phase after the α -addition and cyclisation steps to produce an organic solution of the TIP. The intermediates generated from TRIS-base addition are less hydrophobic due to the multiple hydroxyl groups and therefore do not transfer across the phase barrier during the reaction; (iii) The monophasic chloroform methodology for TIP synthesis requires the amine to be soluble in organic solvents, which TRIS-base is not. Changing the solvent system to a polar protic solvent was not an option as this lead to the formation of pseudo-base by the addition of solvent to the phenanthridinium moiety. The formation of the pseudo-base product was confirmed by a ^1H NMR spectroscopy experiment: TEA was added to a solution of BEP in CD_3OD and the ^1H NMR spectrum was obtained (Figure 50).

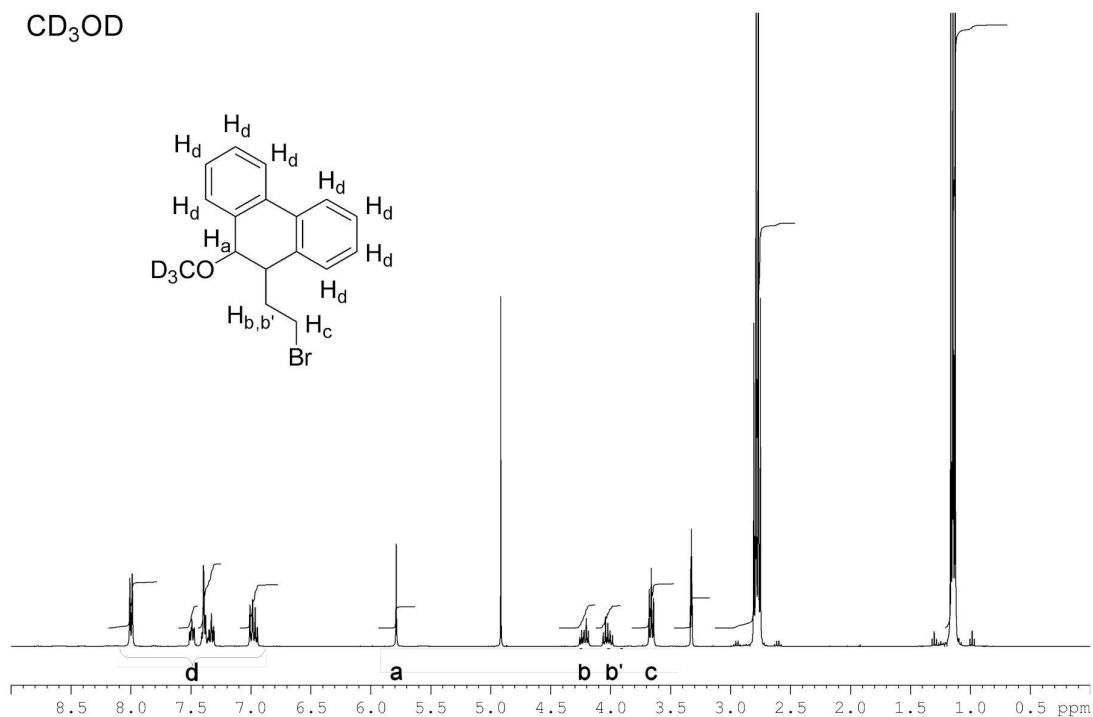
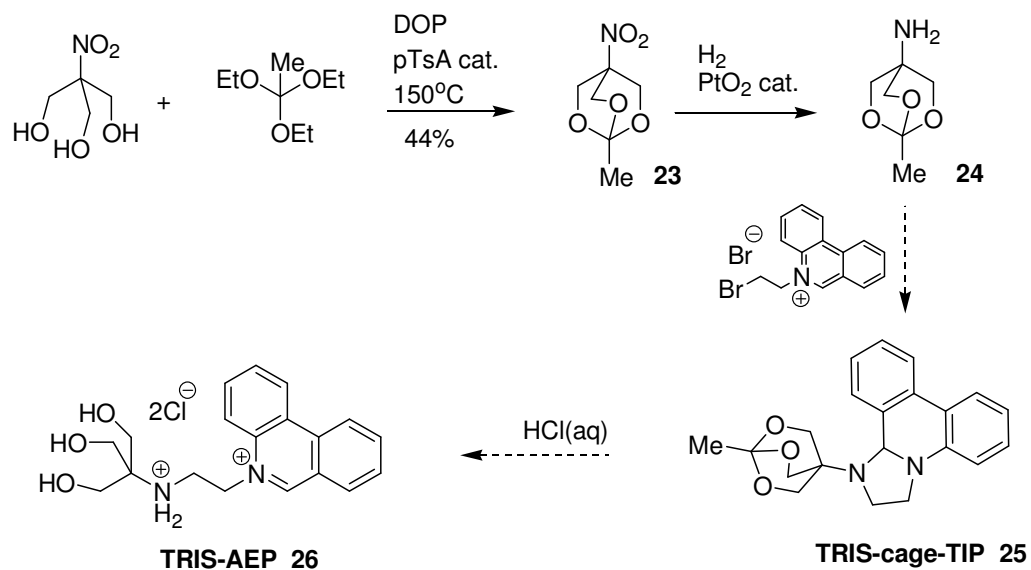


Figure 50. ¹H NMR of methoxy-BEP pseudo-base product.

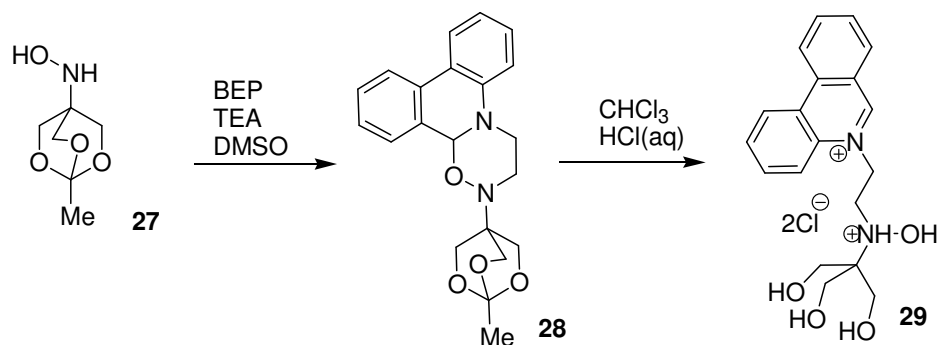
The synthesis of a protected TRIS-base analogue was therefore proposed as an alternative amine substrate that could react cleanly with the BEP reagent and then be deprotected to produce the desired aromatic frameworks.



Scheme 29. Synthesis of protected "TRIS-cage" and proposed reaction with BEP and aqueous acid deprotection.

The synthesis of the amino orthoacetate **24** is a reported procedure and should have been a simple 2-step synthesis, however the hydrogenation step was not as easy as expected. The apparatus available for high pressure hydrogenations was an H-cube flow system so development of a new procedure that was compatible with this kit was initially investigated. A range of parameters were investigated, specifically catalyst type, pressure, temperature, flow rate and reaction time, in an attempt to develop a compatible procedure however no amino orthoacetate **24** was ever synthesised. Conversion of the nitro starting material **23** to the hydroxylamine intermediate was relatively successful and produced the hydroxylamine in reproducible yields of ~75%. With the hydroxylamine in hand we decided to proceed and investigate the reaction of this compound with the BEP starting material, fortunately this reaction was successful and led to the synthesis of a new oxadiazinophenanthridine motif.

The reaction of hydroxylamine **27** with BEP and TEA in DMSO led to the formation of the 2-(1-methyl-2,6,7-trioxa-bicyclo[2.2.2]oct-4-yl)-3,4-dihydro-2H,12*b*H-1-oxa-2,4a-diazatriphenylene, **28** (Scheme 30).



Scheme 30. Reaction of BEP with TRIS-cage hydroxylamine **25 and the subsequent ring-opening deprotection reaction.**

The structure of **28** was characterised by NMR, MS and IR spectroscopy and fortunately good quality single crystals allowed the structure to be unambiguously assigned using single crystal X-ray diffraction.

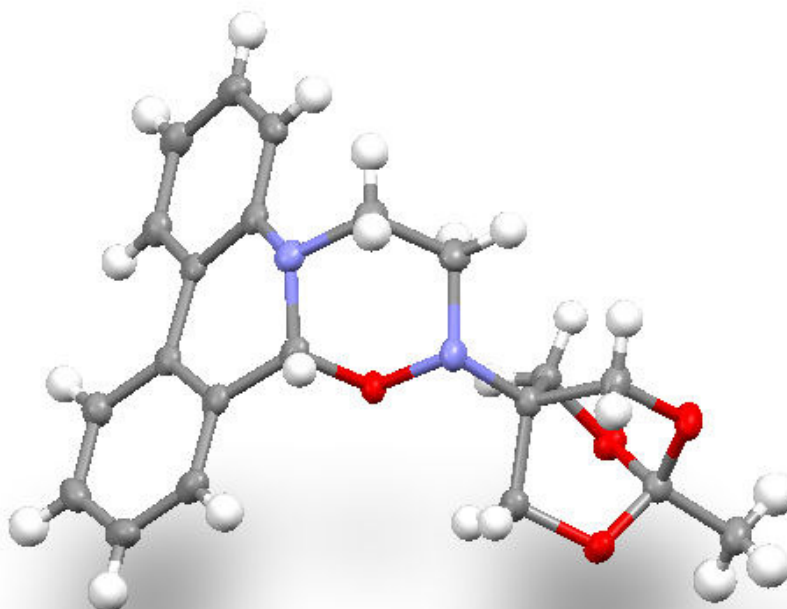


Figure 51. Ball and stick graphical representation of phenthridino-oxadiazine 28.

The six-membered oxadiazine ring can clearly be seen to distort the planarity of the system, similar to the TIPs, and although it is difficult to see from this figure, the angle between the C-N bond of the TRIS-cage sidechain and the plane of the phenanthridine ring system is almost 90° . Isolation of this compound further demonstrated the high reactivity of the BEP and its ability to react with various nucleophiles to generate new heterocyclic frameworks. In the past, BEP has been reacted with primary amines, secondary amines, thiols, and even carbon-based nucleophiles.¹⁸⁶⁻¹⁸⁸ Attempts were made to oxidise the oxadiazinophenanthridine using the standard conditions for TIP-DIP oxidations, however these were unsuccessful. The exchange of the nitrogen at this crucial position appears to produce heterocycles without the same “hydride donor” properties as the TIPs. Dihydropyrrolophenanthridines, generated by nucleophilic attack of BEP with carbon-

based nucleophiles, are also unable to be oxidised under similar conditions.¹⁸⁸ Although the oxadiazinophenanthridine framework does not appear to possess the same redox properties as the TIPs, related phenanthridinotriazine and oxadiazinophenanthridine frameworks have previously been reported to have high levels of fungicidal activity making this discovery even more exciting.¹⁸⁹ The possibility of extending this methodology to other hydroxylamines will therefore be investigated as it could lead to the development of a new family of biologically active heterocycles and a facile route for their synthesis.

Similar to the imidazo ring system of the TIP heterocycles the oxadiazine ring was susceptible to ring opening via protonation. A two-step ring opening and deprotection of **28** could therefore be carried out in a single reaction to afford the ring open analogue **29**. This ligand contained the desired functionality we originally set out to achieve; a phenanthridine-based heterocycle for potential switching and electron transfer and a triol functionality for coordination to the POM metal salt. Attempts to coordinate the ligand to a Mo₆ metal salt to generate the derivatized Anderson cluster were however unsuccessful and no POM-ligand conjugates were obtained. The high charge on the ligand was thought to be the main barrier for ligand coordination.

Eventually a successful procedure for the problematic hydrogenation step (Scheme 29) was found (EtOAc, PtO₂ cat., 7 bar, 24h, autoclave) so the original synthesis could be completed. A ¹H NMR experiment was used to screen the reaction of the amino orthoacetate **24** with BEP and TEA base with positive results. The spectrum obtained (Figure 52) clearly shows the conversion of the BEP starting material to the TIP structure as expected. However attempts were not made to isolate this product as the deprotected AEP derivative **26** would have very similar properties to compound **29** and so would also be unlikely to coordinate to the metal cluster to give the desired hybrid target. Efforts were therefore shifted towards synthesising an aldehyde functionalised heterocycle and a neutral coordinating ligand.

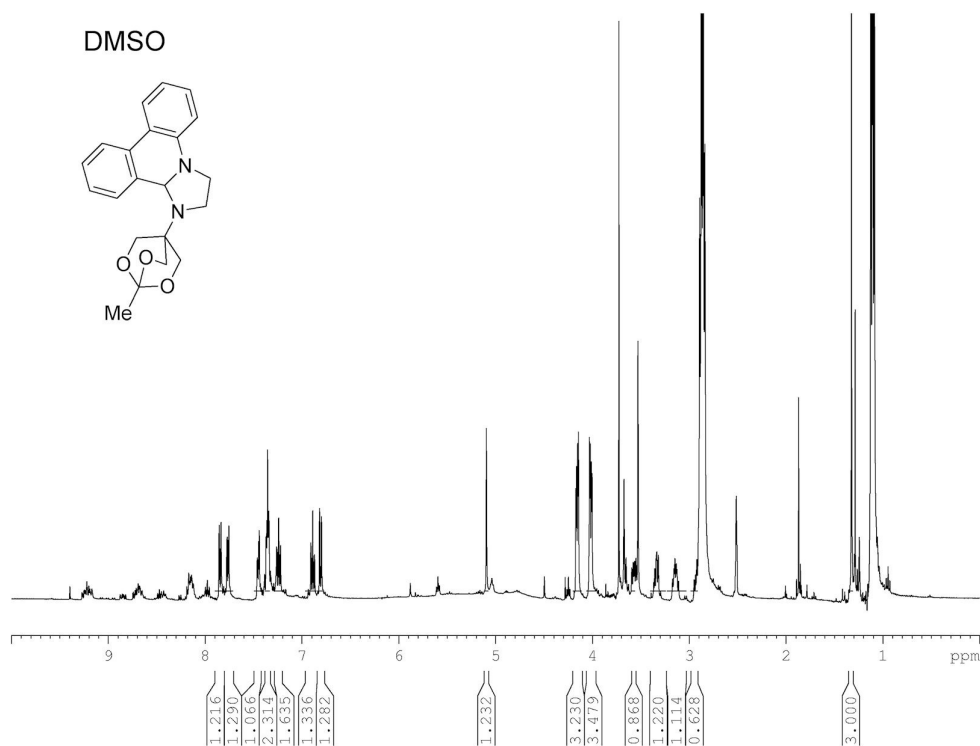
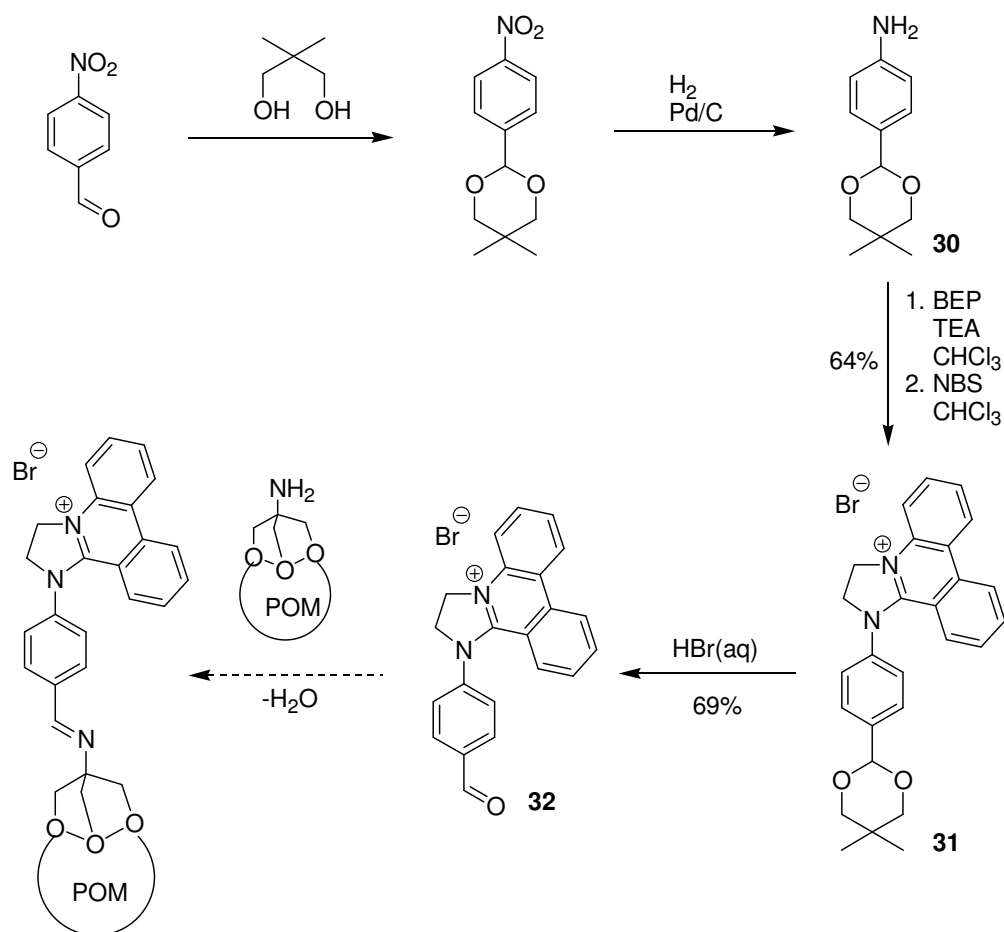


Figure 52. ^1H NMR of crude reaction mixture for the reaction of **24** (**1eq**) with **BEP** (**1eq**) and **TEA** (**3eq**).

7.2 Phenanthridine Aldehyde Ligands

Another route to inorganic-organic hybrid structures is available via combination of a POM cluster functionalised with a “free” TRIS ligand with an organic aldehyde using a Schiff base reaction. This method has been used to create many hybrid structures of varying organic functionality.^{144,190} A synthetic route to DIP-aldehyde **32** was devised with the aim of conjugating it with a TRIS-POM cluster to give the desired hybrid target (Scheme 31).



Scheme 31. Synthesis of organic-POM hybrid via Schiff base reaction of DIP-aldehyde and TRIS-POM.

The protected amine **30** was synthesised *in house*, in two steps, from commercially available *p*-nitrobenzaldehyde. Reaction of the amine with BEP first afforded the acetal protected DIP **31** which could then be easily deprotected in aqueous acid to give the required DIP aldehyde **32**. However subsequent reaction of the DIP-aldehyde with the TRIS-Dawson TBA salt, [C₄H₈NO₃P₂W₁₅V₃O₅₉][C₁₆H₃₆N]₅, did not undergo the desired Schiff base reaction. Instead, when a solution of DIP aldehyde **32** (1eq) in MeCN was added to a solution of TRIS-Dawson TBA salt (1eq) in MeCN, a pale yellow precipitate formed upon mixing. The precipitate was collected by filtration and dried under vacuum. The isolated product (compound **33**) was insoluble in all regular stocked solvents except DMSO and DMF. The product was able to be analysed by ¹H NMR spectroscopy. The

Spectrum obtained showed peaks for the DIP aldehyde and peaks correlating to the methylene and amino protons of the TRIS-Dawson (Figure 53).

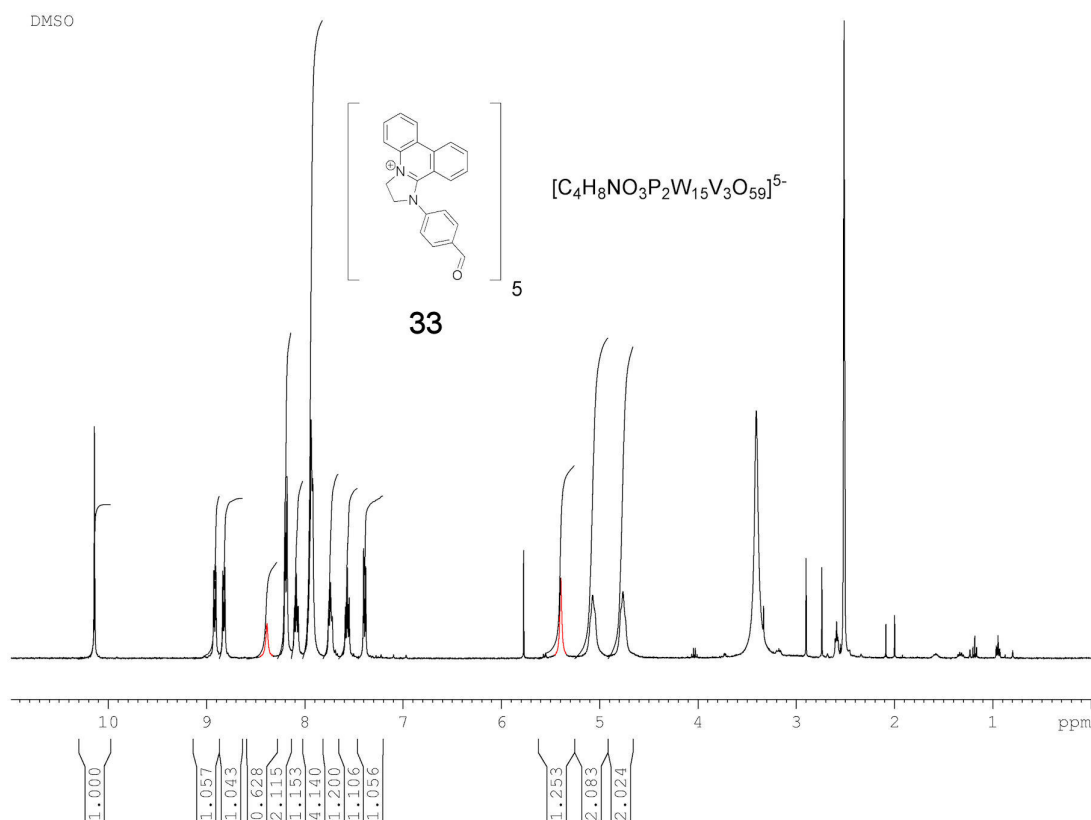


Figure 53. ¹H NMR spectrum of TRIS-Dawson-DIP-aldehyde precipitate (**33**). TRIS proton signals are highlighted in red.

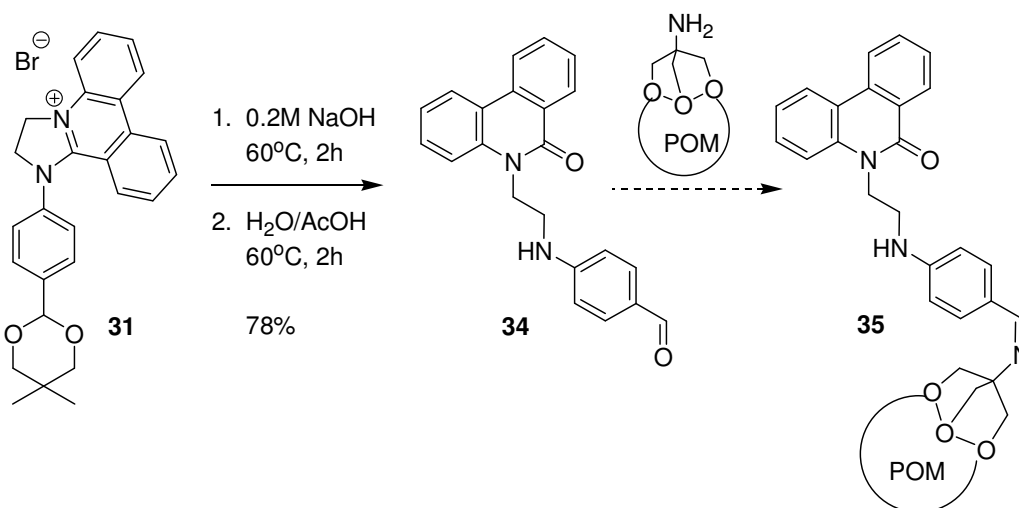
The ratio of the DIP signals to TRIS signals is 5:1 which correlates with the direct cation exchange of the TBA cations for the aldehyde-DIP. As the product obtained was very poorly soluble the only characterisation obtained was the initial ¹H NMR spectrum, attempts to recrystallise the material for single crystal XRD have as yet been unsuccessful.

This result is in correspondence with other results obtained within the Cronin group where DIP cations have been combined with other POM systems to create self assembling microscale tubular structures via cation exchange.^{153,154} The reasons for the formation of these structures is dependent upon the low aqueous solubility of the inorganic-organic

hybrid material formed. This property is not restricted to DIP cations, and microtubes have been grown by the exchange of other aromatic cations such as rhodamine. This has inspired a new area of research for the group where investigations into the combination of POM clusters with aromatic cations of a more interesting nature are now underway.

7.3 Neutral Phenanthridine Ligands

With the competing cation exchange reaction preventing the possibility of the Schiff base reaction of the DIP-aldehyde it was thought that the design of a neutral phenanthridine-aldehyde ligand would increase the probability of a successful combination with the POM cluster. Investigations into creating such a compatible ligand began with the design of the phenanthridinone-aldehyde ligand **34** (Scheme 32).

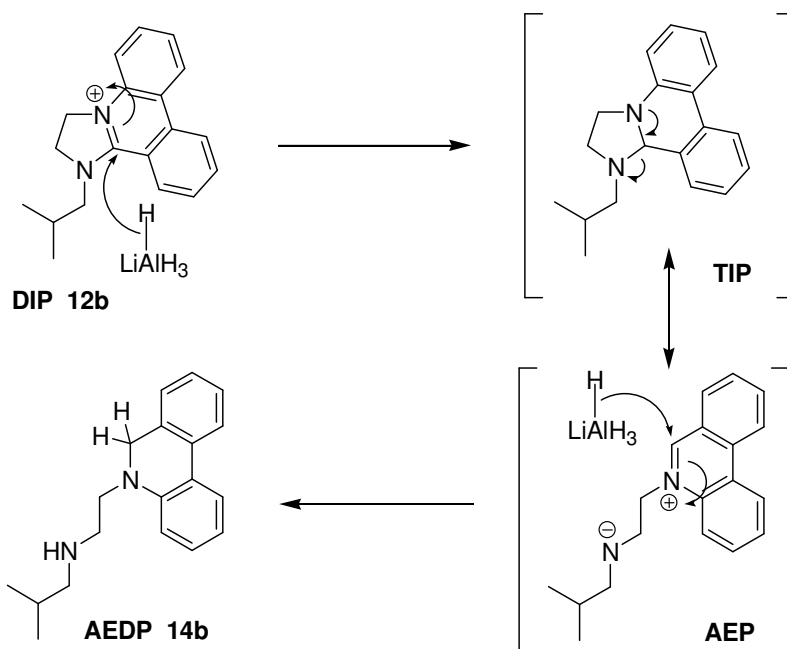


Scheme 32. Synthesis of phenanthridinone-aldehyde ligand.

The phenanthridinone-aldehyde ligand can be isolated directly from the acetal-DIP **30** by stepwise hydrolysis of the DIP and the acetal, affording the required phenanthridinone aldehyde **34** in good yields. Attempts to attach the ligand to both the TRIS-Dawson, [C₄H₈NO₃P₂W₁₅V₃O₅₉][TBA]₅, and bis-TRIS-Manganese Anderson, [MnMo₆O₂₄(C₄H₈N)₂][TBA]₃, are underway but have not yet yielded crystals. Obtaining a material with the switchable and redox functionality of the AEP/TIP system is not possible

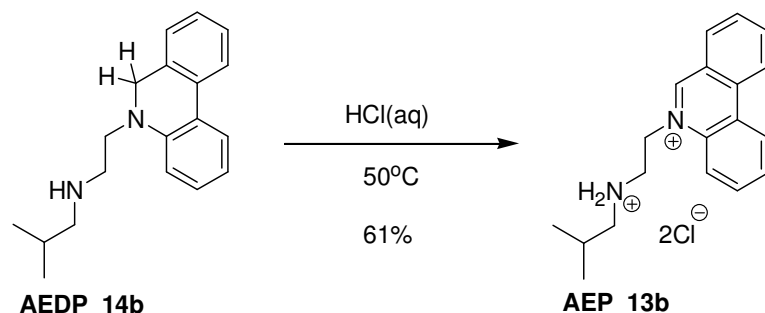
using this synthesis as the phenanthridinone moiety is not susceptible to cyclisation. However structures from combination of these ligands with POMs could lead to materials with interesting interactions within the crystal lattice due to the possibilities of H-bonding from the amine and carbonyl groups and π -stacking of the phenanthridinone rings.

Initial investigative studies have shown that the synthesis of an analogous reduced phenanthridine compound could also be a viable route to TIP-aldehyde ligands from DIP-acetal **31**: DIP frameworks have a very high reduction potential so chemical reduction by reducing agents such as sodium cyanoborohydride, sodium borohydride and sodium dithionite have been unsuccessful. Using a much stronger reducing agent like lithium aluminium hydride has yielded a successful method for DIP reduction, however the reduction product was not the expected TIP framework. Reduction of isobutyl-DIP **12b** with LiAlH_4 led to isolation of the isobutyl-AEDP not the isobutyl-TIP. The LiAlH_4 must reduce the DIP to the TIP form but as the TIP is in equilibrium with the AEP form a second, easier reduction of the phenanthridinium/imidazol moiety lead to the AEDP product **14b** obtained. The proposed mechanism for this conversion is shown in (Scheme 33).



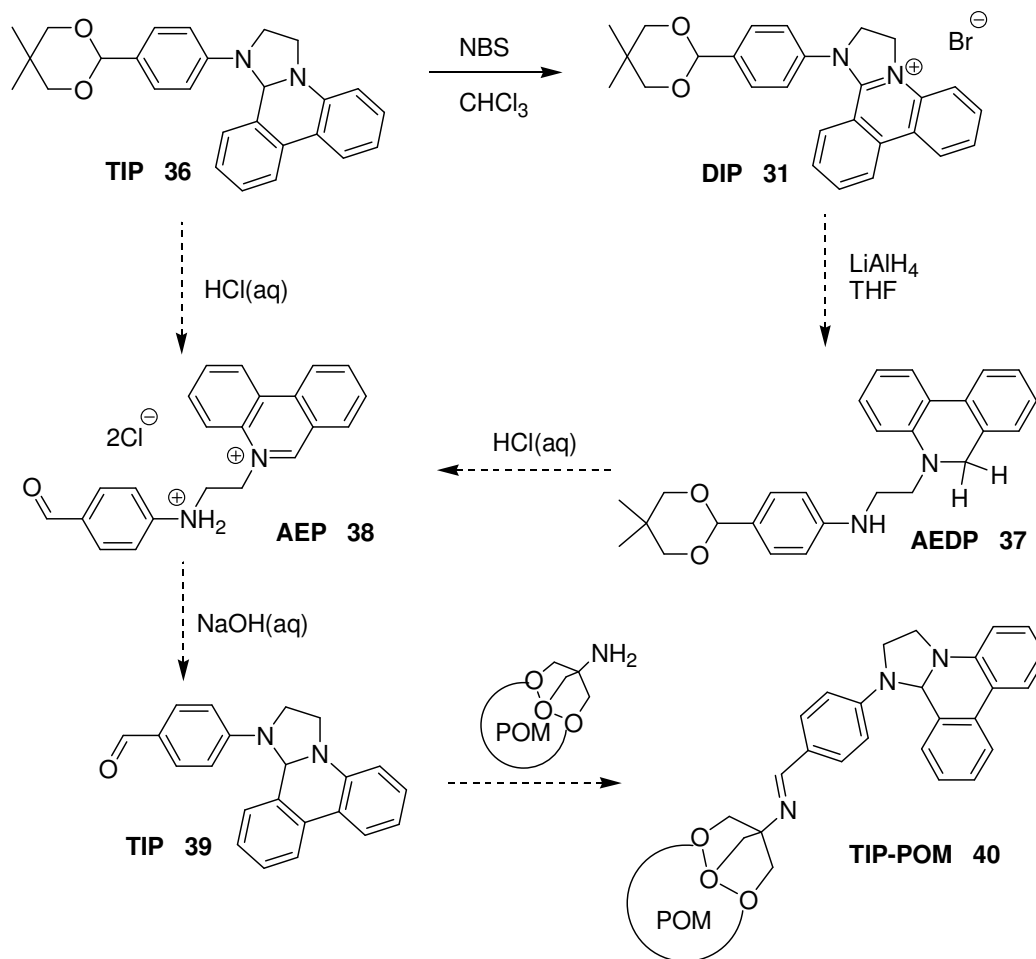
Scheme 33. Mechanism for the reduction of isobutyl-DIP to isobutyl-AEDP.

The AEDP frameworks can be easily reoxidised to the AEP form simply by heating in aqueous acid (Scheme 34).



Scheme 34. Reoxidation of AEDP to AEP in aqueous acid.

Combination of these reduction and oxidation steps could therefore form a synthetic route to the TIP-aldehyde ligand **39** from the DIP-acetal **31**. This synthesis could however be greatly simplified by isolating the TIP-acetal **36** since the TIP-aldehyde **39** could be easily produced from here in a simple two step reaction (Scheme 35).



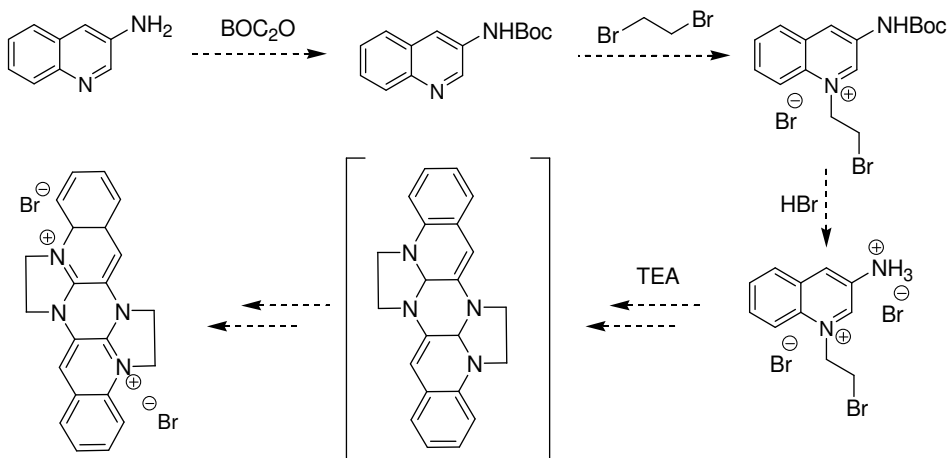
Scheme 35. Proposed scheme for the synthesis of AEP/TIP-aldehyde ligands.

The electrochemical properties of the TIP-POM conjugate **40** could then be studied which would hopefully lead to some interesting electron transfer mechanisms between the POM cluster and the ligand.

8 CONCLUSIONS AND FUTURE WORK

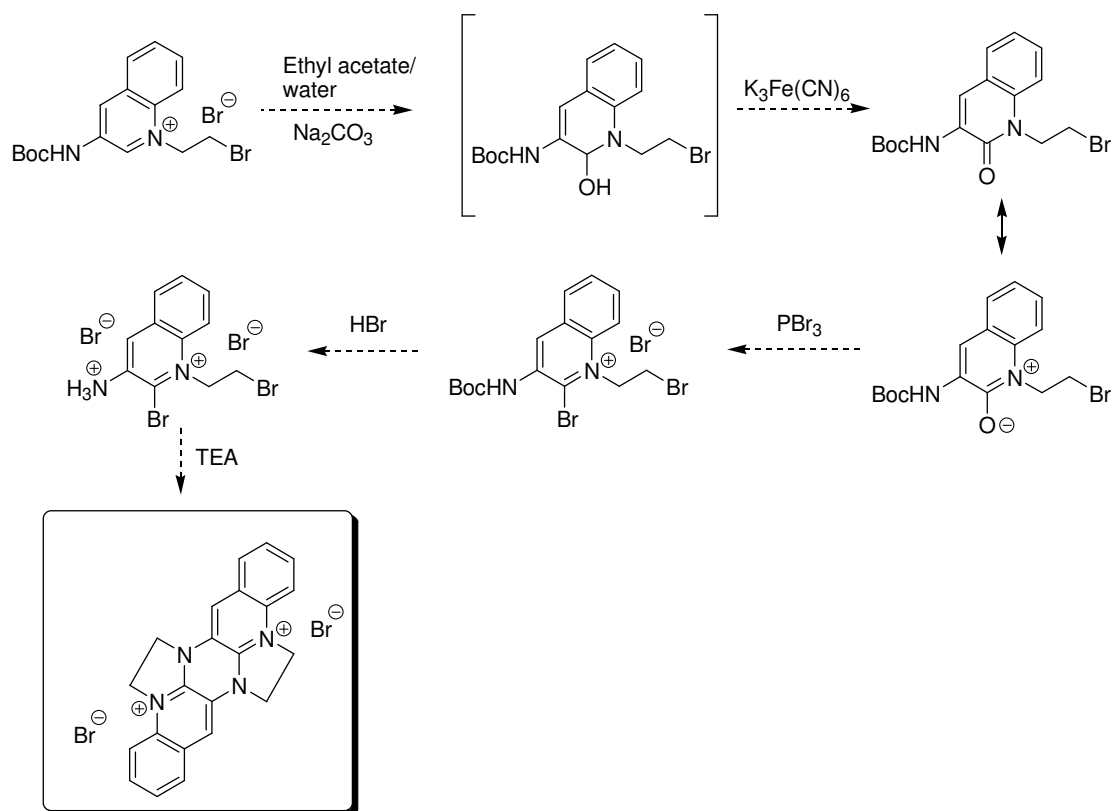
8.1 Macrocyclic Polycations

2-bromoethyl alkylated *N*-heterocycles like quinoline had been previously shown to react with primary amines in a 3-step cascade reaction to form DIQ type cationic frameworks.¹²¹ The application of this multi-step reaction sequence to amino-quinolines was investigated with the aim of generating complex polycationic macrocycles via a simple one pot methodology. 4-aminoquinoline was selected as the initial candidate but failed to yield any macrocyclic products. The position of the amino functionality relative to the quinoline-*N* proved to be a key factor for the reactivity of the alkylated substrates and consequently the reasons for the different reactivities of 4-aminoquinoline observed. Conjugation between the amine and the quinolinium-*N* centre severely reduces the nucleophilicity of the amine and renders it unreactive towards the electrophilic iminium centre. The 4-position of quinoline is also a poor location for the amine functionality due to the steric influence of the benzo ring, which hinders nucleophilic attack of the amine. 3-aminoquinolines overcame these problems with reactivity, and was proven to retain amine nucleophilicity even after alkylation of the quinoline-*N*. This was only demonstrated with simple *N*-methylated analogues as direct bromoethylation of 3-aminoquinoline was not possible without an appropriate protection strategy. 3-Amino-1-(2-bromoethyl)-quinolininium bromide has been proposed as a suitable substrate for future attempts to create cyclic oligomers using this reaction methodology. The proposed synthesis is shown in Scheme 36.



Scheme 36. Proposed synthesis of 3-amino-1-(2-bromoethyl)-quinolininium bromide and subsequent multi-step dimerization.

There are no foreseeable issues with the synthetic route to the alkylated substrate and the multi-step reaction should proceed at least as far as the α -addition and cyclisation steps as the substrate fulfils the criteria required for a successful multi-step reaction: The amine is not fully conjugated and should therefore retain nucleophilicity even after alkylation, the amine is sterically unhindered, and the relative orientation of the amine and iminium moieties should favour dimerization/cyclisation over linear polymerization. Isolation of the neutral unoxidised dimer would be the most likely product from this reaction due to the difficulties previously encountered with oxidation of aryl-tetrahydroimidazoquinolines. Oxidation could be encouraged by insertion of a bromine at the 2-position of the quinolinium substrate (Scheme 37). The increased steric hindrance introduced by the bromine ortho to the amine would hopefully be overcome by the increased electrophilicity of the iminium centre.

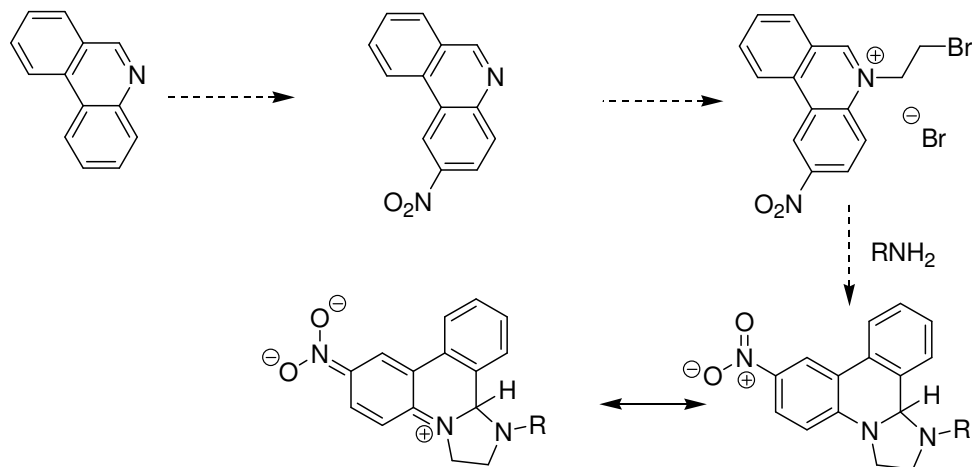


Scheme 37. Proposed α -bromination strategy for DIQ-macrocycle/dimer synthesis.

8.2 TIP Synthesis and Applications

A methodology for the isolation of 1,2,3,12b-tetrahydroimidazo[1,2-*f*]phenanthridines has been developed. The mechanism for their formation from the reaction of primary amines with the BEP cation involves an α -addition followed by an intramolecular cyclisation. The inhibition of oxidative hydride loss from the TIP framework is dependent upon the availability of the *N* lone pairs of the incoming amine nucleophile, which can be finely tuned by partial conjugation with substituted phenyl side-chains. The steric bulk of the amine side-chain can also inhibit hydride transfer and stabilise the TIP framework. Both the electronic and steric influences are very sensitive and a balance in size and conjugation must be achieved for reaction success, i.e. if the level of conjugation is too high, or the amine is too sterically crowded, then the α -addition and cyclisation steps cannot proceed; if the level of conjugation is too low, or the amine is insufficiently crowded, then there is no inhibition of the hydride transfer.

The initial synthetic methodology developed is unquestionably limited to mainly aryl primary amines, however our investigations and demonstrated understanding of the reaction processes should enable modification of our procedures to accommodate other primary amines and enhance the scope of the methodology. An immediate plan for future work will therefore involve functionalizing the phenanthridine ring to investigate the subsequent effects electron withdrawing groups and various positions will have on the stability of the TIP frameworks. For example, nitration of the phenanthridine ring should reduce the electron density of the phenanthridine ring and could increase the stability of TIPs formed from unhindered aliphatic amines (Scheme 38). The electron withdrawing effect of the nitro group removes the electron density from the phenanthridine-*N* in the same way the phenyl rings of aryl-TIPs remove electron density from the amino-*N*. The facile oxidation to the DIP form could therefore be inhibited, even for TIPs formed from the addition of aliphatic amines. Potential problems with the regioselectivity of nitration of phenanthridine¹⁹¹ and reduced nucleophilicity of nitro-phenanthridine would need to be addressed as part of this investigation.



Scheme 38. Nitration of phenanthridine and subsequent stabilization of the TIP formed.

Other ways to increase the scope of the reaction could be to investigate the application of the methodology to other *N*-heterocycles such as quinolines, quinazolines and pteridines to isolate their tetrahydroimidazo derivatives.

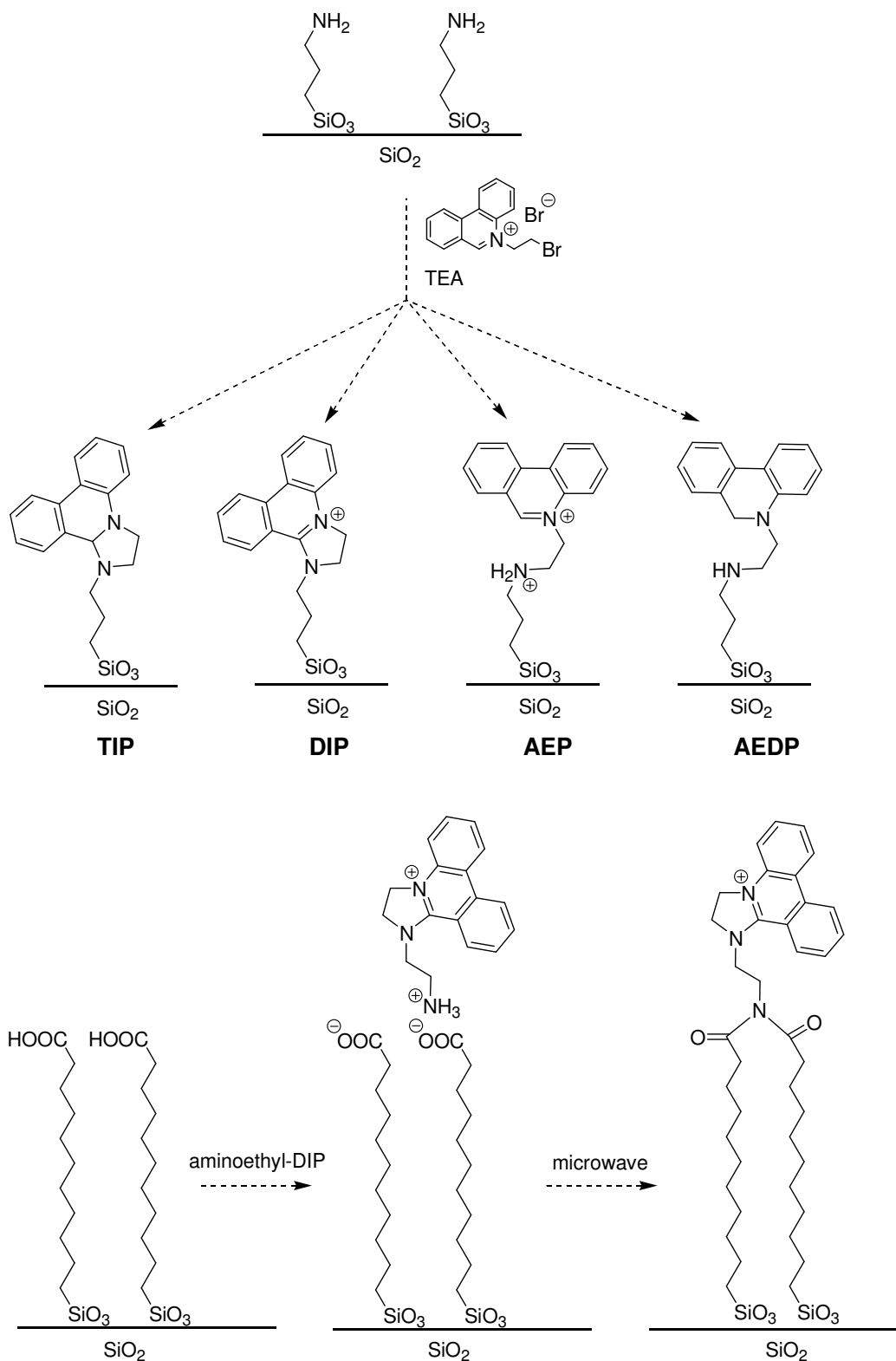
Exploiting the reductive nature of the TIP framework is also a priority for any future work in this area. Similar aryl-fused 5-membered di-nitrogen ring systems, such as 2,3-dihydrobenzo[*d*]imidazoles, have highly selective reducing properties and have been used in the reductive dehalogenation of α -halo ketones, aldehydes, esters, lactones, and carboxylic acids, cleanly and almost quantitatively.^{192,193} TIPs could potentially carry out the same conversions equally as well; they have comparable levels of tenability, their syntheses are easy, but they are also chiral, making them a potentially useful addition to the reagents currently used to carry out such conversions.

8.3 Lockable Molecular Switch

Acid induced ring opening of the TIP framework leads to the formation of AEP dication. The reverse, base induced cyclisation reaction was also found to be possible. The cyclisation process between these heterocyclic systems can operate reversibly in both monophasic and biphasic conditions using pH control. Reduction and oxidation of the

AEPs and TIPs, respectively, can be used to irreversibly inhibit this process. These reversible and irreversible switching methods were used to form the basis of a solution-based “lockable molecular switch”. Attempts to immobilize the switchable frameworks on gold substrates, with the hope of enhancing or altering the device performance, were unfortunately unsuccessful. None of the disulfide analogues that were synthesised showed any evidence of adsorption onto the gold substrates. It was thought that steric and electronic repulsion between the heterocycles and the gold surface were the reasons for lack of adsorption. Disulfide analogues with longer lipoic acid linkers were synthesised to overcome these issues, however, gold was later deemed to be an inappropriate choice of substrate for the development of a robust switching device and work on this project was halted.

Continuation of this work therefore requires a robust substrate-heterocycle linker that will be stable to repeated exposures of the switching conditions, and will also allow for structural distinction of the monolayers in each of the four switching states. A good candidate for future surface studies could therefore be SiO₂ substrates¹⁹⁴ functionalized with DIP-alkylsilanes. Self-assembled monolayers on silicon oxide have very high thermal stabilities (150°C in air),¹⁹⁵⁻¹⁹⁸ are stable to harsh oxidizing (KMnO₄)¹⁹⁹ and reducing (LiAlH₄)²⁰⁰ conditions, and are stable in mildly acidic aqueous media (0.1N HCl for more than 40 h).²⁰¹ The only drawback could be the potential hydrolysis of the Si – O bonds in aqueous base (0.1N NaOH resulted in immediate degradation)²⁰¹ however much milder non-nucleophilic bases like TEA could be used for the cyclisation switching step. A simple procedure for the synthesis of these monolayers could be achieved by the *in situ* derivatization of amino terminated monolayers by the addition of BEP (Scheme 39, top). The amino terminated monolayers can be easily synthesised from commercial reagents and materials.²⁰² Another potential route to SAMs functionalized with DIP-type heterocycles could be via microwave-induced imide formation¹⁹⁹ (Scheme 39, bottom). The SAMs formed should be stable to the conditions required for interconversion of all forms of the heterocyclic component; DIP, TIP, AEP, and AEDP.



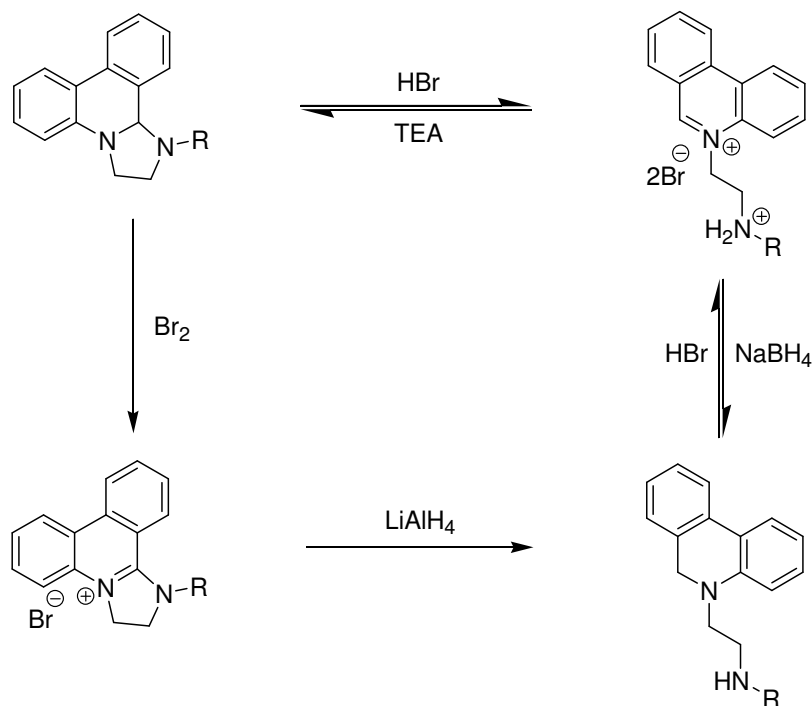
Scheme 39. (top) *In situ* derivatization of amino terminated alkylsilane monolayers to form switchable heterocycles chemisorbed on the silicon oxide substrate. (bottom) Microwave-induced imide formation in SAMs.

8.4 Bioassay Results

A library of compounds consisting of AEP/TIP/DIP frameworks was synthesised and their cytotoxic activities towards human ovarian cancer cell lines were established. A large amount of structural overlap of the amine side-chains was built into the library to allow the best comparison of the SARs for each of the heterocyclic motifs. The following observations and inferences were made for the data obtained: (i) IC_{50} values for the AEP/TIPs are in the μM concentration range, comparable to DIPs; (ii) the activities of AEPs and TIPs appear to be related, suggesting a common active species; (iii) interconversion of AEPs and TIPs *in vitro* is thought to be the reason for the association in their activities; (iv) RF values for AEP/TIPs are typically ≤ 1 and so are not susceptible to the same resistance mechanisms as cisplatin; (v) consequently the induction of cell death by AEP/TIPs is not dependent upon the presence of mismatch repair function. These results are promising and have taken this project closer to realising its goal of creating chemotherapeutics with high toxicity and high selectivity. The next stage for clinical evaluation of these compounds will be *in vivo* assays with human tumour xenografts in mice. These tests will provide data on the compound stabilities and metabolism, bioavailabilities, tumour suppression, and therapeutic indices. The 15 AEP compounds will be screened for *in vivo* activity and selectivity using this assay. Since the AEPs and TIPs consistently gave similar results *in vitro* but the aqueous solubility of the AEPs is significantly better, only the AEP compounds have been selected for the initial *in vivo* testing.

8.5 IP-POM Hybrids

The synthesis of an imidazophenanthridine-based POM hybrid was attempted via TRIS-base ligand derivatization and metal coordination, and via Schiff base condensation of organic aldehydes and TRIS-POM conjugates. Neither route resulted in the successful isolation of a hybrid structure, however much has been learned about the synthesis of such materials and new discoveries were made that could have interesting applications in other areas. In the search for a neutral organic aldehyde ligand two new procedures were developed for the conversion of DIPs and AEDPs which could benefit future developments of the “lockable molecular switch” (Scheme 40).

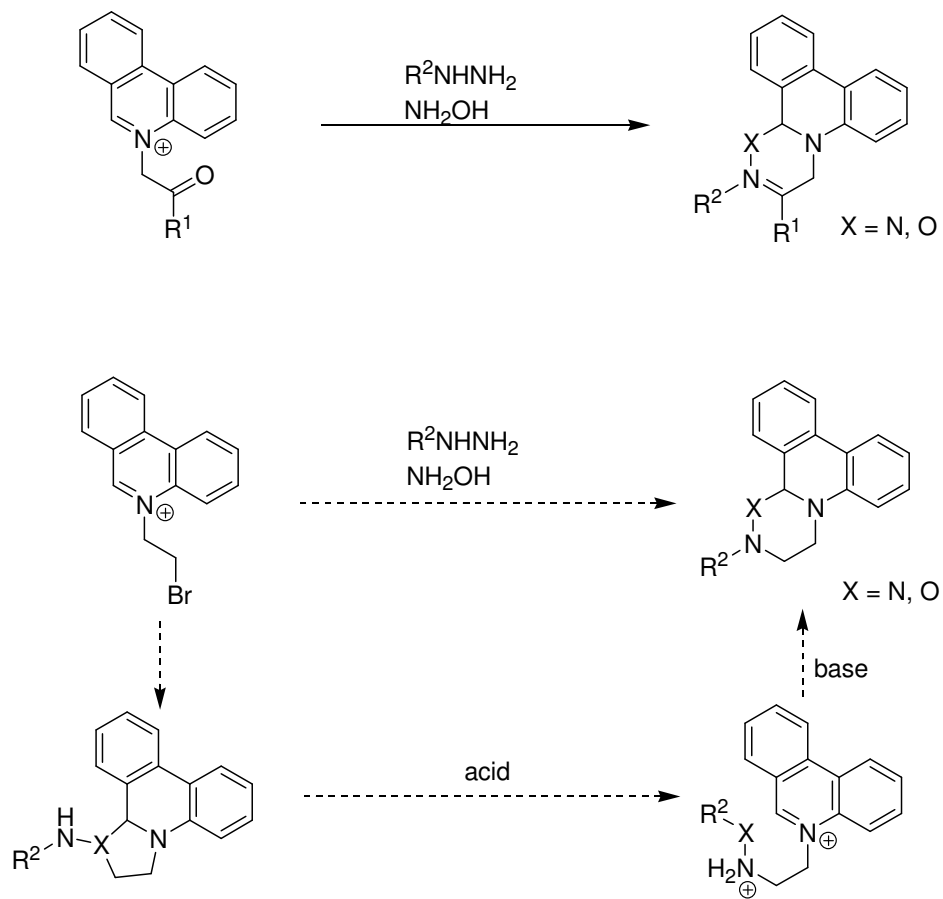


Scheme 40. Potential new switching methods for further development of the molecular switch.

The DIP reduction and AEDP oxidation methodologies complete the switching loop by offering “unlocking” or “reset” procedures to allow complete interconversion of all four switching forms.

In the search for suitable TRIS-base protecting strategies an oxadiazinophenanthridine motif was discovered by reaction of a hydroxylamine with the BEP. Related oxadiazinophenanthridine and phenanthridinotriazine compounds have been synthesised by the reaction of hydroxylamines and hydrazines with 5-(2-oxopropyl)-phenanthridinium cations (Scheme 41, top). These compounds were shown to have excellent fungicidal properties.¹⁸⁹ The reaction of BEP with these nucleophiles could therefore lead to the generation of new heterocycles with potentially high biological activities. The reaction of BEP with hydrazines has been previously used to produce DIP frameworks in the past.¹²⁹ The initial reaction mechanism must therefore favour α -addition, followed by a 5-*exo-tet* cyclisation to form the kinetically favoured 5-membered ring TIP product. However if the

TIP intermediate is acidified and the imidazo ring is opened then the product may be able to rearrange upon basification to give the 6-membered triazine ring.



Scheme 41. (top) Synthesis of phenanthridinotriazine fungicides. (bottom) Proposed synthesis of analogous phenanthridinotriazine compounds from BEP.

Experimental

9 EXPERIMENTAL

9.1 Materials

Solvents for synthesis (AR grade) were supplied by *Fisher Chemicals* and *Riedel-de Haen*. Nitrogen Gas was supplied by *B.O.C. Ltd.* and was of commercial grade. Deuterated solvents were obtained from *Goss Scientific Instruments Ltd.* and *Cambridge Isotope Laboratories Inc.* All other reagents were supplied by *Sigma-Aldrich Chemical Company Ltd.*, *Fisher Chemicals*, and *Lancaster Chemicals Ltd.* Column chromatographies were performed on Silica gel 60 obtained from *Merck*. All commercial starting materials were used as supplied, without further purification. Reactions requiring dry conditions were undertaken in AR grade solvent previously dried using a *Pure Solv 400-5-MD Solvent Purification System*.

9.2 Instrumentation

The following instruments were used for all analytical and spectroscopic measurements:

Melting point:	Stuart Scientific SMP1 melting point apparatus, using capillary tubes. The given temperatures are uncorrected
pH measurements:	Hanna Instruments HI 9025C microcomputer pH meter with a BCH combination pH electrode (309-1065) and HI 7669/2W temperature probe
Elemental analysis :	EA 1110 CHNS, CE-440 Elemental Analyser.
Mass spectrometry:	Kratos Kompact MALDI III; (ES) LCT Micromass TOF; (LSIMS) Micromass Zabspec; (CI / EI) Micromass Prospec; JEOL JMS 700 (FAB / EI / CI).
FT-IR spectroscopy:	Shimadzu FTIR-8300 and Jasco FTIR-410 spectrometers, data manipulation with Shimadzu HyperIR and JASCO software.
UV-Vis spectroscopy :	Shimadzu UV-3101PC UV-VIS-NIR Scanning Spectrophotometer. Data manipulation with Shimadzu software.
NMR spectroscopy:	Bruker DPX-400 and Avance-400 (400 MHz ¹ H, 100 MHz ¹³ C, 2D experiments). Data manipulation with Bruker Topspin.
Single X-ray crystallography:	Bruker Nonius X8 Advance diffractometer equipped with an APEXIICCD detector. Oxford Diffraction Gemini S Ultra diffractometer. Data manipulation with SHELXS-97 and SHELXL-97 via WinGX.
Cyclic Voltammetry:	VoltaLab PG301; Dynamic-EIS voltametry and CH Instruments 620A electrochemical workstation
Fluorescence spectroscopy:	Shimadzu spectrofluorophotometer RF-5301PC

9.3 Methods

When required, syntheses were carried out under nitrogen (oxygen free, dried over calcium chloride) using standard Schlenk line techniques. All reactions were carried out using oven-dried glassware. Reactions monitored by TLC were developed under UV, ninhydrin, iodine or phosphomolybdic acid; the *R_f* and eluent are given for characterised compounds purified using column chromatography. Melting points are given in degrees Celsius and are uncorrected. Peaks from mass spectroscopy are given in *m/z* (with *m* = mass in Dalton and *z* = charge), starting from the molecular peak, with relative % to basis peak. Infra red spectra were obtained using KBr disc, CaF windows or a Golden Gate; peaks are quoted in wave numbers (ν) (cm^{-1}) and their relative intensity are reported as follows: s = strong, m = medium, w = weak, b = broad. UV spectroscopy measurements are reported by plotting the wavelength (λ) in nm against Absorbance; Molar absorption coefficient (ϵ) is in $\text{M}^{-1}\cdot\text{cm}^{-1}$). All NMR spectra were recorded at room temperature unless otherwise stated. Chemical shifts (δ) are given in ppm relative to residual solvent peak. Coupling constants (*J*) are given in Hz. Signal multiplicities are expressed as follows: s = singlet, d = doublet, t = triplet, q = quartet, m = multiplet, brd = broad. The degree of substitution at carbon positions was determined by DEPT experiments. X-ray analyses were performed using suitable single crystals mounted onto the end of a thin glass fiber using Fomblin oil. X-ray diffraction intensity data were measured at on an Oxford Diffraction Gemini S Ultra diffractometer or a Bruker Nonius X8 Advance diffractometer equipped with an APEXIICCD detector. Structure solution and refinement was carried out with SHELXS-97¹⁹¹ and SHELXL-97¹⁹² via WinGX.¹⁹³ Corrections for incident and diffracted beam absorption effects were applied using analytical and empirical methods.¹⁹⁴

9.4 Electrochemical Data

9.4.1 Cyclic voltammetry studies of DIPs (12a, b, i, j, t)

The redox behavior of compounds **12(a, b, i, j, t)** were studied in (0.1 M TBAPF₆) acetonitrile solution using glassy carbon (3 mm) as the working electrode, platinum mesh as the auxiliary and Ag/AgCl as the reference electrode. Figure S1 shows the main characteristic peaks associated with the redox couples of compounds **12(a, b, i, j, t)** in the range of +1.950 V and -1.950 V vs Ag/AgCl at a scan rate of 50 mV s⁻¹. The form of the CV diagram remained identical no matter the scanning potential direction. In all cases, at the aforementioned scan rate and scanning towards the negative region of potential values, one reversible and two ill-defined irreversible reductions have been revealed while at the positive region of potential values, two irreversible oxidation peaks observed. In the case of compound **12i** a third quasireversible oxidation peak was observed at higher potential values.

Compounds **12(a, b, i, j, t)**, incorporate the same aromatic carbon architecture and reveal similar redox behavior. The relative redox potential values are summarized in Table S1.

Table S1. Cyclic voltammetry data for compounds 12(a, b, i, j, t) at 100 mV/sec.

Compound	Oxidation couples		Reduction couples	
	$E_{1/2}$ (V)		$E_{1/2}$ (V)	ΔE (V)
12t	+1.348		-0.084(ill defined)	-
	+0.895		-1.047	0.139
12j	+1.326		-0.007(ill defined)	-
	+0.958		-1.193	0.115
12b	+1.320		0.064(ill defined)	-
	+0.912		-1.279	0.156
12a	+1.314		0.013(ill defined)	-
	+0.888		-1.302	0.121
12i	-		0.002(ill defined)	-
	+1.595		-1.227	0.167
	+1.307		-	-
	+0.885		-	-

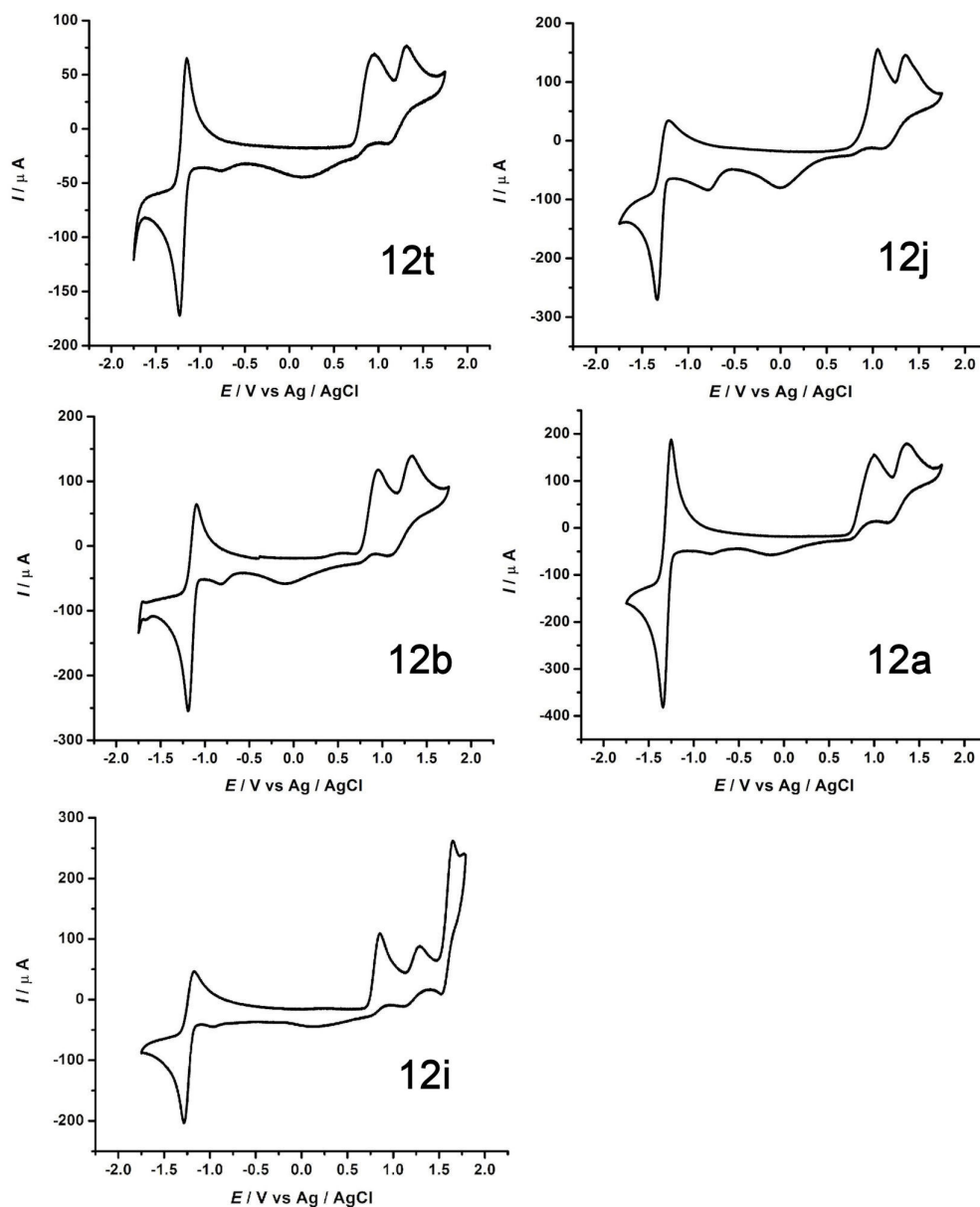


Figure S1. CV diagrams of compounds; 4a, R = cyclohexyl; 4b, R = isobutyl; 4i, R = 3,4-dimethoxyphenyl; 4j, R = phenyl; 4t, R = 3,4-difluorophenyl. Conditions: 1 mM of the compound; 0.1 M TBAPF₆ as supporting electrolyte; at 25 °C using glassy carbon working electrode (3 mm); the potentials are reported relative to Ag/AgCl reference electrode; scan rate 50 mVs⁻¹.

Figure S2 represents the voltammogram of compound **12j** at different scan rates (50, 100, 200, 300, 400 mV/sec). The potential values, up to the value of 120, are proportional to

scan rate indicating a surface confined effect while up to 400 mV/sec the effect becomes diffusion controlled. The same behaviour was observed for the other 4 compounds as well.

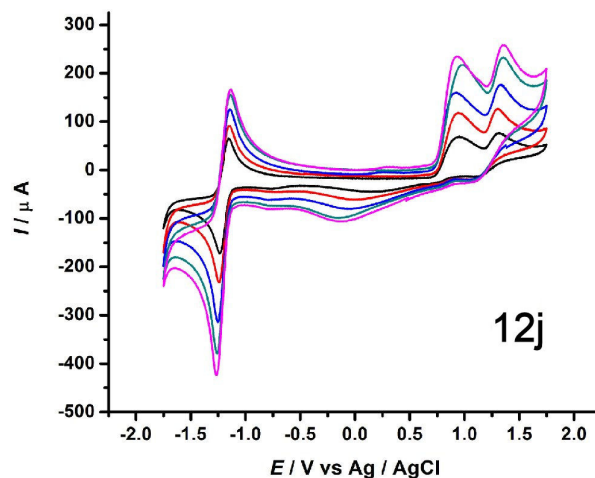


Figure S2. CV diagram of compound 12j (R = phenyl) at scan rates (from inner to outer) 50, 100, 200, 300 and 400 mV/sec.

9.4.2 Cyclic voltammetry studies of DIP 12b and AEP 13b

The following electrochemical experiments were performed using a CH Instruments 620A electrochemical workstation. The electrolyte solution (0.1 M) was prepared from recrystallised Bu_4NPF_6 using dry acetonitrile. A three electrode configuration was used with a platinum disc working electrode, a platinum wire counter electrode and a Ag/AgCl reference electrode. The solution was purged with nitrogen prior to recording the electrochemical data, and all measurements were recorded under a nitrogen atmosphere.

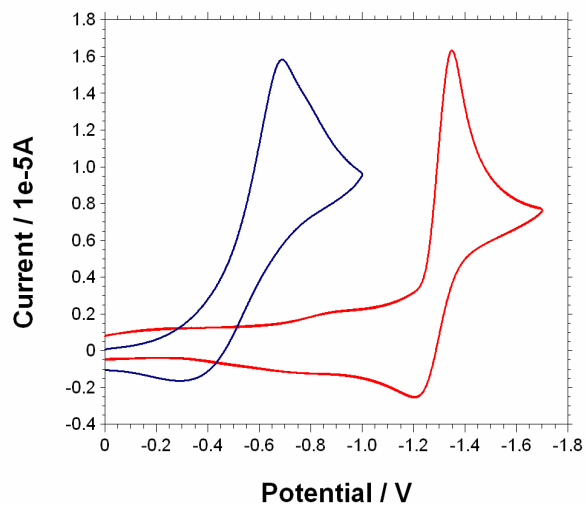


Figure S3. Cyclic voltammograms of compounds 13b (blue line) and 12b (red line) (5 mg) in acetonitrile (8 ml). Scan rate = 100 mVs^{-1} .

9.4.3 Square wave voltammetry studies of DIP 12b and AEP 13b

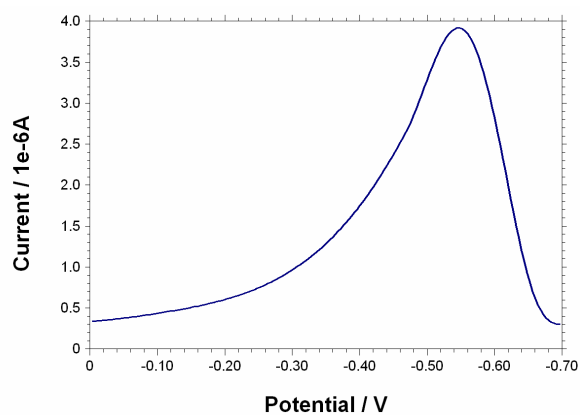


Figure S4. Square wave voltammogram of compound 13b (5 mg) in acetonitrile (8 ml).

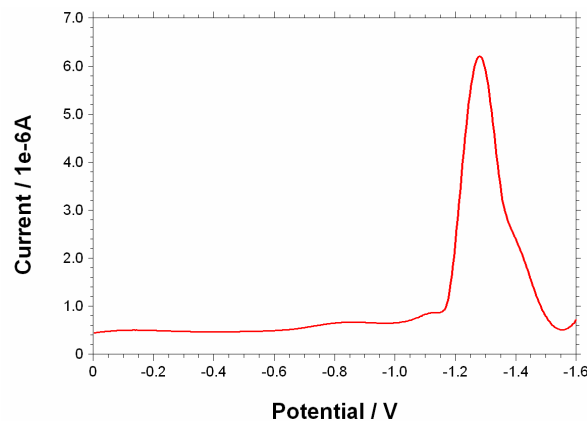


Figure S5. Square wave voltammogram of compound **12b** (5mg) in acetonitrile (8 ml).

9.5 UV Spectra Conditions (Ref. Figure 33)

UV spectra of compounds **TIP 11b**, **DIP 12b**, **AEP 13b**, and **AEDP 14b**.

Samples prepared as 4×10^{-5} M solutions in acetonitrile, scan range 240-400 nm, slit width 2 nm.

The sample of **TIP 11b** was prepared by basification of a biphasic solution of **AEP 13b** (35.1 mg, 0.1 mmol) in H_2O (~1 mL) and DCM (~1 mL) with Na_2CO_3 (~50 mg) followed by separation of layers and removal of DCM solvent under vacuum. The residue was immediately redissolved in acetonitrile and diluted to the desired concentration.

The sample of **AEDP 14b** was prepared by reduction of a biphasic solution of **AEP 13b** (35.1 mg, 0.1 mmol) in H_2O (~1 mL) and DCM (~1 mL) with NaBH_4 (~10 mg) followed by separation of layers and removal of DCM solvent under vacuum. The residue was immediately redissolved in acetonitrile and diluted to the desired concentration.

9.6 Fluorescence Spectra Conditions (Ref. Figure 33)

DIP 12b spectrum conditions: 4×10^{-6} M, excitation wavelength 320 nm, scan range 330-630 nm, slit (ex) 3 nm, slit (em) 5 nm.

TIP 11b spectrum conditions: 4×10^{-5} M, excitation wavelength 320 nm, scan range 330-630 nm, slit (ex) 1.5 nm, slit (em) 3 nm.

AEP **13b** spectrum conditions: 4×10^{-5} M, excitation wavelength 246 nm, scan range 330-630 nm, slit (ex) 3 nm, slit (em) 3 nm.

AEDP **14b** spectrum conditions: 4×10^{-5} M, excitation wavelength 320 nm, scan range 330-630 nm, slit (ex) 3 nm, slit (em) 3 nm.

The sample of TIP **11b** was prepared by basification of a biphasic solution of AEP **3b** (35.1 mg, 0.1 mmol) in H₂O (~1 mL) and DCM (~1 mL) with Na₂CO₃ (~50 mg) followed by separation of layers and removal of DCM solvent under vacuum. The residue was immediately redissolved in acetonitrile and diluted to the desired concentration.

The sample of AEDP **4** was prepared by reduction of a biphasic solution of AEP **3b** (35.1 mg, 0.1 mmol) in H₂O (~1 mL) and DCM (~1 mL) with NaBH₄ (~10 mg) followed by separation of layers and removal of DCM solvent under vacuum. The residue was immediately redissolved in acetonitrile and diluted to the desired concentration.

9.7 In Situ Monitored ¹H NMR Experiments

9.7.1 TIP-AEP hydride transfer initiation via acidification (Ref. Figure 19)

A monophasic solution of TIP **11b** was prepared by addition of isobutylamine (0.40 mmol, 4.0 eq) to BEP **10** (0.10 mmol, 1.0 eq) in D₆-DMSO (1.0 mL). Addition of DCl (0.125 mmol, 1.25 eq) resulted in the complete conversion of TIP **11b** to equimolar amounts of DIP **12b** and AEDP **14b**.

9.7.2 Bromoaniline isomer comparison (Ref. Figure 20)

2- or 4-Bromoaniline (0.054 mmol, 1.0 eq) and TEA (23 μL, 0.162 mmol, 3.0 eq) was added to a solution of BEP **10** (20 mg, 0.054 mmol, 1.0 eq) in D₆-DMSO (0.8 mL) and the reaction progress monitored by ¹H NMR spectroscopy.

9.7.3 Adamantyl and isobutyl comparison (Ref. Figure 21 & Figure 22)

A solution of isobutyl-TIP **11b** suitable for ^1H NMR analysis was prepared by addition of isobutylamine (2.8 μL , 0.028 mmol, 1.0 eq) to a biphasic solution of BEP **10** (10 mg, 0.028 mmol, 1.0 eq) in 5% Na_2CO_3 (aq) (0.8 mL) and CHCl_3 (0.8 mL) and shaking vigorously in an NMR tube for 2 min. The layers were then separated and the organic layer was concentrated under vacuum to give a colourless oily residue which was immediately redissolved in D_6 -DMSO (0.8 mL). A solution of BEP **10** (10 mg, 0.028 mmol, 1.0 eq) in D_6 -DMSO (0.8 mL) was then added to the solution, analysing the solutions by ^1H NMR spectroscopy both before and after the addition.

A similar reaction was repeated for adamantyl-TIP: A solution of BEP **10** (10 mg, 0.028 mmol, 1.0 eq) in D_6 -DMSO (0.8 mL) was added to a solution of adamantyl-TIP **3f** (10 mg, 0.028 mmol, 1.0 eq) in D_6 -DMSO (0.8 mL), analysing the solutions by ^1H NMR spectroscopy both before and after the addition.

9.7.4 4-Fluorophenyl-TIP/AEP cyclisation reversibility (Ref. Figure 30)

In an NMR tube, 4-fluorophenyl-TIP **11n** (10 mg, 0.032 mmol) was dissolved in D_6 -DMSO. DCI (35% wt., 1 drop) was added and the tube was shaken vigorously. TEA (3 drops) was then added and the tube was shaken vigorously. ^1H NMR spectra were obtained before and after each addition.

9.7.5 Monophasic isobutyl-AEP/TIP conversion via pH jump (Ref. Figure 34)

In an NMR tube, isobutyl-AEP **13b** (10 mg, 0.032 mmol) was dissolved in D_6 -DMSO. TEA (53 μL 0.38 mmol, ~ 12 eq) was then added and the tube was shaken vigorously. ^1H NMR spectra were obtained before and after the addition of TEA.

9.7.6 Incremental isobutyl-AEP/TIP conversion in biphasic system (Ref. Figure 35)

In an NMR tube, AEP **13b** (40 mg, 0.114 mmol) was dissolved in D_2O (1.0 mL) and CDCl_3 (1.0 mL) and cyclohexane (1 drop) were added. A 1N Na_2CO_3 solution in D_2O was added in 30 μL portions (150 μL , 0.15 mmol in total) and the CDCl_3 layer was analysed by

¹H NMR spectroscopy. The D₂O layer was then replaced with fresh D₂O (1.0 mL), a 0.5M solution of DCl in D₂O was then added in 30 μL portions and the CDCl₃ layer was analysed by ¹H NMR spectroscopy.

9.7.7 Br₂ oxidation of isobutyl-TIP (Ref. Figure 40)

In an NMR tube, a 5% Na₂CO₃ solution in D₂O (0.8 mL) was added to a suspension of AEP **13b** (15 mg, 0.043 mmol) in CDCl₃ (0.8 mL) and the tube shaken vigorously. The aqueous phase was removed and replaced with fresh D₂O (0.8 mL). Bromine (2 drops) was added, the tube was shaken again and an orange precipitate formed (DIP product). The reaction mixture was filtered and a ¹H NMR spectrum of the CDCl₃ filtrate was obtained.

9.7.8 BEP methoxy adduct formation (Ref. Figure 50)

TEA (23 μL, 0.167 mmol, 3.0 eq) was added to a solution of BEP **10** (20 mg, 0.056 mmol, 1.0 eq) in CD₃OD (0.8 mL) and a ¹H NMR spectrum was obtained.

9.7.9 TRIS-cage-TIP (Ref. Figure 52)

To a solution of **1-methyl-2,6,7-trioxa-bicyclo[2.2.2]oct-4-ylamine** (10 mg, 0.069 mmol, 1.0 eq) and TEA (29 μL, 0.207 mmol, 3.0 eq) in D₆-DMSO (0.8 mL) was added BEP **10** (25 mg, 0.069 mmol, 1.0 eq). A ¹H NMR spectrum was obtained after ~20 min.

9.8 In Situ Monitored UV Switching Experiments

9.8.1 pH switching of isobutyl-AEP/TIP (Ref. Figure 36)

The initial sample was prepared as a 5×10⁻⁵ M solution of AEP **13b** (2.2 mg, 0.005 mmol) in H₂O (100 mL) with a drop of 48% HBr_(aq) to reduce the pH to ~3. DCM (100 mL) was added and the biphasic solution was then basified to ~pH 9 by drop-wise addition of TEA. The solution was re-acidified to ~pH 3 by drop-wise addition of 48% HBr_(aq). This cycle repeated 3 times. The solution was stirred thoroughly during each addition and left to separate for >2min after each addition. UV spectra were obtained for both the aqueous and

organic layers after each addition. Note: The lack of accuracy for pH measurements was due to incompatibility of pH probe with DCM so universal indicator paper was used instead.

9.8.2 NaBH₄ reduction of isobutyl-AEP (Ref. Figure 37)

A 5×10^{-5} M aqueous solution of AEP **13b** was prepared (2.2 mg in 100 mL). DCM (100 mL) was added, followed by NaBH₄ (6.3 mg, 0.1 mmol, 20 eq) and the reaction stirred for ~2 min. TEA was added drop-wise to basify the aqueous phase. 48% HBr_(aq) was added to acidify the aqueous layer. The solution was stirred thoroughly during each addition and left to separate for >2min after each addition. UV spectra were obtained for both the aqueous and organic layers after each addition. Note the shift in absorbance maxima upon re-acidification at the end of the experiment can be explained by protonation of the AEDP product.

9.8.3 Br₂ oxidation of isobutyl-TIP (Ref. Figure 39)

The initial sample was prepared as a 5×10^{-5} M solution of AEP **13b** (2.2 mg, 0.005 mmol) in H₂O (100 mL). DCM (100 mL) was added and the biphasic solution was then basified to ~pH 8 with TEA (3.5 μ L, 0.025 mmol, 5.0 eq). Bromine was then added and the reaction progress was followed using UV spectroscopy. 48% HBr (1 drop) was added at the end of the experiment to show the AEP starting material could not be reformed by re-acidification of the solution. The increase in absorbance upon acidification can be explained by the removal of hydroxide ions that cause DIP **12b** to exist as its pseudo base analogue at high pH.

9.9 MTT Assays

Drug sensitivity is determined by a tetrazolium dye-based microtitration assay.¹⁷⁸ The cell lines used were the human ovarian cancer cell line A2780 and 2 cisplatin resistant derivatives (A2780/cp70 and MCP1).¹⁷³ Both resistant cell lines have lost expression of a component (MLH1) of the DNA mismatch repair pathway. Cells were plated out in 96 well plates at a density of 500 – 1000 cells/well and allowed to attach and grow for 2 days. Cells were exposed to the drug at a range of concentrations for 24 hours and then the

medium was replaced with drug free medium for a further 3 days. On the final day MTT (50 μ l of a 5mg/ml solution) was added to the medium (200 μ l) in each well and the plates were incubated at 37°C for 4h in the dark. Medium and MTT were then removed and the MTT-formazan crystals were dissolved in DMSO (200 μ l). Glycine buffer (25 μ l per well, 0.1M, pH 10.5) was added and the absorbance measured at 570nm in a multiwell plate reader. A typical dose-response curve consisted of 8 drug concentrations and 2 wells were used per drug concentration. Results are expressed in terms of the drug concentration required to kill 50% of the cells (IC_{50}) estimated as the absorbance value equal to 50% of that of the untreated control wells.

The RF value is the resistance factor. It is calculated by dividing the IC_{50} value for a given drug for the cisplatin resistant cell lines by that obtained for the cisplatin sensitive A2780 cell line. Where the RF is less than 1 it means that the cisplatin resistant cell lines is more sensitive to the drug than is the A2780 cell line.

9.10 Crystallography

Structures were solved using Patterson or Direct methods with SHELXS-97²⁰³ or SIR-92²⁰⁴ using WinGX²⁰⁵ routines. Refinement was accomplished by full matrix least-squares on F^2 via SHELXL-97. All non-hydrogen atoms were refined anisotropically unless stated otherwise. Hydrogen atom positions were calculated using standard geometric criteria and refined using a riding model. All data manipulation and presentation steps were performed using WinGX. Details of interest about the structure refinement are given in the tables. The following quantities are given in the information for each structure and were calculated as follows:

9.10.1 1-(4-Fluorophenyl)-1,2,3,12b-tetrahydroimidazo[1,2-f]phenanthridine (11n)

Empirical formula	$C_{21}H_{17}FN_2$
Formula weight	316.37
Temperature	100(2) K
Wavelength	0.71073 Å
Crystal system, space group	Monoclinic, P21/c
Unit cell dimensions	$a = 7.8862(2)$ Å $\alpha = 90.00^\circ$ $b = 39.4824(12)$ Å $\beta = 93.878(2)^\circ$ $c = 10.0829(3)$ Å $\gamma = 90.00^\circ$
Volume	3132.29(16) Å ³
Z, Calculated density	8, 1.342 Mg/m ³
Absorption coefficient	0.088 mm ⁻¹
F(000)	1328
Crystal size	0.16 x 0.14 x 0.10 mm
Theta range for data collection	2.0 to 23.4°
Limiting indices	-8 ≤ h ≤ 8, -41 ≤ k ≤ 43, -11 ≤ l ≤ 11
Reflections collected / unique	19890 / 4474 [R(int) = 0.0762]
Completeness to theta =	23.4 100.0 %
Absorption correction	Empirical
Max. and min. transmission	0.982 and 0.996
Refinement method	Full-matrix least-squares on F ²
Data / restraints / parameters	4474 / 0 / 443
Goodness-of-fit on F ²	0.957
Final R indices [I > 2σ(I)]	R1 = 0.0485, wR2 = 0.0912
R indices (all data)	R1 = 0.1018, wR2 = 0.1161
Largest diff. peak and hole	0.182 and -0.202 e.Å ⁻³

9.10.2 2-(1-Methyl-2,6,7-trioxa-bicyclo[2.2.2]oct-4-yl)-3,4-dihydro-2H,12bH-1-oxa-2,4a-diazatriphenylene (28)

Empirical formula	C ₂₁ H ₂₂ N ₂ O ₄
Formula weight	366.41
Temperature	293(2) K
Wavelength	1.54184 Å
Crystal system, space group	Orthorhombic, P2(1)2(1)2(1)
Unit cell dimensions	$a = 5.92460(10)$ Å $\alpha = 90.00^\circ$ $b = 12.44370(10)$ Å $\beta = 90.00^\circ$ $c = 23.2846(2)$ Å $\gamma = 90.00^\circ$
Volume	1716.63(4) Å ³
Z, Calculated density	4, 1.418 Mg/m ³
Absorption coefficient	0.807 mm ⁻¹
F(000)	776
Crystal size	0.43 x 0.10 x 0.09 mm
Theta range for data collection	3.55 to 62.41°
Limiting indices	-6 ≤ h ≤ 6, -10 ≤ k ≤ 13, -26 ≤ l ≤ 26
Reflections collected / unique	5971 / 2406 [R(int) = 0.0163]
Completeness to theta =	62.41 100.0 %
Absorption correction	Analytical
Max. and min. transmission	0.834 and 0.949
Refinement method	Full-matrix least-squares on F ²
Data / restraints / parameters	2406 / 0 / 244
Goodness-of-fit on F ²	1.109
Final R indices [I > 2σ(I)]	R1 = 0.0227, wR2 = 0.0572
R indices (all data)	R1 = 0.0236, wR2 = 0.0573
Largest diff. peak and hole	0.108 and -0.139 e.Å ⁻³

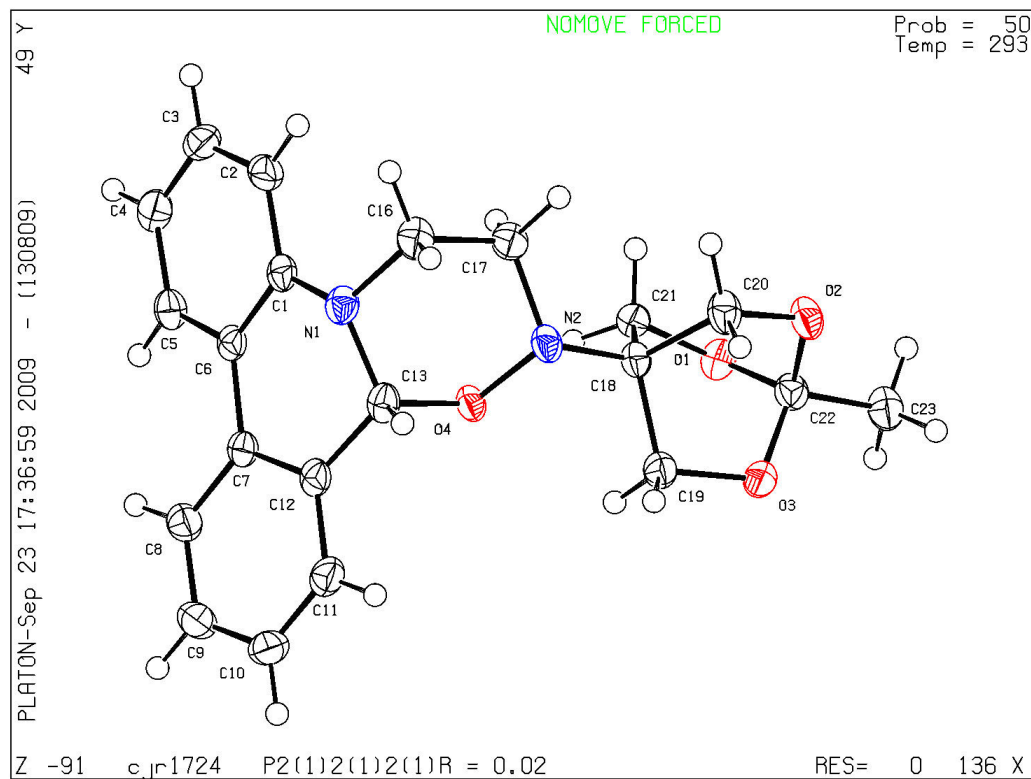
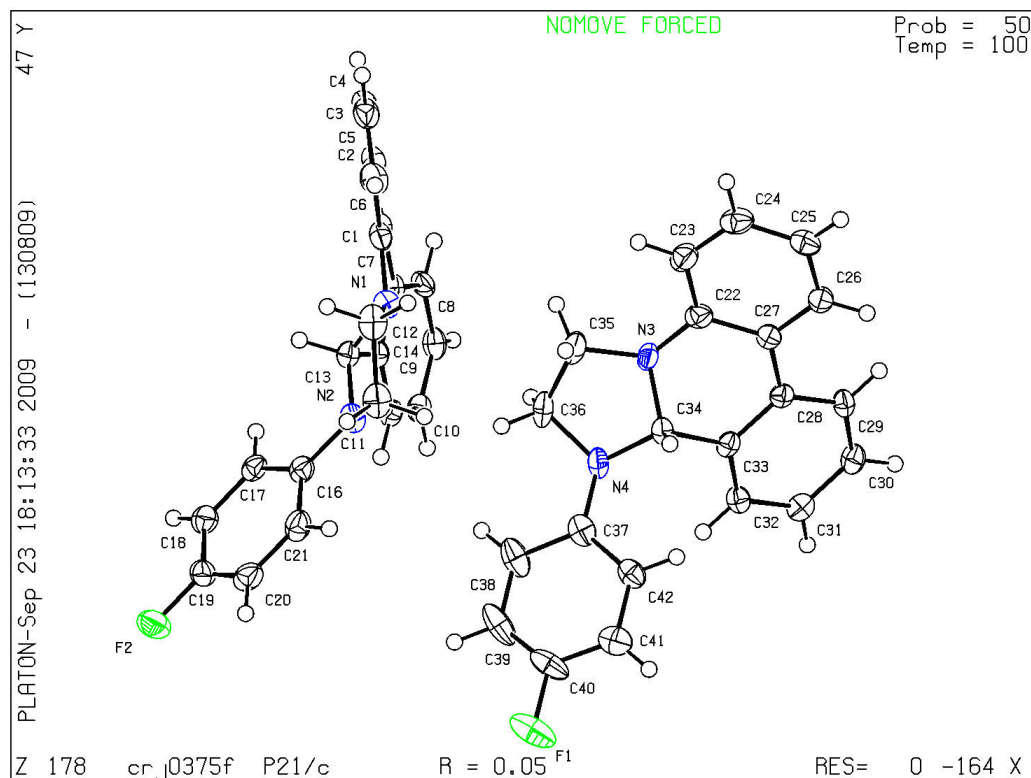
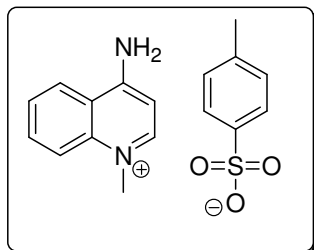


Figure S6. Thermal ellipsoid plots for crystal structures of compounds **11n** (top) and **28** (bottom).

9.11 Syntheses and Analytical Data

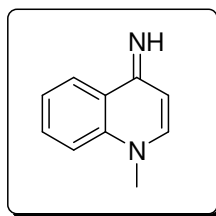
9.11.1 4-Amino-1-methylquinolinium toluene-4-sulfonate (3).



To a suspension of 4-aminoquinoline (500 mg, 3.47 mmol, 1.0 eq) in diethyl ether (20 mL) was added methyl-*p*-toluenesulfonate (642 mg, 4.16 mmol, 1.2 eq). The reaction was stirred at 40 °C for 69 h. The suspension was filtered, washing with more ether, to give a pale yellow solid (1.02 g, 3.08 mmol, 88.8 %): mp 241-243 °C (MeOH); ¹H NMR (DMSO, 400 MHz) δ 9.01 (brd, 2H), 8.51 (d, 1H, J=7.2 Hz), 8.49 (d, 1H, J=7.2 Hz), 8.08 (m, 2H), 7.78 (m, 1Hz), 7.48 (d, 2H, J=8.0 Hz), 7.12 (d, 2H, J=8.0 Hz), 6.79 (d, 1H, J=7.2 Hz), 4.11 (s, 3H), 2.29 (s, 3H); ¹³C NMR (DMSO, 100 MHz) δ 157.9 (C), 146.7 (CH), 145.7 (C), 138.9 (C), 137.6 (C), 134.4 (CH), 128.0 (2 × CH), 126.5 (CH), 125.5 (2 × CH), 124.2 (CH), 118.4 (CH), 116.8 (C), 101.8 (CH), 41.9 (CH₃), 20.8 (CH₃); IR (KBr, cm⁻¹) 3316 (w), 3117 (w), 1680 (m), 1625 (s), 1203 (s), 1182 (s); MS (FAB) *m/z* (%) 159 (M⁺) (100), 147 (32), 136 (53).

Product Reference: Keneford, J. R.; Lourie, E. M.; Morley, J. S.; Simpson, J. C. E.; Williamson, J.; Wright, P. H., J. Chem. Soc. **1952**, 2595-602.

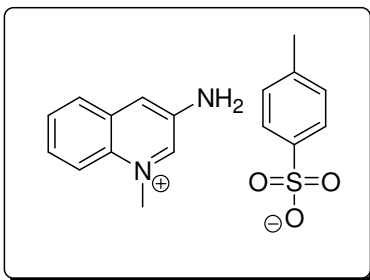
9.11.2 1-Methyl-1*H*-quinolin-4-ylideneamine (4).



To a solution of NaOH (250 mg, 6.25 mmol, 10.3 eq) in H₂O (1 mL) was added 4-amino-1-methylquinolinium toluene-4-sulfonate (200 mg, 0.605 mmol, 1.0 eq) and the reaction heated to reflux for 23 h. The reaction was allowed to cool to rt°C, diluted with H₂O (5 mL) and then extracted with EtOAc (2×10 mL). The combined organic layers were dried over MgSO₄ and concentrated under vacuum to give a white powder (50 mg, 0.32 mmol, 52.3%): ¹H NMR (CDCl₃, 400 MHz) δ 8.48 (dd, 1H, *J*=8.2, 1.4 Hz), δ 7.70 (m, 1H), δ 7.52 (d, 1H, *J*=7.8 Hz), δ 7.42 (m, 2H), δ 6.28 (d, 1H, *J*=7.8 Hz), 3.82 (s, 3H); ¹³C NMR (DMSO, 400 MHz) δ 176.3 (C), 145.0 (CH), 140.6 (C), 132.0 (CH), 126.5 (C), 125.5 (CH), 123.3 (CH), 116.7 (CH), 108.6 (CH), 40.0 (CH₃); IR (KBr, cm⁻¹) 3433 (m), 2945 (w), 1625 (s), 1576 (s), 1493 (m), 1474 (m), 758 (s); MS (EI+) *m/z* (%) 159.1 (M+H)⁺ (100), 131.1 (84), 130.1 (52).

Product Reference: Angyal, C. L.; Werner, R. L., *J. Chem. Soc.* **1952**, 2911-2915

9.11.3 3-Amino-1-methylquinolinium-*p*-toluenesulfonate (7).

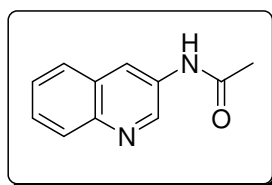


To a solution of 3-aminoquinoline (500 mg, 3.47 mmol, 1.0 eq) in DCM (5 mL) was added methyl-*p*-toluenesulfonate (1.292 g, 6.94 mmol, 2.0 eq) and the resultant yellow solution stirred at room temperature for 18 h. The precipitated product was collected by filtration, washing with DCM (808 mg, 2.45 mmol, 70.6 %): mp 144-146 °C; ¹H NMR (DMSO, 400 MHz) δ 8.84 (d, 1H, *J*=2.4 Hz), 8.22 (d, 1H, *J*=7.6 Hz), 8.08 (d, 1H, *J*=7.6 Hz), 7.98 (d, 1H, *J*=2.4 Hz), 7.79 (m, 2H), 7.48 (d, 2H, *J*=7.8 Hz), 7.12 (d, 2H, *J*=7.8 Hz), 6.60 (brd, 2H), 4.52 (s, 3H), 2.29 (s, 3H); ¹³C NMR (DMSO, 100 MHz) δ 145.8 (C), 143.3 (C), 140.2 (CH), 137.5 (C), 131.8 (C), 130.5 (C), 129.4 (CH), 129.3 (CH), 128.0 (CH), 127.6 (CH), 125.5 (CH), 121.9 (CH), 118.6 (CH), 45.4 (CH₃), 20.8 (CH₃); IR (KBr, cm⁻¹) 3450 (s), 3317 (s), 3196 (s), 3052 (w), 3002 (w), 1636 (s), 1589 (m), 1530 (s), 1380 (m), 1219 (s),

1179 (s), 1120 (s), 1030 (s), 1008 (s); MS (FAB) m/z (%) 160.01 (100) (M+H)⁺, 159.01 (7) (M⁺), 147.17 (2); Anal. Calcd for C₁₇H₁₈N₂ SO₃: C, 61.80; H, 5.49; N, 8.48; Found: C, 61.35; H, 5.44; N, 8.32.

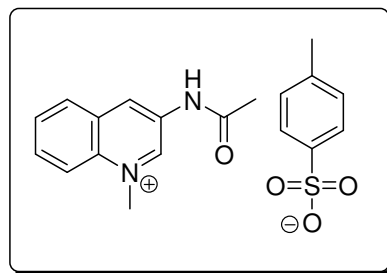
Product Reference: Plakogiannis, F. M.; Lien, E. J. C.; Biles, J. A., *J. Med. Chem.*, **1971**, *14*, 430–432

9.11.4 3-Acetylaminoquinoline (8).



A solution of 3-aminoquinoline (1.0 g, 6.94 mmol, 1.0 eq) in neat acetic anhydride (20 mL) was heated to 90 °C for 1 h. The mother liquor was allowed to cool to room temperature and concentrated to dryness. The residue was partitioned between water and ethyl acetate, the aqueous layer was basified with 10 % aqueous sodium carbonate solution, layers were separated and the aqueous phase further extracted with ethyl acetate. Organic extracts were combined and concentrated to dryness. The crude residue was purified by flash column chromatography, eluent: 0-20 % Methanol in Ethyl acetate. The product was obtained as a white solid (1.079 g, 5.79 mmol, 83.4 %): mp 168-169 °C; R_f = 0.21 in 100% EtOAc; ¹H NMR (CDCl₃, 400 MHz) δ 8.69 (s, 1H), 8.65 (s, 1H), 7.97 (d, 1H, J=7.4 Hz), 7.74 (d, 1H, J=7.4 Hz), 7.57 (t, 1H, J=7.4 Hz), 7.49 (s, 1H), 7.47 (t, 1H, J=7.4 Hz), 2.21 (s, 3H); ¹³C NMR (CDCl₃, 100 MHz) δ 169.0 (C), 145.6 (C), 143.8 (CH), 132.0 (C), 129.0 (CH), 128.4 (CH), 128.3 (C), 127.8 (CH), 127.3 (CH), 124.0 (CH), 24.7 (CH₃); MS (EI) m/z (%) 186.06 (54) (M), 144.05 (100), 117.05 (28), 89.02 (24), 63.02 (11), 43.04 (25).

Product Reference: Dauben, Wm. G.; Vaughan, C. Wheaton, Jr., *J. Am. Chem. Soc.* **1953**, *75*, 4651-5.

9.11.5 3-Acetylamino-1-methylquinolinium *p*-toluenesulfonate (9).

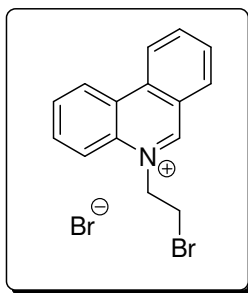
To a suspension of 3-acetylaminoquinoline (200 mg, 1.07 mmol, 1.0 eq) in DCM (5 mL) was added methyl-*p*-toluenesulfonate (398 mg, 2.14 mmol, 2.0 eq) and the reaction stirred at room temperature for 6 d. The mother liquor was filtered to remove insoluble impurities. The filtrate was concentrated to dryness and the crude residue triturated with diethyl ether to give a pale yellow solid product (250 mg, 0.67 mmol, 62.6 %): mp 209-211 °C; ¹H NMR (DMSO, 400 MHz) δ 11.10 (s, 1H), 9.64 (s, 1H), 9.18 (s, 1H), 8.45 (s, 1H), 8.43 (s, 1H), 8.14 (t, 1H, J=7.8 Hz), 7.99 (t, 1H, J=7.8 Hz), 7.48 (d, 2H, J=8.0 Hz), 7.11 (d, 2H, J=8.0 Hz), 4.66 (s, 3H), δ 2.22 (s, 3H), 2.15 (s, 3H); ¹³C NMR (DMSO, 100 MHz) δ 169.7 (C), 145.6 (C), 143.7 (CH), 137.6 (C), 135.2 (C), 133.4 (CH), 133.3 (C), 132.4 (CH), 130.1 (CH), 129.7 (CH), 129.2 (C), 128.1 (CH), 125.4 (CH), 118.9 (CH), 46.0 (CH₃), 23.7 (CH₃), 20.8 (CH₃); IR (KBr, cm⁻¹) 3540 (w), 3222 (w), 3186 (w), 3141 (w), 3079 (m), 3025 (m), 1708 (s), 1605 (s), 1605 (m), 1566 (s), 1521 (s), 1492 (m), 1451 (w), 1424 (m), 1377 (s), 1365 (s), 1264 (s), 1216 (s), 1175 (s), 1119 (s), 1032 (s), 1010 (s); MS (EI) *m/z* (%) 173.1 (1), 159.01 (2), 86 (2), 73.1 (100), 44.1 (100); Anal. Calcd for C₁₉H₂₀N₂SO₃: C, 61.27; H, 5.41; N, 7.52; Found: C, 60.91; H, 5.35; N, 7.46.

3-amino-1-methylquinolinium-*p*-toluenesulfonate (100 mg, 0.30 mmol, 1.0 eq) was suspended in acetic anhydride (2 mL) and heated to 80 °C for 19 h. The reaction mixture was filtered, washing the residue with EtOAc, to give a pale yeallow powder (63 mg, 0.19 mmol, 63.0%): mp 209-211 °C; ¹H NMR (DMSO, 400 MHz) δ 11.10 (s, 1H), 9.64 (s, 1H), 9.18 (s, 1H), 8.45 (s, 1H), 8.43 (s, 1H), 8.14 (t, 1H, J=7.8 Hz), 7.99 (t, 1H, J=7.8 Hz), 7.48 (d, 2H, J=8.0 Hz), 7.11 (d, 2H, J=8.0 Hz), 4.66 (s, 3H), δ 2.22 (s, 3H), 2.15 (s, 3H); ¹³C NMR (DMSO, 100 MHz) δ 169.7 (C), 145.6 (C), 143.7 (CH), 137.6 (C), 135.2 (C),

133.4 (CH), 133.3 (C), 132.4 (CH), 130.1 (CH), 129.7 (CH), 129.2 (C), 128.1 (CH), 125.4 (CH), 118.9 (CH), 46.0 (CH₃), 23.7 (CH₃), 20.8 (CH₃).

Product Reference: Plakogiannis, Fotios M.; Lien, Eric J., *Acta Pharmaceutica Suecica*, **1974**, *11*, 191-195

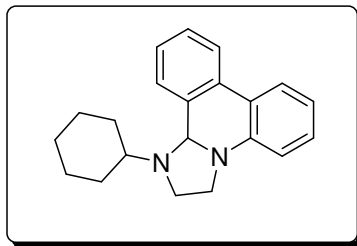
9.11.6 5-(2-Bromoethyl)-phenanthridinium bromide (10).



Phenanthridine (5.74 g, 30 mmol, 1.0 eq) was dissolved in 1,2-dibromoethane (52 mL, 600 mmol, 20.0 eq) and the solution stirred at 90 °C for 6 d. The product was filtered and washed with more dibromoethane (1 mL) every day, returning the mother liquor to the reaction vessel over the 6 d period. The residues collected were combined and washed thoroughly with diethyl ether and dried under vacuum to give the product an off-white solid (10.02 g, 27.30 mmol, 91.0 %): mp 241-243 °C (MeOH-Et₂O); ¹H NMR (DMSO, 400 MHz) δ 10.43 (s, 1H), 9.26 (d, 1H, *J*=8.0 Hz), 9.21 (d, 1H, *J*=8.0 Hz), 8.71 (d, 1H, *J*=8.0 Hz), 8.68 (d, 1H, *J*=8.0 Hz), 8.48 (t, 1H, *J*=8.0 Hz), 8.18 (m, 3H), 5.57 (t, 2H, *J*=6.0 Hz), 4.24 (t, 2H, *J*=6.0 Hz); ¹³C NMR (DMSO, 100 MHz) δ 156.5 (CH), 138.7 (CH), 134.7 (C), 133.1 (CH), 132.7 (C), 132.3 (CH), 130.7 (CH), 130.5 (CH), 125.8 (C), 125.2 (CH), 123.4 (CH), 123.1 (C), 119.9 (CH), 58.1 (CH₂), 30.6 (CH₂); MS (EI+) *m/z* (%) 315.8 (M⁺) (16), 257.9 (6), 236.0 (30), 206.9 (84), 156.1 (19), 101.0 (48).

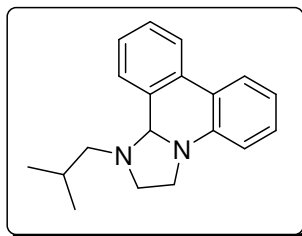
Product Reference: Parenty, A. D. C.; Smith, L. V.; Pickering A. L.; Long, D. -L.; Cronin L., *J. Org. Chem.* **2004**, *69*, 5934-5946.

9.11.7 1-Cyclohexyl-1,2,3,12b-tetrahydroimidazo[1,2-f]phenanthridine (11a).



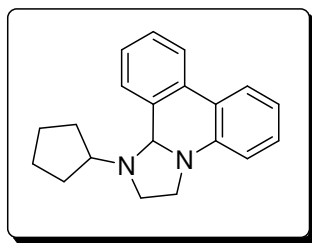
In an NMR tube, BEP **10** (30 mg, 0.082 mmol, 1.0 eq) was suspended in CDCl_3 (1 mL) and D_2O (1 mL). Cyclohexylamine (8 μL , 0.082 mmol, 1.0 eq) and Na_2CO_3 (~50 mg) were then added and the solution was shaken for 1 min. The CDCl_3 layer was then characterized by MS and ^1H and ^{13}C NMR spectroscopy: ^1H NMR (CDCl_3 , 400 MHz) δ 7.82 (d, 1H, $J=8.0$ Hz), 7.77 (d, 1H, $J=8.0$ Hz), 7.51 (d, 1H, $J=8.0$ Hz), 7.38 (m, 2H), 7.28 (t, 1H, $J=8.0$ Hz), 6.93 (t, 1H, $J=8.0$ Hz), 6.75 (d, 1H, $J=8.0$ Hz), 4.99 (s, 1H), 3.47 (m, 1H), 3.30 (m, 3H), 2.78 (m, 1H), 2.01 (m, 2H), 1.85 (m, 2H), 1.69 (m, 1H), 1.32 (m, 5H); ^{13}C NMR (CDCl_3 , 100 MHz) δ 144.0 (C), 135.7 (C), 131.8 (C), 129.0 (CH), 127.5 (CH), 127.3 (CH), 123.7 (CH), 123.5 (CH), 123.1 (C), 123.0 (CH), 118.7 (CH), 113.2 (CH), 75.9 (CH), 60.7 (CH), 46.7 (CH_2), 45.9 (CH_2), 32.9 (CH_2), 27.8 (CH_2), 26.34 (CH_2), 26.25 (CH_2), 25.8 (CH_2); MS (EI+) m/z (%) 304.2 (M^+) (8), 261.1 (10), 193.1 (31), 179.0 (27), 82.9 (93), 44.0 (100).

9.11.8 1-Isobutyl-1,2,3,12b-tetrahydroimidazo[1,2-f]phenanthridine (11b).



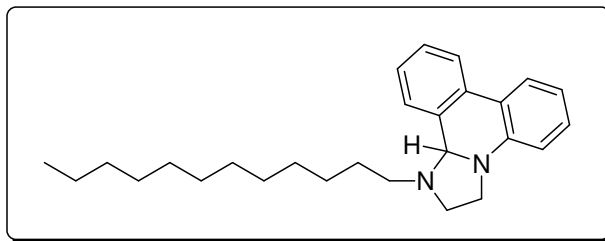
In an NMR tube, BEP **10** (30 mg, 0.082 mmol, 1.0 eq) was suspended in CDCl₃ (1 mL) and D₂O (1 mL). Isobutylamine (8 μL, 0.082 mmol, 1.0 eq) and Na₂CO₃ (~50 mg) were then added and the solution was shaken for 1 min. The CDCl₃ layer was then characterized by MS and ¹H and ¹³C NMR spectroscopy: ¹H NMR (CDCl₃, 400 MHz) δ 7.67 (d, 2H, *J*=7.7 Hz), 7.38 (d, 1H, *J*=7.7 Hz), 7.30-7.21 (m, 2H), 7.15 (t, 1H, *J*=7.7 Hz), 6.78 (t, 1H, *J*=7.7 Hz), 6.58 (d, 1H, *J*=7.7 Hz), 4.78 (s, 1H), 3.41 (m, 2H), 3.27 (m, 1H), 2.85 (m, 1H), 2.33 (m, 2H), 1.78 (m, 1H), 0.98 (d, 3H, *J*=6.6 Hz), 0.90 (d, 3H, *J*=6.6 Hz); ¹³C NMR (CDCl₃, 100 MHz) δ 144.0 (C), 133.2 (C), 132.0 (C), 129.2 (CH), 127.8 (CH), 127.2 (CH), 124.7 (CH), 123.3 (CH), 122.8 (CH), 121.9 (C), 118.2 (CH), 112.7 (CH), 79.7 (CH), 62.0 (CH₂), 51.6 (CH₂), 44.9 (CH₂), 28.2 (CH), 21.2 (CH₃), 20.9 (CH₃); MS (EI+) *m/z* (%) 278.2 (M⁺) (37), 193.1 (100), 178.0 (43).

9.11.9 1-Cyclopentyl-1,2,3,12b-tetrahydroimidazo[1,2-*f*]phenanthridine (11c).



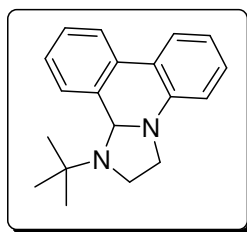
In an NMR tube, BEP **10** (30 mg, 0.082 mmol, 1.0 eq) was suspended in CDCl₃ (1 mL) and D₂O (1 mL). Cyclopentylamine (8 μL, 0.082 mmol, 1.0 eq) and Na₂CO₃ (~50 mg) were then added and the solution was shaken for 1 min. The CDCl₃ layer was then characterized by MS and ¹H and ¹³C NMR spectroscopy: ¹H NMR (CDCl₃, 400 MHz) δ 7.82 (d, 1H, *J*=8.0 Hz), 7.76 (d, 1H, *J*=8.0 Hz), 7.58 (d, 1H, *J*=8.0 Hz), 7.38 (m, 2H), 7.28 (t, 1H, *J*=8.0 Hz), 6.93 (t, 1H, *J*=8.0 Hz), 6.77 (d, 1H, *J*=8.0 Hz), 4.92 (s, 1H), 3.38 (m, 4H), 3.24 (m, 1H), 1.87 (m, 2H), 1.75 (m, 2H), 1.58 (m, 4H); ¹³C NMR (CDCl₃, 100 MHz) δ 144.0 (C), 135.0 (C), 131.8 (C), 129.0 (CH), 127.6 (CH), 127.3 (CH), 124.3 (CH), 123.4 (CH), 122.8 (CH), 122.8 (C), 118.6 (CH), 113.5 (CH), 78.2 (CH), 63.7 (CH), 48.3 (CH₂), 46.3 (CH₂), 31.3 (CH₂), 29.5 (CH₂), 24.2 (CH₂), 24.1 (CH₂); MS (EI+) *m/z* (%) 290.1 (M⁺) (30), 193.1 (100), 179.0 (74).

9.11.10 1-Dodecyl-1,2,3,12b-tetrahydroimidazo[1,2-f]phenanthridine (11d).



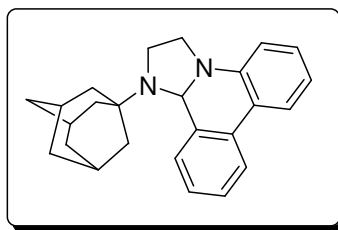
In an NMR tube, BEP **10** (30 mg, 0.082 mmol, 1.0 eq) was suspended in CDCl₃ (1 mL) and D₂O (1 mL). Dodecylamine (19 μL, 0.082 mmol, 1.0 eq) and Na₂CO₃ (~50 mg) were then added and the solution was shaken for 1 min. The CDCl₃ layer was then characterized by MS and ¹H and ¹³C NMR spectroscopy. ¹H NMR (CDCl₃, 400 MHz) δ 7.78 (m, 2H), 7.36 (m, 3H), 7.25 (t, 1H, *J*=8.0 Hz), 6.87 (t, 1H, *J*=8.0 Hz), 6.69 (d, 1H, *J*=8.0 Hz), 4.88 (s, 1H), 3.56 (m, 1H), 3.48 (m, 1H), 3.41 (m, 1H), 2.96 (m, 1H), 2.70 (m, 1H), 2.53 (m, 1H), 1.63 (m, 2H), 1.29 (m, 18H), 0.91 (t, 3H, *J*=6.8 Hz); ¹³C NMR (CDCl₃, 100 MHz) δ 144.1 (C), 132.8 (C), 131.9 (C), 129.2 (CH), 127.9 (CH), 127.2 (CH), 124.9 (CH), 123.3 (CH), 122.7 (CH), 121.7 (C), 118.2 (CH), 112.7 (CH), 79.5 (CH), 53.7 (CH₂), 51.2 (CH₂), 45.2 (CH₂), 31.9 (CH₂), 29.69 (CH₂), 29.65 (CH₂), 29.4 (CH₂), 29.2 (CH₂), 27.5 (CH₂), 22.7 (CH₂), 14.2 (CH₃); MS (CI⁺) *m/z* (%) 407.5 (M+17) (100), 391.5 (M+H)⁺ (59).

9.11.11 1-Tert-butyl-1,2,3,12b-tetrahydroimidazo[1,2-f]phenanthridine (11e).



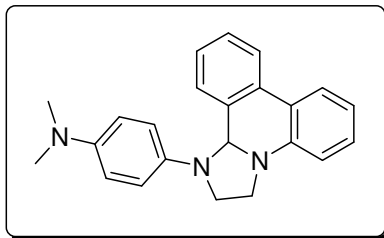
In an NMR tube, BEP **10** (30 mg, 0.082 mmol, 1.0 eq) was suspended in CDCl₃ (1 mL) and tert-butylamine (50 μL, 0.98 mmol, 12.0 eq) was added and the solution was shaken for ~5 min. The CDCl₃ layer was then washed with D₂O (~1 mL) and excess solvents were removed under vacuum. The oily yellow residue was redissolved in CDCl₃ and characterized by MS and ¹H and ¹³C NMR spectroscopy: ¹H NMR (CDCl₃, 400 MHz) δ 7.74 (d, 1H, *J*=8.0 Hz), 7.60 (m, 2H), 7.26 (m, 2H), 7.18 (m, 2H), 6.83(t, 1H, *J*=8.0 Hz), 6.66 (d, 1H, *J*=8.0 Hz), 4.86 (s, 1H), 3.38 (m, 1H), 3.19 (m, 3H), 1.11 (s, 9H); ¹³C NMR (CDCl₃, 100 MHz) δ 143.7 (C), 136.7 (C), 132.1 (C), 128.8 (CH), 127.12 (CH), 127.06 (CH), 124.0 (CH), 123.6 (C), 123.5 (CH), 123.0 (CH), 118.5 (CH), 113.8 (CH), 74.5 (CH), 55.1 (CH₂), 47.3 (CH₂), 46.9 (C), 28.2 (3 × CH₃); MS (EI+) *m/z* (%) 278 (M⁺) (20), 263 (100), 219 (61), 209 (23), 193 (39), 178 (51).

9.11.12 1-Adamantyl-1,2,3,12b-tetrahydroimidazo[1,2-*f*]phenanthridine (11f).



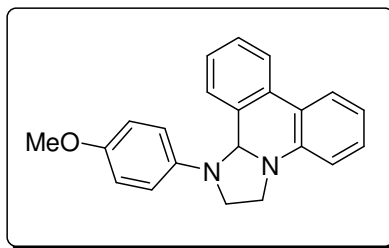
General TIP synthesis method. Product isolated as a pale yellow powder (493.1 mg, 1.38 mmol, 72.6 %): mp 87-89 °C (Et₂O); ¹H NMR (DMSO, 400 MHz) δ 7.85 (d, 1H, *J*=7.6 Hz), 7.73 (m, 1H), δ 7.63 (m, 1H), 7.34 (m, 2H), 7.24 (t, 1H, *J*=7.6 Hz), 6.88 (t, 1H, *J*=7.6 Hz), 6.76 (d, 1H, *J*=7.6 Hz), 4.96 (s, 1H), 3.64 (m, 1H), δ 3.26 (m, 1H), 2.95 (m, 1H), 2.04 (s, 3H), 1.85 (m, 3H), 1.62 (m, 10H); ¹³C NMR (CDCl₃, 100 MHz) δ 143.8 (C), 137.0 (C), 132.12 (C), 128.8 (CH), 127.1 (CH), 127.0 (CH), 124.0 (CH), 123.54 (C), 123.48 (CH), 122.9 (CH), 118.5 (CH), 113.6 (CH), 76.7 (CH), 55.2 (C), 47.5 (CH₂), 44.9 (CH₂), 41.1 (3 × CH₂), δ 36.8 (3 × CH₂), δ 29.6 (3 × CH); IR (KBr, cm⁻¹) 3736 (w), 2901 (m), 2359 (m), 1603 (m), 1444 (m), 1211 (w), 746 (s); MS (CI+) *m/z* (%) 413 (35), 399 (11), 357 (M+H)⁺ (100), 356 (59), 221 (11), 180 (18), 178 (14), 79 (43); HRMS (CI+) Calcd for (C₂₅H₂₉N₂)⁺, 357.2331; Found, 357.2333.

9.11.13 1-(4-Dimethylaminophenyl)-1,2,3,12b-tetrahydroimidazo[1,2-f]phenanthridine (11g).



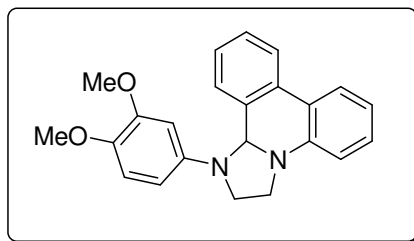
General TIP synthesis method. Product isolated as a pale grey powder (574 mg, 1.68 mmol, 88.1%): mp 197-199 °C (Et₂O); ¹H NMR (CDCl₃, 400 MHz) δ 7.89 (d, 1H, *J*=7.8 Hz), 7.79 (d, 1H, *J*=7.8 Hz), 7.42 (t, 1H, *J*=7.8 Hz), 7.34 (t, 1H, *J*=7.8 Hz), 7.26 (m, 2H), 7.04 (t, 1H, *J*=7.8 Hz), 6.83 (m, 3H), 6.77 (m, 2H), 5.30 (s, 1H), 4.15 (m, 1H), 3.80 (m, 1H), 3.68 (m, 1H), 3.37 (m, 1H), 2.91 (s, 6H); ¹³C NMR (CDCl₃, 100 MHz) δ 144.4 (C), 143.7 (C), 141.4 (C), 134.6 (C), 131.9 (C), 129.1 (CH), 127.7 (CH), 127.2 (CH), 124.6 (CH), 124.2 (C), 123.7 (CH), 123.3 (CH), 119.7 (CH), 115.6 (2 × CH₂), 115.0 (2 × CH₂), 112.8 (CH), 75.6 (CH), 52.1 (CH₂), 44.8 (CH₂), 41.9 (2 × CH₃); IR (KBr, cm⁻¹) 3433 (w), 3045 (w), 2927 (w), 2870 (w), 2841 (w), 2787 (w), 1597 (m), 1514 (s), 1493 (m), 1442 (m), 1372 (m), 1337 (m), 1297 (s), 1210 (m), 809 (m), 749 (s), 734 (m); MS (FAB) *m/z* (%) 342.4 (M+H)⁺ (100), 206.6 (10), 193.7 (37), 180.8 (23), 136.3 (25); HRMS (FAB) Calcd for (C₂₃H₂₄N₃)⁺, 342.1970; Found, 342.1965.

9.11.14 1-(4-Methoxyphenyl)-1,2,3,12b-tetrahydroimidazo[1,2-f]phenanthridine (11h).



General TIP synthesis method. Product isolated as an off-white powder (561 mg, 1.71 mmol, 89.4%): mp 167-169 °C (Et₂O); ¹H NMR (CDCl₃, 400 MHz) δ 7.88 (d, 1H, *J*=7.7 Hz), 7.79 (d, 1H, *J*=7.7 Hz), 7.42 (t, 1H, *J*=7.7 Hz), 7.34 (t, 1H, *J*=7.7 Hz), 7.28 (t, 1H, *J*=7.7 Hz), 7.20 (d, 1H, *J*=7.7 Hz), 7.04 (t, 1H, *J*=7.7 Hz), 6.90 (d, 2H, *J*=9.1 Hz), 6.83 (d, 1H, *J*=7.7 Hz), 6.74 (d, 2H, *J*=9.1 Hz), 5.29 (s, 1H), 4.14 (m, 1H), 3.81 (m, 1H), 3.68 (m, 1H), 3.38 (m, 1H); ¹³C NMR (CDCl₃, 100 MHz) δ 152.5 (C), 143.6 (C), 143.4 (C), 134.4 (C), 131.9 (C), 129.2 (CH), 127.8 (CH), 127.2 (CH), 124.5 (CH), 124.2 (C), 123.7 (CH), 123.4 (CH), 119.9 (CH), 115.4 (2 × CH), 114.6 (2 × CH), 112.9 (CH), 75.6 (CH), 55.8 (CH₃), 52.0 (CH₂), 44.8 (CH₂); IR (KBr, cm⁻¹) 3435 (w), 3054 (w), 2983 (w), 2929 (m), 2871 (m), 2851 (w), 2830 (w), 2774 (w), 1600 (m), 1510 (s), 1442 (s), 1371 (s), 1290 (s), 1245 (s), 1180 (m), 1037 (s), 814 (s), 754 (s), 734 (m); MS (EI+) *m/z* (%) 328.2 (M⁺) (24), 193.1 (100), 165.1 (14), 82.9 (25); HRMS (EI+) Calcd for C₂₂H₂₀N₂O, 328.1576; Found, 328.1575.

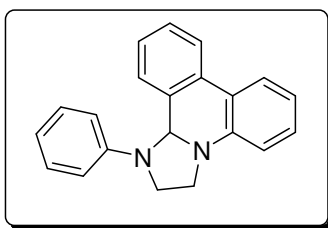
9.11.15 1-(3,4-Dimethoxyphenyl)-1,2,3,12b-tetrahydroimidazo[1,2-*f*]phenanthridine (11i).



General TIP synthesis method. Product isolated as a cream powder (610 mg, 1.70 mmol, 89.1%): mp 148-150 °C (Et₂O); ¹H NMR (CDCl₃, 400 MHz) δ 7.88 (d, 1H, *J*=7.7 Hz), 7.79 (d, 1H, *J*=7.7 Hz), 7.42 (t, 1H, *J*=7.7 Hz), 7.35 (t, 1H, *J*=7.7 Hz), 7.29 (t, 1H, *J*=7.7 Hz), 7.23 (d, 1H, *J*=7.7 Hz), 7.05 (t, 1H, *J*=7.7 Hz), 6.84 (d, 1H, *J*=8.6 Hz), 6.82 (d, 1H, *J*=7.7 Hz), 6.42 (d, 1H, *J*=2.8 Hz), 6.29 (dd, 1H, *J*=8.6 Hz, 2.8 Hz), 5.32 (s, 1H), 4.14 (m, 1H), 3.85 (m, 1H), 3.69 (m, 1H), 3.39 (m, 1H); ¹³C NMR (CDCl₃, 100 MHz) δ 149.6 (C), 143.9 (C), 143.5 (C), 142.0 (C), 134.4 (C), 131.9 (C), 129.2 (CH), 127.9 (CH), 127.2 (CH), 124.5 (CH), 124.2 (C), 123.7 (CH), 123.4 (CH), 120.0 (CH), 112.9 (CH), 112.6 (CH), 105.5 (CH), δ 100.1 (CH), 75.5 (CH), 56.6 (CH₃), 55.9 (CH₃) 51.9 (CH₂), 44.8 (CH₂); IR

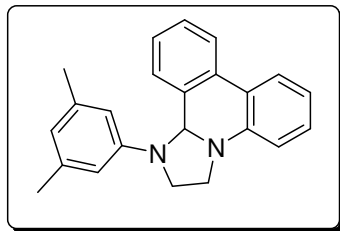
(KBr, cm^{-1}) 3434 (w), 2996 (w), 2966 (w), 2933 (w), 2879 (w), 2830 (w), 1601 (m), 1515 (s), 1493 (s), 1447 (s), 1247 (s), 1012 (m), 770 (s), 731 (m); MS (FAB) m/z (%) 359.3 ($\text{M}+\text{H}^+$) (100), 193.6 (35), 180.8 (33), 155.1 (24), 137.3 (13); HRMS (FAB) Calcd for $(\text{C}_{23}\text{H}_{23}\text{N}_2\text{O}_2)^+$, 359.1760; Found, 359.1758.

9.11.16 1-(Phenyl)-1,2,3,12b-tetrahydroimidazo[1,2-*f*]phenanthridine (11j).



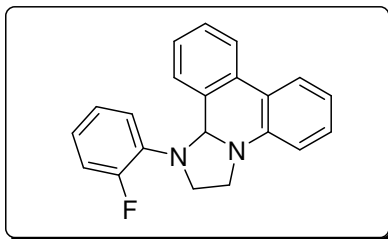
General TIP synthesis method. Product isolated as an orange powder (165 mg, 0.47 mmol, 87.4%): mp 196-197 °C (Et_2O); ^1H NMR (CDCl_3 , 400 MHz) δ 7.78 (dd, 1H, $J=8.0, 1.2$ Hz), 7.68 (d, 1H, $J=8.0$ Hz), 7.32 (td, 1H, $J=8.0, 1.2$ Hz), 7.20 (m, 4H), 7.10 (d, 1H, $J=8.0$ Hz), 6.95 (td, 1H, $J=8.0, 1.2$ Hz), 6.75 (m, 2H), 6.67 (d, 2H, $J=8.0$ Hz), 5.25 (s, 1H), 4.01 (m, 1H), 3.80 (m, 1H), 3.58 (m, 1H), 3.28 (m, 1H); ^{13}C NMR (DMSO, 100 MHz) δ 148.6 (C), 143.2 (C), 133.7 (C), 131.5 (C), 129.2 (CH), 128.9 (CH), 127.7 (CH), 126.9 (CH), 123.9 (CH), 123.6 (CH), 123.31 (CH), 123.25 (C), 119.6 (CH), 117.8 (CH), 114.0 (CH), 113.1 (CH), 74.5 (CH), 50.9 (CH_2), 44.3 (CH_2); IR (KBr, cm^{-1}): 3443 (w), 3057 (w), 2935 (w), 2879 (w), 2811 (w), 1259 (w), 1598 (s), 1487 (s), 1442 (s), 1324 (s), 1301 (m), 1210 (w), 1016 (w), 753 (s), 694 (m); MS (FAB) m/z (%) 299.3 ($\text{M}+\text{H}^+$) (100), 180.8 (21), 155.1 (46), 137.3 (40), 121.5 (16); HRMS (FAB) Calcd for $(\text{C}_{21}\text{H}_{19}\text{N}_2)^+$, 299.1548; Found, 299.1551.

9.11.17 1-(3,5-Dimethylphenyl)-1,2,3,12b-tetrahydroimidazo[1,2-f]phenanthridine (11k).



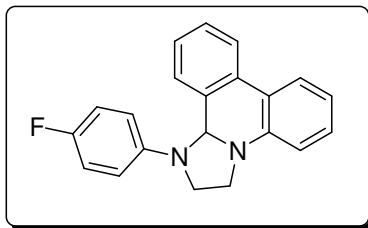
General TIP synthesis method. Product isolated as a pale peach powder (590 mg, 1.81 mmol, 94.6%): mp 195-196 °C (Et₂O); ¹H NMR (CDCl₃, 400 MHz) δ 7.77 (d, 1H, *J*=7.7 Hz), 7.67 (d, 1H, *J*=7.7 Hz), 7.31 (t, 1H, *J*=7.7 Hz), 7.22 (t, 1H, *J*=7.7 Hz), 7.16 (t, 1H, *J*=7.7 Hz), 7.11 (d, 1H, *J*=7.7 Hz), 6.92 (t, 1H, *J*=7.7 Hz), 6.71 (d, 1H, *J*=7.7 Hz), 6.43 (s, 1H), 6.31 (s, 2H), 5.22 (s, 1H), 3.97 (m, 1H), 3.78 (m, 1H), 3.53 (m, 1H), 3.23 (m, 1H), 2.19 (s, 6H); ¹³C NMR (CDCl₃, 100 MHz) δ 149.1 (C), 143.5 (C), 138.8 (2 × C), 134.5 (C), 131.9 (C), 129.2 (CH), 127.8 (CH), 127.2 (CH), 124.6 (CH), 124.3 (C), 123.7 (CH), 123.4 (CH), 120.2 (CH), 119.1 (CH), 113.0 (2 × CH), 112.1 (CH), 75.0 (CH), 51.2 (CH₂), 44.8 (CH₂), 21.7 (2 × CH₃); IR (KBr, cm⁻¹) 3433 (w), 3033 (w), 3008 (w), 2877 (w), 2835 (w), 1611 (s), 1496 (m), 1446 (s), 1349 (s), 1224 (m), 1195 (m), 817 (m), 778 (m), 733 (s), 687 (m); MS (FAB) *m/z* (%) 327.4 (M+H)⁺ (100), 193.7 (32), 180.8 (21), 149.2 (12); HRMS (FAB) Calcd for (C₂₃H₂₃N₂)⁺, 327.1861; Found, 327.1862.

9.11.18 1-(2-Fluorophenyl)-1,2,3,12b-tetrahydroimidazo[1,2-f]phenanthridine (11m).



General TIP synthesis method. Product isolated as a pale orange powder (411 mg, 1.30 mmol, 68.0%): mp 158-159 °C (Et₂O); ¹H NMR (CDCl₃, 400 MHz) δ 7.88 (d, 1H, *J*=7.8 Hz), 7.79 (d, 1H, *J*=7.8 Hz), 7.41 (t, 1H, *J*=7.8 Hz), 7.35 (t, 1H, *J*=7.8 Hz), 7.24 (t, 1H, *J*=7.8 Hz), 7.15 (m, 2H), 7.06 (t, 1H, *J*=7.8), 7.00 (t, 1H, *J*=7.8 Hz), 6.92 (m, 1H), 6.84 (d, 1H, *J*=7.8 Hz), 6.76 (t, 1H, *J*=7.8 Hz), 5.44 (s, 1H), 4.35 (m, 1H), 3.73 (m, 2H), 3.33 (m, 1H); ¹³C NMR (CDCl₃, 100 MHz) δ 154.55 (C), 152.1 (C), 143.8 (C), 137.9 (C), 133.8 (C), 132.0 (C), 129.2 (CH), 128.0 (CH), 127.2 (CH), 124.2 (CH), 123.8 (CH), 123.4 (CH), 120.4 (CH), 120.0 (CH), 116.9 (CH), 116.8 (CH), 116.4 (CH), 112.8 (CH), 74.8 (CH), 53.1 (CH₂), 45.2 (CH₂); IR (KBr, cm⁻¹) 3426 (w), 3061 (w), 2955 (w), 2897 (w), 2818 (w), 2758 (w), 1639 (w), 1503 (s), 1447 (s), 1369 (s), 1329 (s), 1302 (s), 1237 (m), 1214 (s), 1042 (m), 757 (s), 741 (s); MS (FAB) *m/z* (%) 317.3 (M+H)⁺ (100), 180.8 (28), 155.1 (34), 137.3 (30); HRMS (FAB) Calcd for (C₂₁H₁₈FN₂)⁺, 317.1454; Found, 317.1459.

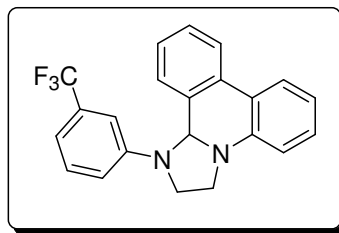
9.11.19 1-(4-Fluorophenyl)-1,2,3,12b-tetrahydroimidazo[1,2-*f*]phenanthridine (11n).



General TIP synthesis method. Product isolated as a white powder (514 mg, 1.63 mmol, 85.1%): mp 181-183 °C (Et₂O); ¹H NMR (CDCl₃, 400 MHz) δ 7.89 (d, 1H, *J*=8.0 Hz), δ 7.80 (d, 1H, *J*=8.0 Hz), 7.43 (t, 1H, *J*=8.0 Hz), 7.35 (t, 1H, *J*=8.0 Hz), 7.29 (t, 1H, *J*=8.0 Hz), 7.16 (d, 1H, *J*=8.0 Hz), 7.03 (m, 3H), 6.84 (d, 1H, *J*=8.0 Hz), 6.71 (d, 1H, *J*=9.2 Hz), 6.69 (d, 1H, *J*=9.2 Hz), 5.29 (s, 1H), 4.13 (m, 1H), 3.83 (m, 1H), 3.69 (m, 1H), 3.40 (m, 1H); ¹³C NMR (CDCl₃, 100 MHz) δ 157.3 (C), 155.0 (C), 145.4 (C), 143.4 (C), 134.0 (C), 131.9 (C), 129.2 (CH), 128.0 (CH), 127.2 (CH), 124.3 (CH), 123.4 (CH), 123.5 (CH), 120.1 (CH), 115.7 (CH), 115.4 (CH), 115.0 (CH), 114.9 (CH), 113.0 (CH), 75.5 (CH), 51.7 (CH₂), 44.9 (CH₂); IR (KBr, cm⁻¹) 3442 (w), 3060 (w), 2959 (w), 2891 (w), 2817 (w), 2756 (w), 1600 (m), 1510 (s), 1485 (m), 1441 (m), 1366 (m), 1317 (m), 1236 (m), 1209

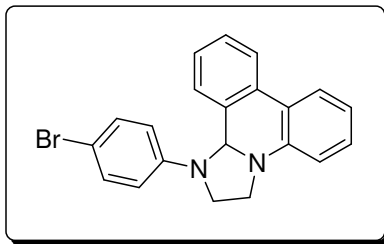
(m), 1158 (m); MS (FAB) m/z (%) 317.3 (M+H)⁺ (100), 180.8 (17); HRMS (FAB) Calcd for (C₂₁H₁₈FN₂)⁺, 317.1454; Found, 317.1458.

9.11.20 1-(3-Trifluoromethylphenyl)-1,2,3,12b-tetrahydroimidazo[1,2-f]phenanthridine (11p).



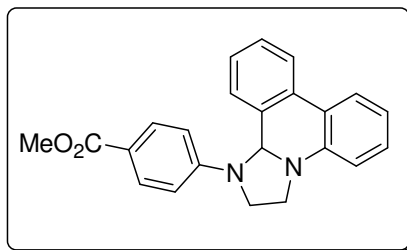
General TIP synthesis method. Product isolated as an orange solid (530 mg, 1.45 mmol, 75.7%): mp 147-149 °C (Et₂O); ¹H NMR (CDCl₃, 400 MHz) δ 7.90 (d, 1H, *J*=7.7 Hz), 7.82 (d, 1H, *J*=7.7 Hz), 7.45 (t, 1H, *J*=7.7 Hz), 7.37 (m, 2H), 7.29 (t, 1H, *J*=7.7 Hz), 7.15 (m, 3H), 7.00 (s, 1H), 6.87 (m, 2H), 5.37 (s, 1H), 4.13 (m, 1H), 3.92 (m, 1H), 3.71 (m, 1H), 3.43 (m, 1H); ¹³C NMR (CDCl₃, 100 MHz) δ 148.8 (C), 143.1 (C), 133.5 (C), 131.9 (C), 131.6 (C), 131.3 (C), 129.5 (CH), 129.3 (CH), 128.1 (CH), 127.3 (CH), 124.3 (C), 124.0 (CH), 123.8 (CH), 123.7 (CH), 120.3 (CH), 116.8 (CH), 114.5 (CH), 113.3 (CH), 110.4 (CH), 75.0 (CH), 50.9 (CH₂), 44.9 (CH₂); IR (KBr, cm⁻¹) 3418 (m), 3066 (w), 2936 (w), 2888 (w), 2827 (w), 1602 (m), 1489 (m), 1445 (s), 1362 (s), 1349 (s), 1158 (m), 1114 (s), 1073 (m), 865 (m), 753 (s); MS (FAB) m/z (%) 367.3 (M+H)⁺ (100), 307.1 (8), 180.8 (12), 154.9 (6); HRMS (FAB) Calcd for (C₂₂H₁₈F₃N₂)⁺, 367.1422; Found, 367.1431.

9.11.21 1-(4-Bromophenyl)-1,2,3,12b-tetrahydroimidazo[1,2-*f*]phenanthridine (11r).



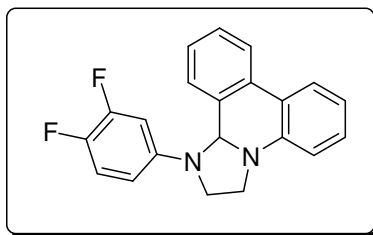
General TIP synthesis method. Product isolated as a brown powder (560 mg, 1.48 mmol, 77.7%): mp 196-197 °C (Et₂O); ¹H NMR (CDCl₃, 400 MHz) δ 7.78 (d, 1H, *J*=7.7 Hz), 7.70 (d, 1H, *J*=7.7 Hz), 7.33 (t, 1H, *J*=7.7 Hz), 7.27 (m, 2H), 7.25 (t, 1H, *J*=7.7 Hz), 7.18 (t, 1H, *J*=7.7 Hz), 7.03 (d, 1H, *J*=7.7 Hz), 6.96 (t, 1H, *J*=7.7 Hz), 6.74 (d, 1H, *J*=7.7 Hz), 6.54 (d, 2H, *J*=9.0 Hz), 5.18 (s, 1H), 3.98 (m, 1H), 3.73 (m, 1H), δ 3.58 (m, 1H), 3.29 (m, 1H); ¹³C NMR (CDCl₃, 100 MHz) δ 147.70 (C), 143.2 (C), 133.7 (C), 131.9 (C), 131.8 (2 × CH), 129.3 (CH), 128.0 (CH), 127.2 (CH), 124.23 (C), 124.18 (CH), 123.8 (CH), 123.6 (CH), 120.2 (CH), 115.7 (2 × CH), 113.1 (CH), 110.1 (C), 75.1 (CH), 51.0 (CH₂), 44.9 (CH₂); IR (KBr, cm⁻¹) 3443 (w), 3063 (w), 2932 (w), 2882 (w), 2839 (w), 1590 (s), 1488 (s), 1460 (s), 1443 (s), 1360 (s), 1345 (s), 1326 (s), 1307 (s), 745 (s), 731 (s); MS (FAB) *m/z* (%) 379.1 (M+H)⁺ (91), 377.1 (M+H)⁺ (100), 307.3 (13), 180.8 (39), 155.1 (19); HRMS (FAB) Calcd for (C₂₁H₁₈BrN₂)⁺, 377.0653, 379.0635; Found, 377.0648, 379.0634.

9.11.22 1-(4-Methylacetatephenyl)-1,2,3,12b-tetrahydroimidazo[1,2-*f*]phenanthridine (11s).



General TIP synthesis method. Product isolated as a pale peach powder (460 mg, 1.29 mmol, 67.6%): mp 167-168 °C (Et₂O); ¹H NMR (CDCl₃, 400 MHz) δ 7.99 (d, 2H, *J*=9.0 Hz), 7.90 (d, 1H, *J*=7.7 Hz), 7.81 (d, 1H, *J*=7.7 Hz), 7.44 (t, 1H, *J*=7.7 Hz), 7.36 (t, 1H, *J*=7.7 Hz), 7.28 (t, 1H, *J*=7.7 Hz), 7.13 (d, 1H, *J*=7.7 Hz), 7.08 (t, 1H, *J*=7.7 Hz), 6.87 (d, 1H, *J*=7.7 Hz), 6.75 (d, 2H, *J*=9.0 Hz), 5.43 (s, 1H), 4.09 (m, 1H), 3.99 (m, 1H), 3.91 (s, 3H), 3.70 (m, 1H), 3.45 (m, 1H); ¹³C NMR (CDCl₃, 100 MHz) δ 204.4 (C), 167.2 (C), 151.7 (C), 142.9 (C), 133.2 (C), 131.9 (C), 131.2 (CH), 129.3 (CH), 128.1 (CH), 127.2 (CH), 124.3 (C), 124.1 (CH), 123.8 (CH), 123.7 (CH), 123.0 (CH), 120.4 (CH), 119.3 (C), 113.4 (CH), 74.6 (CH), 51.7 (CH₃), 50.1 (CH₂), 45.0 (CH₂); IR (KBr, cm⁻¹) 3400 (w), 2938 (w), 2878 (w), 2839 (w), 1709 (s), 1598 (s), 1516 (m), 1493 (m), 1432 (w), 1279 (s), 1186 (m), 1115 (m), 768 (m), 751 (m), 733 (m); MS (FAB) *m/z* (%) 357 (M+H)⁺ (100), 193 (36), 154 (31), 136 (20); HRMS (FAB) Calcd for (C₂₃H₂₁N₂O₂)⁺, 357.1603; Found, 357.1602.

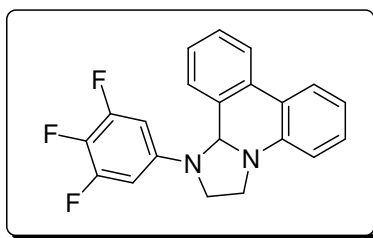
9.11.23 1-(3,4-Difluorophenyl)-1,2,3,12b-tetrahydroimidazo[1,2-*f*]phenanthridine (11t).



General TIP synthesis method. Product isolated as a pale yellow powder (625 mg, 1.87 mmol, 97.9%): mp 154-155 °C (Et₂O); ¹H NMR (CDCl₃, 400 MHz) δ 7.89 (d, 1H, *J*=7.7 Hz), 7.80 (d, 1H, *J*=7.7 Hz), 7.45 (t, 1H, *J*=7.7 Hz), 7.36 (t, 1H, *J*=7.7 Hz), 7.30 (t, 1H, *J*=7.7 Hz), 7.09 (m, 3H), 6.85 (d, 1H, *J*=7.7 Hz), 6.57 (m, 1H), δ 6.41 (m, 1H), 5.25 (s, 1H), 4.08 (m, 1H), 3.81 (m, 1H), 3.69 (m, 1H), 3.41 (m, 1H); ¹³C NMR (CDCl₃, 100 MHz) δ 151.8 (dd, *J*_{C-F} = 245, 14 Hz, C), 145.8 (C), 144.7 (dd, *J*_{C-F} = 245, 14 Hz, C), 143.1 (C), 133.5 (C), 131.9 (C), 129.3 (CH), 128.1 (CH), 127.3 (CH), 124.2 (C), 124.1 (CH), 123.8 (CH), 123.6 (CH), 120.3 (CH), 117.4 (d, *J*_{C-F} = 20 Hz, CH), 113.2 (CH), 109.0 (CH), 103.1 (d, *J*_{C-F} = 20 Hz, CH), 75.4 (CH), 51.4 (CH₂), 44.9 (CH₂), ¹⁹F NMR (CDCl₃, 376 MHz): δ -

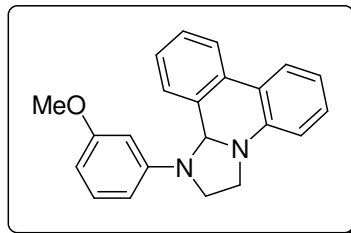
136.7 (s, 1F), -152.7 (s, 1F); IR (KBr, cm^{-1}) 3419 (w), 3062 (w), 3031 (w), 2943 (w), 2888 (w), 2826 (w), 2760 (w), 2675 (w), 1627 (m), 1581 (s), 1520 (s), 1452 (s), 1348 (s), 1224 (s), 817 (s); MS (FAB) m/z (%) 335.2 ($\text{M}+\text{H}^+$) (100), 206.6 (12), 180.8 (51), 157.0 (20); HRMS (FAB) Calcd for $(\text{C}_{21}\text{H}_{17}\text{F}_2\text{N}_2)^+$, 335.1360; Found, 335.1363.

9.11.24 1-(3,4,5-Trifluorophenyl)-1,2,3,12b-tetrahydroimidazo[1,2-f]phenanthridine (11u).



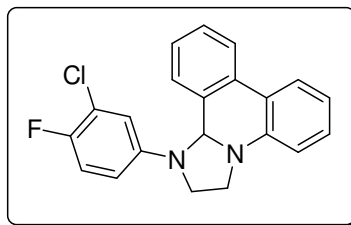
General TIP synthesis method. Product isolated as a pale yellow powder (404 mg, 1.15 mmol, 60.1%): mp 192-194 °C; ^1H NMR (CDCl_3 , 400 MHz) δ 7.78 (d, 1H, $J=8.0$ Hz), 7.70 (d, 1H, $J=8.0$ Hz), 7.35 (t, 1H, $J=8.0$ Hz), 7.23 (m, 2H), 6.99 (m, 2H), 6.75 (d, 1H, $J=8.0$ Hz), 6.22 (m, 2H), 5.12 (s, 1H), 3.92 (m, 1H), 3.68 (m, 1H), 3.57 (m, 1H), 3.31 (m, 1H); ^{13}C NMR (CDCl_3 , 100 MHz) δ 142.8 (C), 133.0 (C), 131.9 (C), 129.3 (CH), 128.2 (CH), 127.4 (CH), 124.2 (C), 123.8 (2 \times CH), 123.7 (CH), 120.5 (CH), 113.4 (CH), 97.9 (CH), 97.6 (CH), 75.3 (CH), 51.0 (CH_2), 45.0 (CH_2); IR (KBr, cm^{-1}) 3736 (w), 3070 (w), 2887 (w), 2359 (w), 1602 (w), 1527 (m), 1253 (m), 1037 (m), 756 (s); MS (EI+) m/z (%) 352 (M^+) (17), 193 (88), 165 (20), 78 (100), 63 (100), 45 (18); HRMS (EI+) Calcd for $\text{C}_{21}\text{H}_{15}\text{F}_3\text{N}_2$, 335.1360; Found, 335.1363.

9.11.25 1-(3-Methoxyphenyl)-1,2,3,12b-tetrahydroimidazo[1,2-f]phenanthridine (11y).



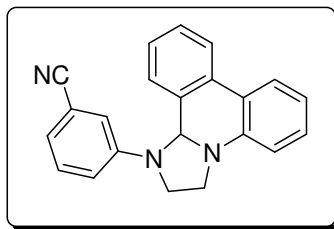
General TIP synthesis method. Product isolated as a pale orange powder (400 mg, 1.22 mmol, 63.8%): mp 122-124 °C (Et₂O); ¹H NMR (CDCl₃, 400 MHz) δ 7.89 (d, 1H, *J*=7.7 Hz), 7.79 (d, 1H, *J*=7.7 Hz), 7.42 (t, 1H, *J*=7.7 Hz), 7.35 (t, 1H, *J*=7.7 Hz), 7.28 (t, 1H, *J*=7.7 Hz), 7.23 (d, 1H, *J*=7.7 Hz), 7.21 (t, 1H, *J*=8.2 Hz), 7.05 (t, 1H, *J*=7.7 Hz), 6.84 (d, 1H, *J*=7.7 Hz), 6.45 (dd, 1H, *J*=8.2 Hz, 2.2 Hz), 6.39 (dd, 1H, *J*=8.2 Hz, 2.2 Hz), 6.34 (t, 1H, *J*=2.2 Hz), 5.34 (s, 1H), 4.09 (m, 1H), 3.91 (m, 1H), 3.81 (s, 3H), 3.68 (m, 1H), 3.39 (m, 1H); ¹³C NMR (CDCl₃, 100 MHz) δ 160.6 (C), 150.1 (C), 143.3 (C), 143.1 (C), 131.8 (C), 129.8 (CH), 129.2 (CH), 127.8 (CH), 127.2 (CH), 124.5 (CH), 124.4 (C), 123.7 (CH), 123.4 (CH), 120.0 (CH), 113.0 (CH), 107.1 (CH), 103.1 (CH), 100.7 (CH), 75.1 (CH), 55.2 (CH₃), 51.0 (CH₂), 44.9 (CH₂); IR (KBr, cm⁻¹) 3434 (w), 3062 (w), 3032 (w), 3000 (w), 2970 (w), 2936 (w), 2879 (w), 2838 (m), 2772 (w), 2675 (w), 1601 (s), 1491 (s), 1442 (s), 1358 (s), 1237 (s), 1168 (s), 1041 (s), 768 (s); MS (FAB) *m/z* (%) 329.3 (M+H)⁺ (100), 180.8 (26), 155.1 (23), 137.3 (22), 84.9 (16); HRMS for (C₂₂H₂₁N₂O)⁺ calcd: 329.1654, obsd 329.1655.

9.11.26 1-(3-Chloro-4-fluorophenyl)-1,2,3,12b-tetrahydroimidazo[1,2-f]phenanthridine (11z).



General TIP synthesis method. Product isolated as an off-white powder (418 mg, 1.19 mmol, 62.4%): mp 164-165 °C (Et₂O); ¹H NMR (CDCl₃, 400 MHz) δ 7.89 (d, 1H, *J*=7.7 Hz), 7.81 (d, 1H, *J*=7.7 Hz), 7.45 (t, 1H, *J*=7.7 Hz), 7.36 (t, 1H, *J*=7.7 Hz), 7.31 (t, 1H, *J*=7.7 Hz), 7.13 (d, 1H, *J*=7.7 Hz), 7.07 (t, 1H, *J*=7.7 Hz), 7.06 (t, 1H, *J*=9.1 Hz), 6.85 (d, 1H, *J*=7.7 Hz), 6.78 (dd, 1H, *J*=6.0 Hz, *J*=3.2 Hz), 6.57 (dt, 1H, *J*=9.1 Hz, *J*=3.2 Hz), 5.27 (s, 1H), 4.08 (m, 1H), 3.81 (m, 1H), 3.69 (m, 1H), 3.40 (m, 1H); ¹³C NMR (CDCl₃, 100 MHz) δ 151.4 (d, *J*_{C-F}=238 Hz, CF), 145.8 (C), 143.1 (C), 133.5 (C), 131.9 (C), 129.3 (CH), 128.1 (CH), 127.3 (CH), 124.2 (C), 124.0 (CH), 123.8 (CH), 123.6 (CH), 121.2 (d, *J*_{C-F}=20 Hz, CCl), 120.3 (CH), 116.6 (d, *J*_{C-F}=20 Hz, CH), 115.3 (CH), 113.2 (CH), 113.0 (CH), 75.3 (CH), 51.4 (CH₂), 44.9 (CH₂); ¹⁹F NMR (CDCl₃, 400 MHz): δ -130.1 (s), IR (KBr, cm⁻¹) 3433 (w), 3034 (w), 2937 (w), 2879 (w), 2845 (w), 2764 (w), 1600 (m), 1505 (s), 1445 (m), 1361 (m), 1328 (m), 1239 (s), 834 (m), 756 (s), 734 (s); MS (FAB) *m/z* (%) 351.2 (M+H)⁺ (100), 180.8 (33); HRMS (FAB) for (C₂₁H₁₇ClFN₂)⁺ calcd 351.1064, obsd 351.1069.

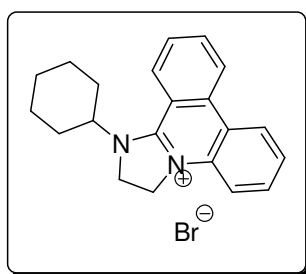
9.11.27 1-(3-Cyano-phenyl)-1,2,3,12b-tetrahydro-imidazo[1,2-f]phenanthridine (11a')



General TIP synthesis method. Product isolated as a pale peach powder (386 mg, 1.19 mmol, 62.5%): mp 175-177 °C (Et₂O); ¹H NMR (CDCl₃, 400 MHz) δ 7.78 (d, 1H, *J*=7.8 Hz), 7.69 (d, 1H, *J*=7.8 Hz), 7.33 (t, 1H, *J*=7.8 Hz), 7.23 (m, 2H), 7.18 (t, 1H, *J*=7.8 Hz), 7.01 (d, 1H, *J*=7.8 Hz), 6.96 (m, 2H), 6.87 (s, 1H), 6.81 (dd, 1H, *J*=8.4 Hz, *J*=2.2 Hz), 6.74 (d, 1H, *J*=7.8 Hz), 5.20 (s, 1H), 3.96 (m, 1H), δ 3.74 (m, 1H), 3.57 (m, 1H), 3.29 (m, 1H); ¹³C NMR (CDCl₃, 100 MHz) δ 148.7 (C), 142.9 (C), 133.0 (C), 131.9 (C), 129.9 (CH), 129.4 (CH), 128.2 (CH), 127.4 (CH), 124.3 (C), 123.86 (CH), 123.85 (CH), 123.8 (CH), 121.4 (CH), 120.5 (CH), 119.4 (C), 118.0 (CH), 116.6 (CH), 113.4 (CH), 113.0 (C), 75.0

(CH), 50.7 (CH₂), 45.0 (CH₂); IR (KBr, cm⁻¹) 3433 (w), 3061 (w), 2946 (w), 2886 (w), 2846 (w), 2766 (w), 2225 (m), 1596 (s), 1572 (m), 1491 (s), 1444 (s), 1359 (s), 1339 (s), 1304 (m), 1161 (m); 850 (m), 778 (s), 756 (s), 683 (m); MS (FAB) *m/z* (%) 324 (M+H)⁺ (100), 193 (32), 180 (20); HRMS (FAB) for (C₂₂H₁₈N₃)⁺ calcd 324.1501, obsd 324.1500.

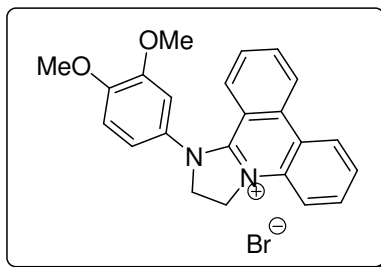
9.11.28 1-Cyclohexyl-2,3-dihydro-1H-imidazo[1,2-f]phenanthridinium bromide (12a).



A solution of cyclohexylamine (218 μ L, 1.91 mmol, 1.0 eq) in 5% Na₂CO₃ aqueous solution (20mL) was added to a suspension of BEP **10** (700 mg, 1.91 mmol, 1.0 eq) in ethyl acetate (30mL). The resultant biphasic solution was stirred at room temperature under N₂ for 1 h. Layers were separated and the organic layer was washed with water (3 \times 10 mL) and brine (1 \times 10 mL). NBS (340 mg, 1.91 mmol, 1.0 eq) was added and the reaction was stirred for 30 min. The resultant suspension was filtered, washing the residue with acetone. The residue was dried under vacuum and collected as a pale yellow solid (678 mg, 1.77 mmol, 92.6%): mp 293-294 $^{\circ}$ C (MeOH-Et₂O); ¹H NMR (CDCl₃ MHz) δ 8.64 (d, 1H, *J*=8.0), 8.42 (d, 1H, *J*=8.0 Hz), 8.30 (d, 1H, *J*=8.0 Hz), 8.07 (t, 1H, *J*=8.0 Hz), 7.83 (t, 1H, *J*=8.0 Hz), 7.79 (t, 1H, *J*=8.0 Hz), 7.65 (d, 1H, *J*=8.0 Hz), 7.58 (t, 1H, *J*=8.0 Hz), 5.17 (t, 2H, *J*=10.6 Hz), 4.74 (t, 2H, *J*=10.6 Hz), 4.57 (m, 1H), 2.26 (m, 2H), 2.06 (m, 2H), 1.99 (m, 2H), 1.84 (m, 1H), 1.52 (m, 2H), 1.37 (m, 1H); ¹³C NMR (DMSO, 100 MHz) δ 152.6 (C), 135.0 (CH), 135.0 (C), 133.0 (C), 131.4 (CH), 129.5 (CH), 127.8 (CH), 125.0 (CH), 124.3 (CH), 123.8 (CH), 119.8 (C), 115.72 (CH), 115.65 (C), 57.6 (CH), 45.8 (CH₂), 44.7 (CH₂), 30.2 (2 \times CH₂), 24.6 (CH₂), 24.5 (2 \times CH₂); MS (FAB) *m/z* (%) 303.3 (M⁺) (100), 221.5 (11), 176.8 (11), 155.0 (32).

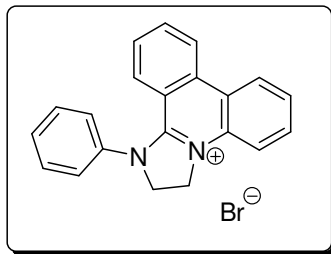
Product Reference: Parenty, A. D. C., University of Glasgow, 2004.

9.11.29 1-(3,4-Dimethoxyphenyl)-2,3-dihydro-1H-imidazo[1,2-f]phenanthridinium bromide (12i).



To a suspension of **BEP 10** (1.00 g, 2.72 mmol, 2.0 eq) in CHCl_3 (25 mL) was added was added TEA (568 μL , 4.08 mmol, 3.0 eq) and 3,4-dimethoxyaniline (209 mg, 1.36 mmol, 1.0 eq). The reaction was stirred under N_2 for 24 h. Solvent was removed under vacuum and the residue was triturated with water (2×2 mL) then acetone (~ 30 mL) to give a pale yellow powder after drying under vacuum (338 mg, 0.77 mmol, 56.8 %): mp 307-308 $^\circ\text{C}$ (decomp) (MeOH-Et₂O); ^1H NMR (DMSO, 400 MHz): δ 8.91 (d, 1H, $J=8.2$ Hz), 8.82 (d, 1H, $J=8.2$ Hz), 8.07 (t, 1H, $J=8.2$ Hz), 7.93 (t, 1H, $J=8.2$ Hz), 7.83 (d, 1H, $J=8.2$ Hz), 7.71 (t, 1H, $J=8.2$ Hz), 7.61 (t, 1H, $J=8.2$ Hz), 7.41 (m, 2H), 7.26 (m, 2H), 4.93 (t, 2H, $J=10.4$ Hz), 4.59 (m, 2H), 3.89 (s, 3H), 3.75 (s, 3H); ^{13}C NMR (DMSO, 100 MHz) δ 152.6 (C), 150.0 (C), 149.7 (C), 135.3 (CH), 135.0 (C), 132.6 (C), 131.5 (CH), 128.7 (CH), 127.1 (CH), 125.6 (CH), 124.2 (CH), 124.1 (CH), 120.3 (C), 118.9 (CH), 116.1 (CH), 115.1 (C), 112.6 (CH), 110.2 (CH), 55.8 ($2 \times \text{CH}_3$), 54.6 (CH_2), 46.7 (CH_2); IR (KBr, cm^{-1}) 3024 (w), 2960 (w), 2361 (w), 1595 (m), 1577 (s), 1514 (m), 1442 (m), 1307 (m), 1261 (s), 1240 (m), 1022 (m), 754 (s); MS (FAB) m/z (%) 357.4 (M^+) (100), 307.2 (32), 290.3 (12), 155.0 (43), 138.2 (42); HRMS (FAB) for ($\text{C}_{23}\text{H}_{21}\text{N}_2\text{O}_2^+$) calcd 357.1603, obsd 357.1600.

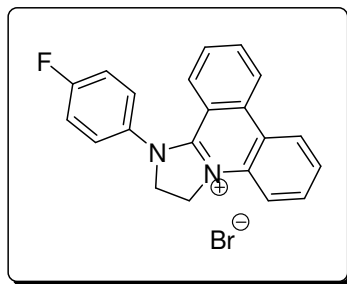
9.11.30 1-Phenyl-2,3-dihydro-1*H*-imidazo[1,2-*f*]phenanthridinium bromide (12j).



NBS (299 mg, 1.68 mmol, 1.0 eq) was added to a solution of 1-phenyl-1,2,3,12b-tetrahydroimidazo[1,2-*f*]phenanthridine (500 mg, 1.68 mmol, 1.0 eq) in chloroform (30 mL) and the resultant suspension was stirred at room temperature for 1.5 h. Solvent was removed under vacuum and the residue was triturated with ethyl acetate (3 × 20 mL) and diethyl ether (3 × 20 mL). The product was collected by filtration and dried under vacuum to give a pale peach powder (549 mg, 1.58 mmol, 86.6%): mp >340 °C (MeOH-Et₂O); ¹H NMR (DMSO, 400 MHz) δ 8.93 (d, 1H, J=8.0 Hz), 8.83 (d, 1H, J=8.0 Hz), 8.07 (t, 1H, J=8.0 Hz), 7.94 (t, 1H, J=8.0 Hz), 7.85 (d, 1H, J=8.0 Hz), 7.71 (m, 6H), 7.55 (t, 1H, J=8.0 Hz), 7.29 (d, 1H, J=8.0 Hz), 4.96 (t, 2H, J=10.6 Hz), 4.62 (t, 2H, J=10.6 Hz); ¹³C NMR (DMSO, 100 MHz) δ 152.7 (C), 139.2 (C), 135.3 (CH), 135.2 (C), 132.6 (C), 131.6 (CH), 130.8 (2 × CH), 130.1 (CH), 128.6 (CH), 127.0 (CH), 126.7 (2 × CH), 125.8 (CH), 124.3 (CH), 124.1 (CH), 120.5 (C), 116.2 (CH), 115.4 (C), 54.4 (CH₂), 46.9 (CH₂).

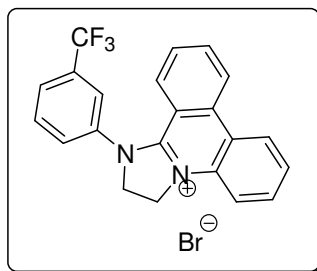
Product Reference: Parenty, A. D. C.; Smith, L. V.; Pickering A. L.; Long, D. -L.; Cronin L., *J. Org. Chem.* **2004**, *69*, 5934-5946.

9.11.31 1-(4-Fluorophenyl)-2,3-dihydro-1*H*-imidazo[1,2-*f*]phenanthridinium bromide (12n).



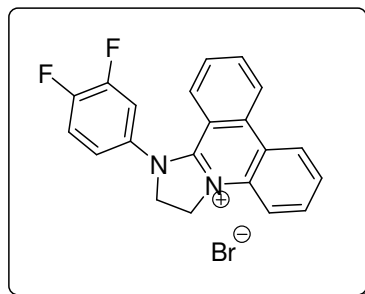
To a solution of 1-(4-fluorophenyl)-1,2,3,12b-tetrahydro-imidazo[1,2-*f*]phenanthridine (250 mg, 0.79 mmol, 1.0 eq) in CHCl_3 (30 mL) was added NBS (140 mg, 0.79 mmol, 1.0 eq) and the reaction was stirred at room temperature for 1h. The reaction mixture was then concentrated under vacuum and the residue was triturated with acetone to give a pale peach powder after drying (250 mg, 0.63 mmol, 80.1%): mp $>350^\circ\text{C}$ (MeOH-Et₂O); ¹H NMR (DMSO, 400 MHz) δ 8.94 (d, 1H, $J=8.0$ Hz), 8.84 (d, 1H, $J=8.0$ Hz), 8.08 (t, 1H, $J=8.0$ Hz), 7.95 (t, 1H, $J=8.0$ Hz), 7.83 (m, 3H), 7.73 (t, 1H, $J=8.0$ Hz), 7.59 (m, 3H), 7.31 (d, 1H, $J=8.0$ Hz), 4.95 (t, 2H, $J=10.2$ Hz), 4.60 (t, 2H, $J=10.2$ Hz); ¹³C NMR (DMSO, 100 MHz) δ 162.3 (d, $J_{\text{C-F}}=247.8$ Hz, C), 152.7 (C), 135.38 (C), 135.35 (CH), 135.1 (C), 132.5 (C), 131.6 (CH), 129.3 (CH), 128.8 (CH), 127.0 (CH), 125.8 (CH), 124.2 (d, $J_{\text{C-F}}=24.3$ Hz, CH), 120.4 (C), 118.0 (CH), 117.8 (CH), 116.2 (CH), 115.2 (C), 54.5 (CH₂), 46.9 (CH₂); IR (cm⁻¹) 1577 (m), 1394 (m), 1219 (m), 848 (m), 790 (m), 756 (s), 669 (m); MS (FAB) m/z (%) 315.3 (M⁺) (100); HRMS (FAB) for (C₂₁H₁₆FN₂)⁺ calcd 315.1298, obsd 315.1299.

9.11.32 1-(3-Trifluoromethylphenyl)-2,3-dihydro-1H-imidazo[1,2-f]phenanthridinium bromide (12p).



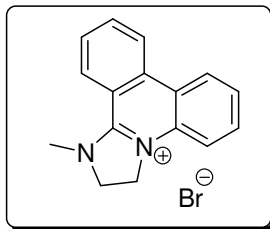
To a suspension of BEP **10** (700 mg, 1.91 mmol, 1.0 eq) in CHCl_3 (40 mL) was added 3-(trifluoromethyl)-aniline (239 μL , 1.91 mmol, 1.0 eq) and TEA (798 μL , 5.73 mmol, 3.0 eq). The resultant suspension was stirred under a nitrogen atmosphere for 5 h. The reaction mixture was transferred to a separating funnel and washed with water (2 \times 20 mL) and brine (1 \times 20 mL). The organic phase was then dried over MgSO_4 and the solvent was removed under vacuum to give a yellow oil. The oily residue was redissolved in CHCl_3 (50 mL) and NBS (340 mg, 1.91 mmol, 1.0 eq) was added. The reaction was stirred at room temperature for 2 h then filtered, yielding a pale yellow powder after drying under vacuum (498 mg). The filtrate was concentrated under vacuum and the residue was triturated with acetone to yield a second batch of product (128 mg). Combined yield (626 mg, 1.41 mmol, 73.6%): mp >350 $^\circ\text{C}$ (MeOH-Et₂O); ^1H NMR (DMSO, 400 MHz) δ 8.97 (d, 1H, $J=8.0$ Hz), 8.87 (d, 1H, $J=8.0$ Hz), 8.21 (s, 1H), 8.08 (m, 3H), 7.92 (m, 3H), 7.76 (t, 1H, $J=8.0$ Hz), 7.60 (t, 1H, $J=8.0$ Hz), 7.28 (d, 1H, $J=8.0$ Hz), 5.00 (t, 2H, $J=10.2$ Hz), 4.69 (t, 2H, $J=10.2$ Hz); ^{13}C NMR (DMSO, 100 MHz) δ 152.9 (C), 140.2 (C), 135.5 (CH), 135.2 (C), 132.5 (C), 132.1 (CH), 131.7 (CH), 130.9 (CH), 128.7 (CH), 127.0 (CH), 126.5 (CH), 126.1 (CH), 124.5 (CH), 124.1 (CH), 123.8 (CH), 120.7 (C), 116.4 (CH), 115.1 (C), 54.1 (CH₂), 47.2 (CH₂); IR (cm^{-1}) 3032 (w), 1577 (m), 1539 (m), 1325 (m), 1128 (m), 756 (m), 704 (m); MS (FAB) m/z (%) 365 (M^+) (70), 307 (26), 289 (18), 154 (100), 136 (70); HRMS (FAB) for $(\text{C}_{22}\text{H}_{16}\text{F}_3\text{N}_2)^+$ calcd 365.1266, obsd 365.1270.

9.11.33 1-(3,4-Difluorophenyl)-2,3-dihydro-1H-imidazo[1,2-*f*]phenanthridinium bromide (12t).



NBS (340 mg, 1.91 mmol, 1.0 eq) was added to a solution of 1-difluorophenyl-1,2,3,12b-tetrahydroimidazo[1,2-*f*]phenanthridine (640 mg, 1.91 mmol, 1.0 eq) in chloroform (30 mL) and the resultant suspension was stirred at room temperature for 1 h. Solvent was removed under vacuum and the residue was triturated with acetone to give the product as a pale orange powder after drying under vacuum (700 mg, 1.69 mmol, 88.7%): mp 355-356 °C (MeOH-Et₂O); ¹H NMR (DMSO, 400 MHz) δ 8.95 (d, 1H, *J*=8.2 Hz), 8.86 (d, 1H, *J*=8.2 Hz), 8.12 (t, 1H, *J*=8.2 Hz), 7.96 (m, 2H), 7.88 (d, 1H, *J*=8.2 Hz), 7.78 (m, 2H), 7.64 (m, 2H), 7.41 (d, 1H, *J*=8.2 Hz), 4.97 (t, 2H, *J*=10.5 Hz), 4.61 (t, 2H, *J*=10.6 Hz); ¹³C NMR (DMSO, 100 MHz) δ 152.9 (C), 150.1 (dd, *J*_{C-F} = 252, 13.6 Hz, C), 150.0 (dd, *J*_{C-F} = 252, 13.6 Hz, C), 135.8 (C), 135.5 (CH), 135.1 (C), 132.4 (C), 131.6 (CH), 129.0 (CH), 127.3 (CH), 126.0 (CH), 124.5 (CH), 124.3 (CH), 124.1 (CH), 120.6 (C), 119.7 (d, *J*_{C-F} = 19 Hz, CH), 116.9 (d, *J*_{C-F} = 19 Hz, CH), 116.4 (CH), 115.0 (C), 54.3 (CH₂), 47.1 (CH₂); IR (KBr, cm⁻¹) 3024 (w), 2359 (w), 2332 (w), 1595 (w), 1577 (m), 1541 (m), 1508 (s), 1456 (m), 1267 (m), 754 (s); MS (FAB) *m/z* (%) 333 (M⁺) (100), 307 (53), 289 (53); HRMS (FAB) for (C₂₁H₁₅F₂N₂)⁺ calcd 333.1203, obsd 333.1205.

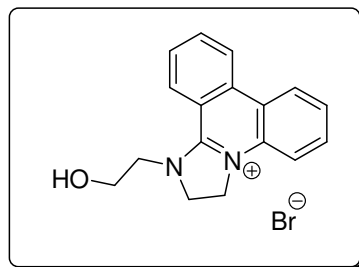
9.11.34 1-Methyl-2,3-dihydro-1*H*-imidazo[1,2-*f*]phenanthridinium bromide (12b').



To a biphasic solution of methylamine hydrochloride (460 mg, 6.81 mmol, 5.0 eq) in EtOAc (20 mL) and 5% Na₂CO₃ (10 mL) was added BEP **10** (500 mg, 1.362 mmol, 1.0 eq). The reaction was stirred under nitrogen for 5 min, the aqueous layer was removed and the organic layer washed with H₂O (1 × 10 mL) then brine (1 × 10 mL). NBS (242 mg, 1.36 mmol, 1.0 eq) was added and the reaction stirred under nitrogen for 1 h. The precipitated product was filtered, washing with diethyl ether and drying under vacuum to give a pale yellow powder as the product (419 mg, 1.33 mmol, 97.6%): mp >350°C (MeOH-Et₂O); ¹H NMR (DMSO, 400 MHz) δ 8.88 (d, 1H, J=8.0 Hz), 8.71 (d, 1H, J=8.0 Hz), 8.69 (d, 1H, J=8.0 Hz), 8.14 (t, 1H, J=8.0 Hz), 7.90 (t, 1H, J=8.0 Hz), 7.81 (t, 1H, J=8.0 Hz), 7.62 (d, 1H, J=8.0 Hz), 7.60 (t, 1H, J=8.0 Hz), 4.69 (t, 2H, J=10.6 Hz), 4.33 (t, 2H, J=10.6 Hz), 3.76 (s, 3H); ¹³C NMR (DMSO, 100 MHz) δ 153.3 (C), 135.2 (CH), 134.7 (C), 132.9 (C), 131.4 (CH), 129.1 (CH), 128.3 (CH), 125.0 (CH), 124.1 (CH), 123.9 (CH), 119.7 (C), 116.0 (C), 115.6 (CH), 53.0 (CH₂), 45.7 (CH₂), 38.1 (CH₃).

Product Reference: Smith, L. V.; Parenty, A. D. C.; Guthrie, K. M.; Plumb, J.; Brown, R.; Cronin, L. *Chembiochem* **2006**, *7*, 1757-1763.

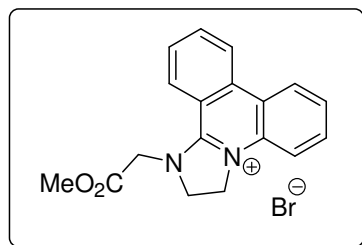
9.11.35 1-(2-Hydroxy-ethyl)-2,3-dihydro-1*H*-imidazo[1,2-*f*]phenanthridinium bromide (12f').



To a suspension of BEP **10** (1.00 g, 2.72 mmol, 1.0 eq) in EtOAc (40 mL) was added a solution of ethanolamine (197 μ L, 3.26 mmol, 1.2 eq) in 5% Na₂CO₃ (aq). The resultant biphasic solution was stirred under a nitrogen atmosphere for 2.5 h. The reaction mixture was transferred to a separating funnel and the layers were separated, washing the organic phase with H₂O (2 \times 20 mL). The combined organics were dried over MgSO₄ and filtered before adding NBS (484 mg, 2.72 mmol, 1.0 eq). The reaction was stirred at room temperature for 2 h. The precipitated product was collected by filtration and dried under vacuum to yield the product as a pale yellow powder. The product was recrystallized from EtOH (621 mg, 1.80 mmol, 66.1%): mp 205-207 °C (EtOH); ¹H NMR (DMSO, 400 MHz) δ 8.89 (d, 1H, *J*=7.8 Hz), 8.78 (d, 1H, *J*=7.8 Hz), 8.73 (d, 1H, *J*=7.8 Hz), 8.14 (t, 1H, *J*=7.8 Hz), 7.86 (t, 1H, *J*=7.8 Hz), 7.85 (t, 1H, *J*=7.8 Hz), 7.66 (d, 1H, *J*=7.8 Hz), 7.62 (t, 1H, *J*=7.8 Hz), 4.74 (t, 2H, *J*=10.6 Hz), 4.48 (t, 1H, *J*=10.6 Hz), 4.20 (t, 2H, *J*=5.3 Hz), 3.94 (t, 2H, *J*=5.3 Hz); ¹³C NMR (DMSO, 100 MHz) δ 153.8 (C), 135.2 (CH), 134.7 (C), 132.9 (C), 131.4 (CH), 129.0 (CH), 128.2 (CH), 125.1 (CH), 124.1 (CH), 123.9 (CH), 119.8 (C), 115.8 (CH), 115.6 (C), 58.1 (CH₂), 52.6 (CH₂), 51.3 (CH₂), 46.0 (CH₂); MS (FAB) *m/z* (%) 265.2 (M⁺) (100), 219.4 (13).

Product Reference: Parenty, A. D. C.; Smith, L. V.; Pickering A. L.; Long, D. -L.; Cronin L., *J. Org. Chem.* **2004**, *69*, 5934-5946.

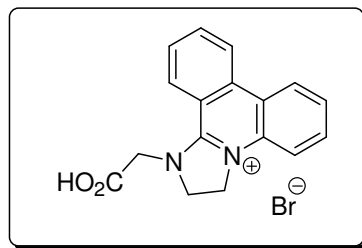
9.11.36 1-Methoxycarbonylmethyl-2,3-dihydro-1*H*-imidazo[1,2-*f*]phenanthridinium bromide (12g').



To a suspension of of BEP **10** (700 mg, 1.91 mmol, 1.0 eq) in EtOAc (30 mL) was added a solution of glycine methyl ester hydrochloride (240 mg, 1.91 mmol, 1.0 eq) and triethanolamine (1.425 g, 9.55 mmol, 5.0 eq) in H₂O (30 mL). The reaction was stirred at room temperature under nitrogen for 1 h. The layers were separated and the organic layer was washed with H₂O (2 × 20 mL) and dried over MgSO₄. NBS (306 mg, 1.72 mmol, 0.9 eq) was then added and the solution was stirred in the dark for 1 h. The resultant suspension was filtered, washing the residue with Et₂O and drying under vacuum to give a pale yellow powder (583 mg, 1.56 mmol, 90.8%): mp 230 °C (decomp); ¹H NMR (DMSO, 400 MHz) δ 8.96 (d, 1H, *J*=8.2 Hz), 8.81 (d, 1H, *J*=8.2 Hz), 8.36 (d, 1H, *J*=8.2 Hz), 8.18 (t, 1H, *J*=8.2 Hz), 7.90 (t, 1H, *J*=8.2 Hz), 7.89 (t, 1H, *J*=8.2 Hz), 7.76 (d, 1H, *J*=8.2 Hz), 7.70 (t, 1H, *J*=8.2 Hz), 5.22 (s, 2H), 4.87 (t, 2H, *J*=10.6 Hz), 4.36 (t, 2H, *J*=10.6 Hz), 3.79 (s, 3H); ¹³C NMR (DMSO, 100 MHz) δ 186.2 (C), 153.8 (C), 135.5 (CH), 134.6 (C), 132.3 (C), 131.5 (CH), 129.5 (CH), 127.1 (CH), 125.7 (CH), 124.2 (CH), 123.9 (CH), 120.0 (C), 116.3 (CH), 115.1 (C), 53.0 (CH₃), 52.1 (CH₂), 51.7 (CH₂), 46.3 (CH₂).

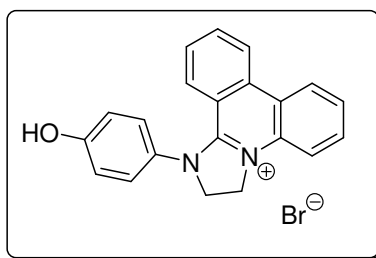
Product Reference: Smith, L. V.; de la Fuente, J. M.; Guthrie, K. M.; Parenty, A. D. C.; Cronin, L. *New J. Chem.* **2005**, 29, 1118-1120.

9.11.37 1-Carboxymethyl-2,3-dihydro-1H-imidazo[1,2-f]phenanthridinium bromide (12h').



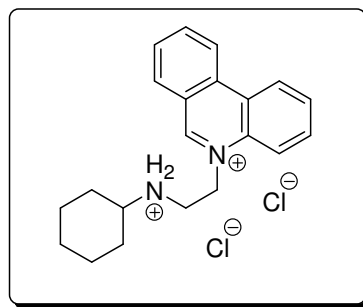
48 % HBr (aq) (5 mL) was added to a solution of 1-methoxycarbonylmethyl-2,3-dihydro-1H-imidazo[1,2-f]phenanthridinium bromide (400 mg, 1.07 mmol, 1.0 eq) in H₂O (10 mL) and the reaction solution stirred for 2 h. The solvents were removed under vacuum to give a pale peach powder (344 mg, 0.96 mmol, 89.8%): mp 280 °C (decomp); ¹H NMR (DMSO, 400 MHz) δ 8.95 (d, 1H, *J*=8.0 Hz), 8.79 (d, 1H, *J*=8.0 Hz), 8.39 (d, 1H, *J*=8.0 Hz), 8.17 (t, 1H, *J*=8.0 Hz), 7.90 (t, 1H, *J*=8.0), 7.89 (t, 1H, *J*=8.0), 7.74 (d, 1H, *J*=8.0 Hz), 7.68 (t, 1H, *J*=8.0 Hz), 5.12 (s, 2H), 4.86 (t, 2H, *J*=10.5 Hz), 4.36 (t, 2H, *J*=10.5 Hz); ¹³C NMR (MeOD, 100 MHz) δ 170.5 (C), 156.1 (C), 137.1 (C), 136.8 (CH), 134.2 (C), 132.8 (CH), 130.5 (CH), 128.3 (CH), 127.2 (CH), 125.5 (CH), 125.1 (CH), 122.1 (C), 117.1 (CH), 53.6 (CH₂), 52.9 (CH₂), 47.7 (CH₂); IR (KBr, cm⁻¹) 3429 (w), 2779 (m), 2588 (m), 2506 (m), 1714 (s), 1573 (s), 1549 (s), 1449 (m), 1401 (m), 1300 (m), 1259 (s), 1201 (s), 1108 (w), 753 (m), 715 (m), 631 (m); MS (FAB) *m/z* (%) 307.3 (26), 279.3 (M⁺) (100), 155.1 (64), 137.3 (61); HRMS (FAB) for (C₁₇H₁₅N₂O₂)⁺ calcd 279.1134, obsd 279.1138.

9.11.38 1-(4-Hydroxy-phenyl)-2,3-dihydro-1H-imidazo[1,2-f]phenanthridin-4ium bromide (12i').



To a solution of BEP **10** (500 mg, 1.36 mmol, 2.0 eq) in MeOH (15 mL) was added a solution of 4-aminophenol (74 mg, 0.68 mmol, 1.0 eq) and TEA (285 μ L, 2.04 mmol, 3.0 eq) in MeOH (5 mL). The reaction mixture was shaken vigorously for 1 min then left to stand for 24 h. Brown crystals were filtered, washing them with MeOH and diethyl ether before drying under vacuum. The product was collected as a brown crystalline solid (194 mg, 0.49 mmol, 72.4%): mp $>350^{\circ}\text{C}$; ^1H NMR (DMSO, 400 MHz) δ 8.88 (d, 1H, J=8.0 Hz), 8.78 (d, 1H, J=8.0 Hz), 8.05 (t, 1H, J=8.0 Hz), 7.91 (t, 1H, J=8.0 Hz), 7.79 (d, 1H, J=8.0 Hz), 7.69 (t, 1H, J=8.0 Hz), 7.57 (t, 1H, J=8.0 Hz), 7.53 (d, 2H, J=9.2 Hz), 7.37 (d, 1H, J=8.0 Hz), 7.03 (d, 2H, J=9.2 Hz), 4.89 (t, 2H, J=10.6 Hz), 4.52 (t, 2H, J=10.6 Hz); ^{13}C NMR (DMSO, 100 MHz) δ 158.4 (C), 152.5 (C), 135.2 (CH), 134.9 (C), 132.7 (C), 131.5 (CH), 129.9 (C), 128.6 (CH), 128.1 (2 \times CH), 126.9 (CH), 125.5 (CH), 124.2 (CH), 124.0 (CH), 120.2 (C), 117.1 (2 \times CH), 116.0 (CH), 115.4 (C), 54.6 (CH₂), 46.6 (CH₂); IR (KBr, cm^{-1}) 3448 (w), 3108 (s), 3021 (m), 1609 (s), 1595 (s), 1576 (s), 1547 (s), 1513 (s), 1494 (s), 1446 (s), 1391 (m), 1303 (s), 1262 (s), 1227 (s), 1166 (s), 845 (s), 788 (s), 751 (s), 718 (s), 666 (s); MS (FAB) m/z (%) 313 (14) (M⁺), 232 (17), 157 (32), 79 (100); Anal. Calcd for C₂₁H₁₇BrN₂O: C, 64.13; H, 4.36; N, 7.12; Found: C, 63.96; H, 4.33; N, 7.08.

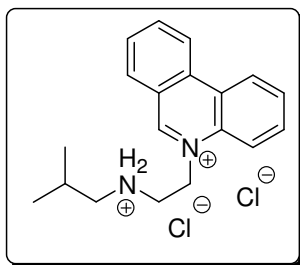
9.11.39 5-(2-Cyclohexylaminoethyl)-phenanthridinium chloride; hydrochloride (13a).



To a suspension of BEP **10** (700 mg, 1.91 mmol, 1.0 eq) in DCM (40 mL) was added cyclohexylamine (219 μ L, 1.91 mmol, 1.0 eq) and 5% Na₂CO₃ (20 mL). The reaction mixture was stirred for 3 hr under nitrogen before transferring to a separating funnel.

Phases were separated and the organic phase was washed with water (1 × 10 mL) then extracted into 1N HCl (2 × 20 mL). The acidic extract was concentrated under vacuum and the residue triturated with acetone to afford a pale yellow powder as the product (691 mg, 1.83 mmol, 95.9%): mp 252-253 °C; ¹H NMR (D₂O, 400 MHz) δ 9.90 (s, 1H), 8.94 (d, 1H, *J*=8.2 Hz), 8.85 (d, 1H, *J*=8.2 Hz), 8.40 (d, 1H, *J*=8.2 Hz), 8.26 (m, 2H), 7.99 (m, 3H), 5.36 (t, 2H, *J*=6.8 Hz), 3.74 (t, 2H, *J*=6.8 Hz), 3.07 (m, 1H), 1.93 (m, 2H), 1.67 (m, 2H), 1.50 (m, 1H), 1.11 (m, 5H); ¹³C NMR (D₂O, 100 MHz) δ 155.5 (CH), 139.0 (CH), 135.2 (C), 132.8 (CH), 132.5 (CH), 132.4 (C), 130.6 (CH), 130.5 (CH), 126.2 (C), 124.9 (CH), 123.3 (C), 122.6 (CH), 118.3 (CH), 58.4 (CH), 53.6 (CH₂), 42.2 (CH₂), 28.6 (2×CH₂), 24.3 (CH₂), 23.8 (2×CH₂); IR (KBr, cm⁻¹) 3405 (m), 2963 (m), 2857 (m), 2627 (m), 2490 (m), 2431 (m), 2368 (w), 1626 (s), 1582 (m), 1448 (m), 1347 (m), 1261 (m), 1030 (m), 916 (m), 761 (s); 610 (m); MS (FAB) *m/z* (%) 305.4 (M⁺) (100), 155.1 (25), 137.3 (16); HRMS (FAB) for (C₂₁H₂₅N₂)⁺ calcd 305.2018, obsd 305.2016.

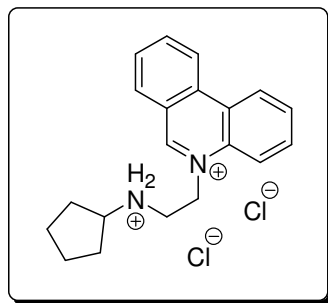
9.11.40 5-(2-Isobutylaminoethyl)-phenanthridinium chloride; hydrochloride (13b).



BEP **10** (250 mg, 0.68 mmol, 1.0 eq) was added to a biphasic solution of isobutylamine (67.5 μL, 0.68 mmol, 1.0 eq) in ethyl acetate (20 mL) and 5% Na₂CO₃ aqueous solution (20 mL). The solution was stirred at room temperature for 3 h before transferring it to a separating funnel, where the phases were separated and the organic phase was washed with water (2 × 5 mL) and brine (1 × 5 mL). Conc. HCl (3 drops) was then added to the organic layer to form the hydrochloride salt. Evaporation of the solvent and trituration of the residue with diethyl ether yielded the product as a pale yellow solid (187 mg, 0.53 mmol, 78.3%): mp 234-235 °C; ¹H NMR (DMSO, 400 MHz) δ 10.72 (s, 1H), 10.08 (s, 2H), 9.25

(d, 1H, $J=8.0$ Hz), 9.18 (d, 1H, $J=8.0$ Hz), 8.89 (d, 1H, $J=8.0$ Hz), 8.60 (d, 1H, $J=8.0$ Hz), 8.43 (t, 1H, $J=8.0$ Hz), 8.15 (m, 3H), 5.69 (t, 2H, $J=6.2$ Hz), 3.69 (m, 2H), 2.84 (m, 2H), 2.10 (sept, 1H, $J=6.8$ Hz), 0.99 (d, 6H, $J=6.8$ Hz); ^{13}C NMR (DMSO, 100 MHz) δ 157.4 (CH), 138.2 (CH), 134.7 (C), 133.3 (C), 133.1 (CH), 132.0 (CH), 130.3 (CH), 130.2 (CH), 126.1 (C), 125.1 (CH), 123.8 (C), 123.1 (CH), 120.0 (CH), 54.3 (CH₂), 53.1 (CH₂), 45.5 (CH₂), 25.4 (CH), 20.3 (2 \times CH₃); IR (KBr, cm⁻¹) 3412 (s), 2959 (m), 2706 (m), 1627 (s), 1535 (m), 1451 (s), 761 (s); MS (EI+) m/z (%) 280.3 (M⁺) (11), 278.3 (5), 235.2 (36), 194.2 (100), 180.2 (30), 165.1 (23); HRMS (FAB) for (C₁₉H₂₃N₂)⁺ calcd 279.1861, obsd 279.1862.

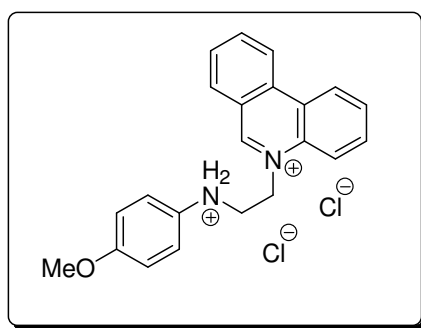
9.11.41 5-(2-Cyclopentylaminoethyl)-phenanthridinium chloride; hydrochloride (13c).



To a suspension of BEP **10** (700 mg, 1.91 mmol, 1.0 eq) in DCM (40 mL) was added cyclopentylamine (188 μL , 1.91 mmol, 1.0 eq) and 5% Na₂CO₃ (20 mL). The reaction mixture was stirred for 2.5 hr under nitrogen before transferring to a separating funnel. Phases were separated and the organic phase was washed with water (1 \times 10 mL) then extracted into 1N HCl (2 \times 20 mL). The acidic extract was concentrated under vacuum and the residue triturated with acetone to afford a pale yellow powder as the product (647 mg, 1.78 mmol, 93.2%): mp 255-257 $^{\circ}\text{C}$; ^1H NMR (D₂O, 400 MHz) δ 9.89 (s, 1H), 8.88 (d, 1H, $J=8.2$ Hz), 8.79 (d, 1H, $J=8.2$ Hz), 8.39 (d, 1H, $J=8.2$ Hz), 8.25 (m, 2H), 8.06-7.93 (m, 3H), 5.37 (t, 2H, $J=6.8$ Hz), 3.73 (t, 2H, $J=6.8$ Hz), 3.53 (p, 1H, $J=7.1$ Hz), 1.96 (m, 2H), 1.54 (m, 6H); ^{13}C NMR (D₂O, 100 MHz) δ 155.3 (CH), 138.9 (CH), 135.0 (C), 132.7 (CH), 132.5 (CH), 132.2 (C), 130.6 (CH), 130.4 (CH), 126.0 (C), 124.7 (CH), 123.1 (C),

122.5 (CH), 118.2 (CH), 60.4 (CH), 53.5 (CH₂), 44.0 (CH₂), 29.0 (2×CH₂), 23.4 (2×CH₂); IR (KBr, cm⁻¹) 3405 (m), 2960 (m), 2646 (m), 2438 (w), 1627 (s), 1581 (m), 1535 (m), 1453 (m), 1348 (w), 920 (w), 760 (s), 611 (w), 493 (w); MS (FAB) 291.0 (M⁺) (100), 180.1 (22); HRMS (FAB) for (C₂₀H₂₃N₂)⁺ calcd 291.1861, obsd 291.1864.

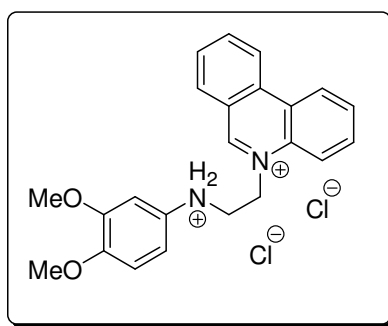
9.11.42 5-(2-(4-Methoxyphenyl)-aminoethyl)-phenanthridinium chloride; hydrochloride (13h).



To a suspension of BEP **10** (700 mg, 1.91 mmol, 1.0 eq) in CHCl₃ (50 mL) was added *p*-anisidine (235 mg, 1.91 mmol, 1.0 eq) and TEA (798 μL, 5.73 mmol, 3.0 eq). The resultant suspension was stirred under a nitrogen atmosphere for 20 min. The reaction mixture was transferred to a separating funnel and washed with water (2×20 mL) and 5% Na₂CO₃ (aq) (2×20 mL). The organic phase was then dried over MgSO₄ and the solvent was removed under vacuum to give an off-white powder. The dry residue was dissolved in DCM (50 mL) and extracted into 0.1 M HCl (2×20 mL). The aqueous extracts were combined and concentrated under vacuum to give an orange oil which was vitrified by addition of acetone. The product was collected by filtration, dried under vacuum and collected as pale peach powder (626 mg, 1.56 mmol, 81.7 %): mp 205-207 °C (MeOH-Et₂O); ¹H NMR (CD₃OD, 400 MHz) δ 10.20 (s, 1H), 9.19 (d, 1H, *J*=7.8 Hz), 9.12 (d, 1H, *J*=7.8 Hz), 8.69 (d, 1H, *J*=7.8 Hz), 8.59 (d, 1H, *J*=7.8 Hz), 8.46 (t, 1H, *J*=7.8 Hz), 8.24 (t, 1H, *J*=7.8 Hz), 8.19 (t, 1H, *J*=7.8 Hz), 8.15 (t, 1H, *J*=7.8 Hz), 7.32 (d, 2H, *J*=8.9 Hz), 6.91 (d, 2H, *J*=8.9 Hz), 5.65 (t, 2H, *J*=6.3 Hz), 4.21 (t, 2H, *J*=6.3 Hz), 3.76 (s, 3H); ¹³C NMR (DMSO, 100 MHz) δ 157.0 (CH), 138.2 (CH), 134.6 (C), 133.2 (C), 133.0 (CH), 132.1 (CH), 130.3 (CH), 130.2 (CH), 126.0 (C), 125.1 (CH), 123.6 (C), 123.1 (CH), 119.9 (CH),

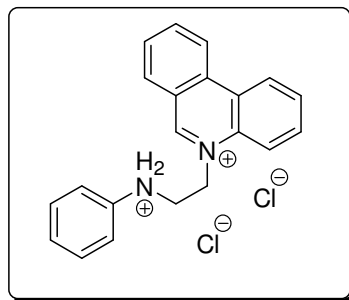
114.8 (CH), 55.4 (CH₃), 54.2 (CH₂), 47.2 (CH₂); IR (cm⁻¹) 2999 (w), 2588 (w), 2314 (w), 1630 (w), 1535 (w), 1514 (s), 1450 (m), 1259 (m), 1022 (m), 769 (s); MS (FAB) *m/z* (%) 329.2 (M⁺) (100), 193.6 (10), 180.8 (15); HRMS (FAB) for (C₂₂H₂₁N₂O)⁺ calcd 329.1654, obsd 329.1659.

9.11.43 5-(2-(3,4-Dimethoxyphenyl)-aminoethyl)-phenanthridinium chloride; hydrochloride (13i).



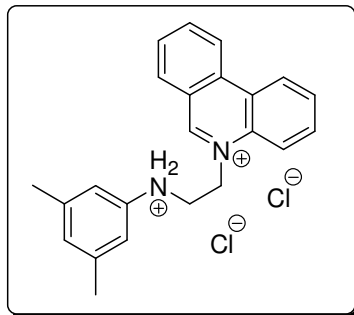
To a suspension of 1-(3,4-dimethoxyphenyl)-1,2,3,12b-tetrahydroimidazo[1,2-*f*]phenanthridine (100 mg, 0.32 mmol) in MeOH (4 mL) was added conc. HCl (4 drops) and the resultant solution was stirred for 5 min. The solution was then concentrated under vacuum to give an orange oil which was vitrified by addition of acetone. The product was collected by filtration and dried under vacuum and collected as pale yellow powder (61 mg, 0.14 mmol, 50.0 %): mp 187-189 °C (MeOH-Et₂O); ¹H NMR (DMSO, 400 MHz) δ 10.23 (s, 1H), 9.22 (d, 1H, *J*=8.0 Hz), 9.15 (d, 1H, *J*=8.0 Hz), 8.75 (d, 1H, *J*=8.0 Hz), 8.53 (d, 1H, *J*=8.0 Hz), 8.42 (t, 1H, *J*=8.0 Hz), 8.14 (m, 3H), 6.67 (d, 1H, *J*=8.0 Hz), 6.38 (brd, 1H), 6.32 (brd, 1H), 5.37 (t, 2H, *J*=5.8 Hz), 3.86 (t, 2H, *J*=5.8 Hz); ¹³C NMR (DMSO, 100 MHz) δ 156.6 (CH), 149.5 (C), 138.1 (CH), 134.5 (C), 133.2 (C), 132.9 (CH), 132.1 (CH), 130.33 (CH), 130.25 (CH), 125.9 (C), 125.1 (CH), 123.4 (C), 123.1 (CH), 119.9 (CH), 113.1 (CH), 56.1 (CH₃), 55.7 (CH₂), 55.3 (CH₃), 46.4 (CH₂); IR (KBr, cm⁻¹) 3433 (m), 3005 (w), 2590 (w), 2214 (w), 1626 (s), 1515 (s), 1448 (m), 1263 (m), 1018 (m), 758 (s); MS (FAB) *m/z* (%) 359.4 (M⁺) (100), 193.7 (13), 180.8 (34); HRMS (FAB) for (C₂₃H₂₃N₂O₂)⁺ calcd 359.1760, obsd 359.1767.

9.11.44 5-(2-Phenylaminoethyl)-phenanthridinium chloride; hydrochloride (13j).



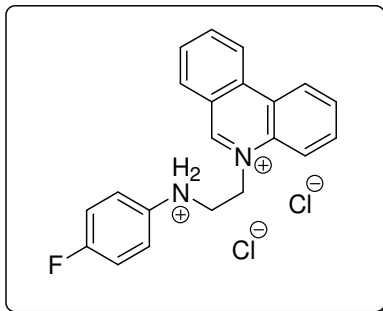
1-phenyl-1,2,3,12b-tetrahydroimidazo[1,2-*f*]phenanthridine (200 mg, 0.671 mmol, 1.0 eq) was dissolved in chloroform (6 mL), conc. HCl (3-5 drops) was added and the reaction stirred at room temperature for 30 min. The reaction mixture was diluted with water (10 mL). Layers were then separated and the organic layer further extracted with water (2 × 10 mL). The combined aqueous extracts were concentrated under vacuum to give an orange oil. Addition of acetone crystallized out a pale yellow solid product which was collected by filtration (224 mg, 0.603 mmol, 90.0%): mp 212-214 °C; ¹H NMR (D₂O, 400 MHz) δ 9.42 (s, 1H), 8.74 (d, 1H, *J*=7.8 Hz), 8.63 (d, 1H, *J*=7.8 Hz), 8.33 (d, 1H, *J*=7.8 Hz), 8.13 (t, 1H, *J*=7.8 Hz), 8.09 (d, 1H, *J*=7.8 Hz), 8.01 (t, 1H, *J*=7.8 Hz), 7.93 (t, 1H, *J*=7.8 Hz), 7.81 (t, 1H, *J*=7.8 Hz), 6.72 (t, 2H, *J*=7.6 Hz), 6.36 (t, 1H, *J*=7.6 Hz), 6.32 (d, 2H, *J*=7.6 Hz), 5.15 (t, 2H, *J*=5.3 Hz), 3.86 (t, 2H, *J*=5.3 Hz); ¹³C NMR (DMSO, 100 MHz) δ 156.0 (CH), 138.0 (CH), 134.4 (C), 133.2 (C), 132.8 (CH), 132.0 (CH), 130.4 (CH), 130.3 (CH), 129.1 (CH), 125.9 (C), 125.1 (CH), 123.4 (C), 123.1 (CH), 119.9 (CH), 113.0 (CH), 58.8 (CH₂), 42.2 (CH₂); IR (KBr, cm⁻¹) 3406 (m), 3066 (w), 2579 (m), 2336 (m), 1626 (s), 1446 (m), 761 (s); MS (FAB) *m/z* (%) 299.3 (M⁺) (64), 232.3 (17), 179.7 (15), 158.0 (64), 81.1 (100); HRMS (FAB) for (C₂₁H₁₉N₂)⁺ calcd 299.1548, obsd 299.1547.

9.11.45 5-(2-(3,5-Dimethylphenyl)-aminoethyl)-phenanthridinium chloride; hydrochloride (13k).



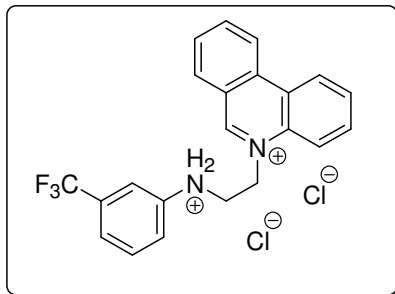
To a suspension of BEP **10** (700 mg, 1.91 mmol, 1.0 eq) in CHCl_3 (40 mL) was added 3,5-dimethylaniline (238 μL , 1.91 mmol, 1.0 eq) and TEA (798 μL , 5.73 mmol, 3.0 eq). The resultant suspension was stirred under a nitrogen atmosphere for 40 min. The reaction mixture was transferred to a separating funnel and washed with water (2 \times 20 mL) and 5% Na_2CO_3 (aq) (2 \times 20 mL). The organic phase was then dried over MgSO_4 and the solvent removed under vacuum to give an off-white powder. The dry residue was dissolved in DCM (30 mL) and extracted into 1.0 M HCl (2 \times 20 mL). The aqueous extracts were combined and concentrated under vacuum to give a mobile yellow oil which was vitrified by addition of acetone. The product was collected by filtration under a flow of nitrogen due to the hygroscopic nature of the product, which was then dried under vacuum and collected as pale orange powder (620 mg, 1.55 mmol, 81.3 %): mp 207-209 $^\circ\text{C}$ (MeOH-Et₂O); ^1H NMR (D_2O , 400 MHz) δ 9.45 (s, 1H), 8.76 (d, 1H, $J=7.8$ Hz), 8.62 (d, 1H, $J=7.8$ Hz), 8.34 (d, 1H, $J=7.8$ Hz), 8.16 (t, 1H, $J=7.8$ Hz), 8.05 (m, 2H), 7.97 (t, 1H, $J=7.8$ Hz), 7.83 (t, 1H, $J=7.8$ Hz), 5.84 (s, 2H), 5.73 (s, 1H), 5.23 (t, 2H, $J=4.8$ Hz), 3.95 (t, 2H, $J=4.8$ Hz), 1.51 (s, 6H); ^{13}C NMR (D_2O , 100 MHz) δ 154.8 (CH), 140.4 (C), 139.4 (CH), 134.7 (C), 132.7 (C), 132.6 (CH), 132.5 (CH), 131.7 (C), 130.8 (CH), 130.4 (CH), 125.7 (C), 124.9 (CH), 122.8 (C), 122.5 (CH), 118.7 (CH), 50.0 (CH_2), 44.2 (CH_2), 19.5 (2 \times CH_3); IR (cm^{-1}) 2336 (w), 1627 (w), 923 (w), 854 (w), 765 (s); MS (FAB) m/z (%) 327.3 (M^+) (100), 206.5 (8), 193.6 (20), 180.8 (34), 149.1 (18); HRMS (FAB) for $(\text{C}_{23}\text{H}_{24}\text{N}_2)^{2+}$ calcd 328.1939, obsd 328.1935.

9.11.46 5-(2-(4-Fluorophenyl)-aminoethyl)-phenanthridinium chloride; hydrochloride (13n).



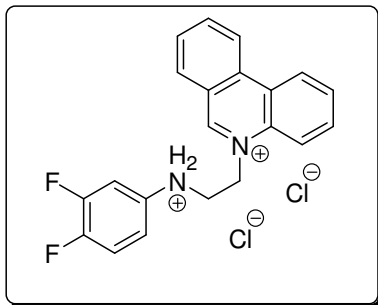
A solution of 1-(4-fluorophenyl)-1,2,3,12b-tetrahydroimidazo[1,2-*f*]phenanthridine (100 mg, 0.32 mmol) in DCM (30 mL) was extracted with 1.0 M HCl (2×20 mL). The aqueous extracts were combined and concentrated under vacuum to give a yellow oil which was vitrified by addition of acetone. The product was collected by filtration, dried under vacuum, and collected as pale yellow powder (108 mg, 0.28 mmol, 86.7 %): mp 220-222 °C (MeOH-Et₂O); ¹H NMR (D₂O, 400 MHz) δ 9.61 (s, 1H), 8.68 (d, 1H, *J*=8.0 Hz), 8.60 (d, 1H, *J*=8.0 Hz), 8.20 (d, 1H, *J*=8.0 Hz), 8.15 (m, 2H), 7.96 (t, 1H, *J*=8.0 Hz), 7.86 (m, 2H), 7.03 (m, 2H), 6.72 (m, 2H), 5.38 (t, 2H, *J*=5.8 Hz), 4.13 (t, 2H, *J*=5.8 Hz); ¹³C NMR (D₂O, 100 MHz) δ 161.6 (d, *J*_{C-F}=246.0 Hz, C), 155.2 (CH), 139.1 (CH), 135.2 (C), 132.6 (CH), 132.5 (CH), 132.2 (C), 130.7 (CH), 130.5 (CH), 130.2 (C), 126.2 (C), 124.9 (CH), 123.2 (C), 123.1 (CH), 122.7 (CH), 118.6 (CH), 117.0 (d, *J*_{C-F}=23.0 Hz, CH), 54.2 (CH₂), 46.4 (CH₂); IR (KBr, cm⁻¹) 3439 (s), 3055 (w), 2563 (w), 2362 (w), 1625 (s), 1509 (s), 1233 (w), 759 (s); MS (FAB) *m/z* (%) 317 (M⁺) (14), 307 (28), 289 (18), 147 (91), 136 (100); HRMS (FAB) for (C₂₁H₁₈FN₂)⁺ calcd 317.1454, obsd 317.1450.

9.11.47 5-(2-(3-Trifluoromethylphenyl)-aminoethyl)-phenanthridinium chloride; hydrochloride (13p).



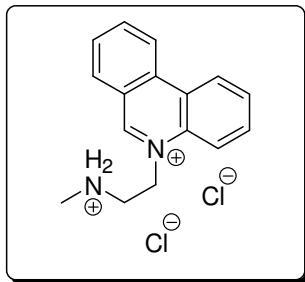
To a suspension of BEP **10** (700 mg, 1.91 mmol, 1.0 eq) in CHCl_3 (50 mL) was added TEA (798 μL , 5.73 mmol, 3.0 eq) and 3-(trifluoromethyl)aniline (239 μL , 1.91 mmol, 1.0 eq). The reaction was stirred under N_2 for 3.5 h. The reaction mixture was transferred to a separating funnel and the layers were separated, washing the organic layer further with H_2O (2 \times 20 mL) before drying over MgSO_4 . Solvent was then removed under vacuum to give a yellow oil, addition of MeOH (20 mL) precipitated a pale yellow solid which was collected by filtration. The Filter residue was resuspended in MeOH (10 mL) and acidified with conc. HCl (5 drops). The reaction was stirred for 5 min then solvent was removed under vacuum to give an orange oil, addition of acetone vitrified the oil to give a pale orange crystalline solid which was collected by filtration and dried under vacuum (404 mg, 0.92 mmol, 48.1 %): mp 203-205 $^\circ\text{C}$ (MeOH-Et $_2\text{O}$); ^1H NMR (CD_3OD , 400 MHz) δ 9.92 (s, 1H), 9.15 (d, 1H, $J=8.0$ Hz), 9.05 (d, 1H, $J=8.0$ Hz), 8.71 (d, 1H, $J=8.0$ Hz), 8.45 (d, 1H, $J=8.0$ Hz), 8.39 (t, 1H, $J=8.0$ Hz), 8.20 (m, 2H), 8.06 (t, 1H, $J=8.0$ Hz), 7.09 (t, 1H, $J=8.0$ Hz), 6.69 (d, 1H, $J=8.0$ Hz), 6.50 (s, 1H), 5.36 (t, 2H, $J=5.2$ Hz), 4.01 (t, 2H, $J=5.2$ Hz); ^{13}C NMR (CD_3OD , 100 MHz) δ 156.8 (CH), 149.1 (C), 139.6 (CH), 136.7 (C), 134.9 (C), 133.89 (CH), 133.56 (CH), 132.31 (C), 131.85 (CH), 131.6 (CH), 131.0 (CH), 128.0 (C), 126.9 (C), 126.4 (CH), 125.1 (C), 124.2 (CH), 120.5 (CH), 116.7 (CH), 114.6 (CH), 108.8 (CH), 59.4 (CH_2), 42.9 (CH_2); IR (KBr, cm^{-1}) 3262 (m), 3008 (m), 2268 (m), 1627 (s), 1534 (m), 1447 (s), 1326 (s), 1123 (s), 872 (m), 766 (s); MS (FAB) m/z (%) 367.3 (M^+) (100); HRMS (FAB) for $(\text{C}_{22}\text{H}_{18}\text{F}_3\text{N}_2)^+$ calcd 367.1422, obsd 367.1424.

9.11.48 5-(2-(3,4-Difluorophenyl)-aminoethyl)-phenanthridinium chloride; hydrochloride (13t).



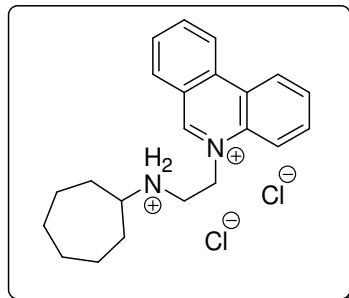
A solution of 1-(4-fluorophenyl)-1,2,3,12b-tetrahydroimidazo[1,2-f]phenanthridine (100 mg, 0.32 mmol) in DCM (30 mL) was extracted with 1.0 M HCl (2×20 mL). The aqueous extracts were combined and concentrated under vacuum to give a yellow oil which was vitrified by addition of acetone. The product was collected by filtration, dried under vacuum and collected as pale yellow powder (56 mg, 0.14 mmol, 45.8 %): mp 165-167 °C (MeOH-Et₂O); ¹H NMR (D₂O, 400 MHz) δ 8.81 (d, 1H, *J*=8.0 Hz), 8.70 (d, 1H, *J*=8.0 Hz), 8.35 (d, 1H, *J*=8.0 Hz), 8.18 (m, 2H), 8.02 (t, 1H, *J*=8.0 Hz), 7.96 (t, 1H, *J*=8.0 Hz), 7.86 (t, 1H, *J*=8.0 Hz), 8.66 (m, 1H), 6.20 (m, 1H), 6.13 (m, 1H), 5.22 (t, 2H, *J*=5.6 Hz), 3.88 (t, 2H, *J*=5.6 Hz); ¹³C NMR (DMSO, 100 MHz) δ 156.1 (CH), 150.0 (dd, *J*_{C-F}=242.0, 13.6 Hz, CF), 145.0 (d, *J*_{C-F}=13.6 Hz, CH), 141.3 (dd, *J*_{C-F}=242.0, 13.6 Hz, CF), 138.0 (CH), 134.4 (C), 133.1 (C), 132.8 (CH), 132.0 (CH), 130.4 (CH), 130.3 (CH), 125.9 (C), 125.0 (CH), 123.4 (C), 123.1 (CH), 119.9 (CH), 117.4 (d, *J*_{C-F}=, 13.6 Hz, CH), 108.3 (CH), 100.4 (d, *J*_{C-F}=, 13.6 Hz, CH), 56.78 (CH₂), 41.9 (CH₂); IR (KBr, cm⁻¹) 3432 (m), 3000 (m), 2568 (w), 2135 (w), 1629 (m), 1517 (s), 1452 (m), 1294 (m), 754 (s); MS (FAB) *m/z* (%) 335.3 (M⁺) (100), 307.4 (23), 155.2 (44), 137.4 (44); HRMS (FAB) for (C₂₁H₁₇F₂N₂)⁺ calcd 335.1360, obsd 335.1365.

9.11.49 **5-(2-Methylaminoethyl)-phenanthridinium** **chloride;**
hydrochloride (13b').



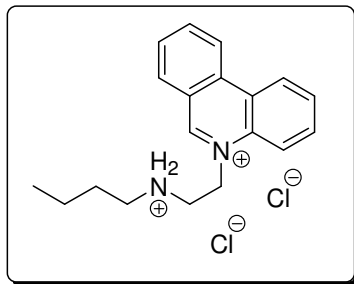
To a suspension of BEP **10** (500 mg, 1.36 mmol, 1.0 eq) in EtOAc (20 mL) was added methylamine hydrochloride (460 mg, 6.81 mmol, 5.0 eq) and 5% Na₂CO₃ (10 mL). The reaction mixture was stirred for 5 min at room temperature before transferring to a separating funnel. Phases were separated and the organic phase was washed with water (1 × 10 mL) then extracted into 1N HCl (1 × 10 mL). The acidic extract was concentrated under vacuum and the residue triturated with acetone to afford a white powder as the product (356 mg, 1.15 mmol, 84.7%): mp 254-255 °C; ¹H NMR (D₂O, 400 MHz) δ 9.91 (s, 1H), 8.90 (d, 1H, *J*=8.2 Hz), 8.81 (d, 1H, *J*=8.2 Hz), 8.40 (d, 1H, *J*=8.2 Hz), 8.29-8.24 (m, 2H), 7.99 (m, 3H), 5.40 (t, 2H, *J*=6.6 Hz), 3.76 (t, 2H, *J*=6.6 Hz), 2.69 (s, 3H); ¹³C NMR (D₂O, 100 MHz) δ 155.5 (CH), 139.1 (CH), 135.3 (C), 132.9 (CH), 132.6 (CH), 132.5 (C), 130.8 (CH), 130.6 (CH), 126.3 (C), 125.0 (CH), 123.3 (C), 122.7 (CH), 118.4 (CH), 53.5 (CH₂), 46.7 (CH₂), 33.5 (CH₃); IR (KBr, cm⁻¹) 3447 (m), 2999 (m), 2682 (m), 2406 (m), 1626 (s), 1534 (m), 1447 (m), 1345 (m), 1259 (m), 1154 (w), 1032 (m), 760 (s), 719 (m), 613 (w); MS (FAB) *m/z* (%) 237.4 (M⁺) (100), 206.6 (26), 180.8 (87), 60.4 (51); HRMS (FAB) for (C₁₆H₁₇N₂)⁺ calcd 237.1392, obsd 237.1391.

9.11.50 5-(2-Cycloheptylaminoethyl)-phenanthridinium chloride; hydrochloride (13c').

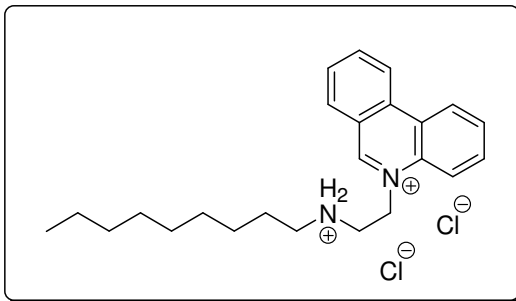


To a suspension of BEP **10** (700 mg, 1.91 mmol, 1.0 eq) in DCM (40 mL) was added cycloheptylamine (243 μ L, 1.91 mmol, 1.0 eq) and 5% Na_2CO_3 (20 mL). The reaction mixture was stirred for 2.5 hr under nitrogen before transferring to a separating funnel. Phases were separated and the organic phase was washed with water (1 \times 10 mL) then extracted into 1N HCl (2 \times 20 mL). The acidic extract was concentrated under vacuum and the residue triturated with acetone to afford a pale yellow powder as the product (740 mg, 1.89 mmol, 99.0%): mp 254-255 $^\circ\text{C}$; ^1H NMR (D_2O , 400 MHz) δ 9.74 (s, 1H), 8.53 (d, 1H, $J=8.4$ Hz), 8.43 (d, 1H, $J=8.4$ Hz), 8.21 (d, 1H, $J=8.4$ Hz), 8.12 (d, 1H, $J=8.4$ Hz), 8.03 (t, 1H, $J=8.4$ Hz), 7.89 (t, 1H, $J=8.4$ Hz), 7.78 (m, 2H), 5.21 (t, 2H, $J=6.8$ Hz), 3.60 (t, 2H, $J=6.8$ Hz), 3.19 (m, 1H), 1.85 (m, 2H), 1.45 (m, 4H), 1.28 (m, 6H); ^{13}C NMR (D_2O , 100 MHz) δ 155.4 (CH), 138.9 (CH), 135.1 (C), 132.7 (CH), 132.5 (CH), 132.3 (C), 130.6 (CH), 130.47 (CH), 126.05 (C), 124.81 (CH), 123.18 (C), 122.5 (CH), 118.3 (CH), 60.7 (CH), 53.5 (CH_2), 42.6 (CH_2), 30.2 ($2\times\text{CH}_2$), 27.1 ($2\times\text{CH}_2$), 23.0 ($2\times\text{CH}_2$); IR (KBr, cm^{-1}) 3397 (m), 2928 (m), 2857 (m), 2694 (m), 2455 (m), 1627 (s), 1579 (m), 1534 (m), 1448 (m), 1347 (m), 1261 (m), 1032 (m), 920 (m), 762 (s), 721 (m), 610 (m), 494 (m); MS (FAB) m/z (%) 319 (M^+) (59), 307 (27), 289 (23), 180 (8), 154 (100), 136 (75); HRMS (FAB) for $(\text{C}_{22}\text{H}_{27}\text{N}_2)^+$ calcd 319.2174, obsd 319.2176.

9.11.51 5-(2-Butylaminoethyl)-phenanthridinium chloride; hydrochloride (13d').

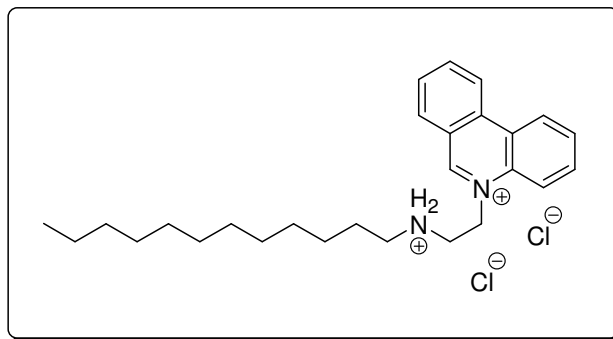


To a suspension of BEP **10** (700 mg, 1.91 mmol, 1.0 eq) in DCM (40 mL) was added cyclopentylamine (189 μ L, 1.91 mmol, 1.0 eq) and 5% Na_2CO_3 (20 mL). The reaction mixture was stirred for 2.5 hr under nitrogen before transferring to a separating funnel. Phases were separated and the organic phase was washed with water (1×10 mL) then extracted into 1N HCl (2×20 mL). The acidic extract was concentrated under vacuum and the residue triturated with acetone to afford a pale yellow powder as the product (579 mg, 1.65 mmol, 86.4%): mp 223-224 $^\circ\text{C}$; ^1H NMR (D_2O , 400 MHz) δ 9.87 (s, 1H), 8.68 (d, 1H, $J=8.4$ Hz), 8.59 (d, 1H, $J=8.4$ Hz), 8.35 (d, 1H, $J=8.4$ Hz), 8.23 (d, 1H, $J=8.4$ Hz), 8.18 (t, 1H, $J=8.4$ Hz), 8.03 (t, 1H, $J=8.4$ Hz), 7.92 (m, 2H), 5.36 (t, 2H, $J=6.6$ Hz), 3.74 (t, 2H, $J=6.6$ Hz), 3.05 (t, 2H, $J=7.4$ Hz), 1.58 (p, 1H, $J=7.4$ Hz), 1.29 (sext, 2H, $J=7.4$ Hz), 0.81 (t, 3H, $J=7.4$ Hz); ^{13}C NMR (D_2O , 100 MHz) δ 155.5 (CH), 139.1 (CH), 135.2 (C), 132.8 (CH), 132.6 (CH), 132.5 (C), 130.7 (CH), 130.6 (CH), 126.2 (C), 124.9 (CH), 123.3 (C), 122.7 (CH), 118.4 (CH), 53.5 (CH_2), 48.3 (CH_2), 45.2 (CH_2), 27.4 (CH_2), 19.1 (CH_2), 12.7 (CH_3); IR (KBr, cm^{-1}) 3375 (m), 2963 (s), 2702 (m), 2409 (m), 2359 (m), 1628 (s), 1535 (m), 1459 (s), 1262 (m), 1155 (m), 1040 (m), 761 (s), 720 (m); MS (FAB) m/z (%) 279 (M^+) (100), 180 (24), 154 (37), 136 (32); HRMS (FAB) for $(\text{C}_{19}\text{H}_{23}\text{N}_2)^+$ calcd 279.1861, obsd 279.1858.

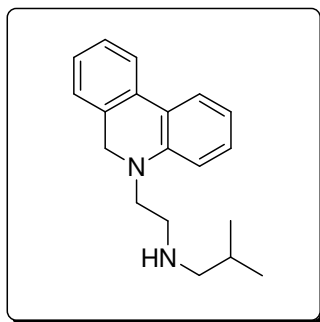
9.11.52 5-(2-Nonylaminoethyl)-phenanthridinium chloride; hydrochloride (13e').

To a suspension of BEP **10** (700 mg, 1.91 mmol, 1.0 eq) in DCM (40 mL) was added cyclopentylamine (350 μ L, 1.91 mmol, 1.0 eq) and 5% Na_2CO_3 (20 mL). The reaction mixture was stirred for 2.5 hr under nitrogen before transferring to a separating funnel. Phases were separated and the organic phase was washed with water (1 \times 10 mL) then extracted into 1N HCl (2 \times 20 mL). The acidic extract was concentrated under vacuum and the residue triturated with acetone to afford a pale yellow powder as the product (511 mg, 1.21 mmol, 63.5%): mp 213-215 $^\circ\text{C}$; ^1H NMR (D_2O , 400 MHz) δ 9.88 (s, 1H), 8.81 (d, 1H, $J=8.2$ Hz), 8.72 (d, 1H, $J=8.2$ Hz), 8.35 (d, 1H, $J=8.2$ Hz), 8.23 (d, 1H, $J=8.2$ Hz), 8.20 (t, 1H, $J=8.2$ Hz), 8.00 (t, 1H, $J=8.2$ Hz), 7.93 (t, 1H, $J=8.2$ Hz), 7.90 (t, 1H, $J=8.2$ Hz), 5.34 (t, 2H, $J=6.7$ Hz), 3.70 (t, 2H, $J=6.7$ Hz), 2.95 (t, 2H, $J=7.7$ Hz), 1.51 (q, 2H, $J=7.7$ Hz), 1.10 (m, 12H), 0.67 (t, 3H, $J=6.7$ Hz); ^{13}C NMR (D_2O , 100 MHz) δ 156.2 (CH), 139.9 (CH), 136.2 (C), 133.6 (CH), 133.3 (CH), 131.5 (CH), 131.3 (CH), 127.2 (C), 125.8 (CH), 124.2 (C), 123.5 (CH), 119.0 (CH), 54.1 (CH_2), 49.2 (CH_2), 45.8 (CH_2), 31.5 (CH_2), 28.8 (CH_2), 28.7 (CH_2), 28.5 (CH_2), 26.0 (CH_2), 25.8 (CH_2), 22.4 (CH_2), 13.8 (CH_3); IR (KBr, cm^{-1}) 3409 (s), 2924 (s), 2853 (s), 2727 (m), 2399 (w), 1626 (s), 1536 (m), 1458 (s), 1348 (m), 1263 (m), 1150 (w), 1032 (m), 758 (s), 720 (m), 611 (m), 493 (w); MS (FAB) m/z (%) 349.6 (M^+) (100), 180.0 (18), 171.1 (17); HRMS (FAB) for $(\text{C}_{24}\text{H}_{33}\text{N}_2)^+$ calcd 349.2644, obsd 349.2642.

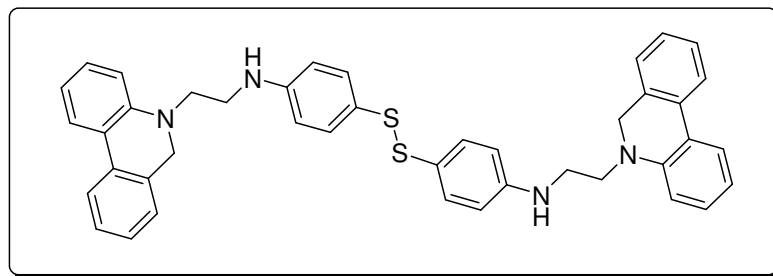
9.11.53 5-(2-Dodecylaminoethyl)-phenanthridinium chloride; hydrochloride (13j').



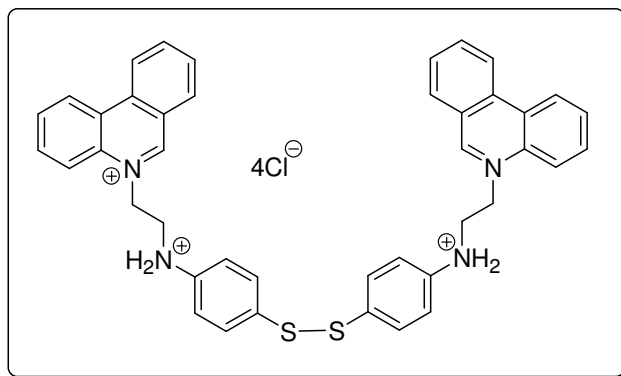
To a suspension of BEP **10** (700 mg, 1.91 mmol, 1.0 eq) in DCM (40 mL) was added cyclopentylamine (354 mg, 1.91 mmol, 1.0 eq) and 5% Na₂CO₃ (20 mL). The reaction mixture was stirred for 4 hr under nitrogen before transferring to a separating funnel. Phases were separated and the organic phase was washed with water (1 × 10 mL). Addition of 1N HCl (40 mL) gave an emulsion which was concentrated under vacuum and the residue triturated with acetone to afford a pale peach powder as the product (742 mg, 1.60 mmol, 83.8%): mp 212-213 °C; ¹H NMR (D₄-Methanol, 400 MHz) δ 9.87 (s, 1H), 8.56 (d, 1H, *J*=8.2 Hz), 8.49 (d, 1H, *J*=8.2 Hz), 8.14 (d, 1H, *J*=8.2 Hz), 8.06 (d, 1H, *J*=8.2 Hz), 7.83 (t, 1H, *J*=8.2 Hz), 7.62 (t, 1H, *J*=8.2 Hz), 7.55 (t, 1H, *J*=8.2 Hz), 7.52 (t, 1H, *J*=8.2 Hz), 5.06 (t, 2H, *J*=6.7 Hz), 3.30 (t, 2H, *J*=6.7 Hz), 2.72 (m, 1H), 2.55 (t, 2H, *J*=7.7 Hz), 1.94 (p, 2H, *J*=7.7 Hz), 0.74 (m, 18H), 0.30 (t, 3H, *J*=7.7 Hz); ¹³C NMR (D₄-Methanol, 100 MHz) δ 156.3 (CH), 138.4 (CH), 135.4 (C), 133.0 (C), 132.8 (CH), 132.2 (CH), 130.2 (CH), 130.0 (CH), 126.3 (C), 124.7 (CH), 123.7 (C), 122.6 (CH), 118.9 (CH), 53.2 (CH₂), 48.2 (CH₂), 45.2 (CH₂), 31.3 (CH₂), 29.0 (CH₂), 28.9 (CH₂), 28.8 (CH₂), 28.5 (CH₂), 25.8 (CH₂), 25.6 (CH₂), 22.0 (CH₂), 12.8 (CH₃); IR (KBr, cm⁻¹) 3433 (m), 2921 (s), 2848 (m), 2671 (w), 2413 (w), 1629 (m), 1454 (m), 1363 (w), 764 (m), 722 (w); MS (FAB) *m/z* (%) 391.4 (M⁺) (100), 212.7 (27), 180.8 (30); HRMS (FAB) for (C₂₇H₃₉N₂)⁺ calcd 391.3113, obsd 391.3111.

9.11.54 5-(2-Isobutylaminoethyl)-6H-phenanthridine (14b).

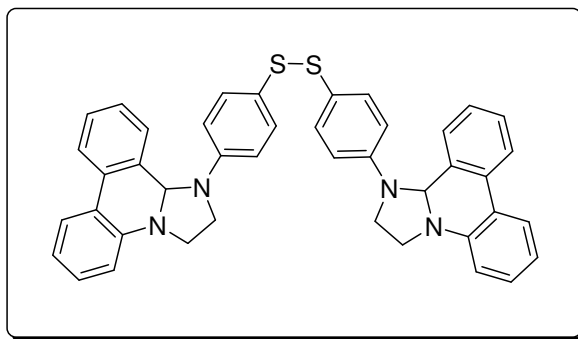
In an NMR tube, 5-(2-isobutylaminoethyl)-phenanthridinium chloride; hydrochloride (30 mg, 0.085 mmol, 1.0 eq) was dissolved in D₂O (1 mL). CDCl₃ (1 mL) was then added followed by sodium cyanoborohydride (6.4 mg, 0.102 mmol, 1.2 eq) and the reaction shaken until a biphasic solution formed. The aqueous phase was removed and the organic layer was washed with a 5% Na₂CO₃ in D₂O solution (2 × 1 mL). The organic layer was concentrated under vacuum to give the product as a yellow oil (20 mg, 0.713 mmol, 71.3%): ¹H NMR (DMSO, 400 MHz) δ 7.74 (d, 1H, *J*=8.0 Hz), 7.73 (d, 1H, *J*=8.0 Hz), 7.30 (t, 1H, *J*=8.0 Hz), 7.23 (t, 1H, *J*=8.0 Hz), 7.18 (m, 2H), 6.83 (d, 1H, *J*=8.0 Hz), 7.75 (t, 1H, *J*=8.0 Hz), 4.32 (s, 2H), 3.38 (t, 2H, *J*=8.0 Hz), 2.76 (t, 2H, *J*=8.0 Hz), 2.37 (d, 2H, *J*=7.6 Hz), 1.65 (sept, 1H, *J*=6.8 Hz), 0.87 (d, 6H, *J*=6.8 Hz); ¹³C NMR (DMSO, 100 MHz) δ 146.0 (C), 132.6 (C), 131.6 (C), 129.1 (C), 128.1 (CH), 127.5 (CH), 126.9 (CH), 125.7 (CH), 123.6 (CH), 122.1 (CH), 117.4 (CH), 112.3 (CH), 57.7 (CH₂), 51.9 (CH₂), 50.1 (CH₂), 45.2 (CH₂), 28.0 (CH), 20.8 (2×CH₃); IR (KBr, cm⁻¹) 3424 (w), 3067 (w), 2954 (m), 2352 (w), 2251 (w), 1602 (m), 1496 (s), 1444 (s), 1289 (w), 1103 (w), 749 (s); MS (EI) *m/z* (%) 280.2 (M⁺) (31), 235.1 (79), 194.0 (100), 180.0 (63), 165.1 (41), 152.0 (19), 86.1 (32); HRMS (EI) for C₁₉H₂₄N₂ calcd 280.1939, obsd 280.1936.

9.11.55 AEDP disulfide (15)

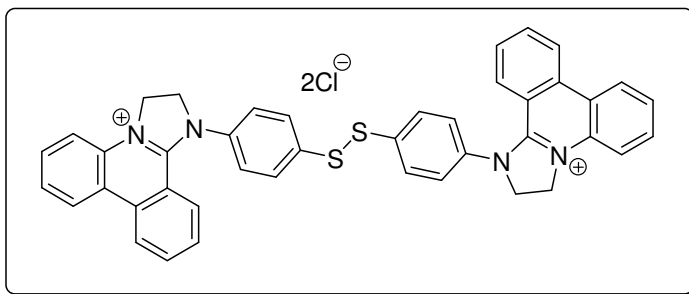
To a solution of AEP disulfide (220 mg, 0.27 mmol, 1.0 eq) in MeOH (25 mL) was added NaBH₄ (82 mg, 2.18 mmol, 8.0 eq). The reaction was stirred at room temperature for 5 h. A 5% Na₂CO₃ (aq) solution (10 mL) was added to the reaction mixture and the precipitated product was collected by filtration. The dried product was a pale beige powder (127 mg, 0.19 mmol, 70.1%): mp > 160°C (degrad); ¹H NMR (CDCl₃, 400 MHz) δ 7.77 (m, 2H), δ 7.37 (m, 2H), δ 7.25 (m, 3H), δ 7.13 (d, 1H, *J*=8.0 Hz), δ 6.92 (t, 1H, *J*=8.0 Hz), δ 6.84 (d, 1H, *J*=8.0 Hz), δ 6.54 (d, 2H, *J*=8.0 Hz), δ 4.29 (s, 2H), δ 4.11 (s, 1H), δ 3.58 (t, 2H, *J*=6.0 Hz), δ 3.47 (t, 2H, *J*=6.0 Hz); ¹³C NMR (CDCl₃, 100 MHz) δ 148.5 (C), 145.9 (C), 134.4 (CH), 132.7 (C), 132.1 (C), 129.2 (CH), 127.9 (CH), 127.2 (CH), 125.7 (CH), 124.1 (CH), 123.6 (C), 122.6 (CH), 118.9 (CH), 113.33 (C), 113.30 (CH), 112.6 (CH), 52.9 (CH₂), 49.5 (CH₂), 40.3 (CH₂); IR (cm⁻¹) 3304 (w), 1592 (m), 1444 (s), 868 (m), 749 (s); MS (FAB) *m/z* (%) 329.0 (42), 307.0 (18), 289.0 (10), 176.7 (100); Anal. Calcd for C₄₂H₃₈N₄S₂ C, 76.10; H, 5.78; N, 8.45; Found C, 73.27; H, 5.74; N, 8.45.

9.11.56 AEP disulfide (16).

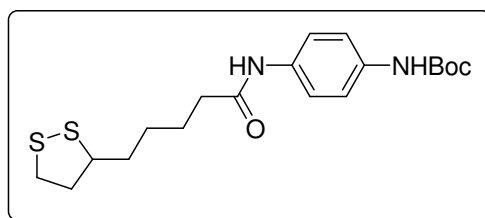
To a suspension of TIP disulfide (200 mg, 0.304 mmol, 1.0 eq) in MeOH (20 mL) was added HCl conc. (1.0 mL) and the reaction stirred for 20 min. Solvents were removed under vacuum and the oily residue was vitrified with acetone. The product was collected by filtration to give an orange powder (221 mg, 0.275 mmol, 90.3%, hygroscopic): mp 193-197 °C; ^1H NMR (CD_3OD , 400 MHz) δ 9.97 (s, 1H), 8.84 (d, 1H, $J=8.0$ Hz), 8.71 (d, 1H, $J=8.0$ Hz), 8.62 (d, 1H, $J=8.0$ Hz), 8.35 (d, 1H, $J=8.0$ Hz), 8.18 (t, 1H, $J=8.0$ Hz), 8.12 (t, 1H, $J=8.0$ Hz), 8.02 (t, 1H, $J=8.0$ Hz), 7.89 (t, 1H, $J=8.0$ Hz), 6.76 (d, 2H, $J=8.4$ Hz), 6.38 (d, 2H, $J=8.4$ Hz), 5.36 (brd, 2H), 3.93 (brd, 2H); ^{13}C NMR (CD_3OD , 100 MHz) δ 156.8 (CH), 147.7 (C), 139.6 (CH), 136.3 (C), 134.6 (C), 134.0 (CH), 133.8 (2 \times CH), 133.7 (CH), 131.8 (CH), 131.5 (CH), 127.6 (C), 126.8 (C), 126.2 (CH), 124.8 (C), 124.1 (CH), 120.6 (CH), 114.9 (2 \times CH), 58.7 (CH_2), 43.7 (CH_2); IR (cm^{-1}) 3337 (m), 3017 (w), 1626 (m), 1590 (m), 1449 (m), 1259 (m), 1015 (m), 821 (m), 757 (s), 719 (m); MS (FAB) m/z (%) 659.9 (M^+) (49), 331.1 ($\text{M}^{2+}/2$) (100), 181.7 (86); HRMS (FAB) for $\text{C}_{21}\text{H}_{19}\text{N}_2\text{S}$ calcd 331.1269, obsd 331.1263.

9.11.57 TIP disulfide (17).

To a solution of 4-aminophenyl disulfide (236 mg, 0.96 mmol, 1.0 eq) and TEA (798 μ L, 5.73 mmol, 3.0 eq) in MeCN (25 mL) was added BEP **10** (1.91 mmol, 2.0 eq). The resultant suspension was stirred under a nitrogen atmosphere for 5 h at room temperature. The reaction mixture was filtered, washing the residue with a little MeOH. After drying under vacuum the product was obtained as a dirty yellow powder (550 mg, 0.83 mmol, 87.4%): mp 190-192 $^{\circ}$ C; 1 H NMR (CDCl_3 , 400 MHz) δ 7.87 (d, 2H, $J=8.0$ Hz), 7.78 (d, 2H, $J=8.0$ Hz), 7.42 (m, 6H), 7.34 (m, 2H), 7.26 (d, 2H, $J=8.0$ Hz), 7.14 (d, 2H, $J=8.0$ Hz), 7.05 (m, 2H), 6.83 (d, 2H, $J=8.0$ Hz), 6.68 (d, 4H, $J=8.0$ Hz), 5.32 (s, 2H), 4.07 (m, 2H), 3.89 (m, 2H), 3.67 (m, 2H), 3.39 (m, 2H); 13 C NMR (CDCl_3 , 100 MHz) δ 148.9 (C), 143.1 (C), 133.9 (C), 133.6 (CH), 132.9 (C), 131.9 (C), 129.2 (CH), 128.0 (CH), 127.2 (CH), 125.4 (C), 124.2 (CH), 123.8 (CH), 123.6 (CH), 120.2 (CH), 114.4 (CH), 113.2 (CH), 75.0 (CH), 50.7 (CH₂), 44.9 (CH₂); IR (KBr, cm^{-1}) 3384 (w), 3060 (w), 3030 (w), 2933 (w), 2883 (w), 2808 (w), 1587 (s), 1490 (s), 1446 (s), 1357 (s), 1232 (m), 1187 (m), 1087 (m), 1016 (m), 816 (s), 755 (s), 729 (s); MS (FAB) m/z (%) 659.1 (M+H)⁺ (35), 329.1 (100), 193.6 (52), 180.7 (67); HRMS (FAB) for (C₄₂H₃₅N₄S₂)⁺ calcd 659.2303, obsd 659.2299.

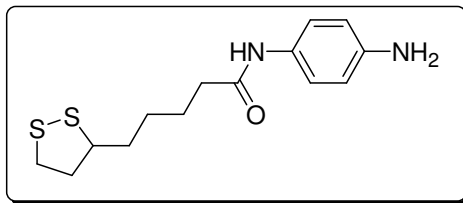
9.11.58 DIP disulfide (18).

NH_4Cl (100 mg, 1.87 mmol, 12.3 eq) was added to a suspension of TIP disulfide (100 mg, 0.152 mmol, 1.0 eq) in DMSO (2 mL) and the reaction was heated to boiling for ~ 2min. The reaction was allowed to cool before acetone was added to precipitate the product. The crude product was collected by filtration. The crude residue was triturated with water and dried under vacuum to give a pale brown powder (98 mg, 0.134 mmol, 88.5%): mp > 250°C (degrad); ^1H NMR (DMSO, 400 MHz) δ 8.93 (d, 1H, J=8.0 Hz), 8.84 (d, 1H, J=8.0 Hz), 8.03 (t, 1H, J=8.0 Hz), 7.94 (t, 1H, J=8.0 Hz), 7.89 (d, 2H, J=8.4 Hz), 7.88 (m, 2H), 7.81 (d, 2H, J=8.4 Hz), 7.72 (m, 2H), 4.97 (t, 2H, J=10.6 Hz), 4.62 (t, 2H, J=10.6 Hz); ^{13}C NMR (DMSO, 100 MHz) δ 152.5 (C), 138.5 (C), 137.3 (C), 135.3 (CH), 135.1 (C), 132.5 (C), 131.6 (CH), 128.9 (2 \times CH), 128.7 (CH), 127.9 (2 \times CH), 130.0 (CH), 125.8 (CH), 124.4 (CH), 124.1 (CH), 120.4 (C), 116.3 (CH), 115.1 (C), 54.3 (CH_2), 47.1 (CH_2); IR (cm^{-1}) 3122 (m), 3029 (m), 2808 (m), 1577 (m), 1396 (s), 1311 (m), 1024 (w), 752 (m); MS (FAB) m/z (%) 655.9 (M^+) (12), 328.0 ($\text{M}^{2+}/2$) (67), 171.8 (100); HRMS (FAB) for $\text{C}_{21}\text{H}_{16}\text{N}_2\text{S}$ calcd 328.1034, obsd 328.1032.

9.11.59 [4-(5-[1,2]Dithiolan-3-yl)pentanoylamino)-phenyl]-carbamic acid tert-butyl ester (19).

To a solution of Lipoic acid (2.00 g, 9.69 mmol, 1.0 eq) and *N*-Boc-p-phenylenediamine (2.00 g, 9.69 mmol, 1.0 eq) in toluene (70 mL) was added p-Bromobenzoic acid (40 mg, 0.19 mmol, 0.02 eq). The reaction was refluxed through a Soxhlet condenser containing 3Å molecular sieves for 44 hrs. Solvent was removed under vacuum to give a grey powder as the crude product. Purification by flash column chromatography afforded the pure product as a beige powder (2.91 g, 7.34 mmol, 75.8%): mp 177-179 °C; Rf = 0.38 in 3:2 PE/EtOAc; ¹H NMR (CDCl₃, 400 MHz) δ 7.46 (d, 2H, *J*=8.2 Hz), 7.34 (d, 2H, *J*=8.2 Hz), 7.07 (s, 1H), 6.45 (s, 1H), 3.62 (m, 1H), 3.19 (m, 2H), 2.50 (m, 1H), 2.38 (m, 2H), 1.96 (m, 1H), 1.79 (m, 4H), 1.58 (m, 2H), 1.54 (s, 9H); ¹³C NMR (CDCl₃, 100 MHz) δ 170.9 (C), 152.9 (C), 134.7 (C), 133.2 (C), 120.8 (CH), 119.2 (CH), 56.4 (CH), 40.3 (CH₂), 38.5 (CH₂), 37.3 (CH₂), 34.7 (CH₂), 28.9 (CH₂), 28.4 (3×CH₃), 25.3 (CH₂); IR (KBr, cm⁻¹) 3331 (s), 2923 (m), 1694 (s), 1660 (s), 1539 (s), 1520 (s), 1404 (s), 1310 (m), 1245 (m), 1160 (s), 1058 (m), 834 (m); MS (CI) *m/z* (%) 397.4 (M+H)⁺ (8), 297.3 (14), 179.2 (32), 153 (31), 107.2 (19); Anal. Calcd for C₁₉H₂₈N₂O₃S₂ C, 57.54; H, 7.12; N, 7.06; Found C, 57.33; H, 7.06; N, 7.28; HRMS (CI) for (C₁₉H₂₉N₂O₃S₂)⁺ calcd 397.1620, obsd 397.1621.

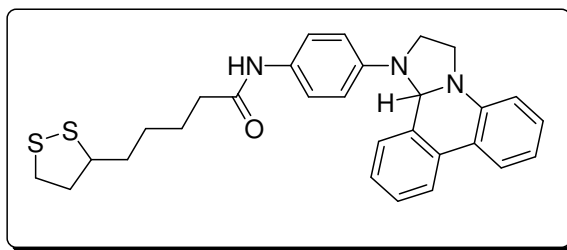
9.11.60 5-[1,2]Dithiolan-3-yl-pentanoic acid (4-amino-phenyl)-amide (20).



To a solution of [4-(5-[1,2]Dithiolan-3-yl-pentanoylamino)-phenyl]-carbamic acid tert-butyl ester (1.20 g, 4.04 mmol) in MeOH (150 mL) was added conc. HCl (10 mL) and the reaction was stirred at room temperature for 18 hrs. The reaction mixture was reduced to half volume and then partitioned between H₂O (200 mL) and Et₂O (200 mL). The layers were separated and the aqueous layer was washed with a further portion of Et₂O (100 mL). The aqueous layer was then neutralized by addition of solid NaHCO₃ and extracted into Et₂O (3 × 100 mL). The combined ether extracts were dried over MgSO₄ and concentrated under vacuum to give a brown oil (320 mg, 1.08 mmol, 35.6%): ¹H NMR (CDCl₃, 400

MHz) δ 7.29 (d, 2H, $J=8.0$ Hz), δ 7.09 (brd, 1H), δ 6.67 (d, 2H, $J=8.0$ Hz), δ 3.60 (m, 1H), δ 3.52 (brd, 2H), δ 3.17 (m, 2H), δ 2.49 (m, 1H), δ 2.35 (t, 2H, $J=7.4$ Hz), δ 1.94 (m, 1H), δ 1.77 (m, 4H), δ 1.42 (m, 2H); ^{13}C NMR (CDCl_3 , 100 MHz) δ 136.7 (C), 134.2 (C), 122.8 (CH), 119.4 (CH), 56.4 (CH), 40.3 (CH_2), 38.5 (CH_2), 37.3 (CH_2), 34.7 (CH_2), 28.9 (CH_2), 25.3 (CH_2); MS (EI+) m/z (%) 296.2 (M^+) (82), 150.1 (21), 108.1 (100).

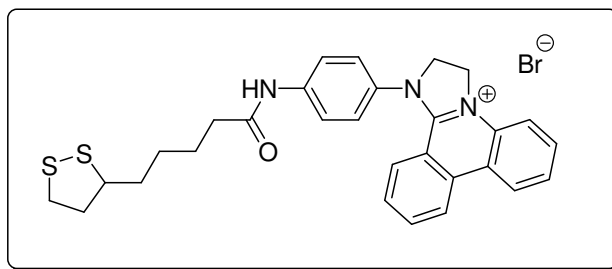
9.11.61 5-[1,2]Dithiolan-3-yl-pentanoic acid [4-(2,3-dihydro-12bH-imidazo[1,2-f]phenanthridin-1-yl)-phenyl]-amide (21).



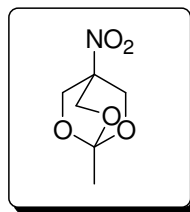
To a solution of 5-[1,2]Dithiolan-3-yl-pentanoic acid (4-amino-phenyl)-amide (320 mg, 1.08 mmol, 1.0 eq) and TEA (452 μL , 5.73 mmol, 3.0 eq) in CHCl_3 (30 mL) was added 5-(2-Bromo-ethyl)-phenanthridinium bromide (317 mg, 0.864 mmol, 0.8 eq). The resultant suspension was stirred under a nitrogen atmosphere for 0.5 h. The reaction mixture was transferred to a separating funnel and washed with water (3 \times 15 mL). The organic phase was then dried over MgSO_4 and the solvent removed under vacuum to give the crude product as an orange foam. Trituration with MeOH afforded the product as an off-white powder (349 mg, 0.697 mmol, 64.4%): mp 131-133 $^\circ\text{C}$; ^1H NMR (DMSO, 400 MHz) δ 9.64 (s, 1H), 7.91 (d, 1H, $J=7.8$ Hz), 7.84 (d, 1H, $J=7.8$ Hz), 7.44 (d, 2H, $J=8.9$ Hz), 7.41 (t, 1H, $J=7.8$ Hz), 7.31 (t, 1H, $J=7.8$ Hz), 7.27 (t, 1H, $J=7.8$ Hz), 6.99 (m, 2H), 6.87 (d, 1H, $J=7.8$ Hz), 6.67 (d, 2H, $J=8.9$ Hz), 5.20 (s, 1H), 4.09 (m, 1H), 3.95 (m, 1H), 3.77 (m, 1H), 3.65 (m, 2H), 3.17 (m, 2H), 2.43 (m, 1H), 2.57 (m, 1H), 1.89 (m, 1H), 1.69 (m, 1H), 1.60 (m, 4H), 1.41 (m, 2H); ^{13}C NMR (CDCl_3 , 100 MHz) δ 171.3 (C), 146.3 (C), 143.7 (C), 134.4 (C), 132.2 (C), 129.5 (CH), 129.2 (C), 128.2 (CH), 127.6 (CH), 124.7 (CH), 124.5 (C), 124.1 (CH), 123.8 (CH), 122.2 (CH), 120.3 (CH), 114.6 (CH), 113.3 (CH), 75.6 (CH), 56.8 (CH), 51.6 (CH_2), 45.2 (CH_2), 40.6 (CH_2), 38.8 (CH_2), 37.6 (CH_2), 35.0 (CH_2), 29.3 (CH_2), 25.8 (CH_2); IR (KBr, cm^{-1}) 3295 (w), 3033 (w), 2926 (m), 1652 (s), 1601 (s), 1515

(s), 1445 (s), 1299 (s), 1158 (s), 819 (m), 750 (s), 730 (s); MS (FAB) m/z (%) 502.4 (M+H)⁺ (61), 414.4 (100), 180.8 (43); HRMS (FAB) for (C₂₉H₃₂N₃OS₂)⁺ calcd 502.1987, obsd 502.1982.

9.11.62 1-[4-(5-[1,2]Dithiolan-3-yl-pentanoylamino)-phenyl]-2,3-dihydro-1H-imidazo[1,2-f]phenanthridin-4-ylum bromide (22).

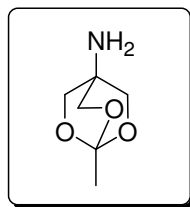


To a solution of Lipoic amine SM (130 mg, 0.44 mmol, 1.0 eq) and TEA (275 μ L, 1.97 mmol, 4.5 eq) in CHCl₃ (10 mL) was added 5-(2-Bromo-ethyl)-phenanthridinium bromide (240 mg, 0.66 mmol, 1.5 eq) and the reaction was stirred at room temperature for 4 d. Solvents were removed under vacuum and the brown residue was triturated with acetone then sonicated in H₂O and filtered to give a brown powder after drying under vacuum (55 mg, 0.095 mmol, 21.5%): mp 252-258 °C (degrad); ¹H NMR (DMSO, 400 MHz) δ 10.32 (brd, 1H), 8.91 (d, 1H, $J=8.0$ Hz), 8.82 (d, 1H, $J=8.0$ Hz), 8.07 (t, 1H, $J=8.0$ Hz), 7.88 (m, 3H), 7.83 (d, 1H, $J=8.0$ Hz), 7.71 (t, 1H, $J=8.0$ Hz), 7.65 (d, 2H, $J=8.0$ Hz), 7.60 (t, 1H, $J=8.0$ Hz), 7.40 (d, 1H, $J=8.0$ Hz), 4.93 (t, 2H, $J=10.6$ Hz), 4.57 (t, 2H, $J=10.6$ Hz), 3.67 (m, 1H), 3.19 (m, 2H), 2.44 (m, 2H), 1.92 (m, 1H), 1.72 (m, 1H), 1.65 (m, 4H), 1.45 (m, 2H); ¹³C NMR (DMSO, 100 MHz) δ 171.7 (C), 152.5 (C), 140.6 (C), 135.3 (CH), 135.0 (C), 133.3 (CH), 132.6 (C), 131.5 (C), 128.7 (CH), 127.2 (CH), 127.0 (CH), 125.7 (CH), 124.3 (CH), 124.1 (CH), 120.5 (CH), 120.3 (C), 116.5 (CH), 115.3 (C), 56.2 (CH), 54.1 (CH₂), 46.8 (CH₂), 38.1 (CH₂), 34.2 (CH₂), 28.4 (CH₂), 24.8 (CH₂); IR (cm⁻¹) 3041 (w), 2933 (w), 1680 (m), 1602 (m), 1575 (m), 1541 (s), 1516 (s), 1442 (m), 1311 (m), 756 (s); MS (FAB) m/z (%) 500.1 (M⁺) (69), 232.3 (39), 179.7 (39), 157.9 (98), 81.0 (100); HRMS (FAB) for (C₂₉H₃₀N₃OS₂)⁺ calcd 500.1830, obsd 500.1828.

9.11.63 1-Methyl-4-nitro-2,6,7-trioxabicyclo[2.2.2]octane (23).

Synthetic procedure derived from synthesis of Yokoyama *et al.*:²⁰⁶ In a 250 mL RB flask fitted with a distillation condenser; 2-(hydroxymethyl)-2-nitro-1,3-propanediol (28.9 g, 190.9 mmol, 1.0 eq) was suspended in dioctylphthalate (90 mL). Triethyl orthoacetate (35 mL, 190.9 mmol, 1.0 eq) was added and the reaction mixture was heated to 120°C for 2 hrs. The distillation condenser was replaced with a vertical air condenser and a catalytic amount of *p*-toluenesulfonic acid (5-10 mg) and a further portion of DOP (50 mL) were added. The pressure was reduced to < 50 mbar and the reaction was heated to 160°C for a further 2 hrs. The crude product sublimed and crystallized on the condenser. The crude material was recrystallized from hexane to give white needle-like crystals (12.70 g, 72.5 mmol, 38.0%): mp 113-115 °C (Hexane); ¹H NMR (CDCl₃, 400 MHz) δ 4.43 (s, 6H), 1.55 (s, 3H); ¹³C NMR (CDCl₃, 100 MHz) δ 110.1 (CMe), 75.4 (CNO₂), 67.6 (3×CH₂), 22.1 (CH₃); IR (KBr, cm⁻¹) 3489 (w), 3049 (m), 2916 (m), 1560 (s), 1302 (s), 1126 (s), 1029 (s), 863 (s); MS (CI) *m/z* (%) 176.2 (M+H)⁺ (100), 149.2 (29), 131.2 (37).

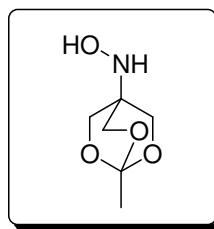
Product Reference: Yokoyama, Y.; Padias, A. B.; Bratoeff, E. A.; Hall, H. K. *Macromolecules* **1982**, *15*, 11-17.

9.11.64 1-Methyl-2,6,7-trioxabicyclo[2.2.2]oct-4-ylamine (24).

Autoclave: 1-methyl-4-nitro-2,6,7-trioxa-bicyclo[2.2.2]octane (3.87 g, 22.10 mmol), 10% Pd/C (1200 mg), EtOAc (50 mL), 6 bar, 10d. Product isolated as a white solid after EtOAc recryst. (1.211 g, 8.34 mmol, 37.7%): mp 90-100 °C; ^1H NMR (CDCl_3 , 400 MHz) δ 3.82 (s, 6H), δ 1.43 (s, 3H), δ 1.18 (brd, 2H); ^{13}C NMR (CDCl_3 , 100 MHz) δ 108.3 (C), δ 72.7 ($3\times\text{CH}_2$), δ 45.0 (C), 22.9 (CH_3); IR (cm^{-1}) 3313 (m), 3265 (m), 2953 (m), 1626 (m), 1560 (m), 1402 (m), 1294 (m), 1120 (s), 1047 (s), 1043 (s); MS (CI) m/z (%) 299.16 (40), 164.92 (M+18) (23), 147.13 (M+2) (100), 145.14 (M $^+$) (43), 116.54 (29).

Product Reference: Yokoyama, Y.; Padias, A. B.; Bratoeff, E. A.; Hall, H. K. *Macromolecules* **1982**, *15*, 11-17.

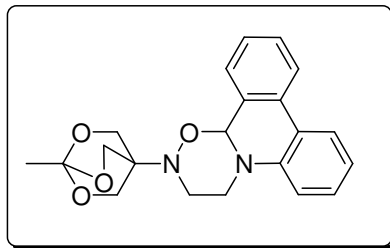
9.11.65 *N*-(1-methyl-2,6,7-trioxa-bicyclo[2.2.2]oct-4-yl)-hydroxylamine (27).



H-Cube: 10% Pd/C catcart®, EtOAc, 0.5 mL/min, rt°C, 20 bar, 3 d. 1-methyl-4-nitro-2,6,7-trioxa-bicyclo[2.2.2]octane (4.23 g, 24.17 mmol) in EtOAc (400 mL) was continuously flowed through the system for 3 d. The solvent was removed under vacuum to give the product as a white powder (3.30g, 20.48 mmol, 84.8%): mp 155-157 °C; ^1H NMR (CDCl_3 , 400 MHz) δ 5.01 (brd, 2H), 4.04 (s, 6H), 1.49 (s, 3H); ^{13}C NMR (CDCl_3 , 100 MHz) δ 108.9 (C), 68.7 ($3\times\text{CH}_2$), 52.9 (C), 22.9 (CH_3); IR (KBr, cm^{-1}) 3105 (m), 3097 (m), 2953 (m), 1739 (w), 1552 (m), 1388 (m), 1190 (M), 1126 (m), 1047 (s), 1030 (s); MS (CI) m/z (%) 162.1 (M+H) $^+$ (100), 146.1 (69).

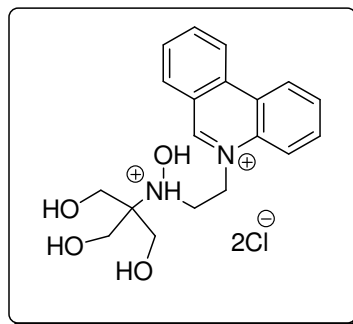
Product Reference: Studer, A., *Angew. Chem. Int. Ed.* **2000**, *39*, 1108-1111.

9.11.66 **2-(1-Methyl-2,6,7-trioxa-bicyclo[2.2.2]oct-4-yl)-3,4-dihydro-2H,12bH-1-oxa-2,4a-diaza-triphenylene (28).**



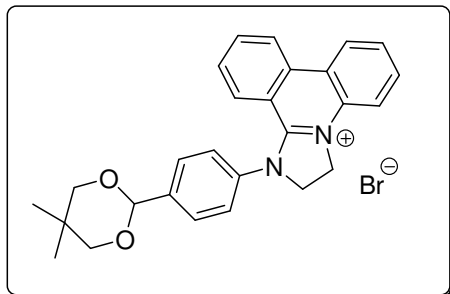
BEP **10** (400 mg, 1.09 mmol, 1.0 eq) was added to a solution of *N*-(1-methyl-2,6,7-trioxa-bicyclo[2.2.2]oct-4-yl)-hydroxylamine (158 mg, 0.98 mmol, 0.9 eq) and TEA (456 μ L, 3.27 mmol, 3.0 eq) in DMSO (20 mL) and the reaction was stirred at room temperature for 1.5 hrs. MeOH (80 mL) and H₂O (20 mL) were added to precipitate the product which was collected by filtration, washing with MeOH. After drying under vacuum the product was obtained as a white powder (194 mg, 0.53 mmol, 54.2%): mp 215-217 °C (DMSO-MeOH); ¹H NMR (CDCl₃, 400 MHz) δ 7.91 (d, 2H, *J*=8.0 Hz), 7.50 (m, 1H), 7.39 (s, 2H), 7.33 (t, 1H, *J*=8.0 Hz), 7.00 (t, 1H, *J*=8.0 Hz), 6.95 (d, 1H, *J*=8.0 Hz), 6.13 (s, 1H), 4.22 (d, 1H, *J*=11.2 Hz), 4.12 (d, 3H, *J*=7.6 Hz), 4.06 (d, 3H, *J*=7.6 Hz), 3.56 (t, 1H, *J*=11.2 Hz), 3.19 (t, 1H, *J*=11.2 Hz), 2.79 (d, 1H, *J*=11.2 Hz), 1.47 (s, 3H); ¹³C NMR (CDCl₃, 100 MHz) δ 140.9 (C), 131.0 (C), 129.7 (CH), 129.4 (CH), 127.9 (CH), 127.6 (C), 127.5 (CH), 124.0 (CH), 121.9 (CH), 121.3 (C), 119.4 (CH), 112.8 (CH), 108.8 (C), 89.8 (CH), 67.1 (3 \times CH₂), 55.6 (C), 46.7 (CH₂), 45.4 (CH₂), 22.8 (CH₃); IR (cm⁻¹) 2958 (w), 2895 (w), 1604 (w), 1494 (w), 1447 (w), 1296 (m), 1122 (s), 1070 (m), 864 (s); MS (FAB) *m/z* (%) 367.3 (M+H)⁺ (100), 307.1 (18), 206.6 (23), 193.7 (18); Anal. Calcd for C₂₁H₂₂N₂O₄ C, 68.84; H, 6.05; N, 7.65; Found C, 68.34; H, 5.96; N, 7.58; HRMS (FAB) for (C₂₁H₂₃N₂O₄)⁺ calcd 367.1658, obsd 367.1654.

9.11.67 5-(2-(1-Methyl-2,6,7-trioxo-bicyclo[2.2.2]oct-4-yl)-hydroxylaminoethyl)-phenanthridinium chloride; hydrochloride (29).



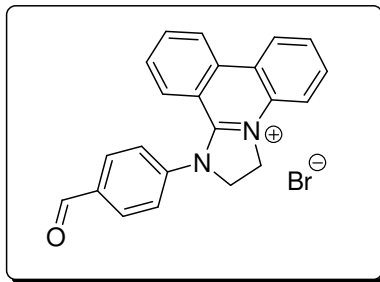
To a solution of 2-(1-methyl-2,6,7-trioxo-bicyclo[2.2.2]oct-4-yl)-3,4-dihydro-2*H*,12*bH*-1-oxa-2,4a-diazatriphenylene (100 mg, 0.28 mmol, 1.0 eq) in CHCl_3 (10 mL) was added 5*N* HCl (aq) (10 mL), and the reaction was stirred for ~15 min. The layers were separated and the organic phase was further extracted with 1*N* HCl (aq) (5 mL). The combined aqueous extracts were heated to reflux for 3h. The solvent was removed under vacuum and the residue was triturated with acetone. Filtration and drying under vacuum afforded the product as a pale yellow powder (104 mg, 0.25 mmol, 91.4%): mp 158-160 °C; ^1H NMR (D_2O , 400 MHz) δ 9.69 (s, 1H), 8.77 (d, 1H, $J=8.0$ Hz), 8.70 (d, 1H, $J=8.0$ Hz), 8.34 (d, 1H, $J=8.0$ Hz), 8.30 (d, 1H, $J=8.0$ Hz), 8.20 (t, 1H, $J=8.0$ Hz), 7.99 (t, 1H, $J=8.0$ Hz), 7.92 (m, 2H), 5.13 (t, 2H, $J=5.2$ Hz), 3.59 (t, 2H, $J=5.2$ Hz), 3.41 (s, 6H); ^{13}C NMR (D_2O , 100 MHz) δ 155.1 (CH), 138.4 (CH), 134.8 (C), 132.5 (CH), 132.2 (CH), 130.3 (CH), 125.9 (C), 124.6 (CH), 123.0 (C), 122.5 (118.6), 69.6 (C), 59.4 ($3\times\text{CH}_2$), 54.9 (CH_2), 51.4 (CH_2); IR (cm^{-1}) 3266 (w), 1749 (s), 1627 (m), 1448 (m), 1360 (m), 1228 (s), 1064 (s), 912 (m), 759 (s); MS (FAB) m/z (%) 343.3 (M^+) (100), 295.3 (7), 206.6 (10), 103.8 (32); HRMS (FAB) for $(\text{C}_{19}\text{H}_{23}\text{N}_2\text{O}_4)^+$ calcd 343.1658, obsd 343.1676.

9.11.68 1-[4-(5,5-Dimethyl-[1,3]dioxan-2-yl)-phenyl]-2,3-dihydro-1*H*-imidazo[1,2-*f*]phenanthridin-4-ylum bromide (31).



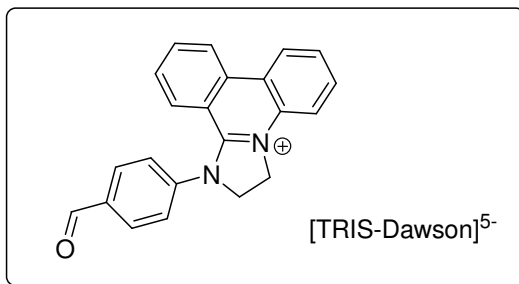
To a solution of 4-(5,5-dimethyl-[1,3]dioxan-2-yl)-phenylamine (169 mg, 0.817 mmol, 1.0 eq) and TEA (342 μ L, 2.451 mmol, 3.0 eq) in CHCl_3 (30 mL) was added BEP **10** (300 mg, 0.817 mmol, 1.0 eq) and the reaction stirred at room temperature for 2 hrs. The reaction mixture was concentrated under vacuum and the foam-like residue was triturated with MeOH to give a pale peach powder. The residue was redissolved in CHCl_3 (30 mL) and NBS (131 mg, 0.735 mmol, 0.9 eq) was added. After stirring the reaction mixture for 1 h the solvent was removed under vacuum. Trituration of the residue with acetone and drying the residue under vacuum afforded the product as a white powder (255 mg, 0.519 mmol, 63.5%): mp 318-319 $^\circ\text{C}$ (MeOH-Et₂O); ^1H NMR (DMSO, 400 MHz) δ 8.93 (d, 1H, $J=8.0$ Hz), 8.84 (d, 1H, $J=8.0$ Hz), 8.08 (t, 1H, $J=8.0$ Hz), 7.94 (t, 1H, $J=8.0$ Hz), 7.86 (d, 1H, $J=8.0$ Hz), 7.59 (m, 5H), 7.58 (t, 1H, $J=8.0$ Hz), 7.35 (d, 1H, $J=8.0$ Hz), 5.58 (s, 1H), 4.96 (t, 2H, $J=10.6$ Hz), 4.61 (t, 2H, $J=10.6$ Hz), 3.76 (d, 2H, $J=10.8$ Hz), 3.72 (d, 2H, $J=10.8$ Hz), 1.24 (s, 3H), 0.81 (s, 1H); ^{13}C NMR (DMSO, 100 MHz) δ 152.5 (C), 140.2 (C), 139.5 (C), 135.4 (CH), 135.1 (C), 132.6 (C), 131.6 (CH), 128.6 (3 \times CH), 126.9 (CH), 126.4 (2 \times CH), 125.8 (CH), 124.4 (CH), 124.1 (CH), 120.4 (C), 116.3 (CH), 115.2 (C), 99.9 (CH), 76.6 (CH₂), 54.4 (CH₂), 47.0 (CH₂), 29.9 (C), 22.8 (CH₃), 21.4 (CH₃); IR (cm^{-1}) 2937 (w), 2862 (w), 1575 (s), 1545 (s), 1390 (s), 1215 (m), 1111 (s), 1099 (s), 1016 (m), 842 (m); MS (FAB) m/z (%) 411.2 (M⁺) (100); HRMS (FAB) for (C₂₇H₂₇N₂O₂)⁺ calcd 411.2073, obsd 411.2069.

9.11.69 1-(4-Formylphenyl)-2,3-dihydro-1H-imidazo[1,2-f]phenanthridin-4-ylum bromide (32).



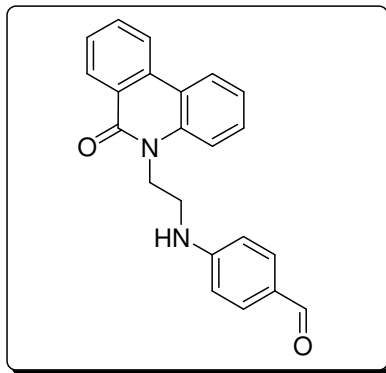
To a suspension of 1-[4-(5,5-dimethyl-[1,3]dioxan-2-yl)-phenyl]-2,3-dihydro-1H-imidazo[1,2-f]phenanthridin-4-ylum bromide (150 mg, 0.305 mmol, 1.0 eq) in H₂O (15 mL) was added con. HBr (48% by wt, 2 mL) and the reaction stirred at 90°C for 2 hrs. The suspension was filtered and the residue was dried under vacuum to give a yellow powder (85 mg, 0.210 mmol, 68.8%): mp 350-352 °C; ¹H NMR (DMSO, 400 MHz) δ 10.15 (s, 1H), 8.95 (d, 1H, *J*=8.0 Hz), 8.87 (d, 1H, *J*=8.0 Hz), 8.24 (d, 2H, *J*=8.0 Hz), 8.12 (t, 1H, *J*=8.0 Hz), 7.94 (m, 4H), 7.76 (t, 1H, *J*=8.0 Hz), 7.57 (t, 1H, *J*=8.0 Hz), 7.40 (d, 1H), 5.00 (t, 2H, *J*=10.6 Hz), 4.68 (t, 2H, *J*=10.6 Hz); ¹³C NMR (DMSO, 100 MHz) δ 192.4 (CH), 152.6 (C), 144.3 (C), 136.3 (C), 135.6 (CH), 135.2 (C), 132.4 (C), 131.6 (CH), 128.8 (CH), 127.3 (CH), 127.0 (CH), 126.1 (CH), 124.4 (CH), 124.1 (CH), 120.8 (C), 116.4 (CH), 115.1 (C), 53.9 (CH₂), 47.2 (CH₂); IR (cm⁻¹) 3045 (w), 1697 (m), 1572 (s), 1541 (s), 1309 (m), 819 (m), 794 (m), 752 (s), 719 (m); MS (FAB) *m/z* (%) 325.2 (M⁺) (16), 307.1 (46), 289.1 (18), 155.0 (100), 137.2 (71); HRMS (FAB) for (C₂₂H₁₇N₂O)⁺ calcd 325.1341, obsd 325.1339.

9.11.70 TRIS-Dawson 1-(4-formylphenyl)-2,3-dihydro-1*H*-imidazo[1,2-*f*]phenanthridin-4-ylum salt (33).

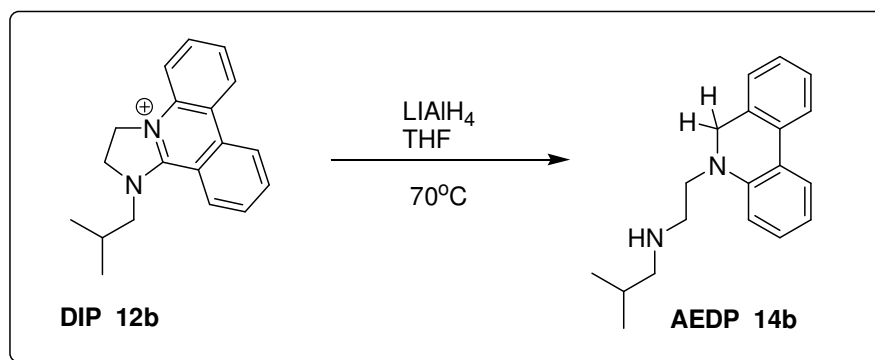


A solution of TRIS-Dawson TBA salt (30 mg, 0.0058 mmol, 1.0 eq) in MeCN (0.5 mL) was added to a solution of DIP-aldehyde **32** (2.3 mg, 0.0058 mmol, 1.0 eq) in MeCN and the mixed solution was left to stand for 1 h. The precipitate was collected by filtration and dried to give a greenish yellow powder (28 mg, 0.0049 mmol, 85%): ¹H NMR (DMSO, 400 MHz) δ 10.14 (s, 10H), 8.94 (d, 10H, *J*=8.0 Hz), 8.86 (d, 10H, *J*=8.0 Hz), 8.39 (s, 3H), 8.23 (d, 20H, *J*=8.0 Hz), 8.11 (t, 10H, *J*=8.0 Hz), 7.93 (m, 40H), 7.75 (t, 10H, *J*=8.0 Hz), 7.56 (t, 10H, *J*=8.0 Hz), 7.39 (d, 10H), 5.40 (s, 6H), 5.07 (brd, 20H), 4.77 (brd, 20H); ¹³C NMR (DMSO, 100 MHz) δ 192.3 (CH), 152.5 (C), 144.3 (C), 136.2 (C), 135.5 (CH), 135.2 (C), 132.4 (C), 131.7 (CH), 131.6 (CH), 128.7 (CH), 127.3 (CH), 127.0 (CH), 126.1 (CH), 124.3 (CH), 124.0 (CH), 120.7 (C), 116.6 (CH), 114.0 (C), 54.0 (CH₂), 47.3 (CH₂); IR (cm⁻¹) 3457 (w), 3050 (w), 1693 (w), 1573 (m), 1522 (m), 1308 (m), 1084 (m), 949 (m), 903 (m), 808 (s), 716 (s); Anal. Calcd for [NH₂C(CH₂O)₃P₂W₁₂V₃O₅₉] [C₂₂H₁₇N₂O]₅ C, 24.19; H, 1.66; N, 2.72; Found C, 22.12; H, 1.68; N, 2.60).

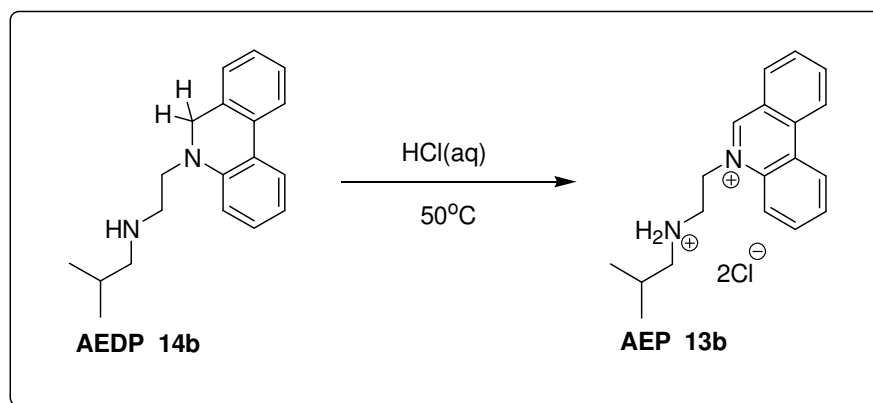
9.11.71 4-[2-(6-Oxo-6H-phenanthridin-5-yl)-ethylamino]-benzaldehyde (34).



DIP basic hydrolysis and acetal acid hydrolysis: A Mixture of DIP-aldehyde and DIP acetal (814 mg) was suspended in ~0.2M NaOH (150 mL) and heated to 60°C for 16 hrs. The reaction mixture was cooled and filtered to give a pale peach solid residue. The residue was resuspended in H₂O (50 mL), AcOH (20 mL) was added and the reaction was heated to 60°C for a further 2 hrs. The reaction mixture was filtered and after drying under vacuum the product was collected as an off-white powder (490 mg, 1.43 mmol, ~78%): mp 196-198 °C; ¹H NMR (CDCl₃, 400 MHz) δ 9.62 (s, 1H), 8.49 (d, 1H, *J*=8.0 Hz), 8.27 (d, 1H, *J*=8.0 Hz), 8.23 (d, 1H, *J*=8.0 Hz), 7.74 (t, 1H, *J*=8.0 Hz), 7.56 (m, 3H), 7.48 (t, 1H, *J*=8.0 Hz), 7.37 (d, 1H, *J*=8.0 Hz), 7.30 (t, 1H, *J*=8.0 Hz), 6.57 (d, 2H, *J*=8.8 Hz), 5.44 (brd, 1H), 4.71 (t, 2H, *J*=5.6 Hz), 3.66 (dt, 2H, *J*=5.2, 5.6 Hz); ¹³C NMR (CDCl₃, 100 MHz) δ 190.1 (C), 162.5 (C), 153.3 (C), 136.8 (C), 133.6 (C), 132.9 (CH), 132.2 (CH), 129.8 (CH), 128.6 (CH), 128.1 (CH), 126.1 (C), 125.0 (C), 123.7 (CH), 122.8 (CH), 121.7 (CH), 119.5 (C), 114.6 (CH), 111.6 (CH), 41.8 (CH₂), 41.7 (CH₂); IR (cm⁻¹) 3379 (w), 1651 (s), 1589 (s), 1556 (s), 1533 (m), 1437 (m), 1354 (m), 1317 (m), 1161 (s), 804 (m); MS (EI+) *m/z* (%) 342.2 (M⁺) (20), 209.1 (73), 196.1 (81), 179.3 (64), 147.1 (94); HRMS (EI+) for C₂₂H₁₈N₂O₂ calcd 342.1368, obsd 342.1370.

9.11.72 LiAlH₄ DIP reduction.

To a suspension of isobutyl-DIP (500 mg, 1.40 mmol, 1.0 eq) in dry THF (10 mL) was added a solution of LiAlH₄ (2.0 M in THF, 7 mL, 14.0 mmol, 10.0 eq) dropwise over ~5 min. The reaction was heated to reflux (70°C) and stirred for 18 h (note: reaction was complete after 2 h). The reaction was cooled to rt°C and quenched by dropwise addition of H₂O (2 mL). The resultant suspension was filtered and the filtrate was reduced by volume to ~10 mL before partitioning between H₂O (20 mL) and Et₂O (100 mL). The layers were separated and the organic layer was washed with H₂O (20 mL) before drying over MgSO₄ and concentrating under vacuum. The crude product was purified by flash column chromatography (~15g silica, Et₂O then 5% TEA in Et₂O). The product was collected as a yellow oil (114 mg, 0.41 mmol, 29.0 %): ¹H NMR (CDCl₃, 400 MHz) δ 7.64 (m, 2H), 7.22 (t, 1H, *J*=8.0 Hz), 7.14 (m, 2H), 7.04 (d, 1H, *J*=8.0 Hz), 6.76 (m, 2H), 4.24 (s, 2H), 3.43 (t, 2H, *J*=8.0 Hz), 2.86 (t, 2H, *J*=8.0 Hz), 2.39 (d, 2H, *J*=7.6 Hz), 1.68 (sept, 1H, *J*=6.8 Hz), 0.81 (d, 6H, *J*=6.8 Hz); ¹³C NMR (DMSO, 100 MHz) δ 146.2 (C), 132.9 (C), 132.2 (C), 129.1 (C), 127.7 (CH), 127.0 (CH), 125.6 (CH), 123.9 (CH), 122.5 (CH), 118.2 (CH), 112.6 (CH), 58.2 (CH₂), 53.1 (CH₂), 50.8 (CH₂), 46.2 (CH₂), 28.4 (CH), 20.8 (2×CH₃).

9.11.73 AEDP acidic oxidation.

A mixture of isobutyl-AEDP **14b** (80 mg, 0.28mmol) in H₂O (5mL) was acidified by addition of HCl conc. (0.5 mL) and the reaction stirred at 50°C for 24 h. The solvent was removed under vacuum and the oily residue was vitrified by addition of acetone. The product was filtered and dried to give a pale yellow powder (61 mg, 0.17 mmol, 61.0 %): ¹H NMR (DMSO, 400 MHz) δ 10.72 (s, 1H), 10.08 (s, 2H), 9.25 (d, 1H, J=8.0 Hz), 9.18 (d, 1H, J=8.0 Hz), 8.89 (d, 1H, J=8.0 Hz), 8.60 (d, 1H, J=8.0 Hz), 8.43 (t, 1H, J=8.0 Hz), 8.15 (m, 3H), 5.69 (t, 2H, J=6.2 Hz), 3.69 (m, 2H), 2.84 (m, 2H), 2.10 (sept, 1H, J=6.8 Hz), 0.99 (d, 6H, J=6.8 Hz).

Publications

The following articles and communications were published as a result of work undertaken over the course of this Ph.D. programme:

“Fine Tuning Reactivity: Synthesis and Isolation of 1,2,3,12b-tetrahydroimidazo[1,2-f]phenanthridines” Richmond, C. J.; Eadie, R. M.; Parenty, A. D. C.; Cronin, L. *J. Org. Chem.* **2009**, *74*, 8196-8202.

“A New C-C Bond Forming Annulation Reaction Leading to pH Switchable Organic Materials” Kitson, P. J.; Parenty, A. D. C.; Richmond, C. J.; Long, D. L.; Cronin, L. *Chem. Commun.* **2009**, *27*, 4067-4069.

“Realization of a “Lockable” molecular switch via pH- and redox-modulated cyclization” Richmond, C. J.; Parenty, A. D. C.; Song, Y. F.; Cooke, G.; Cronin, L. *J. Am. Chem. Soc.* **2008**, *130*, 13059-13065.

“A general and efficient five-step one-pot procedure leading to nitrogen-bridgehead heterocycles containing an imidazole ring” Parenty, A. D. C.; Song, Y. F.; Richmond, C. J.; Cronin, L. *Org. Lett.* **2007**, *9*, 2253-2256.

References

- (1) Sneader, W. *Drug Discovery: The Evolution of Modern Medicines*; John Wiley and Sons Ltd: Chichester, 1985.
- (2) Lednicer, D. *Strategies for Organic Drug Synthesis and Design*; Second ed.; John Wiley and Sons Inc.: Hoboken, New Jersey, 2009.
- (3) McLaren, K. *The Colour Science of Dyes and Pigments*; Second ed.; Adam Hilger Ltd: Bristol, 1986.
- (4) Campbell, I. M. *Introduction to Synthetic Polymers*; Oxford University Press Inc.: New York, 1994.
- (5) Izaat, R. M.; Christensen, J. J. *Synthesis of Macrocycles: The Design of Selective Complexing Agents*; John Wiley and Sons Inc.: New York, 1987.
- (6) Bradshaw, J. S. *Aza-crown macrocycles*; John Wiley & Sons: Chichester, 1993.
- (7) Dalgarno, S. J.; Thallapally, P. K.; Barbour, L. J.; Atwood, J. L. *Chem. Soc. Rev.* **2007**, *36*, 236-245.
- (8) Yoon, J.; Kim, S. K.; Singh, N. J.; Kim, K. S. *Chem. Soc. Rev.* **2006**, *35*, 355-360.
- (9) Li, J.; Loh, X. J. *Adv. Drug Delivery Rev.* **2008**, *60*, 1000-1017.
- (10) Parker, D. *Macrocyclic Synthesis*; Oxford University Press Inc.: Oxford, 1996.
- (11) Gutsche, C. D. *Calixarenes*; The Royal Society of Chemistry: Cambridge, 1989.
- (12) Ananchenko, G. S.; Udachin, K. A.; Pojarova, M.; Dubes, A.; Ripmeester, J. A.; Jebors, S.; Coleman, A. W. *Cryst. Growth Des.* **2006**, *6*, 2141-2148.
- (13) Liu, L.; Zakharov, L. N.; Golen, J. A.; Rheingold, A. L.; Hanna, T. A. *Inorg. Chem.* **2008**, *47*, 11143-11153.
- (14) Liu, S.; Ruspic, C.; Mukhopadhyay, P.; Chakrabarti, S.; Zavalij, P. Y.; Isaacs, L. J. *Am. Chem. Soc.* **2005**, *127*, 15959-15967.
- (15) Bowman-James, K. *Acc. Chem. Res.* **2005**, *38*, 671-678.
- (16) Gibson, S. E.; Lecci, C. *Angew. Chem. Int. Ed.* **2006**, *45*, 1364-1377.
- (17) Schalley, C. A.; Reckien, W.; Peyerimhoff, S.; Baytekin, B.; Vögtle, F. *Chem. Eur. J.* **2004**, *10*, 4777-4789.
- (18) Gokel, G. W. *Crown Ethers and Cryptands*; The Royal Society of Chemistry: London, 1991.
- (19) Curtis, W. D.; Laidler, D. A.; Stoddart, J. F.; Jones, G. H. *J. Chem. Soc.-Perkin Trans. 1* **1977**, 1756-1770.
- (20) Ouchi, M.; Inoue, Y.; Liu, Y.; Nagamune, S.; Nakamura, S.; Wada, K.; Hakushi, T. *Bull. Chem. Soc. Jpn.* **1990**, *63*, 1260-1262.
- (21) Stoddart, J. F. *Top. Stereochem.* **1987**, *17*, 207-288.
- (22) Bako, P.; Bako, T.; Meszaros, A.; Keglevich, G.; Szollosy, A.; Bodor, S.; Mako, A.; Toke, L. *Synlett.* **2004**, 643-646.
- (23) Ashton, P. R.; Preece, J. A.; Stoddart, J. F.; Tolley, M. S.; White, A. J. P.; Williams, D. J. *Synthesis* **1994**, 1344-1352.
- (24) Ashton, P. R.; Preece, J. A.; Stoddart, J. F.; Tolley, M. S. *Synlett.* **1994**, 789-792.
- (25) Jose, N.; Sengupta, S.; Basu, J. K. *J. Mol. Catal. A-Chem.* **2009**, *309*, 153-158.
- (26) Pedersen, C. J. *J. Am. Chem. Soc.* **1967**, *89*, 7017-7036.
- (27) Hiraoka, M. *Crown Ethers and Analogous Compounds*; Elsevier: Amsterdam ; New York, 1992.
- (28) Dietrich, B.; Lehn, J. M.; Sauvage, J. P. *Tetrahedron Lett.* **1969**, 2885-&.
- (29) Dietrich, B.; Lehn, J. M.; Sauvage, J. P.; Blanzat, J. *Tetrahedron* **1973**, *29*, 1629-1645.

-
- (30) Alcock, N. W.; Curzon, E. H.; Moore, P. *J. Chem. Soc.-Dalton Trans.* **1984**, 2813-2820.
- (31) Parker, D. *Chem. Soc. Rev.* **1990**, *19*, 271-291.
- (32) Hosseini, M. W.; Lehn, J. M. *Helv. Chim. Acta* **1987**, *70*, 1312-1319.
- (33) Brand, G.; Hosseini, M. W.; Ruppert, R. *Helv. Chim. Acta* **1992**, *75*, 721-728.
- (34) Ransohoff, J. E. B.; Staab, H. A. *Tetrahedron Lett.* **1985**, *26*, 6179-6182.
- (35) Newkome, G. R.; Lee, H. W. *J. Am. Chem. Soc.* **1983**, *105*, 5956-5957.
- (36) Bell, T. W.; Cragg, P. J.; Drew, M. G. B.; Firestone, A.; Kwok, D. I. A. *Angew. Chem. Int. Ed.* **1992**, *31*, 345-347.
- (37) Bell, T. W.; Cragg, P. J.; Drew, M. G. B.; Firestone, A.; Kwok, D. I. A. *Angew. Chem. Int. Ed.* **1992**, *31*, 348-350.
- (38) Bell, T. W.; Cragg, P. J.; Drew, M. G. B.; Firestone, A.; Kwok, A. D. I.; Liu, J.; Ludwig, R. T.; Papoulis, A. T. *Pure Appl. Chem.* **1993**, *65*, 361-366.
- (39) Bell, T. W.; Firestone, A.; Ludwig, R. *J. Chem. Soc.-Chem. Commun.* **1989**, 1902-1904.
- (40) Kim, J.; Jung, I.-S.; Kim, S.-Y.; Lee, E.; Kang, J.-K.; Sakamoto, S.; Yamaguchi, K.; Kim, K. *J. Am. Chem. Soc.* **2000**, *122*, 540-541.
- (41) Lee, J. W.; Samal, S.; Selvapalam, N.; Kim, H.-J.; Kim, K. *Acc. Chem. Res.* **2003**, *36*, 621-630.
- (42) Buschmann, H. J.; Schollmeyer, E. *J. Incl. Phenom. Mol. Recogn. Chem.* **1997**, *29*, 167-174.
- (43) Karcher, S.; Kornmüller, A.; Jekel, M. *Acta Hydroch. Hydrob.* **1999**, *27*, 38-42.
- (44) Li, S. Y.; Sun, B.; Xiao, Z. C.; Huang, M. H.; Xie, W. X.; Liu, J. M. *Chin. Chem. Lett.* **2009**, *20*, 640-642.
- (45) Okada, Y.; Mizutani, M.; Ishii, F.; Nishimura, J. *Tetrahedron Lett.* **1998**, *39*, 8461-8464.
- (46) Mullen, K. M.; Beer, P. D. *Chem. Soc. Rev.* **2009**, *38*, 1701-1713.
- (47) Crowley, J. D.; Goldup, S. M.; Lee, A. L.; Leigh, D. A.; McBurney, R. T. *Chem. Soc. Rev.* **2009**, *38*, 1530-1541.
- (48) Stoddart, J. F. *Chem. Soc. Rev.* **2009**, *38*, 1521-1529.
- (49) Prikhod'ko, A. I.; Sauvage, J.-P. *J. Am. Chem. Soc.* **2009**, *131*, 6794-6807.
- (50) Zhao, Y. L.; Trabolsi, A.; Stoddart, J. F. *Chem. Commun.* **2009**, 4844-4846.
- (51) Mihail, B.; Yves-Marie, L.; Luca, P.; Marco, M.; Nelsi, Z.; Gavin, V.; Arie van der, L.; Eddy, P.; Jean-Marie, L. *Eur. J. Inorg. Chem.* **2009**, *2009*, 2621-2628.
- (52) Stoddart, J. F. *Chem. Soc. Rev.* **2009**, *38*, 1802-1820.
- (53) Coskun, A.; Friedman, D. C.; Li, H.; Patel, K.; Khatib, H. A.; Stoddart, J. F. *J. Am. Chem. Soc.* **2009**, *131*, 2493-2495.
- (54) Zheng, Y. B.; Yang, Y.-W.; Jensen, L.; Fang, L.; Juluri, B. K.; Flood, A. H.; Weiss, P. S.; Stoddart, J. F.; Huang, T. J. *Nano Lett.* **2009**, *9*, 819-825.
- (55) Dietrich-Buchecker, C.; Colasson, B.; Fujita, M.; Hori, A.; Geum, N.; Sakamoto, S.; Yamaguchi, K.; Sauvage, J.-P. *J. Am. Chem. Soc.* **2003**, *125*, 5717-5725.
- (56) Zhang, W. Y.; Dichtel, W. R.; Stieg, A. Z.; Benitez, D.; Gimzewski, J. K.; Heath, J. R.; Stoddart, J. F. *Proc. Natl. Acad. Sci. U. S. A.* **2008**, *105*, 6514-6519.
- (57) *The Oxford Paperback Dictionary*; Oxford University Press: Oxford, 1994.
- (58) Balzani, V.; Credi, A.; Venturi, M. *Molecular Devices and Machines - A Journey into the Nano World*; Wiley-VCH: Weinheim, 2003.
- (59) Saha, S.; Flood, A. H.; Stoddart, J. F.; Impellizzeri, S.; Silvi, S.; Venturi, M.; Credi, A. *J. Am. Chem. Soc.* **2007**, *129*, 12159-12171.
- (60) Nguyen, T. D.; Tseng, H. R.; Celestre, P. C.; Flood, A. H.; Liu, Y.; Stoddart, J. F.; Zink, J. I. *Proc. Natl. Acad. Sci. U. S. A.* **2005**, *102*, 10029-10034.

-
- (61) Koumura, N.; Zijlstra, R. W. J.; van Delden, R. A.; Harada, N.; Feringa, B. L. *Nature* **1999**, *401*, 152-155.
- (62) Dulic, D.; Kudernac, T.; Puzys, A.; Feringa, B. L.; van Wees, B. J. *Adv. Mater.* **2007**, *19*, 2898-+.
- (63) Xie, N.; Chen, Y. *J. Mater. Chem.* **2006**, *16*, 982-985.
- (64) Rurack, K.; Danel, A.; Rotkiewicz, K.; Grabka, D.; Spieles, M.; Rettig, W. *Org. Lett.* **2002**, *4*, 4647-4650.
- (65) Wilson, T. M.; Tauber, M. J.; Wasielewski, M. R. *J. Am. Chem. Soc.* **2009**, *131*, 8952-8957.
- (66) Kawai, S. H.; Gilat, S. L.; Lehn, J. M. *J. Chem. Soc.-Chem. Commun.* **1994**, 1011-1013.
- (67) Kawai, S. H.; Gilat, S. L.; Ponsinet, R.; Lehn, J. M. *Chem. Eur. J.* **1995**, *1*, 285-293.
- (68) Hanazawa, M.; Sumiya, R.; Horikawa, Y.; Irie, M. *J. Chem. Soc.-Chem. Commun.* **1992**, 206-207.
- (69) Magri, D. C.; Brown, G. J.; McClean, G. D.; de Silva, A. P. *J. Am. Chem. Soc.* **2006**, *128*, 4950-4951.
- (70) Nicoll, D.; McPhee, S. J.; Pignone, M. *Diagnostic Tests*; 4th ed.; Lange Medical Books/McGraw-Hill: London, 2004.
- (71) Goodman, A.; Breinlinger, E.; Ober, M.; Rotello, V. M. *J. Am. Chem. Soc.* **2001**, *123*, 6213-6214.
- (72) Berna, J.; Leigh, D. A.; Lubomska, M.; Mendoza, S. M.; Perez, E. M.; Rudolf, P.; Teobaldi, G.; Zerbetto, F. *Nat. Mater.* **2005**, *4*, 704-710.
- (73) Saha, S.; Stoddart, J. F. *Chem. Soc. Rev.* **2007**, *36*, 77-92.
- (74) Badjic, J. D.; Balzani, V.; Credi, A.; Silvi, S.; Stoddart, J. F. *Science* **2004**, *303*, 1845-1849.
- (75) Ashton, P. R.; Ballardini, R.; Balzani, V.; Baxter, I.; Credi, A.; Fyfe, M. C. T.; Gandolfi, M. T.; Gomez-Lopez, M.; Martinez-Diaz, M. V.; Piersanti, A.; Spencer, N.; Stoddart, J. F.; Venturi, M.; White, A. J. P.; Williams, D. J. *J. Am. Chem. Soc.* **1998**, *120*, 11932-11942.
- (76) Balzani, V.; Clemente-Leon, M.; Credi, A.; Lowe, J. N.; Badjic, J. D.; Stoddart, J. F.; Williams, D. J. *Chem. Eur. J.* **2003**, *9*, 5348-5360.
- (77) Zhang, P.; Terefenko, E. A.; Bray, J.; Deecher, D.; Fensome, A.; Harrison, J.; Kim, C.; Koury, E.; Mark, L.; McComas, C. C.; Mugford, C. A.; Trybulski, E. J.; Vu, A. T.; Whiteside, G. T.; Mahaney, P. E. *J. Med. Chem.* **2009**, *52*, 5703-5711.
- (78) Hartz, R. A.; Ahuja, V. T.; Zhuo, X.; Mattson, R. J.; Denhart, D. J.; Deskus, J. A.; Vrudhula, V. M.; Pan, S.; Ditta, J. L.; Shu, Y.-Z.; Grace, J. E.; Lentz, K. A.; Lelas, S.; Li, Y.-W.; Molski, T. F.; Krishnananthan, S.; Wong, H.; Qian-Cutrone, J.; Schartman, R.; Denton, R.; Lodge, N. J.; Zaczek, R.; Macor, J. E.; Bronson, J. J. *J. Med. Chem.* **2009**, *Advanced article*.
- (79) Fu, G. C. *Acc. Chem. Res.* **2006**, *39*, 853-860.
- (80) Mortimer, R. J.; Dyer, A. L.; Reynolds, J. R. *Displays* **2006**, *27*, 2-18.
- (81) Segura, J. L.; Martin, N.; Guldi, D. M. *Chem. Soc. Rev.* **2005**, *34*, 31-47.
- (82) Crabtree, R. H. *Energy Environ. Sci.* **2008**, *1*, 134-138.
- (83) Pozharskii, A. F.; Soldatenkov, A. T.; Katritzky, A. R. *Heterocycles in Life and Society*; John Wiley and Sons Ltd: Chichester, 1997.
- (84) Barros, T.; Royant, A.; Standfuss, J.; Dreuw, A.; Kuhlbrandt, W. *EMBO J.* **2009**, *28*, 298-306.
- (85) Watson, J. D.; Crick, F. H. C. *Nature* **1953**, *171*, 737-738.

-
- (86) Chen, Z. G.; Stauffacher, C.; Li, Y.; Schmidt, T.; Bomu, W.; Kamer, G.; Shanks, M.; Lomonossoff, G.; Johnson, J. E. *Science* **1989**, *254*, 154-159.
- (87) Berg, J. M.; Tymoczko, J. L.; Stryer, L. *Biochemistry*; 5th ed.; W. H. Freeman: New York, 2002.
- (88) Berger, M.; Gray, J. A.; Roth, B. L. *Annu. Rev. Med.* **2009**, *60*, 355-366.
- (89) Campbell, N. A.; Reece, J. B. *Biology*; 8th ed.; Pearson Benjamin Cummings: San Francisco, 2008.
- (90) Leadley, P. F. *An introduction to Enzyme Chemistry*; The Chemical Society: London, 1978.
- (91) Dixon, M.; Webb, E. C. *Enzymes*; 3rd ed.; Longman Group Ltd: London, 1978.
- (92) Patrick, G. L. *An Introduction to Medicinal Chemistry*; 3rd ed.; Oxford University Press Inc.: New York, 2005.
- (93) Faustman, E. M.; Kirby, Z.; Gage, D.; Varnum, M. *Teratology* **1989**, *40*, 199-210.
- (94) Hudler, G. *Magical Mushrooms, Mischievous Molds*; Princeton University Press: Princeton, NJ, 1998.
- (95) Zheng, W.; RGustafson, D.; Sinha, R.; Cerhan, J.; Moore, D.; Hong, C.; Anderson, K.; Kushi, L.; Sellers, T.; Folsom, A. *J. Natl. Cancer Inst.* **1998**, *90*, 1724-1729.
- (96) Kasprzak, K. S.; Sunderman, F. W.; Salnikow, K. *Mutat. Res., Fundam. Mol. Mech. Mutagen.* **2003**, *533*, 67-97.
- (97) Dunnick, J.; Elwell, M. R.; Radovsky, A. E.; Benson, J. M.; Hahn, F. F.; Nikula, K. J.; Barr, E. B.; Hobbs, C. H. *Cancer Res.* **1995**, *55*, 5251-5256.
- (98) Matsumura, Y.; Ananthaswamy, H. N. *Toxicol. Appl. Pharmacol.* **2004**, *195*, 298-308.
- (99) Parkin, D. M. *Int. J. Cancer* **2006**, *118*, 3030-3044.
- (100) Schernhammer, E. S.; Laden, F.; Speizer, F. E.; Willett, W. C.; Hunter, D. J.; Kawachi, I.; Colditz, G. A. *J. Nat. Cancer Inst.* **2001**, *93*, 1563-1568.
- (101) Bertram, J. S. *Mol. Asp. Med.* **2000**, *21*, 167-223.
- (102) Xu, G.; McLeod, H. L. *Clin. Cancer Res.* **2001**, *7*, 3314-3324.
- (103) *Dorland's Medical Dictionary*; Elsevier 2007.
- (104) Markman, M. *Basic Cancer Medicine*; W. B. Saunders: Philadelphia, Pa.; London, 1997.
- (105) Lawley, P. D.; Brookes, P. *Nature* **1965**, *206*, 480-483.
- (106) Gupta, S. P. *Chem. Rev.* **2002**, *94*, 1507-1551.
- (107) Trzaska, S. *C&EN News* **2005**, *83*, 25.
- (108) Kumar, N. *J. Biol. Chem.* **1981**, *256*, 10435-10441.
- (109) Patlak, M. *FASEB J.* **2002**, *16*, 1-12.
- (110) Peters, G. J.; van der Wilt, C. L.; van Moorsel, C. J. A.; Kroep, J. R.; Bergman, A. M.; Ackland, S. P. *Pharmacol. Ther.* **2000**, *87*, 227-253.
- (111) Bachmeyer, C.; Aractingi, S.; Lionnet, F. *N. Engl. J. Med.* **2008**, *358*, 1362-1369.
- (112) Sauter, C.; Lamanna, N.; Weiss, M. A. *Expert Opin. Drug Metab. Toxicol.* **2008**, *4*, 1217-1222.
- (113) Oettle, H.; Post, S.; Neuhaus, P.; Gellert, K.; Langrehr, J.; Ridwelski, K.; Schramm, H.; Fahlke, J.; Zuelke, C.; Burkart, C.; Gutberlet, K.; Kettner, E.; Schmalenberg, H.; Weigang-Koehler, K.; Bechstein, W.-O.; Niedergethmann, M.; Schmidt-Wolf, I.; Roll, L.; Doerken, B.; Riess, H. *J. Am. Med. Ass.* **2007**, *297*, 267-277.
- (114) Sahasranaman, S.; Howard, D.; Roy, S. *Eur. J. Clin. Pharmacol.* **2008**, *64*, 753-767.
- (115) Champoux, J. J. *Annu. Rev. Biochem.* **2001**, *70*, 369-413.
- (116) Fornari, F. A.; Randolph, J. K.; Yalowich, J. C.; Ritke, M. K.; Gewirtz, D. A. *Mol. Pharmacol.* **1994**, *45*, 649-656.

-
- (117) Evrard, A.; Cuq, P.; Ciccolini, J.; Vian, L.; Cano, J.-P. *Br. J. Cancer* **1999**, *80*, 1726-1733.
- (118) Kim, J.-w.; Dang, C. V. *Cancer Res.* **2006**, *66*, 8927-8930.
- (119) Pelicano, H.; Martin, D. S.; Xu, R. H.; Huang, P. *Oncogene* **2006**, *25*, 4633-4646.
- (120) Pan, J. G.; Mak, T. W. *Sci. STKE* **2007**, *2007*, pe14.
- (121) Parenty, A. D. C.; Smith, L. V.; Pickering, A. L.; Long, D. L.; Cronin, L. *J. Org. Chem.* **2004**, *69*, 5934-5946.
- (122) Guthrie, K. M.; Parenty, A. D. C.; Smith, L. V.; Cronin, L.; Cooper, A. *Biophys. Chem.* **2007**, *126*, 117-123.
- (123) Smith, L. V.; de la Fuente, J. M.; Guthrie, K. M.; Parenty, A. D. C.; Cronin, L. *New J. Chem.* **2005**, *29*, 1118-1120.
- (124) Parenty, A. D. C.; Smith, L. V.; Guthrie, K. M.; Long, D. L.; Plumb, J.; Brown, R.; Cronin, L. *J. Med. Chem.* **2005**, *48*, 4504-4506.
- (125) Smith, L. V.; Parenty, A. D. C.; Guthrie, K. M.; Plumb, J.; Brown, R.; Cronin, L. *ChemBioChem* **2006**, *7*, 1757-1763.
- (126) Saar, K.; Lindgren, M.; Hansen, M.; Eiriksdottir, E.; Jiang, Y.; Rosenthal-Aizman, K.; Sassian, M.; Langel, U. *Anal. Biochem.* **2005**, *345*, 55-65.
- (127) Parenty, A. D. C., University of Glasgow, 2004.
- (128) Baldwin, J. E.; Thomas, R. C.; Kruse, L. I.; Silberman, L. *J. Org. Chem.* **1977**, *42*, 3846-3852.
- (129) Smith, L. V., University of Glasgow, 2005.
- (130) Botar, B.; Geletii, Y. V.; Kogerler, P.; Musaev, D. G.; Morokuma, K.; Weinstock, I. A.; Hill, C. L. *J. Am. Chem. Soc.* **2006**, *128*, 11268-11277.
- (131) Kim, W. B.; Voithl, T.; Rodriguez-Rivera, G. J.; Evans, S. T.; Dumesic, J. A. *Angew. Chem. Int. Ed.* **2005**, *44*, 778-782.
- (132) Judd, D. A.; Nettles, J. H.; Nevins, N.; Snyder, J. P.; Liotta, D. C.; Tang, J.; Ermolieff, J.; Schinazi, R. F.; Hill, C. L. *J. Am. Chem. Soc.* **2001**, *123*, 886-897.
- (133) Rhule, J. T.; Hill, C. L.; Judd, D. A. *Chem. Rev.* **1998**, *98*, 327-357.
- (134) Fleming, C.; Long, D. L.; McMillan, N.; Johnston, J.; Bovet, N.; Dhanak, V.; Gadegaard, N.; Kogerler, P.; Cronin, L.; Kadodwala, M. *Nat. Nanotechnol.* **2008**, *3*, 229-233.
- (135) Ritchie, C.; Ferguson, A.; Nojiri, H.; Miras, H. N.; Song, Y. F.; Long, D. L.; Burkholder, E.; Murrie, M.; Kogerler, P.; Brechin, E. K.; Cronin, L. *Angew. Chem. Int. Ed.* **2008**, *47*, 5609-5612.
- (136) Pope, M.; Muller, A. *Polyoxometalate chemistry: from topology via self-assembly to applications*; Kluwer Academic Publishers: Dordrecht, Boston, 2001.
- (137) Pope, M. T. *Heteropoly and Isopoly Oxometalates*; Springer-Verlag: Berlin, 1983.
- (138) Liu, Y.; Liu, S. X.; Ji, H. M.; Zhang, S. W.; Cai, L. L.; Cao, R. G. *J. Clust. Sci.* **2009**, *20*, 535-543.
- (139) Zhang, L.-Z.; Gu, W.; Dong, Z.; Liu, X.; Li, B.; Liu, M.-L. *J. Solid State Chem.* **2009**, *182*, 1040-1044.
- (140) Odobel, F.; Severac, M.; Pellegrin, Y.; Blart, E.; Fosse, C.; Cannizzo, C.; Mayer, C. R.; Elliott, K. J.; Harriman, A. *Chem. Eur. J.* **2009**, *15*, 3130-3138.
- (141) Long, D. L.; Kogerler, P.; Farrugia, L. J.; Cronin, L. *Angew. Chem. Int. Ed.* **2003**, *42*, 4180-4183.
- (142) Long, D. L.; Kogerler, P.; Farrugia, L. J.; Cronin, L. *Dalton Trans.* **2005**, 1372-1380.
- (143) McGlone, T.; Streb, C.; Long, D.-L.; Cronin, L. *Chem. Asian J.* **2009**, 9999, NA.
- (144) Song, Y. F.; Long, D. L.; Cronin, L. *Angew. Chem. Int. Ed.* **2007**, *46*, 3900-3904.

-
- (145) Micoine, K.; Hasenknopf, B.; Thorimbert, S.; Lacote, E.; Malacria, M. *Org. Lett.* **2007**, *9*, 3981-3984.
- (146) Bareyt, S.; Piligkos, S.; Hasenknopf, B.; Gouzerh, P.; Lacote, E.; Thorimbert, S.; Malacria, M. *J. Am. Chem. Soc.* **2005**, *127*, 6788-6794.
- (147) Bar-Nahum, I.; Cohen, H.; Neumann, R. *Inorg. Chem.* **2003**, *42*, 3677-3684.
- (148) Pradeep, C. P.; Long, D. L.; Newton, G. N.; Song, Y. F.; Cronin, L. *Angew. Chem.-Int. Edit.* **2008**, *47*, 4388-4391.
- (149) Coronado, E.; Giménez-Saiz, C.; Gómez-García, C. J. *Coord. Chem. Rev.* **2005**, *249*, 1776-1796.
- (150) Li, J. Y.; Li, X.; Zhou, P. X.; Zhang, L.; Luo, S. Z.; Cheng, J. P. *Eur. J. Org. Chem.* **2009**, 4486-4493.
- (151) Cao, R.-G.; Liu, S.-X.; Liu, Y.; Tang, Q.; Wang, L.; Xie, L.-H.; Su, Z.-M. *J. Solid State Chem.* **2009**, *182*, 49-54.
- (152) Wilson, E. F., University of Glasgow, 2009.
- (153) Ritchie, C.; Cooper, G. J. T.; Song, Y.-F.; Streb, C.; Yin, H.; Parenty, A. D. C.; MacLaren, D. A.; Cronin, L. *Nat. Chem.* **2009**, *1*, 47-52.
- (154) Cooper, G. J. T.; Cronin, L. *J. Am. Chem. Soc.* **2009**, *131*, 8368-8369.
- (155) Barrett, A. G. M.; Hennessy, A. J.; Vezouet, R. L.; Procopiou, P. A.; Seale, P. W.; Stefaniak, S.; Upton, R. J.; White, A. J. P.; Williams, D. J. *J. Org. Chem.* **2004**, *69*, 1028-1037.
- (156) Blankenstein, J.; Zhu, J. *Eur. J. Org. Chem.* **2005**, *2005*, 1949-1964.
- (157) Aricó, F.; Chang, T.; Cantrill, S., J.; Khan, S., I.; Stoddart, J. F. *Chem. Eur. J.* **2005**, *11*, 4655-4666.
- (158) Bonaga, L. V. R.; Zhang, H.-C.; Moretto, A. F.; Ye, H.; Gauthier, D. A.; Li, J.; Leo, G. C.; Maryanoff, B. E. *J. Am. Chem. Soc.* **2005**, *127*, 3473-3485.
- (159) Gilchrist, T. L. *Heterocyclic Chemistry*; Longman Scientific and Technical: Harlow, 1985.
- (160) Atkins, T. J. *J. Am. Chem. Soc.* **2002**, *102*, 6364-6365.
- (161) Erhardt, J. M.; Grover, E. R.; Wuest, J. D. *J. Am. Chem. Soc.* **2002**, *102*, 6365-6369.
- (162) Baldwin, J. E. *J. Chem. Soc.-Chem. Commun.* **1976**, 734-736.
- (163) Baldwin, J. E.; Cutting, J.; Dupont, W.; Kruse, L.; Silberman, L.; Thomas, R. C. *J. Chem. Soc.-Chem. Commun.* **1976**, 736-738.
- (164) Baldwin, J. E.; Thomas, R. C.; Kruse, L. I.; Silberman, L. *J. Org. Chem.* **2002**, *42*, 3846-3852.
- (165) McClelland, R. A.; Gedge, S. *J. Am. Chem. Soc.* **1980**, *102*, 5838-5848.
- (166) Huck, N. P. M.; Feringa, B. L. *J. Chem. Soc.-Chem. Commun.* **1995**, 1095-1096.
- (167) Kolega, R. R.; Schlenoff, J. B. *Langmuir* **1998**, *14*, 5469-5478.
- (168) Widrig, C. A.; Chung, C.; Porter, M. D. *J. Electroanal. Chem.* **1991**, *310*, 335-359.
- (169) Thom, I.; Buck, M. *Surf. Sci.* **2005**, *581*, 33-46.
- (170) Geyer, W.; Stadler, V.; Eck, W.; Zharnikov, M.; Golzhauser, A.; Grunze, M. *Appl. Phys. Lett.* **1999**, *75*, 2401-2403.
- (171) Long, Y. T.; Rong, H. T.; Buck, M.; Grunze, M. In *International Conference on Electrified Interfaces*; Elsevier Science Sa: Wolfville, Canada, 2001, p 62-67.
- (172) Raghunand, N.; He, X.; van Sluis, R.; Mahoney, B.; Baggett, B.; Taylor, C. W.; Paine-Murrieta, G.; Roe, D.; Bhujwalla, Z. M.; Gillies, R. J. *Br. J. Cancer* **1999**, *80*, 1005-1011.
- (173) Strathdee, G.; MacKean, M. J.; Illand, M.; Brown, R. *Oncogene* **1999**, *18*, 2335-2341.
- (174) Bignami, M.; Casorelli, I.; Karran, P. *Eur. J. Cancer* **2003**, *39*, 2142-2149.

-
- (175) Schofield, M. J.; Hsieh, P. *Annu. Rev. Microbiol.* **2003**, *57*, 579-608.
- (176) McGuire, W. P., III; Markman, M. *Br. J. Cancer* **2003**, *89*, S3-S8.
- (177) Mosmann, T. *J. Immunol. Methods* **1983**, *65*, 55-63.
- (178) Plumb, J. A.; Milroy, R.; Kaye, S. B. *Cancer Res.* **1989**, *49*, 4435-4440.
- (179) Brana, M. F.; Cacho, M.; Gradillas, A.; de Pascual-Teresa, B.; Ramos, A. *Curr. Pharm. Design* **2001**, *7*, 1745-1780.
- (180) Fink, D.; Nebel, S.; Aebi, S.; Zheng, H.; Cenni, B.; Nehme, A.; Christen, R. D.; Howell, S. B. *Cancer Res.* **1996**, *56*, 4881-4886.
- (181) Guan, W.; Yang, G. C.; Liu, C. G.; Song, P.; Fang, L.; Yan, L. K.; Su, Z. M. *Inorg. Chem.* **2008**, *47*, 5245-5252.
- (182) Han, Z. G.; Zhao, Y. L.; Peng, J.; Feng, Y. H.; Yin, J. N.; Liu, Q. *Electroanalysis* **2005**, *17*, 1097-1102.
- (183) Han, Z. G.; Zhao, Y. L.; Peng, J.; Tian, A. X.; Feng, Y. H.; Liu, Q. *J. Solid State Chem.* **2005**, *178*, 1386-1394.
- (184) Tang, Z. Y.; Liu, S. Q.; Wang, E. K.; Dong, S. J.; Wang, E. B. *Langmuir* **2000**, *16*, 5806-5813.
- (185) Allain, C.; Favette, S.; Chamoreau, L. M.; Vaissermann, J.; Ruhlmann, L.; Hasenknopf, B. *Eur. J. Inorg. Chem.* **2008**, 3433-3441.
- (186) Parenty, A. D. C.; Smith, L. V.; Cronin, L. *Tetrahedron* **2005**, *61*, 8410-8418.
- (187) Kitson, P. J.; Song, Y.-F.; Gamez, P.; de Hoog, P.; Long, D.-L.; Parenty, A. D., C.; Cronin, L. *Inorg. Chem.* **2008**, *47*, 1883-1885.
- (188) Kitson, P. J.; Parenty, A. D. C.; Richmond, C. J.; Long, D. L.; Cronin, L. *Chem. Commun.* **2009**, 4067-4069.
- (189) Coghlan, M. J.; Arnold, W. R.; Caley, B. A. *Pestic. Sci.* **1990**, *29*, 67-73.
- (190) Song, Y. F.; Long, D. L.; Kelly, S. E.; Cronin, L. *Inorg. Chem.* **2008**, *47*, 9137-9139.
- (191) Caldwell, A. G.; Walls, L. P. *J. Chem. Soc.* **1952**, 2156-2164.
- (192) Zhu, X. Q.; Zhang, M. T.; Yu, A.; Wang, C. H.; Cheng, J. P. *J. Am. Chem. Soc.* **2008**, *130*, 2501-2516.
- (193) Chikashita, H.; Ide, H.; Itoh, K. *J. Org. Chem.* **1986**, *51*, 5400-5405.
- (194) Steffen, O.; Bart Jan, R.; David, N. R. *Angew. Chem. Int. Ed.* **2005**, *44*, 6282-6304.
- (195) CalistriYeh, M.; Kramer, E. J.; Sharma, R.; Zhao, W.; Rafailovich, M. H.; Sokolov, J.; Brock, J. D. *Langmuir* **1996**, *12*, 2747-2755.
- (196) Srinivasan, U.; Houston, M. R.; Howe, R. T.; Maboudian, R. *J. Microelectromech. Syst.* **1998**, *7*, 252-260.
- (197) Wang, R. W.; Baran, G.; Wunder, S. L. *Langmuir* **2000**, *16*, 6298-6305.
- (198) Wang, R. W.; Wunder, S. L. *J. Phys. Chem. B* **2001**, *105*, 173-181.
- (199) Maoz, R.; Cohen, H.; Sagiv, J. *Langmuir* **1998**, *14*, 5988-5993.
- (200) Tillman, N.; Ulman, A.; Penner, T. L. *Langmuir* **1989**, *5*, 101-111.
- (201) Wasserman, S. R.; Tao, Y. T.; Whitesides, G. M. *Langmuir* **1989**, *5*, 1074-1087.
- (202) Harnett, C. K.; Satyalakshmi, K. M.; Craighead, H. G. *Appl. Phys. Lett.* **2000**, *76*, 2466-2468.
- (203) Sheldrick, G. M. *Acta Crystallogr. Sect. A* **2008**, *64*, 112-122.
- (204) Altomare, A.; Cascarano, G.; Giacovazzo, C.; Guagliardi, A. *J. Appl. Crystallogr.* **1993**, *26*, 343-350.
- (205) Farrugia, L. J. *J. Appl. Crystallogr.* **1999**, *32*, 837-838.
- (206) Yokoyama, Y.; Padias, A. B.; Bratoeff, E. A.; Hall, H. K. *Macromolecules* **1982**, *15*, 11-17.